

Some pages of this thesis may have been removed for copyright restrictions.

If you have discovered material in AURA which is unlawful e.g. breaches copyright, (either yours or that of a third party) or any other law, including but not limited to those relating to patent, trademark, confidentiality, data protection, obscenity, defamation, libel, then please read our [Takedown Policy](#) and [contact the service](#) immediately

**The characterisation and optimisation of modified herbaceous grasses for identifying
pyrolysis-oil quality traits**

PhD Thesis

ROMANI FAHMI

ASTON UNIVERSITY

10th January 2008

This copy of the thesis has been supplied on condition that anyone who consults it is understood to recognise that its copyright rests with its author and that no quotation from the thesis and no information derived from it may be published without proper acknowledgement.

ASTON UNIVERSITY

The characterisation and optimisation of modified herbaceous grasses for identifying pyrolysis-oil quality traits

ROMANI FAHMI

Doctor of Philosophy 2008

THESIS SUMMARY

The primary objective of this work is to relate the biomass fuel quality to fast pyrolysis-oil quality in order to identify key biomass traits which affect pyrolysis-oil stability. During storage the pyrolysis-oil becomes more viscous due to chemical and physical changes, as reactions and volatile losses occur due to aging. The reason for oil instability begins within the pyrolysis reactor during pyrolysis in which the biomass is rapidly heated in the absence of oxygen, producing free radical volatiles which are then quickly condensed to form the oil. The products formed do not reach thermodynamic equilibrium and in turn the products react with each other to try to achieve product stability. The first aim of this research was to develop and validate a rapid screening method for determining biomass lignin content in comparison to traditional, time consuming and hence costly wet chemical methods such as Klason. *Lolium* and *Festuca* grasses were selected to validate the screening method, as these grass genotypes exhibit a low range of Klason /Acid Digestible Fibre lignin contents. The screening methodology was based on the relationship between the lignin derived products from pyrolysis and the lignin content as determined by wet chemistry. The second aim of the research was to determine whether metals have an affect on fast pyrolysis products, and if any clear relationships can be deduced to aid research in feedstock selection for fast pyrolysis processing. It was found that alkali metals, particularly Na and K influence the rate and yield of degradation as well the char content. Pre-washing biomass with water can remove 70% of the total metals, and improve the pyrolysis product characteristics by increasing the organic yield, the temperature in which maximum liquid yield occurs and the proportion of higher molecular weight compounds within the pyrolysis-oil. The third aim identified these feedstock traits and relates them to the pyrolysis-oil quality and stability. It was found that the mineral matter was a key determinant on pyrolysis-oil yield compared to the proportion of lignin. However the higher molecular weight compounds present in the pyrolysis-oil are due to the lignin, and can cause instability within the pyrolysis-oil. The final aim was to investigate if energy crops can be enhanced by agronomical practices to produce a biomass quality which is attractive to the biomass conversion community, as well as giving a good yield to the farmers. It was found that the nitrogen/potassium chloride fertiliser treatments enhances *Miscanthus* qualities, by producing low ash, high volatiles yields with acceptable yields for farmers. The progress of senescence was measured in terms of biomass characteristics and fast pyrolysis product characteristics. The results obtained from this research are in strong agreement with published literature, and provides new information on quality traits for biomass which affects pyrolysis and pyrolysis-oils.

Keywords: pyrolysis-oil stability, Klason/ADF lignin, biomass pyrolysis characterisation.

Aston University

**The characterisation and optimisation of modified herbaceous grasses for pyrolysis-oil
quality traits**

ROMANI FAHMI

Doctor of Philosophy

ACKNOWLEDGEMENTS

In the beginning I wish to thank GOD ALMIGHTY for safeguarding me, mentally and physically throughout the period of carrying out this research. My unlimited gratitude is for my supervisor Professor AV Bridgwater for his patience, valuable guidance and advice at the time of need.

I would also like to extend my thanks and appreciation to my co-supervisor Dr. J Titiloye and the Bioenergy Research Group in Aston for all their help especially Dr. P Tack for their laboratory support whom without their help this work wouldn't be completed.

A word of thanks also goes to the Supergen staff members for their contribution to make this research possible, in particular I express my thanks to those who are associated in work package 2, Simon Thain and Ian Donnison from IGER, Nicola Yates from Rothamsted and Jenny Jones from Leeds. For the quality, experience, training and knowledge I am indebt to Dr. D. Meier [BFH Institute of Wood Chemistry], Dr Gronli [NTNU] and Professor J. Antal [University of Hawaii].

Special thanks to all my PhD and Post Doctorial colleagues who created the right research environment, and encouraged the scientific discussion forum within our research group. Last but not least I am grateful to my family for their unlimited support and encouragement when times looked grey.

THEOLOGY OF LIFE

VANITY OF ALL VANITIES



Aston University

Content has been removed due to copyright restrictions



Aston University

Content has been removed due to copyright restrictions



Aston University

Content has been removed due to copyright restrictions

**From: The Holy Bible KJV; Book of Proverbs, Ecclesiast, Epistle of James and the 1st
letter from Paul to the Corinthians**

TABLE OF CONTENTS

Table of Contents.....	7
1 Introduction.....	17
1.1 Objectives	17
1.2 Structure of Thesis	19
2 Biological structure of biomass.....	22
2.1 Plant Introduction	22
2.1.1 The Leaf.....	24
2.1.2 The Stem	25
2.1.3 The Roots.....	25
2.2 Biomass Chemical composition.....	26
2.2.1 Cellulose	26
2.2.2 Lignin.....	27
2.2.3 Hemicellulose	28
2.2.4 Inorganic components.....	29
2.2.5 Pectins.....	29
3 Thermal degradation Theory	31
3.1 Background knowledge	31
3.1.1 Slow pyrolysis.....	32
3.1.2 Fast/flash Pyrolysis.....	33
3.2 Common compound degradation mechanism literature review	34
3.2.1 Depolymerisation radical reaction mechanism.....	34
3.2.2 Monomer reversion.....	37
3.3 Pyrolysis compound mechanisms.....	38
3.3.1 Levoglucosan formation	39
3.3.2 5-hydroxymethyl-2-furaldehyde formation	40
3.3.3 Low molecular weight compound formations below 400°C	41
3.3.4 Furfural formation.....	42
3.4 Literature review.....	42
3.4.1 Characterisation of biomass via pyroprobe-GC/MS.....	42
3.4.2 The effect of metals	44

3.4.3	Cellulose and biomass pathway models	46
3.4.4	Hemicellulose pyrolysis.....	50
3.4.5	Lignin pyrolysis.....	51
3.4.6	Agronomical practice.....	54
3.5	Chapter Conclusions	56
4	Materials and Methods.....	58
4.1	Feedstock Characterisation	58
4.1.1	Milling and sieving	58
4.1.2	Particle size	58
4.1.3	Sampling	59
4.1.4	Moisture content	60
4.1.5	Ash content	60
4.1.6	Elemental and metal analysis.....	60
4.1.7	Lignocellulosic determination	61
4.1.8	Statistical analysis [PCA]	61
4.2	Thermogravimetric analysis	62
4.3	Pyroprobe CDS AS-2500 -GC/MS.....	64
4.3.1	Sample sizes.....	65
4.3.2	Sample boats for pyroprobe-GC/MS	66
4.3.3	Turbo mass Gold Gas chromatography/mass spectroscopy	66
4.3.4	Pyroprobe-GC/MS peak identification	68
4.3.5	Pyroprobe-GC/MS repeatability	74
4.4	Conditions for analytical pyrolysis.....	74
4.4.1	Thermal analysis experiments	74
4.4.2	Pyrolysis-GC/MS experiments	74
4.5	Pyrolysis reactor system	76
4.5.1	Overview.....	76
4.5.2	Feed rate Determination.....	78
4.5.3	Fluidised bed reactor.....	78
4.5.4	Residence Time.....	80
4.5.5	Liquid collection systems	81
4.5.6	Limitations of 150 ghr ⁻¹ pyrolysis rig.....	83

4.6	Mass balance.....	84
4.6.1	Liquids	84
4.6.2	Char.....	85
4.6.3	Gas	86
4.6.4	Summary	87
4.7	Pyrolysis-oil background	88
4.7.1	Pyrolysis-oil uses	88
4.8	Pyrolysis-oil analysis	89
4.8.1	Molecular weight: Gel Permeation Chromatography.....	90
4.8.2	Compound identification and quantification: liquid GC/MS	90
4.8.3	Yield determination and water content analysis: Karl Fischer Coulometer.....	91
4.8.4	PH- Metrohm PH meter	92
4.8.5	Elemental method	92
4.8.6	Viscosity- viscometer	92
4.9	Stability theory.....	93
4.9.1	Factors that determine quality and quantity of pyrolysis-oil	95
4.9.2	Inorganic species in pyrolysis-oil	95
4.9.3	Chemical mechanisms within pyrolysis-oil	95
5	Investigation of reference fuels on fast pyrolysis and pyrolysis-oils	96
5.1	Introduction.....	96
5.2	Experimental.....	96
5.2.1	Reference fuel characterisation and analytical pyrolysis conditions	97
5.3	Results & Discussion	97
5.3.1	Reference fuel characterisation.....	97
5.3.2	TGA and pyroprobe-GC/MS results.....	97
5.3.3	Fast pyrolysis experiments on reference fuels.....	100
5.4	Conclusion	116
6	Experimental determination of biomass lignin in <i>Lolium</i> & <i>Festuca</i> grasses using pyroprobe-gc/ms and wet chemistry lignin methods.....	117
6.1	Introduction.....	117
6.2	Experimental.....	118

6.3	Results & Discussion.....	118
6.3.1	Pyroprobe-GC/MS analysis.....	124
6.4	Fast pyrolysis experiments on selected <i>Lolium & Festuca</i> grasses.....	130
6.4.1	Introduction to rig experiments.....	130
6.4.2	Experimental.....	130
6.4.3	Results & Discussion.....	130
6.5	Conclusions.....	144
7	The Effect of metals on pyrolysis and washing treatments for enhancing pyrolysis characteristics	146
7.1	Introduction.....	146
7.2	Experimental.....	146
7.2.1	<i>Lolium</i> and <i>Festuca</i> characterisation	146
7.2.2	Principle component analysis	146
7.2.3	Washing techniques.....	147
7.3	Results & Discussion.....	147
7.3.1	Characterisation results for <i>Lolium</i> and <i>Festuca</i> grasses.....	147
7.3.2	Pyroprobe-GC/MS Results	150
7.3.3	The effect of washing time on willow chip	152
7.3.4	TGA results.....	154
7.3.5	PCA analysis on the effect of lignin on metals.....	157
7.4	Fast pyrolysis experiments on washed feedstocks.....	158
7.4.1	Introduction to rig experiments.....	158
7.4.2	Experimental.....	159
7.4.3	Results & Discussion	159
7.5	Conclusions.....	163
8	Agronomical effects on <i>Miscanthus</i> feedstock quality	166
8.1	Introduction.....	166
8.1.1	Fertiliser treatments and plots.....	167
8.1.2	Grouped fertiliser treatments	167
8.1.3	<i>Miscanthus</i> yield reports per sampling	169
8.2	Experimental.....	169

8.2.1	Miscanthus characterisation.....	169
8.2.2	TGA and Pyroprobe-GC/MS conditions	169
8.3	Results and discussion	170
8.3.1	The agronomical effect of nitrogen fertiliser	170
8.3.2	The agronomical effect of potassium chloride fertiliser	177
8.3.3	The agronomical effect of potassium sulphate applications	185
8.4	Fast pyrolysis experiments on Miscanthus samples studying the effect of fertiliser treatment	191
8.4.1	Introduction to rig experiments.....	191
8.4.2	Experimental.....	192
8.4.3	Results.....	192
8.5	Conclusions.....	199
9	Conclusions and Recommendations.....	202
9.1	Conclusions.....	202
9.2	Recommendations.....	204
10	References.....	207
11	APPENDIX I.....	216
11.1	Publications produced during the PhD course.....	216
11.2	Reference fuels TG & DTG data	217
12	APPENDIX II.....	218
12.1	Agronomical results of Miscanthus	218
12.1.1	The effect of sampling time on TGA	218
12.2	Alkali metal results of Miscanthus treatments.....	219
12.2.1	Nitrogen fertiliser treatments on the leaf content of Miscanthus.....	219
12.2.2	Potassium chloride fertiliser treatments on the leaf content of Miscanthus	220
12.2.3	Potassium sulphate treatment fertiliser treatments on the leaf content of Miscanthus	221
12.2.4	Nitrogen fertiliser treatments on the stem content of Miscanthus.....	222
12.2.5	Potassium chloride fertiliser treatments on the stem content of Miscanthus	223

12.2.6 Potassium sulphate treatment fertiliser treatments on the stem content of Miscanthus	224
13 APPENDIX III	225
13.1 PCA Compounds analysis	225
13.1.1 PCA results from pyroprobe-GC/MS for leaves.....	226
13.1.2 PCA results from pyroprobe-GC/MS for stems	228
13.2 Overview of PCA analysis.....	229
13.2.1 Nitrogen treatments.....	229
13.2.2 Potassium chloride treatments	231
13.2.3 Potassium sulphate treatments	231
13.3 The effect of compound yields during sampling	232

LIST OF FIGURES

Figure 2-1 - Plant shoot and Root systems [3].....	23
Figure 2-2 – Plant cell ultrastructure [3].....	24
Figure 2-3 – The structure of cellulose [β -1,4 linkage]	27
Figure 2-4 - S, G and H monomers of Lignin present in Grasses [10, 11].....	28
Figure 2-5 – The lignin structure within beech wood [2].....	28
Figure 2-6 – The structure of Hemicellulose [3,4]	29
Figure 3-1 – Typical mass balance of wood fast pyrolysis.....	31
Figure 3-2 – Waterloo’s proposed mechanism o fragmentation and depolymerisation of Cellulose Monomers [6, 26, 29]	38
Figure 3-3 – Products derived from Cellulosic glucose including pathway [7, 33]	39
Figure 3-4 - 5-hydroxymethyl-2-furaldehyde formation by dehydration, hydration rearrangement [35].....	41
Figure 3-5 – Madorskey et al., proposed the first model for cellulose [69]	46
Figure 3-6 – Shafizadeh proposed the modified version of his original model, showing the debated Active state [7, 33, 70, 71].	47
Figure 3-7 – Reaction method used by Liden et al and Diebold [27, 86, 100].....	48
Figure 3-8 – Antal’s reaction mechanism for volatile decomposition [9].....	49
Figure 3-9 - The Waterloo Model for Cellulose Decomposition [6, 29].....	50
Figure 3-10 - Antal's proposed lignin reaction pathways in 1985 [33]	53
Figure 4-1 - Perkin Elmer Pyris 1 TGA [133]	63
Figure 4-2 - AS2500 Pyroprobe auto sampler [134]	65
Figure 4-3 - Pyroprobe auto sampler boat and boat position in furnace [134].....	66
Figure 4-4 - Principles of MS analysis [135].....	67
Figure 4-5 - Pyrogram of Avicell cellulose derived compounds.....	69
Figure 4-6 - Pyrogram of Pyrolytic Spruce Lignin Derived compounds	72
Figure 4-7 - Aston's 150 ghr ⁻¹ fluidised bed fast pyrolysis rig	76
Figure 4-8 - The effect of aging on pyrolysis-oil [86].....	94
Figure 4-9 - Average molecular weight vs. viscosity of pyrolysis-oil [86].....	94
Figure 5-1 - Comparison of Total liquid yields from the reference fuels and other feedstocks used in this research in comparison to literature results.	101
Figure 5-2 - The effect of Na and Potassium on total pyrolysis product yields	102
Figure 5-3 - Chromatogram of oil pot 1 from Willow.....	103
Figure 5-4 - Chromatogram of oil pot 2 from Willow.....	105
Figure 5-5 - Relationship between pyroprobe-GC/MS yields to laboratory scale total pyrolysis liquid yields.....	106
Figure 5-6 - Pyroprobe-GC/MS total area yields of key marker yields Vs. GPC results.....	108
Figure 5-7 - Total pyrolysis liquid yields vs. GPC results.....	109
Figure 5-8 - Total liquid yields vs. pH.....	110
Figure 5-9 - The relationship between pyrolysis-oil lignin derived compounds found in oil pot 1 vs. wet chemistry lignin content [%]	111
Figure 5-10 - GPC results of fresh and aged oils vs. wet chemistry lignin content [%]	112
Figure 5-11 - The relationship between the total area for the low molecular weight compounds found in oil pot 2 vs. actual lignin content as measured by wet chemistry [%]	113
Figure 5-12 - Comparison of oil pot 1 composition and methanol evaporated EP/ condenser oil composition.....	114

Figure 5-13 - The effect of aging on Levoglucosan	115
Figure 5-14 - The effect of aging of hydroxyacetaldehyde	115
Figure 6-1 - Relationship between lignin and total metals for <i>Lolium</i> and <i>Festuca</i> grass	120
Figure 6-2 - Relationship of lignin and total metals for species used in this investigation	121
Figure 6-3 - Relationship between biomass components in <i>Lolium</i> and <i>Festuca</i> samples.....	122
Figure 6-4 - Relationship between lignin and holocellulose content in <i>Lolium</i> and <i>Festuca</i> grasses.....	123
Figure 6-5 - (a) Py-GC/MS Chromatogram of a representative grass sample; (b) Partial Least-Squares Factor Loadings.....	125
Figure 6-6 - Pyroprobe-GC-MS predicted vs. actual lignin content [%] as measured by wet chemistry.....	126
Figure 6-7 - Relationship of subunits in <i>Lolium</i> & <i>Festuca</i> samples	127
Figure 6-8 - Relationship between Pyroprobe-GC/MS lignin vs. actual lignin [%] as measured by wet chemistry	127
Figure 6-9 - The screening of other feedstocks by the use of pyroprobe-GC/MS.....	129
Figure 6-10 - TG of <i>Lolium</i> and <i>Festuca</i> grass.....	132
Figure 6-11 - DTG of <i>Lolium</i> and <i>Festuca</i> grass.....	132
Figure 6-12 - TGA results of <i>Lolium</i> and <i>Festuca</i> grasses	133
Figure 6-13 - The comparison of organic composition on grouped compounds in <i>Lolium</i> & <i>Festuca</i> grasses based on Pyrprobe-GC/MS results	135
Figure 6-14 - Average molecular weight of pyrolysis-oil vs. actual lignin content [%] determined by wet chemistry	138
Figure 6-15 - Average molecular weight of pyrolysis-oil vs. viscosity.....	139
Figure 6-16 - Viscosity of pyrolysis-oil vs. actual lignin content [%] as determined by wet chemistry.....	140
Figure 6-17 - Pyrolysis-oil viscosity vs. pyrolysis-oil water content.....	141
Figure 6-18 - PCA analysis of lignin and pyrolysis-oil qualities	143
Figure 7-1 - Unwashed and washed <i>Festuca mairei</i> -4x.....	150
Figure 7-2 - The effect of washing on <i>Festuca mairei</i> -4x levoglucosan peak.....	151
Figure 7-3 - The effect of washing time on Hydroxyacetaldehyde and Levoglucosan from willow chip	153
Figure 7-4 - DTG of temperature programmed pyrolysis of unwashed and washed <i>Festuca</i> Sample F.mairei-4x.....	154
Figure 7-5 - Relationship between the Tmax of cellulose against Na & K level of all unwashed/washed feedstocks	156
Figure 7-6 - Relationship between char yield from TGA pyrolysis against Na & K level for all unwashed/washed feedstocks	156
Figure 7-7 - PCA analysis of Lignin and metals	158
Figure 8-1 - The average ash content of nitrogen fertiliser treatments of the three sampling periods for leaves.....	170
Figure 8-2 - The average ash content of nitrogen fertiliser treatments of the three sampling periods for stems.....	171
Figure 8-3 - The effect of nitrogen treatments and sampling on <i>Miscanthus</i> alkali metal content in leaves.....	172
Figure 8-4 - The effect of nitrogen treatments and sampling on <i>Miscanthus</i> alkali metal content in stems	173
Figure 8-5 - Average dry mass yield of nitrogen fertiliser treatments of the three sampling periods.....	174

Figure 8-6 - Average percentage of leaves present in yields of the nitrogen fertiliser treatments of the three sampling periods.....	174
Figure 8-7 - Volatile and gas yields for leaf material determined by TGA for the nitrogen treatments over the three sampling periods	175
Figure 8-8 - Volatile and gas yields for stem material determined by TGA for the nitrogen treatments over the three sampling periods	176
Figure 8-9 - The average ash content of potassium chloride fertiliser treatments of the three sampling periods for leaves	177
Figure 8-10 - The average ash content of potassium chloride fertiliser treatments of the three sampling periods for stems	178
Figure 8-11 - The effect of potassium chloride treatments and sampling on Miscanthus alkali metal content in leaves.....	179
Figure 8-12 - The effect of potassium chloride treatments and sampling on Miscanthus alkali metal content in stems.....	180
Figure 8-13 - Average dry mass yield of potassium chloride fertiliser treatments of the three sampling periods	181
Figure 8-14 - Average percentage of leaves present in yields of the potassium chloride fertiliser treatments of the three sampling periods.....	182
Figure 8-15 - Volatile and gas yields determined by TGA for the potassium chloride treatments over the three sampling periods for the leaf material.....	183
Figure 8-16 - Volatile and gas yields determined by TGA for the potassium chloride treatments over the three sampling periods for the stem material	183
Figure 8-17 - The average ash content of potassium sulphate fertiliser treatments of the three sampling periods for leaves	185
Figure 8-18 - The average ash content of potassium sulphate fertiliser treatments of the three sampling periods for stems	186
Figure 8-19 - The effect of potassium sulphate treatments and sampling on Miscanthus alkali metal content in leaves.....	186
Figure 8-20 - The effect of potassium sulphate treatments and sampling on Miscanthus alkali metal content in stems.....	187
Figure 8-21 - Average dry mass yield of potassium sulphate treatments of the three sampling periods.....	188
Figure 8-22 - Average percentage of leaves present in yields of the potassium sulphate fertiliser treatments of the three sampling periods.....	189
Figure 8-23 -Volatile and gas yields determined by TGA for the potassium sulphate treatments over the three sampling periods for the leaf material	190
Figure 8-24 - Volatile and gas yields determined by TGA for the potassium sulphate treatments over the three sampling periods for the stem material	191
Figure 8-25 - TG results of the five Miscanthus batches of the five different treatments.....	193
Figure 8-26 - The effect of ash on product distribution.....	195

LIST OF TABLES

Table 4-1 - Assignment of compound composition and gas chromatographic retention times of cellulose [Avicell 99%] derived compounds.....	70
Table 4-2 - Assignment of compound composition and gas chromatographic retention times of Lignin [Spruce pyrolytic lignin] derived compounds.....	73
Table 4-3-Smmary of methods for mass balances.....	87
Table 5-1 – Chemical analysis of reference fuels.....	97
Table 5-2 - ICP analysis of reference fuels [ppm].....	97
Table 5-3 - TGA results of reference fuels.....	98
Table 5-4 - Pyroprobe-GC/MS results of reference fuels.....	99
Table 5-5 - Mass balances of fast pyrolysis experiments on the reference fuels on Aston's 150 ghr ⁻¹ fast pyrolysis rig.....	100
Table 5-6 – Typical compounds found in oil pot 1 and evaporated oils.....	104
Table 5-7 – Typical compounds found in oil pot 2.....	105
Table 5-8 - Oil quality analysis of refrence fuels.....	107
Table 6-1 – Chemical and calorific value analysis of <i>Lolium</i> and <i>Festuca</i> grass samples.....	119
Table 6-2 - Lignin content and ICPES metal analysis in ppm.....	119
Table 6-3 - Elemental analysis of <i>Lolium</i> and <i>Festuca</i> grasses with heating values.....	131
Table 6-4 - Alkali metal content of <i>Lolium</i> and <i>Festuca</i> grasses.....	131
Table 6-5 - Key markers present in <i>Lolium</i> and <i>Festuca</i> samples scaled to 100 %.....	134
Table 6-6 - Mass balance results on <i>Lolium</i> & <i>Festuca</i> grasses on Aston's 1 kghr ⁻¹ fast pyrolysis rig.....	136
Table 6-7 - Oil analysis of <i>Lolium</i> & <i>Festuca</i> grasses.....	137
Table 6-8 - Elemental analysis on <i>Lolium</i> and <i>Festuca</i> oil pot 2.....	138
Table 6-9 - Chemical composition present in <i>Lolium</i> and <i>Festuca</i> pyrolysis-oils.....	142
Table 7-1 - ICP analysis of unwashed <i>Lolium</i> & <i>Festuca</i> grasses [ppm].....	148
Table 7-2 - ICP analysis of washed <i>Lolium</i> & <i>Festuca</i> grasses and other biomass [ppm].....	149
Table 7-3 - The overall effect of washing on pyrolysis products from unwashed/washed F. Mairei-4x [concentration reported as weight per volume].....	152
Table 7-4 - Elemental analysis of washed <i>Festuca arundinacea</i> and washed Switchgrass 2004.....	159
Table 7-5 - Alkali metal content of washed grasses [ppm].....	159
Table 7-6 - Mass balance of washed <i>Lolium</i> <i>Festuca</i> grass and switchgrass 2004 on Aston's 150 ghr ⁻¹ fast pyrolysis rig.....	160
Table 7-7 - Oil quality analysis on washed F. arundinacea and washed Switchgrass 2004 ...	162
Table 8-1 - Treatments for <i>Miscanthus</i>	167
Table 8-2 - CHNO analysis of <i>Miscanthus</i> plots. Oxygen calculated by difference.....	193
Table 8-3 - The five selected treatments for pyrolysis analysis and pyrolysis-oil production	193
Table 8-4 - Pyroprobe-GC/MS of <i>Miscanthus</i> plots.....	194
Table 8-5 - Mass balance of 1st sampling of <i>Miscanthus</i> on Aston's 150 ghr ⁻¹ fast pyrolysis rig.....	196
Table 8-6 - Oil analysis of <i>Miscanthus</i> treatments.....	198

1 INTRODUCTION

The research has two main objectives: Genotypic variation inherent in *Lolium* and *Festuca* species was used to identify biomass traits that may influence the yield and quality of pyrolysis-oils. Studies on *Miscanthus* exploited feedstock quality, as influenced by variation in agronomic practice. Reference fuels were also used to act as comparison standard. The second part of the research is concerned with the screening of biomass lignin, by relating it to the organic vapours from fast pyrolysis. Analytical pyrolysis has been used to validate the quality of the vapours, in which the results were verified on a larger scale by the use of a fast pyrolysis fluidised bed reactor with characterisation of the pyrolysis-oil. The work carried out in this research is associated with the SUPERGEN consortium, in where Rothamsted Research carried out ICP analysis and IGER lignocellulosic determination on the feedstock associated with this research.

1.1 Objectives

The main objectives of the research are:

- [I]. To establish if relationships exist between feedstock and pyrolysis derived products to predict their behaviour under thermal degradation. This would also include the use analytical equipment for screening the quality of biomass, and predicting their pyrolysis-oil yields and stability.
- [II]. To determine whether genotype variation in *Lolium* and *Festuca* feedstocks for lignin content are reflected in yield and quality of pyrolysis product profiles, and to predict their behaviour and yields under fast pyrolysis.
- [III]. The study of the agronomical treatments $[\text{NH}_4\text{NO}_3]$, KCl and K_2SO_4 and harvesting times on *Miscanthus* crops, with the aim to modify the fuel characteristics in optimising pyrolysis conversion.

- [IV]. The investigation on the behaviour of ash/metals on *Lolium* and *Festuca*, Miscanthus and the reference fuels to establish ideal fuel properties ideal for biomass pyrolysis.
- [V]. To establish data sets between the fuel quality and the thermochemical behaviour, in determining factors, which may influence oil stability.
- [VI]. To recommend realistic criteria and approaches for optimising biomass characteristics, which would be beneficial for biomass conversion by fast pyrolysis.

The study utilises genetic variation in grass crop species, and the affect of farming practice on energy crops for identifying quality traits for enhancing pyrolysis characteristics and how much they can be manipulated. The study also includes the possible limitations for farmers and processors, when optimising feedstock characteristics. This in turn would allow realistic recommendations to be made for the most efficient farming practice in growing the feedstock and optimise process conditions for obtaining the optimum pyrolysis liquid quality. The research evaluates if links exist between fuel qualities and farming practice, in order to produce a desirable fuel which can be used for application. This allows limits to be identified on the variability of biomass, which could be used to obtain the optimum fuel quality.

The genotypes used in this investigation are *Lolium* and *Festuca* grasses which are classical genotype feedstocks. The *Lolium* and *Festuca* grasses exhibit a range of gene expression patterns which give rise to variation in ligninExpress genes varying cell wall phenolics and carbohydrates content. The feedstock used for investigating different agronomical practices was *Miscanthus x giganteus*. Miscanthus is a European grass of substantial potential as an energy crop, which produces high crop yield [Ton/Ha], and low ash/metal content than any other non-woody biomass. The Miscanthus crop takes three years to establish when sown and within this growing phase, different fertilisers and harvesting times were implemented to determine their final fuel quality on the crop. Six reference fuels were used to act as a standard for the *Lolium*, *Festuca* and Miscanthus grasses. The reference fuels are willow, straw, reed canary grass, switchgrass as well reed canary grass and switchgrass grown in 2005, in which all the reference fuels have a variation in lignin and alkali metal [ash] content.

The equipment used to analyse these feedstocks for their pyrolysis thermal conversion and behaviour was the TGA (thermogravimetric analyser), pyroprobe-GC/MS unit (pyroprobe-gas

chromatography linked to a mass spectrometer) and Aston's 150 ghr⁻¹ and 1 kghr⁻¹ fluidised bed pyrolysis reactors.

1.2 Structure of Thesis

The thesis is structured into 10 chapters summarised as follows

Chapter 2, Biological structure of biomass

This chapter looks at the biological structure of non-woody biomass plants and their functional roles. Plant anatomy, tissue and cell types are described briefly to provide an insight into lignin/cellulose ratios within the plant. The four main constituents which make up biomass are also examined, which include hemicellulose, cellulose, lignin and metals.

Chapter 3, Thermal degradation theory

Chapter three investigates the principles of thermal degradation, and the chemical reactions of free radical de-polymerisation under the effect of high temperature. Simple reactions have been used to explain and understand the underlying principles of pyrolysis. A comprehensive literature review is also included in this chapter. This was carried out to investigate what work had been carried out in the past to identify possible gaps with in the field, in order for the research to contribute effectively to the field.

Chapter 4, Materials and methods

Pyrolysis equipment used in this research varies from analytical scale units to laboratory reactors. This chapter gives a detailed overview of the TGA [thermogravimetric analysis], pyroprobe-GC/MS and the pyrolysis-oil production rigs 150 ghr⁻¹ and the 1 kghr⁻¹ fluidised bed pyrolysis reactors. Detailed mass balances are also included, in order to demonstrate good closure and hence reliable results. This chapter also reviews the preparation and analysis of the biomass fuels prior to experimental work. This was carried out to provide information on the quality of the feedstock in order to derive relationships with the pyrolysis products, yields and oil quality. This analysis of the biomass prior to experimental includes moisture, ash, proximate analysis, cellulose/lignin content and Induced Coupled Plasma analysis for metal

content. Pyrolysis-oil quality and stability has also been addressed in this chapter to identify key methods which are used to characterise the pyrolysis-oil.

Chapter 5, Investigation of reference fuels on fast pyrolysis and pyrolysis-oils

This chapter investigates how the different reference fuels with its varying composition affect's pyrolysis pathways and products, and the pyrolysis-oil quality. A detailed overview of the reference fuels mass balances and oil characteristics are provided in this chapter, as well as how the pyrolysis liquid characteristics changes at different points of the laboratory scale fast pyrolysis process.

Chapter 6, Experimental determination of biomass lignin in *Lolium* & *Festuca* grasses using pyroprobe-GC/MS and wet chemistry lignin methods

A set of *Lolium* and *Festuca* grasses was used to relate the pyrolysis products to its original constituents, which possessed a wide range of low lignin contents of 2-4 % as measured by Klason and ADF. Pyroprobe-GC/MS and TGA were used to develop the trends and to establish relationships between the feedstocks and the pyrolysis products. Pyrolysis-oil production on Astons 1 kg hr^{-1} scale was used, to produce oils from these species to investigate whether low lignin feedstocks could be beneficial for pyrolysis-oil stability.

Chapter 7, The effect of metals on pyrolysis and washing treatments for enhancing pyrolysis characteristics

This chapter reports on experiments that were conducted on the *Lolium* and *Festuca* grasses to investigate the effect of ash and metal contents on pyrolysis and pyrolysis product yields. It has been shown by other researchers that alkali metals affect the degradation mechanism of biomass during pyrolysis and promote secondary cracking of vapours during the thermochemical process. A number of water washing conditions [pre-treatment] have been used to reduce the metal content within the biomass, to investigate if a relationship exists between the unwashed and washed feedstocks by the use analytical pyrolysis. Pyrolysis-oil production on Astons 150 g hr^{-1} pyrolysis reactor was used to produce oils from these washed species and to investigate whether reducing the metal contents for the low lignin feedstocks was beneficial.

Chapter 8. Agronomical effects on Miscanthus

This chapter investigates and reviews the effect of fertiliser applications and sampling times on Miscanthus which was sown and grown in 2003-2005. 84 Miscanthus samples were provided by Rothamsted along with their ICP metal contents. Feedstock characterisation and analytical pyrolysis was used to discriminate between the different treatment method and sampling periods. Pyrolysis-oil production on the Astons 150 ghr⁻¹ pyrolysis reactor was used to produce oils for the most promising treatment at final harvest. This was carried out to investigate if changes in agronomical practices can improve fast pyrolysis yields and qualities.

Chapter 9. Conclusions and recommendations

The findings of this project are listed within this chapter. The chapter also addresses the problems encountered and how they were resolved, as well as highlighting issues that need to be addressed if progression in this work is to be continued. The chapter also outlines possible future investigations which could be carried out to progress this project field.

2 BIOLOGICAL STRUCTURE OF BIOMASS

This chapter reviews the biological structure of plants and their chemical composition. This is necessary to gain a better understanding of how the plants are currently cultivated and what changes in farming practice can affect the overall biological nature of the plant to benefit fast pyrolysis conversion.

2.1 Plant Introduction

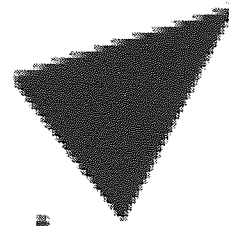
Biomass ranges from woody materials to non-woody materials [1]. Plant material changes as it grows, however there are many common attributes and functions among different non-woody biomass, such as reproduction, photosynthesis and plant biological structures [2]. The height and yield of the plant is dependant on the type of the plant which is being grown and its agronomical conditions which includes its efficiency on minerals, water and sunlight uptake. Fertilisers are used to aid the plant grown and optimise the rate in which the plant grows. In general plants have two main organs which are the root and shoot systems. The root systems are usually found under the ground, and their main functions is to carry the necessary minerals and water to keep the plant alive. The shoot system has the main features of the leaf, bud and stem. This can be seen in Figure 2-1. The cells which consist within the plant have cellulosic walls, nuclei, numerous chloroplasts and vacuoles to store starch as shown in Figure 2-2. The main living cell components within plants are:

- *Middle lamella*: The middle lamella is the first layer formed during cell division. It acts as the depositry to the rest of the cells, and consists predominately of lignin at which most of the lignin molecules are carbon-carbon bonded.
- *Primary wall*: The primary cell wall consists mostly of lignin on the outside of the cell surface. However on the inside of the primary wall, it is dominated by cellulose and allows for carbohydrate storage as well as aiding in cell to cell interaction.
- *2nd Outer wall layer*: The secondary outer wall layer is made predominately of cellulose and some phenolic esters between the walls. The lamella accounts for most of the carbohydrates within plant. Its main function are similar to that of the primary wall layer, however it is more lignified than the secondary outer wall layer.

- *2nd Wall layer*: The secondary wall layer can reach up to 10 μ m, and consists also of cellulose, as well as a number of micro fibrils [which are packed and aligned in parallel] which gives hemicellulose strength to the cell.
- *2nd Outer wall layer*: The secondary outer wall consists of cellulose, lignin, hemicellulose, tertiary lamella and hemicellulose xylans. This aids the cell by building up a resistance to any alkali and chemical attacks to the cell.



Figure 2-1 - Plant shoot and Root systems [3]



Aston University

Illustration removed for copyright restrictions

Figure 2-2 – Plant cell ultrastructure [3]

2.1.1 The Leaf

The tissue within the leaf is surrounded by the epidermis, in which it is coated by a waxy material [cutin] which protects the inner tissue and minimises any water loss [2]. The leaf has an upper and lower epidermis in which the stomata are found. The stomata are surrounded by guard cells which allow gas exchange from oxygen to carbon dioxide in order for photosynthesis to occur. The leaves also consist of veins made of two bundles of elongated cells which are called the xylem [which consists mainly of lignin] and phloem tissues. The xylem tissue bundles are located in the upper epidermis, and are considered as dead cells [3]. The xylem aids the transportation of water and minerals, and is considered to have the property of being brittle which gives strength to the leaf. The phloem tissues are living cells and are located at the lower epidermis, in which its function is to carry the chemical products of photosynthesis to the rest of the plant via the veins to the stem [3,4]. The leaves are the primary site of photosynthesis and it is through the stomata that carbon dioxide and oxygen are exchanged during photosynthesis and photorespiration. During senescence many of the

mineral nutrients are withdrawn from the leaves and exported back into the stem system. As cell death proceeds the tissues become increasingly lignified

2.1.2 The Stem

One of the main functions of the stem is to aid the plant with mechanical strength against aggressive environmental conditions [3]. The majority of the plant's strength is found in the stem, but also provides a more essential by transporting minerals and water to the rest of the plant. The strength of the stem is due to the irregularity of the cell wall thickness. Its structure is similar to that of the leaf, however with three essential tissue regions. The stem has an epidermis [with an outer layer], stomata and guard cell which carries out the same function to that of the leaf [3,4]. The stem structures are round and consistent throughout, however the stem is filled with parenchyma which is equivalent to that of the mesophyll. The outer layer of the stem consists of cortex, which is a necessity for photosynthesis [3]. The xylem within the plant stem has a different arrangement to that of the roots, as the xylems are faced towards the inner/centre core of the stem [usually referred as endarch xylem], while the phloem are on the outer rim of xylem circumference. As the xylem begins to lignify it adds additional mechanical strength to the plant stem.

2.1.3 The Roots

The roots of a plant have the most simplified structure in comparison to the rest of the plant, and have similar characteristics to that of the stem, but with the exception of the vascular bundle which have been bound together to form a single solid cylindrical structure [3]. The centre of the root possesses xylem, while the edge consists of the vascular tissue. The roots possess an additional single layer of cells [endodermis] which is between the vascular tissue and cortex [2]. Endodermis consists mainly of lignin and its function is to uptake certain minerals and soil water [3]. The xylem tissue are located at the core of the root and is shaped like 3/4 branched star [usually referred as exarch xylem], at which the phloem tissue surrounds the outer xylem pronged star, while the whole entire structure is surrounded by the endodermis [3,4]. The exarch xylem and phloem are intertwined together, throughout the roots to give extra support to the base of the plant.

2.2 Biomass Chemical composition

The main components or constituents of biomass are summarised below.

2.2.1 Cellulose

Cellulose is one of many polymers which is found naturally on the earth and are usually referred as polysaccharides. It is regarded as a polysaccharide of beta-D glucopyranose connected to each monomer via glycosidic bonds at the C₁ and C₄ atoms, and repeated consecutively to a degree of polymerisation of 2000-10,000 monomers [DP is the degree of polymerisation or number of monomers]. The structure of cellulose comprises of long linear ribbon like chains which are aggregated in the structural fibrils, in which each fibril can have up to 700 polymeric chains that run in parallel with the hydroxyl groups exposed [4]. The hydroxyl groups can undergo hydrogen bonding within other polymeric molecules within the fibrils. This makes cellulose resistant to solvents and other chemical attacks, as well as having high tensile and temperature strength. Cellulose content within the plant is dependant on the cell wall, and varies from plant to plant by age and location. Cellulose is a crystalline structure of sugar (C₆H₁₀O₅)_n and due to its solid ridged molecular structure it can resist high levels of hydrolysis. When cellulose is heated, it undergoes a rapid decrease in DP due to the hydrolysing of the glycosidic bonds, to form a lower DP known as the active state of cellulose [6]. There are two competing pathways in which cellulose can degrade during pyrolysis; one pathway is the formation of char, while the other being the formation of tar (organic volatiles) [7, 8] at which the yields of char and organics can vary. The thermal degradations of cellulose takes place between 200-400°C, suggesting that the decomposition rate can increase by increasing temperatures and heating rates [6]. The glycosidic bonds can also be broken by the use of alkali metals at high temperatures, and by strong acids. Cellulose itself is a linear molecule, but has the ability to form hydrogen bonds to itself or from an external molecule due to lone pairs on the hydroxyl groups, making it insoluble in water. Pure cellulose within biomass can be easily extracted with high yields, in comparison to the other constituents of biomass, which are entangled within the biomass matrix.

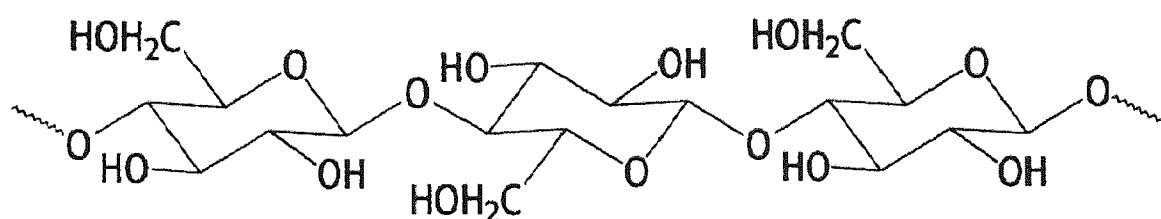
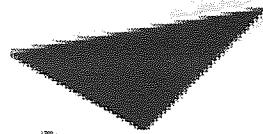


Figure 2-3 – The structure of cellulose [β -1,4 linkage]

2.2.2 Lignin

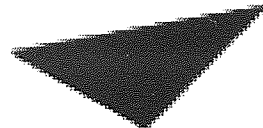
Lignin is the second most abundant organic substance in woody plants [up to 27 % as can be found in some tropical woods], but is usually the least abundant in grasses. It consists of phenolic polymers which is integrated within the cell wall of the plants, in which its main function is to give mechanical strength within the structure and aids the cells in the prevention of microbial attacks [2, 3]. The main units of lignin are monolignols, in which its phytochemical monomer varies from plant to plant and cell types [6], and due to its complexity no standard structure for lignin can be hypothesised accurately. Lignin is usually bonded to phenolic esters [4-hydroxycinnamic acids, p-coumaric and ferulic acids] via covalent bonds, at which its main purpose is to act as an adhesive between the lignin and cellulose structures [shown in Figure 2-5]. Overall lignin structures are complex, in which where specific carbohydrates are linked by the glycosidic bonds in a random unorganised structure [3]. Three types of lignin are present within grasses which are the (H) hydroxylphenylpropane, (G) guaiacylpropane and (S) syringylpropane and are shown in Figure 2-4. Lignin can be isolated by numerous ways from biomass via wet chemistry at which the most common method used is the Klason/ADF, in where sulphuric acid [or any strong acid] is applied to the biomass to hydrolyse the cellulose and hemicellulose. The remaining residue from the biomass/sulphuric acid mixture is of lignin, at which the original structure has not undergone major distortion due to the acid [6]. Since the monomers of lignin are aromatics, a greater temperature is required to decompose the structure during pyrolysis and produce the lignin derived compounds [12].



Aston University

Illustration removed for copyright restrictions

Figure 2-4 - S, G and H monomers of Lignin present in Grasses [10, 11]



Aston University

Illustration removed for copyright restrictions

Figure 2-5 – The lignin structure within beech wood [2]

2.2.3 Hemicellulose

Hemicelluloses are non-cellulosic polysaccharides and are made from pentosans [5 carbons rings, e.g. xylan and arabinan] and hexosans [6 carbons rings, e.g. mannan and galactan]. They act as a supporting substance within the cell wall of the plant, similar to that of cellulose [2]. It is usually found in the secondary cell wall and is entangled with the aromatic polymers

[lignin] as it is cross linked within the matrix of the plant structure. However, they portray a branch structure rather than a linear structure due to the differences in monomers. Due to the monomers of hemicellulose being different to that of cellulose [Its branched nature renders hemicellulose amorphous], they do not possess the same chemical and physical properties. Hemicelluloses are more aqueous soluble, and less resistant to chemical and temperature degradation [5], as it can be hydrolysed by weak acids and be completely degraded within the temperature range of 240-300°C. It is virtually impossible to isolate hemicellulose without modifying its structure, thus synthetic models have been made [10, 13].



Figure 2-6 – The structure of Hemicellulose [3,4]

2.2.4 Inorganic components

The inorganic constituent within biomass which forms the ash, can have a concentration of up to 1.5% of dry mass, and has up to 19 minerals [2]. These include complexes of the following Si, Ca, K, Na and Mg, in addition to smaller amounts of P, Fe, Mn and Al and the mineral content varies throughout the plant but are necessary for plant growth [2]. The micro nutrients are Fe, Mn, Zn, Cu, B, Mo, Cl and Ni, which play a key role in enzyme catalysis within the plant metabolism. This is reviewed in Chapter 3.

2.2.5 Pectins

Polysaccharide pectins are found in the middle lamella and the primary cell wall of dicotyledons and consist's up to 50 % of the cell wall. Pectins are similar to gelling agents, in which its structure is of a linear chain of α -(1-4)-linked D-galacturonic acid and methylgalacturonic acid residues [2, 3]. One of the main functions of pectin is to help the plant

to bind cells together and regulates water within the plant structure, and to act as a thickner as well as a stabiliser. As the plant grows the amount of pectins differs at different parts of the plant, and as the pectin within the plant reduces, the plant becomes softer due to the weakening and breaking of the cell wall. These are insignificant in the context of this thesis.

3 THERMAL DEGRADATION THEORY

Biomass pyrolysis is the thermal degradation of biomass under an inert atmosphere in the absence of oxygen. The products produced from the thermal degradation of biomass are of high and low molecular weight organic compounds. This chapter reviews basic chemistry polymer degradation reactions and mechanisms, as well as giving a literature review on the fundamental work carried out on cellulose and other biomass components under pyrolysis. Other pyrolysis related work which is relevant to this investigation has also been included in this research.

3.1 Background knowledge

In the past ten years there has been a growing interest in fast pyrolysis to produce pyrolysis-oils [14]. The pyrolysis-oils can be used as a transport fuel in diesel engines or as a source of chemicals. The main products from biomass fast pyrolysis are volatiles [which are quenched to produce organic oil], gas and char, and has the advantage of obtaining high yields of pyrolysis-oil. Figure 3-1 shows a typical mass balance of biomass fast pyrolysis.

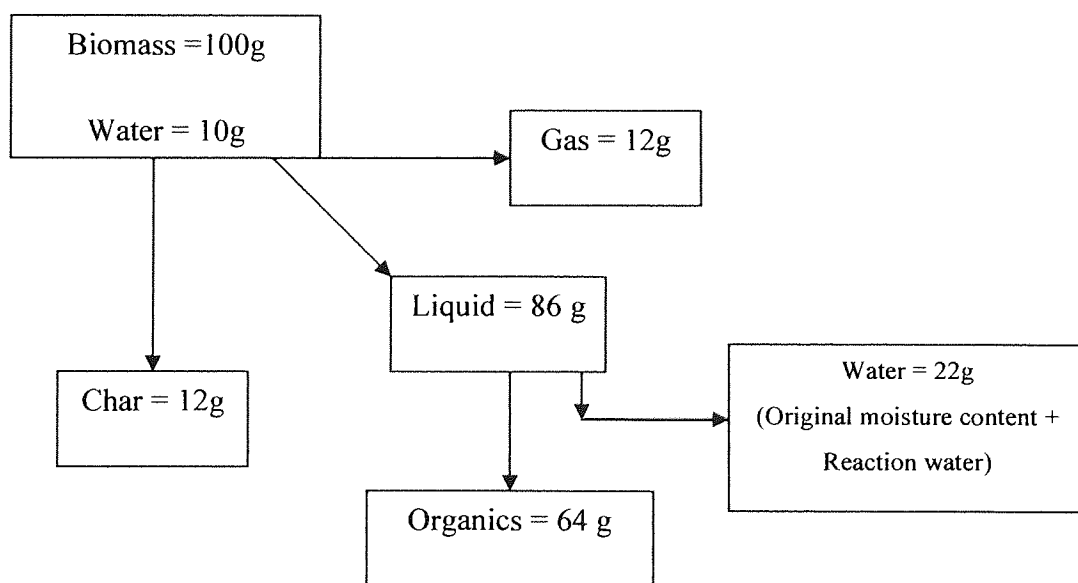


Figure 3-1 – Typical mass balance of wood fast pyrolysis

Thermal degradation has been used in the past for polymers in order to identify the stability of the polymer, and identifying potential uses for its fragments. They can either be used for further reactions or chemical production. However biomass has become more commercialised, as growing concerns of the environment have been raised as industries move towards renewable sources of energy to reduce their carbon emissions.

Dry biomass requires an input energy of 2 MJ/kg for pyrolysis if heated to 500°C; however biomass which has moisture might require higher energy inputs of 3.5 MJ/kg. This implicates that more energy is required to remove the moisture and increase the overall heating requirement for the process. The moisture which is present in the biomass [if not removed] ends up in the pyrolysis-oil after fast pyrolysis [1]. The main elemental groups present in biomass are polysaccharides and carbohydrates which possess C, H, O and N elements. The different bond within the structure suggests that different parts of the biomass have different stabilities.

The volatiles derived from biomass are evolved within the temperature range of 200-450°C, which suggests that the decomposition of cellulose contribute to the majority of the volatiles. The derived organic compounds are then condensed to produce a micro-emulsion in which the continuous phase is an aqueous solution of holocellulose [The sum of cellulose and hemicellulose content] products that stabilises the discontinuous phase of pyrolytic lignin through mechanisms such as hydrogen bonding [15]. Replacing aliphatic covalent bonds with aromatics will increase the thermal stability to a higher temperature of 450-600 °C, but is likely to form a greater yield of char as well as reducing the yields of the volatile [16]. It was found by Uzun et al [17] that biomass particle sizes and heating rate of pyrolysis effects the yields of char and volatiles.

3.1.1 Slow pyrolysis

Slow pyrolysis has been used in the last thousand years to produce chars, methanol/ethanol and tars in furnaces [18-20]. Slow pyrolysis is less energy intensive than fast pyrolysis as low temperatures and heating rates are used, to promote secondary reactions to produce high levels of char and gas. The requirements of slow pyrolysis are:

- Atmospheric pressure

- Low heating rates ranging 0.01°C/s to 2°C/s
- Reactor temperatures of 200-400°C
- Low rate of evolution of volatiles from biomass [minutes to hours]
- Residence times of minutes, hours or days for particles or long solids

Char, volatiles and gases are produced in approximately equal mass proportions due to slow degradation and secondary reactions of the vapours [cracking].

3.1.2 Fast/flash Pyrolysis

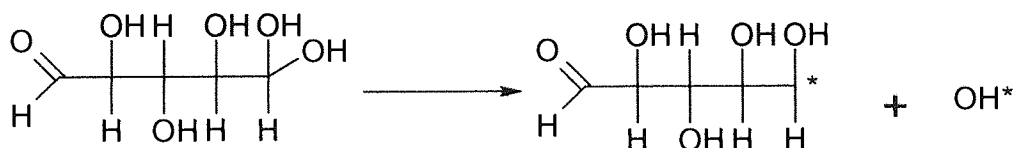
In the early 1980's a distinction between fast and flash pyrolysis was created, but the gap between the two phenomena's disappeared as research developed in pyrolysis. Many researchers have realised that there is no difference between them and the term flash is becoming more abandoned and is adopted as fast [23].

The requirements of fast/flash pyrolysis are:

- Atmospheric pressure
- high heating rates of 10 °C/s to 10⁵°C/s
- Reactor temperatures of 450-550°C
- Fast rate of evolution of volatiles from biomass
- Residence times of 0.5-2 sec for volatiles to maximise high organic volatiles to maximise liquid yield [21,22,24].

3.2 Common compound degradation mechanism literature review

Degradation of polymers via pyrolysis is caused by the dissociation of chemical bonds to form free radicals. Free radicals are a single unpaired electron on an atom or molecule, due to the dissociation of the atom/molecule, and are usually due to UV light providing enough energy to break the bond [30]. It has the characteristics of being very reactive, and can react with any other surrounding molecules to break, add or reform the molecule. Free radicals are different to that of ions due to its unpaired electron, while ions tend to gain or lose an electron in the aid of the formation bonds, thus making the atom/molecule positive or negatively charged [30]. The major products due to degradation are monomers, dimmers and trimmers. The fragmentation depends on the type and strength of the chemical bonds, and the stability of fragment molecule. Long carbon chain tends to break in random fashion to produce smaller molecules similar to its parent molecule. The free radical reaction mechanism takes place when there is a covalent bond within a structure and is broken to form 2 free radicals. i.e. free radical initiation for glucose.



Equation 1-Free radical initiation of Glucose

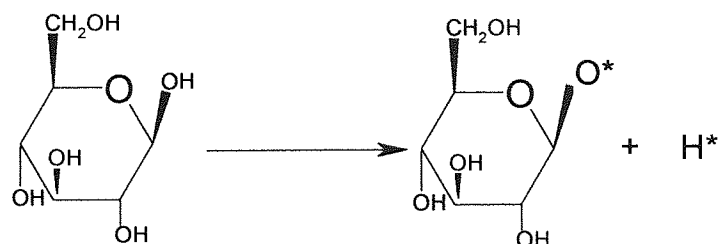
Free radicals are usually formed by breaking the weakest bond in the compound during the pyrolysis degradation process. The composition fragments will depend on the stability of the free radicals to form the fragments.

3.2.1 Depolymerisation radical reaction mechanism

There are various radical reactions

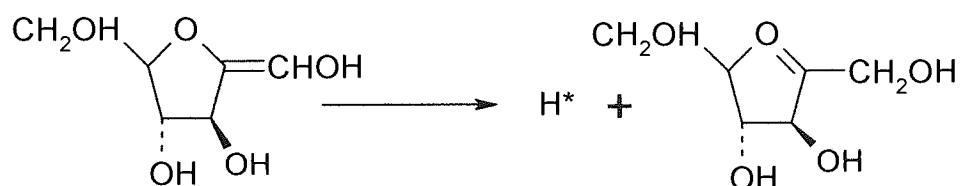
3.2.1.1 *Initiations steps*

Random scission



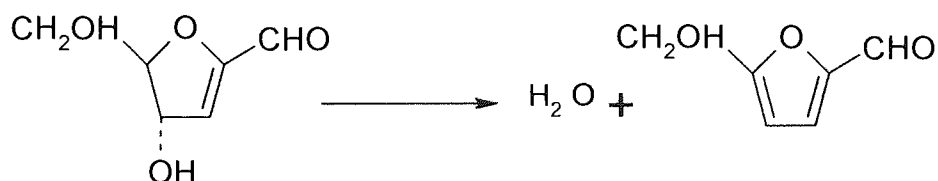
Equation 2 - Random scission of Glucose

This is the most common scission process, where a long chain molecule is broken into a distribution of small molecules. If all the bonds in the chain have the same strength there is no reason for one singular bond to break more intensively than other, suggesting that a wide arrangements of small molecules would be produced [25]. If the free radical dissociates a hydrogen atom from within the molecule, then that specific chain will form a unsaturated bond [double bond], thus creating a free radical on its fragment. The most common of this situation is known as the beta scission. i.e.



Equation 3 – Random Beta scission

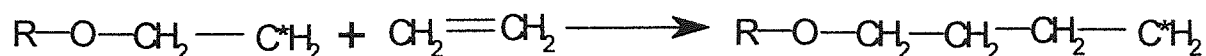
The scission of weak bonds follow the same principles of random scission, but some carbon bonds within the original molecule will have less strength in comparison to the rest of the bonds, thus breaking with less energy and dissociating it from the rest of the structure. When certain species are pyrolysed, no set oligomeric pattern can be observed, and volatiles can be produced as a result. An example of this is dehydration of 5-hydroxymethyl-2-furaldehyde formation.



Equation 4 - Random scission for the formation of water, as in the example of 5-hydroxymethyl-2-furaldehyde formation

3.2.1.2 Propagation

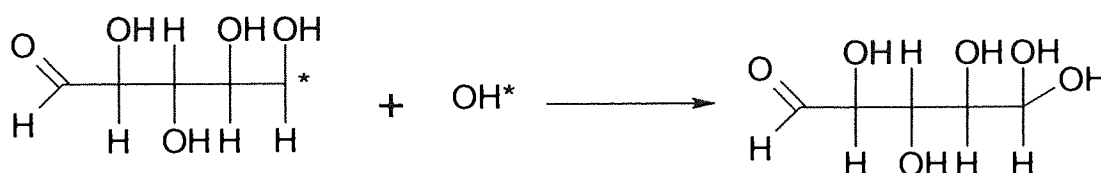
Propagation occurs when the free radical produced attacks another molecule, and either re-configures that molecule or the two molecules combine together to form a new molecule which is higher in molecular weight.



Equation 5 – Propagation from the alkenes to alkanes [straight carbon chains]

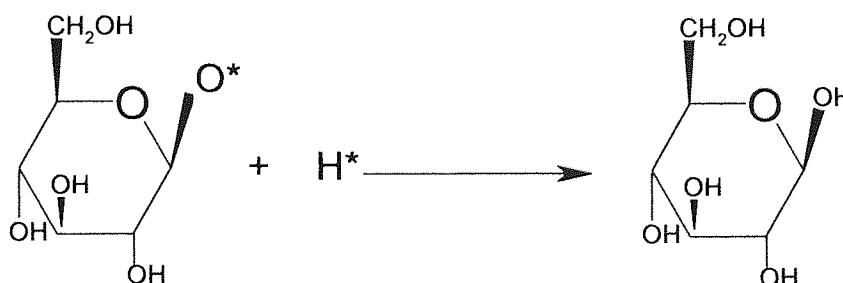
3.2.1.3 Termination

There are 2 types of termination which can occur within chemistry. The first termination is called the first order monomolecular, while the second termination is known as the second order bimolecular termination. The termination step is dependant on the number of molecules present for termination as well as there stability during the intermediate step. The 1st order monomolecular termination unzips the monomer to end the chain with volatilisation of radicals.



Equation 6 – First order termination to form Glucose

The 2nd order bimolecular termination.

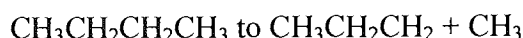


Equation 7 - Second order bimolecular termination on glucose

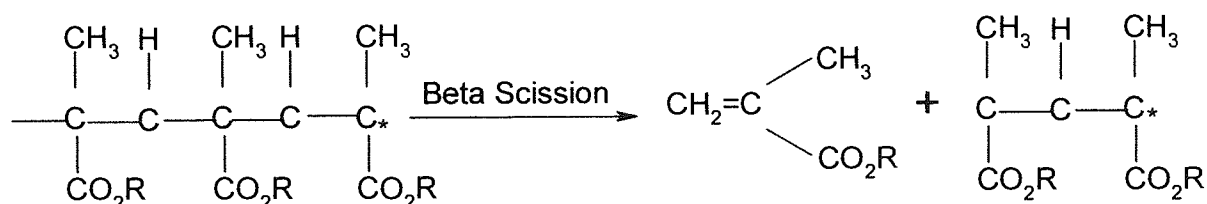
Every act of random scission produces two smaller chains unless the depolymerisation is followed by unzipping of the monomer to the chain end [25]. There is no change in molecular weight in random scission; however a drop in molecular weight can be achieved if the random scission occurs in the presence of free radical termination.

3.2.2 Monomer reversion

An example of polymer to monomer scission is shown below:



Monomer production occurs from a long chain by the use of beta scission which continues with copolymers leading to the production of two monomers/compounds having the original polymerisation ratio [16]. i.e



Equation 8 - Beta scission [volatile evolution]

Scott and Halling et al [28] investigated the chemical mechanisms behind pyrolysis-oil production from cellulose. They gave a detailed explanation for the derivation of cellulose chemicals, and suggested that temperature and metals have an effect of the degradation of cellulose. As temperature increases the cellulose degrades via fragmentation [ring scission] to form hydroxyacetaldehyde, while at lower temperatures the cellulose polymers depolymerise [unzip] to produce levoglucosan. However some researchers suggest that hydroxyacetaldehyde can also be formed from the levoglucosan once scission has taken place [6, 10, 26-28].

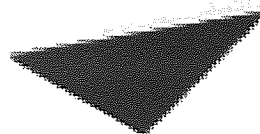


Illustration removed for copyright restrictions

Figure 3-2 – Waterloo's proposed mechanism of fragmentation and depolymerisation of Cellulose Monomers [6, 26, 29]

The Waterloo model [Figure 3-2] shows the cellulose free radical competing mechanism of depolymerisation and fragmentation pathways. The depolymerisation leads to the breaking of the glycosidic bond between the cellulose monomers. Fragmentation occurs at higher temperatures than depolymerisation, and cracks the glucose unit in the cellulose polymer. Other mechanisms such as ionic reactions can be used to understand how certain compounds are also formed [enol and aldehydes] via substitution E1 (S_N1) or E2 (S_N2) pathways for lower molecular weight compounds below 400°C [7, 30-34] .

3.3 Pyrolysis compound mechanisms

The steps involved in the chemical degradation of biomass, is extremely complicated, as many reactions undergo in few seconds. However due to the study of chemical degradation of polysaccharides, an understanding is formed and applied to biomass, due to the leading component in biomass being cellulose. Many researchers such as El Khadem, Boon and M. Antal Jr. [7, 33, 34] were able to explain why some cellulose derived products were made as well as giving possible pathways and reactions. It is suggested that low molecular weight compounds formed below $<400^\circ\text{C}$ are carried out by ionic reactions in the presence of water from dehydration, while larger molecular compounds $>400^\circ\text{C}$ are due to free radical reactions.

3.3.1 Levoglucosan formation

Two mechanisms for the formation of levoglucosan were expressed in literature; the first method is the rupturing [homolytically] of the glycosidic linkage, then depolymerisation occurring via free radicals. The second mechanism is the transglycosylation mechanism which is carried out by depolymerisation followed by a carbonium ion intermediate. Both mechanisms use cellulose [repeated monomer of glucose] as the original reactant to configure its structure until levoglucosan is produced. The two mechanisms can be seen in Figure 3-3, and shows other intermediate products which can be produced from both of the mechanisms.

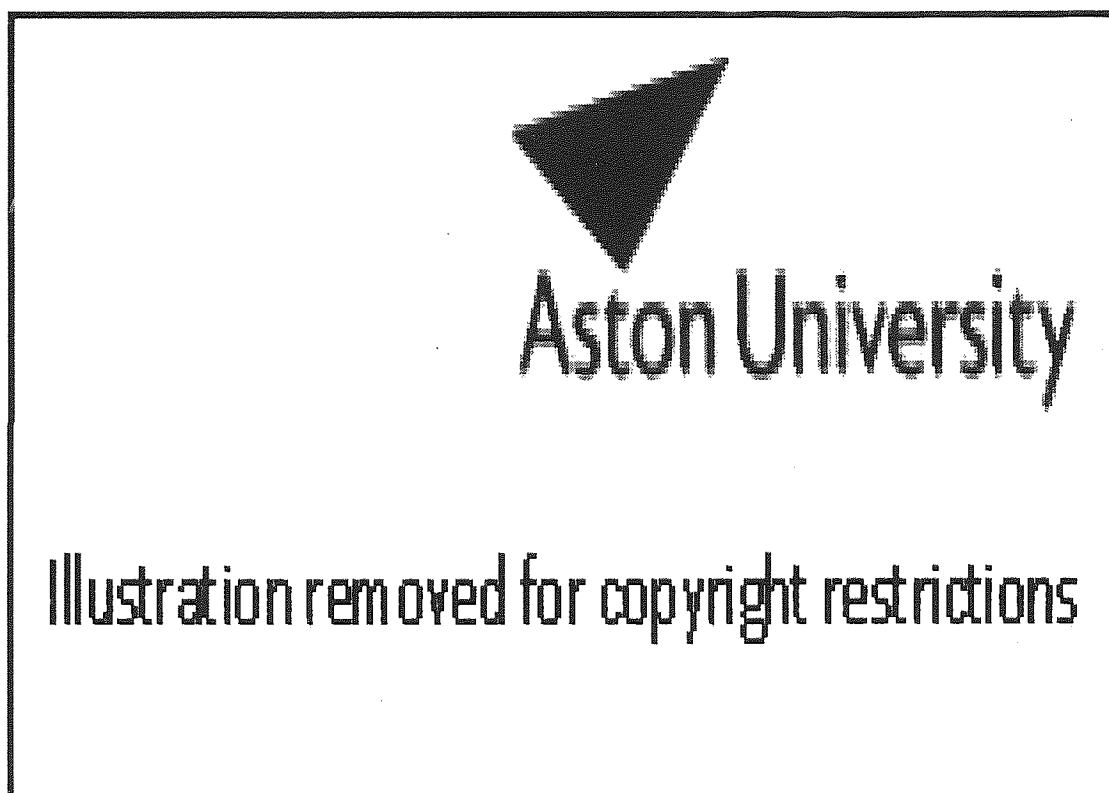


Figure 3-3 – Products derived from Cellulosic glucose including pathway [7, 33]

3.3.1.1 *First mechanism*

This method of free radical reactions was first found by Golova in 1957 and he suggested that the production of levoglucosan has two stages, first being the reduction in DP to about 200 followed by a rapid decomposition via free radicals by breaking the end monomeric unit.

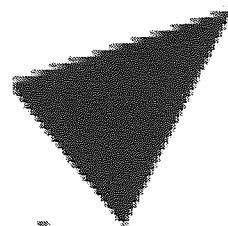
Madorskey contemplated this mechanism with his theories of dehydration with thermal scission of the CO bonds [7]. This mechanism was proven by two other researchers named Arthur and Hinojosa and found that the free radical formation occurred at 250°C, and the cleavage of the 1-4 glycosidic link to form the scission. The researchers concluded that the mechanism which is the rupturing of the glycosidic bond and then thermal depolymerisation via a free radical, and that the hydroxyl group on the methoxyl branch attacks the lone pair of electrons on the oxygen from the ring scission. The molecule then begins to rearranging to form levoglucosan.

3.3.1.2 *Second mechanism*

The second mechanism was found by Kilzer and Broido via heterolytic bond cleavage to form the levoglucosan molecule. They suggested that levoglucosan production was due to a concerted displacement, which resulted in a formation of 1, 4 anhydro alpha D glucopyranose which then rearranges to form levoglucosan. A series of pyrolysis experiments by the use of hexoses and other derived polysaccharides were used to prove this theory. Two modes of reaction can occur depending on the pyrolysis conditions, and the scission of the glucose monomer. The first mode was the formation of the 1, 4 anhydro unit which rearranges itself to form levoglucosan or furfural. The second mode ends with lower molecular volatiles [carbonyl compounds] or condensable products of char by an irreversible carbonium ion mechanism. Levoglucosan yields and other cellulose products was intensively researched by Shafizadeh which back up many other researchers work on the production of cellulose derived compounds.

3.3.2 5-hydroxymethyl-2-furaldehyde formation

The formation of 5-hydroxymethyl-2-furaldehyde from glucose and aldohexoses was found first by Regal and Gaset. High yields of this compound was produced in the temperature range of 175-290°C in the presence of acidic resins. Figure 3-4 shows the structure of a glucose monomer picking a de-protonated H atom to form water as an intermediate product, which can resonate between structures [step 5] via dehydration and hydration [35]. The methodology stated in literature tends to be slow, as the continuous dehydration [loss of water molecules from the structure via hydroxyl groups] process leads to the formation of 5-hydroxymethyl-2-furaldehyde.



Aston University

Illustration removed for copyright restrictions

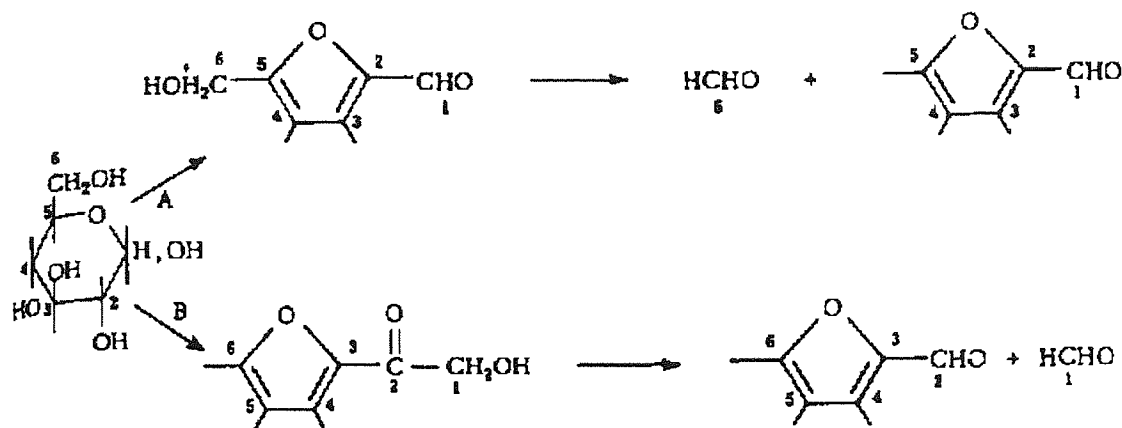
Figure 3-4 - 5-hydroxymethyl-2-furaldehyde formation by dehydration, hydration rearrangement [35]

3.3.3 Low molecular weight compound formations below 400°C

Lower molecular compounds are produced from ionic reaction followed by the dehydration to form water as a by-product. Possible products such as glycerolaldehyde, furan, and acerolyin can be produced. They follow the same mechanism of an E2 reactions where the water molecule is being added, to reform the molecule [mutorotation] to produce the products mentioned. The starting molecule which acts as the reactant, is the glucose monomer which has been broken by scission through the glycosidic bond due to the rapid heating during pyrolysis [7, 36]. The water molecule reacts with the glucose monomer to create a double bond between the C₁ atom and oxygen. Due to the electron density, either mechanisms can occur depending on its level of thermo stability. The ring eventually breaks to form the products.

3.3.4 Furfural formation

Furfural formation from the glucose monomer has two competing pathways. Path A is a simple two step dehydration [by the use of an acid] to produce water and a hexose ring, the continuous dehydration eventually produces the furfural compound. Path B is also a dehydration mechanism to form a carbonyl group [C=O] which the carbon atom is bonded to the hexose ring with a methanol side branch [18].



Equation 9 - Furfural formation by two competing pathways [34]

3.4 Literature review

3.4.1 Characterisation of biomass via pyroprobe-GC/MS

Pyroprobe-GC/MS has been a useful technique to identify compounds which are released during pyrolysis of biomass. O.Faix, D.Meier and I.Fortmann [37-40] have written a number of papers on the thermal degradation products of woods, polysaccharide and wood lignin. They identified 82 lignin derived products 104 derived polysaccharides compounds from pyroprobe-GC/MS; in which all the compounds had specific retention times and Mz. Bremer [41] investigated the volatile contents on lignin and cellulose for different kinds of woods by the use of pyroprobe-GC/MS, by assigning which compounds came from what constitute. It was determined that the subtraction of lignin and cellulose derived compounds from the biomass pyrograms would be suitable for identifying what compounds are derived from hemicellulose.

It was shown by Alves that products derived from pyrolysis could be related back to its original constituents even at low levels [42-44]. J.Rodrigues and D.Meier [45] found that the lignin compounds [monomers S and G] from eucalyptus wood in different proveniences could be identified by pyroprobe-GC/MS and then summated to form areas for the ratio between S/G. It was found that tree provenance varied the S/G ratio significantly with up to 51 % variation relative to the mean. Further work was carried out by JC del Rio and A.Gutierrez [46, 47] as they investigated the degradation of eucalyptus wood to form relationships between the S/G lignin [G-4-hydroxy, 3-methoxyphenyl & S-4-hydroxy, 3,5-dimethoxyphenyl] present in the biomass. A correlation was produced between the yields and the ratio of S/G present in the wood; however a relationship between the lignin/carbohydrate ratios against the yield was unsuccessful. It was clearly seen that individual derived compound from pyrolysis could not be used for relating traditional wet methods of lignin analysis. A second paper was also produced to form a relationship between the S/G against fungi present. It was observed that a decrease in wood lignifications was due to the breaking of ether linked S lignin and enriched G lignin.

B.Scholze and D.Meier [48] reviewed the various yields of pyrolytic lignin by the use of pyroprobe-GC/MS characterisation and Fourier transform infra red. 40 peaks were identified and 9 wavelengths were taken into account which led to the overall conclusion of the investigation. D.Meier and I. Fortmann [49] used pyroprobe-GC/MS peaks to identify and quantify compounds by the use of multi-variance PCA model [Principle Component Analysis] to form relationships between the pyrolysis products and the different wood clones. The use of PCA allowed to discriminate between the genetically modified poplar clones. D.Fabbri and F.Sangiori [50] showed the effectiveness of semi quantitative pyroprobe-GC/MS analysis as they produced a rapid screening method for identifying organic matter in marine sediment, while the chemical alteration of lignocelluloses was investigated by M.Hernandez et al [51]. It was found that the G lignin unit decreases as incubation periods increased. A similar experiment conducted by J.C. Franchini et al [47] were the changes in organic compositions of crop residue. They found that the incubation time affected the relative lignin content by increasing at the expense of the polysaccharide. The characterisation of biomass and other related lignocellulosic materials via analytical pyrolysis has enabled qualitative and quantitative analysis for progression in the study of pyrolysis mechanisms and degradation.

Evans and Milne [52, 53] carried out a number of experiments on free jet molecular beam mass spectroscopy (MBMS) to produce a real time analysis of product evolution for primary, secondary and tertiary products from pyrolysis on a range of feedstocks so that molecular pathways can be determined, for obtaining a greater understanding of fast pyrolysis of biomass. They stated that cracking was reduced significantly at an optimum temperature of 500°C. A list of derived products from biomass pyrolysis [separated in the order of evolution] allowed cellulose pathways to be determined. Evans and Milne suggested that lignin also undergoes depolymerisation due to metals but is greater seen in carbohydrates. Pyrolysis-oils were also analysed by MBMS and suggested that particle size, moisture content and heating rates to produce these oils have only secondary effects on the composition of the oil although the yield varies dramatically.

3.4.2 The effect of metals

Shafizadeh was one of the pioneers in investigating the effect of metals on cellulose by the use of fire retardants [54]. He concluded that the alkali metals especially sodium and potassium effects the degradation of cellulose and derived product yields of low and high molecular weight compounds. Camarero et al [55] investigated wheat straw treatments with magnesium oxidising peroxides. The experiments showed changes in the ratio between the lignin monomers. After enzymatic treatment it was found that there was a decrease in the derived compounds from the S-lignin, and an increase in the H-lignin. Simkovic et al [56] investigated the differences in composition of the degradation products of starch by thermal degradation with and without 3-Cholo-2-hydroxypropyltrimethyl-ammonium chloride. The results also showed that the degradation products were different. I.Tanczos et al [57] carried out similar experiments as they reviewed the affect of two bases (tetramethylammonium hydroxide & NaOH) on cellulose by the use of TG-MS and pyroprobe-GC/MS. It was found that both bases decrease the temperature of decomposition with increasing concentration of lower molecular weight compounds, but both bases gave different decomposition patterns. It was identified that common compounds were found between the degradation of both bases such as cyclopentenone and 2-hydroxy-3methyl 2-cyclopente-1-one suggesting that both bases aid hydrolysis and methylation. It was also found that less char was formed than the cellulose impregnated with NaOH, which agrees with many pyrolysis theories reported in the past, that alkali metals such Na has a major impact in degradation. Szabo, Varhegyi, Till and Faix [58],

investigated different herbaceous grasses to explore the thermal degradation of each specie as well as looking at secondary tar cracking. Their work showed that the char formation can be reduced significantly by using smaller particles, and by the removal of the salts. They showed that low molecular weights were given off as a function of temperature and pressure, suggesting that there was more cellulose than lignin in the species. It is found that acid washing affected both grasses as the peak temperatures and char yields both deviated from its original trials.

An intensive research was carried out on biomass washing [pre-treating] by Hsisheng and Chou Wei [59]. They agreed with previous researchers that washing removes water soluble materials, by reducing its mineral matter and ash content, which intern increased the volatile yields from pyrolysis. It was also reported that cellulose and hemicellulose are responsible for volatile products while lignin are responsible for the contribution to char. This paper also agreed with K.Raveendran, Anuradda Ganesh & C. Khilar [60] which looked more specifically on the alkali metals on biomass such as potassium, sodium and silicon. Their results agreed with the findings from Tanczos, Szabo, Varhegyi, Till and Faix as they reported an increase on the maximum rate of devolatilisation and initial decomposition temperature as metals were removed. These investigations led to a good agreement that inorganic species present in the biomass influences the mechanism and yields of volatiles [61-67]. 16 milled wood lignin [hardwoods and softwoods] were examined with the effect of $ZnCl_2$ and $NaCl$ by E. Jakab, O.Faix and F. Till [68]. It was also found out that softwoods were more reactive than hardwoods due to the fact that it had less methoxyl groups. However the lower the methoxyl groups, the higher the char yield produced from pyrolysis. M.Gronli & G.Varhegyi [67] agreed with the reactivity of soft woods but proved that the decomposition of hardwood cellulose is slightly faster to that of softwood, but clearly stating that the methoxyl groups are found on the wood lignin rather than the cellulose, suggesting that the reactivity of the lignin will be different to the cellulose of the same species. The findings from previous researchers on the effects of metals on pyrolysis of biomass clearly show that metals [especially alkali metals] present in the biomass have an effect on the degradation of pyrolysis, temperature of maximum volatilisation and yields of compounds.

3.4.3 Cellulose and biomass pathway models

To date there are many proposed models and mechanisms for the degradation of cellulosic materials. The aim of a mathematical model is to give a solution for a selected input variable [independent/dependant] which represents the process in question. The main concern in pyrolysis modelling is to identify the affects of the variables on the interaction between volatiles to give a prediction on pyrolysis product yields. The research in this field is essential in pyrolysis development as it aids to develop, optimise and establish reactor designs and conditions.

The first models used for pyrolysis were not based on biomass, but on cellulose. In 1956 Madorskey et al [26, 69] first proposed a simple mechanism [Figure 3-5] in which cellulose had two competing pathways which are dependent on temperature, [below 280°C gave rise to volatiles and water, while above 280°C produced tars].



Aston University

Illustration removed for copyright restrictions

Figure 3-5 – Madorskey et al., proposed the first model for cellulose [69]

Twenty years later Shafizadeh [8, 69] [Figure 3-6] realised that the volatiles are strongly affected by ash and the degree of polymerisation, which were are all dependant on pyrolysis temperature. The Broido and Shafizadeh mechanism suggested that cellulose forms a liquid layer known as the “active cellulose or depolymerised cellulose”, without any notable mass loss, and was later proven by Peacocke [14].

Illustration removed for copyright restrictions

Figure 3-6 – Shafizadeh proposed the modified version of his original model, showing the debated Active state [7, 33, 70, 71].

Towards the 1990's the work by Piskorz et al [26] agreed with Shafizadeh about secondary decomposition of volatiles on the degradation of levoglucosan, and gave a detailed account to all the product distribution of cellulose pyrolysis degradation which accounts for all of the effects including ash and degree of polymerisation.

Work was also carried on hemicellulose and lignin, but not as extensive as cellulose as these components can not be extracted naturally without modification to the original structure, so proposed synthetic models were experimented on. Antal et al [72] proposed a mechanism for lignin which is similar to the pathway of cellulose which included the secondary degradation of the monomer which gave high molecular weight compound volatiles.

Wood pyrolysis has also been investigated, but including mechanisms that are extremely complex and which takes into account such variables as heating rate, temperature and pressure. Evans and Milne [26] developed an accurate model which also adopted the active cellulose and rephrased it to "the active biomass", but they could not prove that at low pressures the biomass would undergo the active liquid state. In the past twenty years four major models were proposed, based on kinetic and stepwise.

Di Blasi [73] based her work on kinetic modelling which took into account the activation energy and rate constants which were obtained via analytical pyrolysis. However it must be

stated here that kinetics data vary from one another due to the nature of equipment, material and conditions used. Later developments in this field allowed such researchers like Di Blasi, Gronli and Galgano to investigate pyrolysis modelling on large biomass particles [74-84]. In spite that they all produced essential results; their results represent a small part of the overall question that needs to be addressed for fast pyrolysis modelling. More accurate models would consider 2 and 3 dimensional analysis and removing some of the assumptions stated in her works [such as constant activation energy and constant wood properties] so that terms can be included to obtain a more accurate solution to the problem. The methods of kinetic modelling developed are sufficient for analytical pyrolysis with mg samples of particle sizes less than 100 μm . However if one wants to investigate larger particle size, with a better representation of fast pyrolysis, kinetic data must be used in conjunction with mass and heat transfer equations which would take into account physical and chemical changes. Liden and Diebold [27], were the first to carry out this reaction pathway models on biomass with use of kinetic modelling [Figure 3-7], followed by Gorton and Knight [100] who also proposed another model, but was critically reviewed by other researchers as not a predictable model for volatile yields.

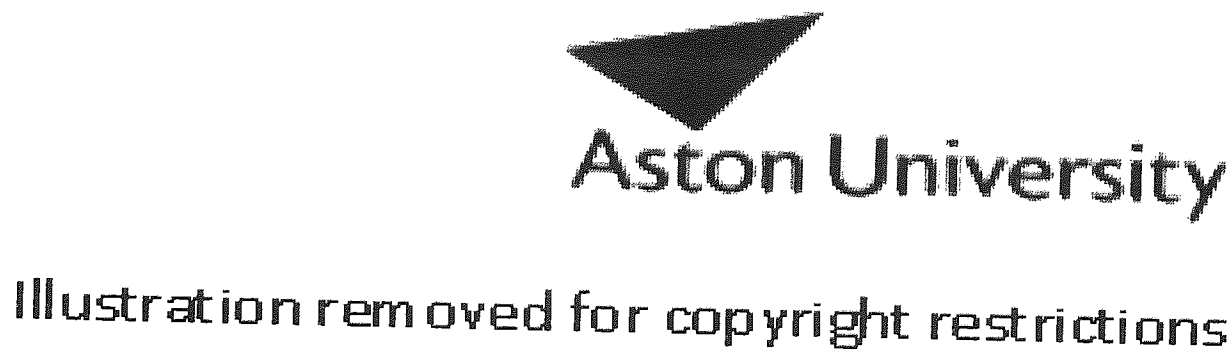


Figure 3-7 – Reaction method used by Liden et al and Diebold [27, 86, 100]

Antal et al [67, 72], followed the footsteps of these researchers and produced a more complex mechanism model where secondary gas phase decomposition is taken into account [Figure 3-8].

Illustration removed for copyright restrictions

Figure 3-8 – Antal's reaction mechanism for volatile decomposition [9]

It has been shown that kinetic modelling is simpler than fast pyrolysis modelling [as it ignores heat and mass transfer effects] as it simplifies the overall kinetic parameters but varies from condition to condition depending on the situation. Overall kinetics data do not predict the yields or behaviour of the feedstock, only on the data which it is based on. Fast pyrolysis has many issues to be taken into account such as fast heating rates, larger sample sizes, no control of sample heating, sample temperatures factors which make modelling more difficult. Nevertheless as far as slow pyrolysis is concerned mass transfer effects can be ignored.

Scott and Halling et al [26-28] investigated the chemical mechanisms to produce pyrolysis-oils from cellulose based on the effect of temperature on cellulose derived products. It was found that two major competing path ways exist, one being the formation of a higher molecular weight compounds like levoglucosan [1, 6 anhydro β -D glucopyranose], while the other being low molecular weight compounds like hydroxyacetaldehyde. They concluded that at higher temperatures cellulose favours the pathway to produce more hydroxyacetaldehyde than levoglucosan. This was explained by thermal degradation theory previously via fragmentation [ring scission] and polymer depolymerisation [unzip] as explained in section 3.2. However some researchers suggest that hydroxyacetaldehyde also can be formed from the levoglucosan once scission has taken place. Further research continued to modify the mechanism to include alkali metals for a more comprehensive model, which is shown in Figure 3-9.

Illustration removed for copyright restrictions

Figure 3-9 - The Waterloo Model for Cellulose Decomposition [6, 29]

This model demonstrated that pyrolysis reactions can be improved at lower temperatures, with the removal of alkali metals to undergo depolymerisation reactions to produce higher molecular weight cellulose compounds.

3.4.4 Hemicellulose pyrolysis

The main authors who carried out work on hemicellulose are Ramiah [87], Williams and Besler [88] and Varhegyi et al [89, 90]. However no global reactions pathways or mechanisms are addressed in this thesis.

Hemicellulose is less abundant than any other component in biomass and degrades at lower temperature than any other component at 150°C-350°C. It gives a high yield of furan derived products as it undergoes fragmentation rather than depolymerisation [21] and contributes to higher levels of char, water and acetic acid during pyrolysis due to its high reactivity. Soltes and Elder [91] suggested that hemicellulose decomposition undergoes a two stage process. The first stage is depolymerisation to water soluble fragments, and the second stage is the decomposition of volatile components. Varhegyi et al found that xylan [component of biomass] degrades at around 200°C and the presence of methanol and 2-furaldehyde in the products [83]. They suggested that the reactions were occurring from the alpha-glycosidic bonds as the beta-glycosidic bond is higher resistant to temperature. Varhegyi et al. also proposed that the formation of 2-furaldehyde at low temperatures of 250-350°C was due to

dehydration of pentose units which were from the uronic units by decarboxylation. Dehydration reactions also form moieties having double bonds, carbonyl groups and conjugated double bond carbonyl groups [92]. The moieties are thought to rearrange, condense and fragment to generate CO and CO₂, formaldehyde and other chemicals such as acetic acid [92].

3.4.5 Lignin pyrolysis

The mechanisms for lignin degradation are still relatively unknown in comparison to cellulose degradation due to the lack of knowledge of the structure. The lignin component in any type of biomass is the most stable as being an aromatic structure. The work carried out on lignin has been based on model compounds in order to mimic degradation pathways during pyrolysis.

An overview of the structure, for biochemical synthesis of lignin and other components of the grass plant cell wall were recently described by Boerjan et al. 2003 [93]. From the three main types of lignin, the [H] type monomer is less abundant in grasses [2] but can still be identified by pyroprobe-GC/MS [37-40, 45] [94]. Most of the mass weight in grass cell walls is composed of polysaccharides. Kleen [95] found that calcium and sodium changed the lignin pyrolysis degradation pattern by allowing for demethoxylation, demethylation and dehydration to occur in the degradation of lignin especially for the guaiacyl monomers. The increase of sodium increased compounds such as phenol, guaicol, coniferyl alcohol and 4-vinyl guaicol, while the untreated products were rich in eugenol and 4-methyl guaicol suggesting that sodium enhances demethylation rather than demethoxylation which back up previous findings by Jakab et al [96]. They also stated that hydrogen and calcium ions were beneficial to anhydrosugars yields from pyrolysis, but the majority of lignin products were overall less influenced by metals.

From TGA analysis of lignin, minor decomposition begins at 240°C, but it is stated that higher temperatures are required to degrade the lignin component [33, 97, 98]. Compounds like coniferyl alcohol and sinapyl alcohol come off at higher temperatures being higher in molecular weight thus requiring a higher energy to break the bonds within the structure and usually occurs in the early stage of pyrolysis by the formation of double bonds.

The research splits lignin pyrolysis into two categories, lignin degradation below 600°C and above 600°C. These are highlighted below:

3.4.5.1 Lignin pyrolysis below 600°C

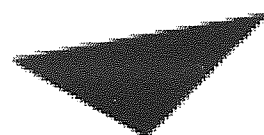
Research in lignin pyrolysis below 600°C has been investigated by numerous researches across the world from different institutions [33, 99-107]. As well as work carried out on Kraft lignin that is used in the paper industry in which Jergers and Klein identified and quantified 33 main products from lignin including guaiacol, cresol, methanol, and other aromatic compounds [108]. Kraft lignin research suggested that higher amounts of monohydroxyl phenolics were produced by increasing pyrolysis holding times and temperatures. Iatridis and Gavalas studied the pyrolysis of Kraft lignin at 400-700°C in which they obtained yields of 60 wt % [109], similar work was also carried out by Nunn et al but using temperatures of 330-1100°C in which they obtained similar yields [110]. From all the work carried out on lignin in which they concluded that the lignin contributes to char formation and withstanding greater temperatures resistance due to the aromatic ring [70, 88] unlike the polysaccharides which degrade further under high temperature producing lower yields of organics.

3.4.5.2 Lignin pyrolysis above 600°C

Lignin pyrolysis above 600°C leads to a complex and incoherent cracking and dehydrogenation, condensation, polymerisation and cyclisation reactions leading to formation of gases and low molecular weight compounds such as carbon monoxide, carbon dioxide, acetic acid and hydroxyacetaldehyde. Heavy organic compounds such as phenols, polyaromatics and benzofurans occur from secondary reactions depending on end point temperature [7, 33, 101-104, 110, 111]. Jergs and Klein proposed that guaiacol and catechol exist as an intermediate during pyrolysis and is very unstable as it can undergo coking reactions to form phenols [108] or methane formation from catechol degradation. Synthetic lignin models were used to investigate pathways of degradation and mechanisms such as Klein and Virk [112]. Mathematical models were also employed to predict levels of char and organics from pyrolysis lignin degradation and the most famous model used is the Monte Carlo simulation [113, 114]. The Monte Carlo consists of two simulations. Simulation one is compromising of the lignin structure and the other being the degradation of oligomers. The pathways used [also included kinetics data] is based on a Markov-chain based simulation of the reaction of lignin polymers which produces yields of hydrocarbons and oxygenated

compounds. Other models such as those developed by Solomon and Anvi et al [115] on lignin were purely based on the prediction of molecular weight distribution of tars. The results obtained by those models were found in good agreement with those obtained by experimental methods.

One reaction pathway has been developed and recognised for complex lignin pyrolysis is by Antal [Figure 3-10], in which it was similar to the principles used for the cellulose as developed by Shafizadeh. Antal assumed that the cellulose and lignin structures had thermally stable rings which were interconnected by ether links in which they were thermally labile during pyrolysis [92].



Aston University

Illustration removed for copyright restrictions

Figure 3-10 - Antal's proposed lignin reaction pathways in 1985 [33]

Figure 3-10 shows that pathway one, two and three occurs at low temperature with an dehydration reaction occurring if there was an increase in temperature and heating rate. This pathway forms monomers. Pathways 4 and 5 are further degradation [cracking] of the monomer if temperatures exceeded above 500°C to produce gases and refractory condensable. Antal suggested that the dehydration and decarboxylation reactions in pathway 5 are the first competitive mechanism for lignin decomposition. Pathway 3 and 6 is assumed to undergo extremely high fast heating rate where char is formed from secondary gases phase reactions. The model suggested by Antal in 1985 was controversial as it was based on the cellulose model by Shafizadeh but further work suggests that a more accurate detail pathway for lignin

degradation could be developed. The work by Nunn et al on milled wood lignin backed up some of the claims by Antal, such as pathway 5 with the formation of carbon monoxide from secondary reactions if the vapour reached 700°C [110]. Nunn et al also showed that at low temperatures below 500°C oxygenated liquids [formaldehyde, methanol and acetaldehyde] are also formed in conjunction with water leading to char yields reaching asymptotic levels at above 980 °C [92]. Nunn also showed that levels of carbon dioxide increased at lower temperatures which were also proposed by Antal's model.

In concluding the lignin degradation mechanisms and pathways, is still relatively unknown due to the variability of composition and structure from different types of biomass lignin, but is shown that the lignin pathways behave similar to that of cellulose in theory, but the process requires more experimental proof to make the hypothesis of the models reality.

3.4.6 Agronomical practice

Growing energy crops for biofuels have shown to be the best way to use surplus agricultural land in Europe for greenhouse gas mitigation [116]. Miscanthus is a potential perennial rhizomatous C₄ grass [originating from south-East Asia] which is a renewable source of biomass which could be used for combustion and pyrolysis applications across Europe [2, 117]. Miscanthus has many genotypes including M x *giganteus*, M. x *sinensis* and M. *sacchariflorus* [118], in which its quality and yield are dependant on its location, soil type and fertiliser application [119]. Field experiments at different locations in Germany have been conducted by Lewandowski [118] and showed that the plant growth and metabolism is dependant on its external physical surroundings, and variation between plots can vary significantly.

H. Schwarz et al [117] investigated Miscanthus x *sinensis* over a three year period, and concluded that the yield was maximised in year three after planting, and that the rate of nitrogen fertiliser applied had no effect on yield which agreed with NG Danalatos [120] as he found that no relationship could be found between yield and nitrogen rate. Jorgensen [121] found similar trends to the effect of nitrogen on M. x *giganteus* grown in Denmark, but also stated that potassium and chlorine levels were the lowest in spring than in winter. Foereid [122] agreed with the outcome of these experiments and also included that organic matter increases with time under Miscanthus cultivation. The mineral uptake of Miscanthus while the

plant is being cultivated effects the yield of the plant as well as the quality of the plant, however Arduini et al [123] suggested that the metals have a threshold on the effect on Miscanthus growth with his field experiments with chromium application.

A number of papers have suggested that delayed harvesting can improve the yield of Miscanthus and feedstock characteristics for its application in combustion [118, 124, 125] by reducing its water content, alkali metal and ash content. Lewandowski suggested that an investigation on the trade off analysis, between the influence of harvest date and the quality of Miscanthus, which should also include a life cycle analysis. This suggests that annual crops contains acceptable alkali metals contents which could be beneficial for combustion and pyrolysis applications [126-128].

Limited papers were found on the agronomical application on the results of combustion and pyrolysis. KO Davidsson [126] investigated the effect of alkali metal release during pyrolysis of straw, and suggested that annual crops contains high levels alkali metals which effects combustion and pyrolysis degradation. He concluded that potassium chloride and sulphur fertiliser affects the metal uptake of straw, and changes rates of degradation by lowering the temperature of maximum alkali metal release. He concluded that lowering chlorine application reduces chlorine content in the plant while potassium reduces yield. His final conclusion also stated that washing could remove the alkali metal and increases the temperature of maximum alkali metal release. This agreed with Lewandowski [129] that combustion was improved by reducing ash, moisture content and alkali metal content, as different fertiliser treatments and harvesting times were conducted on Miscanthus in Germany. He recommended that further investigation on potassium fertiliser had to be conducted, as it impacts negatively on chlorine, potassium and ash concentrations.

3.5 Chapter Conclusions

The literature survey undertaken reveals that simple organic reactions on cellulose can aid in the understanding of complex mechanisms during biomass pyrolysis degradation, to produce a wide range of derived pyrolysis products. Reaction pathways and models have been constructed in the past to describe the mechanisms behind biomass degradation, at which most of the models were based on cellulose. This was due to the fact that biomass consists of mostly polysaccharides thus the degradation of biomass would be similar to that of cellulose. From the main components in biomass, the most unexplained is lignin, due to its unknown complex structure. It can be stated that lignin degradation can have a very small part on the overall degradation of biomass. However this might not be completely true to pyrolysis-oil production and stability, as the majority of heavier molecular weight compounds present in pyrolysis-oil is speculated to originate from the lignin monomers present in the biomass. Intensive work has been carried out on the characterisation of biomass by the use of a pyroprobe-GCMS and TGA. It was shown that analytical pyrolysis has been a useful technique in identifying different types of biomass, as well as understanding the effect of degradation on cellulose and lignin. However from the research carried out on the characterisation of biomass, no evidence was found in correlating the pyrolysis derived products to the constituents of biomass [as determined by wet chemistry]. This inturn would develop an essential method for quantifying lignin/cellulose contents in biomass by the use of analytical pyrolysis.

It was found that the inorganic species present in biomass [necessary for plant growth and optimum yield] became one of the decisive factors which determine the behaviour of the biomass under thermal degradation, in which the results affect the quality and conversion of pyrolysis. The inorganic constituents of biomass can consists of more than 19 metals at which some of the metals can act as a catalyst, that can determine the rate of degradation and yield of char in pyrolysis. Many of the inorganic components are retained in the char and these can catalyse the combustion or gasification of the solid residue. It has been shown that the main metals which affect pyrolysis degradation are sodium, potassium, magnesium and silicates [6, 27, 60, 130]. Furthermore, in combustion, sulphur, sodium, chlorine and potassium in particular, influence the ash chemistry and hence dictate corrosion, slagging and fouling characteristics [6]. Shafizadeh [8] realised that the yield of organic matter to gas and char varies as the inorganic content varies, and that high levels of inorganic species promotes

secondary reactions which would break down the higher molecular compounds to smaller ones, as well as his other findings on the effects of metals on fire retardants. Scott et al [27] developed the "Waterloo model" in which cellulose has two major alternative routes for degradation depending on the amount of alkali metals present. If high levels of alkali metals are present the degradation mechanism favours fragmentation (ring scission) producing lower molecular weight compounds such as hydroxyacetaldehyde, while lower alkali metals contents promotes a de-polymerisation mechanism resulting in higher molecular compounds such as levoglucosan and beta-D-fructose. However optimum yield temperatures vary as the alkali metals in the biomass vary. Teng et al [131] carried out TGA analysis on untreated and water washed rice hulls, and found that the washed rice hull cellulose decomposition peaks occurred at higher temperatures as well as the volatile yield increasing at the expense of the char. Raveendran et al [60, 132] investigated a wide range of biomass with different inorganic species levels to produce a relationship between the change in volatiles to the potassium, zinc and lignin content. It can be seen from the literature that researchers aimed to characterise the behaviour of metals on biomass pyrolysis. The mechanisms behind product formation due to the effect metals during pyrolysis for cellulose and lignin have also shown to be scarce in the field of pyrolysis.

The relationship between the biomass components and the pyrolysis-oil has yet to be developed, as well as identifying fuel traits which could enhance the quality and stability of the pyrolysis-oil. The pyrolysis of feedstocks which have undergone different agronomical treatments has also shown to be absent in pyrolysis research. This area is important to the biomass community as it may lead to the identification of improved agronomic practices to optimize fuel which could optimise fuel characteristics for pyrolysis conversion. This research addresses these issues.

4 MATERIALS AND METHODS

This chapter reviews the materials used, analytical methods and laboratory equipment used in this research, as well as identifying process/feedstock parameters that affects pyrolysis. The analytical units used are the thermogravimetric analyser [TGA], and the pyroprobe-GC/MS. The laboratory scale fast pyrolysis units 150ghr^{-1} / 1 kg hr^{-1} fluidised bed reactors are also described with its mass balances.

This chapter investigates the preparation of the feedstock prior to any pyrolysis. This also includes any analysis to investigate the feedstock characteristics [moisture, ash, and proximate analysis]. Certain techniques and methods were used to study the stability and quality of the pyrolysis-oil from its biomass characteristics. The six reference fuels and Miscanthus agronomical crops were supplied by Rothamsted in 1 Kg bags, while the Lolium and Festuca Grasses were supplied by IGER [Institution of Grassland and Environmental Research].

4.1 Feedstock Characterisation

4.1.1 Milling and sieving

The feedstock was milled by a knife mill by Rothamsted, which had an interchangeable screen with sizes ranging from 100 micron meters to 1 cm. It is then subjected to a sieving process via a sieve shaker. Different sieve mesh sizes were used to obtain different particle size fractions. The mesh screen sieves used, allowed the particle size of a small diameter [less than the mesh diameter] to fall by a continuous shake, this enables the larger particle sizes to stay on the mesh screen and not fall to a lower particle size fraction.

4.1.2 Particle size

A detailed analysis of particle size/mass fractions can be found in Appendix I [Influence of particle size on the analytical and chemical properties of two energy crops]. It was found that different size fractions consist of different chemical properties. Smaller size fractions consist of higher ash contents, with higher metal contents in comparison to that of higher particle size

fractions. The holocellulose and lignin content differ in each particle size fraction, suggesting that plant components such as the xylem and stems are difficult to grind with a traditional knife mill, thus ending in larger size fractions with the majority of these components which includes high level of holocellulose and lignin. This indicates that the process of size reduction does not randomly reduce all different components of biomass material in a uniform manner; instead it causes partial separation of the inorganic and organic matter into different size particles [137]. This would have an affect on fast pyrolysis behaviour in terms of metal content, volatile yields, rates and temperatures for degradations [138]. For this reason all the feedstocks were within a particle size range of 250-355 microns, as it possessed a high ratio of holocellulose/lignin content. The 150 ghr⁻¹ fast pyrolysis experimental rig also used this size fraction since it was used for analytical pyrolysis and to avoid processing problems during the fast pyrolysis runs [review section 4.5].

4.1.3 Sampling

In order to obtain an absolute relationship from any analytical scale pyrolysis units, a large number of replicates must be carried out. This is due to heterogeneous of the biomass sample which is used for analytical pyrolysis analysis. A pure liquid substance would have up to a 10 % deviation from any analytical pyrolysis test [136]. A biomass sample would have a greater standard deviation, as no small sample can represent the overall biomass due to the heterogeneous of different parts of the plant as well its metals content. It was identified early on within this research, that different mass and particle size fractions would consist of different parts of the plant component, in which they would vary in its holocellulose/lignin ratio [a detailed analysis of particle size/mass fractions can be found in Appendix I, Influence of particle size on the analytical and chemical properties of two energy crops]. Samples were taken at random from the feedstock by the use of a Gilson INC. model SP-170 sample divider until a sample size of 3 mg was obtained. For pyroprobe-GC/MS analysis the grass samples were taken at random from the 3 mg sample, and any unused feedstock returned to the original stock. Three replicates were performed for each analysis.

A Perkin Elmer micro balance 2000 was used in weighing samples for analytical pyrolysis, [accurate to 0.001 mg]. The sample size used for pyroprobe-GC/MS analysis was 0.5 mg with 10% accuracy allowance. This is due to the nature of the quartz tube [sample boat for pyroprobe-GC/MS], and sample amount. In order to obtain a more accurate result from

analytical pyrolysis more replicates must be carried out using the pyroprobe-GC/MS on per sample to reduce the standard deviation of 10-20 %.

4.1.4 Moisture content

All feedstocks used were tested for moisture and ash content. The Standards used is the ASTM method. Four weighed pre-dried crucibles with lids are used, at which approximately 2-4 grams of the biomass are placed in each crucible. The lids are placed at an angle so that water vapours can escape from the crucible. The crucibles with their lids are then placed into an oven at 105°C and left for six hours. The samples are then taken out and cooled in desiccators and re-weighed using the same balance. Once the samples are measured, they are placed back into the oven for an hour, and are then taken out and cooled, as they are reweighed. This is done until a constant mass is achieved [139].

4.1.5 Ash content

The samples used for moisture content analysis are also used for ash content analysis. Three samples were placed in a muffle oven pre-heated to 575 °C and left for a minimum of six hours, ensuring that the crucible lids are at an angle so that there are sufficient space for air to creep in and volatiles to escape [139]. The samples are then taken out from the muffle oven and placed in a desiccators and left for one hour. They are then re-weighed, and the ash percentage was calculated by dividing the new weight by the pre-dried weight [weight of the sample after being subjected to the oven at 105 °C] then multiplied by 100. An average was taken from the three samples with a standard deviation of less than 0.5 %.

4.1.6 Elemental and metal analysis

CHN, metals and other inorganic components were determined by digestion, and carried out by Accuris ICPES [Induced coupled plasma emission spectrometer] using the following procedure: The plant materials was dried for four hours at 80°C in an oven and cooled by a desiccator. 0.250 g of the oven dried material was placed in a 25 ml digestion tube, while 5 ml of nitric or perchloric acid was added around the side of the tube ensuring the sample is washed down into the tube. It was then mixed by swirling and held at room temperature for 2 hours [140] prior to heating overnight. 5ml of 25 % of HCl was then added and the mixture heated to 80°C. After cooling; the samples were subjected to ICP analysis. The Elemental

analysis was carried out by an independent laboratory: MEDAC LTD, Brunel Science centre, Cooper's Hill lane, Surrey, TW20-0JZ, UK.

Metal analysis was carried out at Rothamsted Research, Harpenden, Hertfordshire, AL5 2JQ.

4.1.7 Lignocellulosic determination

Lignin and cellulose were analysed by wet chemistry methods which include Klason; Acid Digestible Fibre [ADF], and Neutral Digestible Fibre [NDF] [141]. ADF was determined by storage of the samples under an acid detergent, at which the hemicellulose was dissolved. The residue which remains within the sample consists of mainly lignin [ADF] and cellulose [NDF]. The acid detergent lignin was then determined by further treatment of the ADF residue using a strong acid, to remove any remaining cellulose residue.

Lignocellulosic determination; was carried out at the Institute of Grassland and Environmental Research, Aberystwyth, Wales, SY23 3EB, UK.

4.1.8 Statistical analysis [PCA]

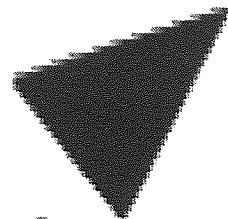
Principle component analysis [PCA] is a commonly used technique for statistics for simplifying data by reducing multivariable to a 2-D plot to characterize the results. The use of principle component analysis allows to identity factors which influence the data so that relationship can be established on a qualitative analysis. PCA uses complex matrices transform in which does not poses fixed vectors, and is completely dependant on the data set. The transformation of the data allows the results to be represented on a new co-ordinate system, in which the greatest variance within the data lies on the first co-ordinate, while the second variance forms the second co-ordinates. PCA has been used in the passed to discriminate the effects of different genotypes, catalysts, reactions and plot locations [43, 49, 155-158] and is considered as a vital tool in identifying affects, trends and patterns on large data sets. PCA will be used for the data produced to identify variables which affect the pyrolysis-oil quality.

4.2 Thermogravimetric analysis

The thermogravimetric analyser [TGA] records the weight change in a sample, as a function of temperature, which allows the identification of phase changes. The results produced enable the calculation of the derivative of peaks, and rates of volatilisation. The maximum temperature which the sample can be heated to is 1000°C with a maximum heating rate of 200°Cmin⁻¹.

The TGA can also produce chemical kinetics' data [activation energy, rate constants, pre-exponential factors and orders] which allows a confident impression on the mechanism of degradation under slow pyrolysis. Previous work had found that heat and mass transfer effects are a dependency on particle size and density of the sample, but slow pyrolysis is kinetic dependant [5, 73] assuming if small particle sizes are used. Different feedstocks have different thermal degradation mechanisms due to natural compositions, thus TGA methods have been used to compare different thermal characteristics from the different types of biomass used in this research.

The TGA has two functions; one being a temperature scan [able to increase/decrease the temperature at different heating rates] and the second being isothermal degradation [fix temperature for a given period of time]. Figure 4-1 shows a schematic of the Perkin Elmer TGA.



Aston University

Illustration removed for copyright restrictions

Figure 4-1 - Perkin Elmer Pyris 1 TGA [133]

The weight loss calculations conducted by the software uses a sensitive balance, of which at one end of the balance a 100mg weight hangs, while at the other end the hang down wire is positioned [where the sample crucible is placed]. Any change in weight from its equilibrium balance will be recorded. A sample weight of 2-3 mg is placed into the crucible in where the sample is subjected to heat from an external furnace. A thermocouple is placed 1-2mm underneath the crucible in the furnace, to measure temperature. The TGA experiments are conducted under an inert atmosphere by the use of nitrogen for pyrolysis degradation to occur.

4.3 Pyroprobe CDS AS-2500 -GC/MS

The advantage of using a pyroprobe is to investigate the breaking of large molecule structures to smaller molecules by applying thermal energy to fracture chemical bonds. The result from pyroprobe-GC/MS enables the study of the formation of volatiles from the original biomass structure by observing their behaviour and stability of their fragments.

The CDS AS-2500 fast pyrolysis auto sampler unit possess an automatic carousel, in which 36 samples can be loaded to pyrolyse the samples automatically. A microcontroller controls the temperature and heating rate of the platinum filament which is placed round the internal furnace. The maximum temperature on the platinum filament is 1400°C; with rates varying from 0.01°C/min to 20,000°C/second for a maximum hold time of 100 seconds. This gives a better representation of fast pyrolysis, such that vapours can be readily analysed in the gas chromatography and mass spectroscopy. Analytical pyrolysis is usually operated with conjunction with a gas chromatography and mass spectroscopy to study complex materials.

Samples are placed in longer quartz tubes and are loaded into the carousel in a vertical position, in which they are dropped into a pyrolysis chamber. The auto sample waits for the GC to be ready, and then activates the pyrolysis chamber to purge with helium, then pyrolyse the sample. The 8-port valve is used to control the purge gas inlet, vent and GC carrier gas as well as ensuring that the sample is purged before being pyrolysed [134]. Figure 4-2 shows the schematic diagram of the CDS AS 2500 auto sampler fast pyrolysis unit.

In theory if the thermal parameters [temperature, heating rate and time] are controlled in a reproducible way, the fragmentation which is a characteristics of the original molecules will be based on the relative strengths of the bonds between its atoms [16].

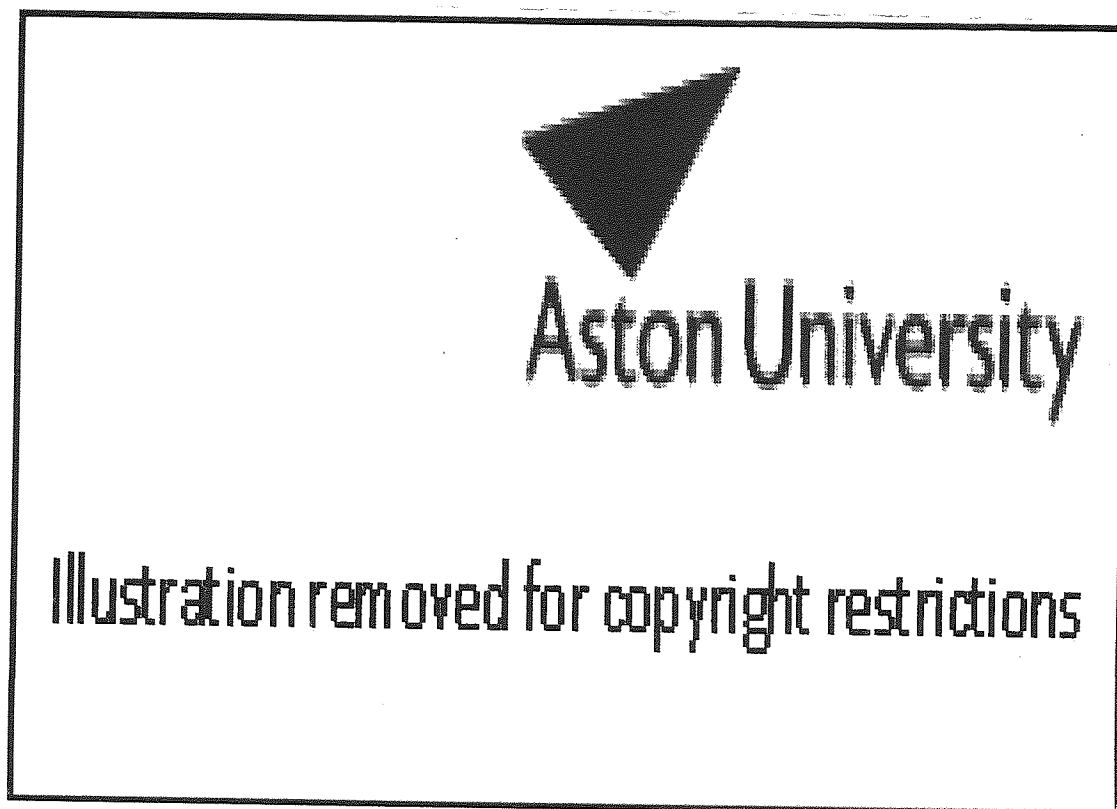


Figure 4-2 - AS2500 Pyroprobe auto sampler [134]

4.3.1 Sample sizes

Sample sizes used are dependant on the gas chromatography capacity and split ratio. Standard gas chromatography can analyse samples of 1 μL which is approximately 1 mg in mass terms. Pure compound substances will completely vaporise when pyrolysed, however using biomass samples around 85% [depending on thermal conversion conditions and yields] will be pyrolysed to condensable and non-condensable vapours, while 15 % will remain as char.

It is recommended that 10-500 μg [0.01-0.5mg] samples should be used if an accurate balance can be used. However if larger samples is used it is suggested that a higher GC split ratio should be employed [136].

4.3.2 Sample boats for pyroprobe-GC/MS

Samples are placed in a quartz tubes and placed into the carousel in an upright position. The quartz tubes are fire polished with a quartz placement rod inserted within the tube to position the sample in the correction position [for effective heat transfer to take place within the pyrolysis chamber] before any sample is placed within the tube.

Samples which melt within the interface or during fast pyrolysis can cause inaccurate results. Quartz wool is placed above the placement rod to minimise any affects of liquid running down the tube and minimise any errors. Figure 4-3 shows a typical pyroprobe sample boat with quartz wool, and sample and placement within the pyrolysis chamber.

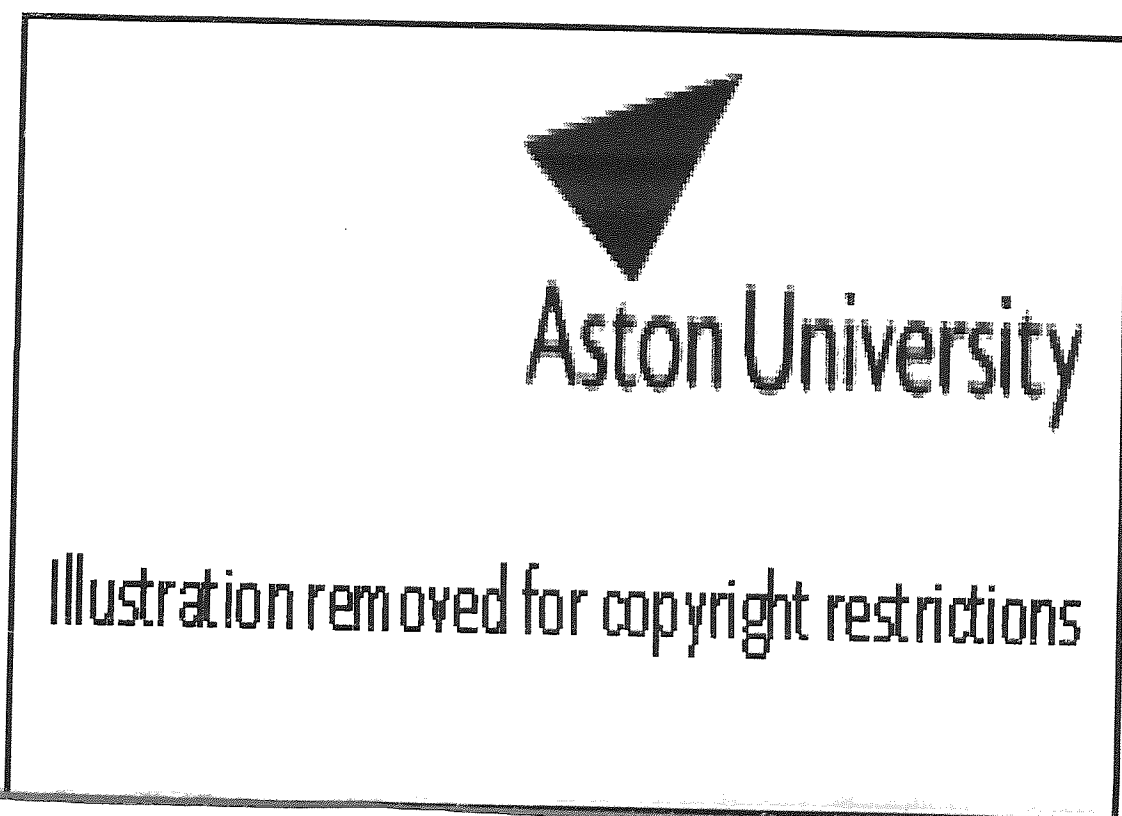


Figure 4-3 - Pyroprobe auto sampler boat and boat position in furnace [134]

4.3.3 Turbo mass Gold Gas chromatography/mass spectroscopy

The Perkin Elmer Turbo mass Gold GC/MS is an analytical laboratory scale gas chromatography and mass spectrometer detector to perform gas/liquid analysis.

The auto system XL gas chromatograph works with accordance to the turbo mass spectroscopy using either an electron ionisation [E.I.] or chemical ionisation [C.I.] to characterise samples by the use of a high performance quadruple filter and mass analyser [135]. The mass spectroscopy system produces positive identification and quantification of compounds which are separated in the mixture via the gas chromatography. The GC/MS system is controlled via a PC which carries out scanning and ion recordings for each sample. Fragmented ions from the quadruple pre-filter and mass analyser, splits the ions which have the selected mass to charge ratio while the low noise photometer operates with a gain of 10^5 that amplifies the ion [135]. Figure 4-4 shows a graphical description of the principles of MS analysis.

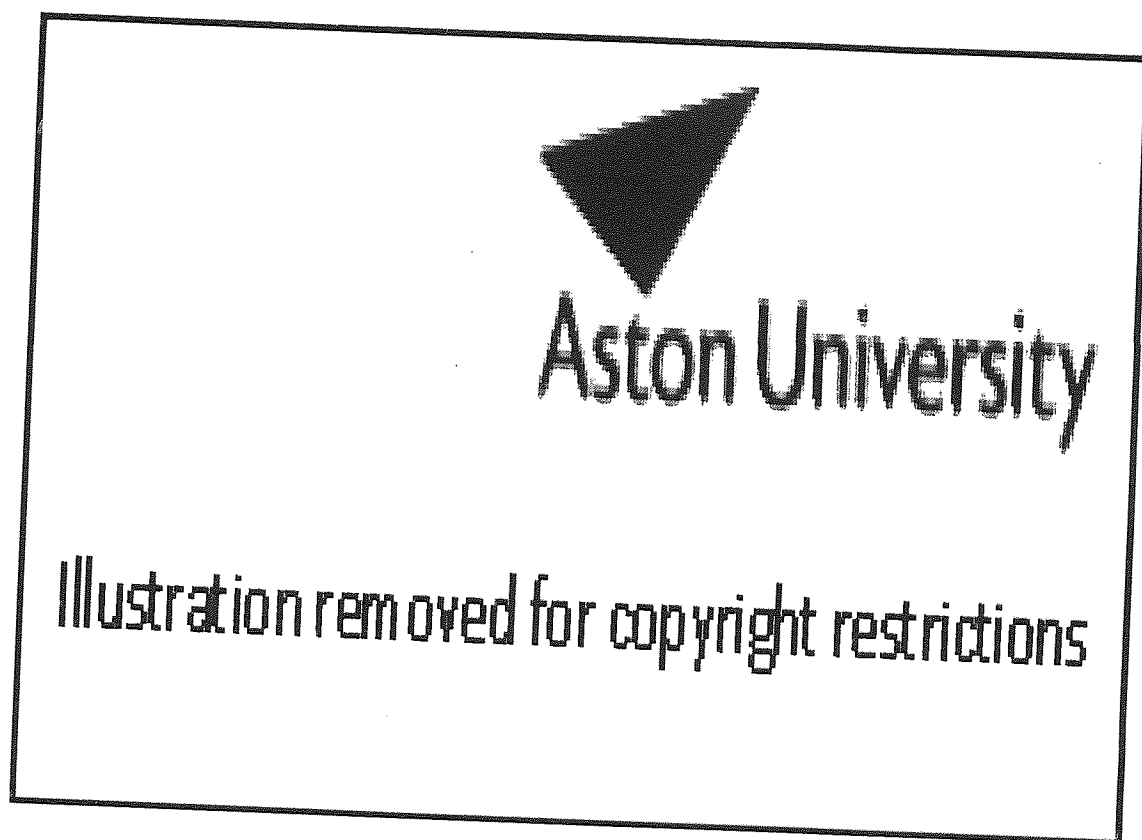


Figure 4-4 - Principles of MS analysis [135]

Gas chromatography and mass spectrometer are well established analytical techniques which have been coupled together to obtain the highest level of chemical analysis. Gas

chromatography is a technique to separate mixtures of compounds to their individual chemical components by their boiling points. By the use of a semi polar capillary column at which on the inside of the inner walls contains a liquid known as the stationary phase which emerges the mixture. Thus the separated components in the GC are usually burnt in a flame known as the flame ionisation detector [F.I.D.]. The chemicals are recorded as peaks, and peak heights and their areas represent the abundance of the compound present in the mixture, thus suggesting lower areas on smaller peaks give lower amounts in the mixture. This corresponds with the amount of a component detected and the time it takes that component to pass through the column [16]. The software adds up all the ion peaks in the mass spectra to give a total ion count (T.I.C.). Scanning can be conducted as well as selected mass ranges (0-1 sec and 0-1000 mass units). The data of scans and masses are recorded on the PC.

The positive fragments [cat ions and radical cat ions] are influenced by an accelerated force in a vacuum through a magnetic field, which are then sorted by a mass to charge ratio [m/e] which is equivalent to its molecular weight per fragment [135].

The carrier gas for the GC is helium; this carries the separated components of the mixture through the GC. The flow rate out of the end of the capillary column into the MS is usually 0.5-3 ml/min. The GC/MS operates usually at 2×10^{-5} Torr with 1 ml/min of helium into the electron ionisation. Once the mass spectra are produced from the analysis of the mixture, peak identification is used to gain an insight of fragmentation or separation of mixtures. The Perkin Elmer turbo GC/MS are accompanied by a search library known as the NIST library/database. 60,000-220,000 stored spectra are found in the NIST library. The large database can be used rapidly to scan the spectra by comparing the mass spectrum of the mixture or fragment component to the library. The end result will be a top 20 compound of best matches giving also a confidence level percentage [135].

4.3.4 Pyroprobe-GC/MS peak identification

4.3.4.1 *Cellulose derived compounds*

To identify the cellulose derived compounds from fast pyrolysis, Avicell cellulose (99% pure) was pyrolysed in the pyroprobe-GC/MS and characterised, a product distribution of more than 104 compounds given off in cellulose [37] according to Meier. The pyrogram of cellulose is shown in Figure 4-5, and the assigned compound peaks can be found in Table 4-1.

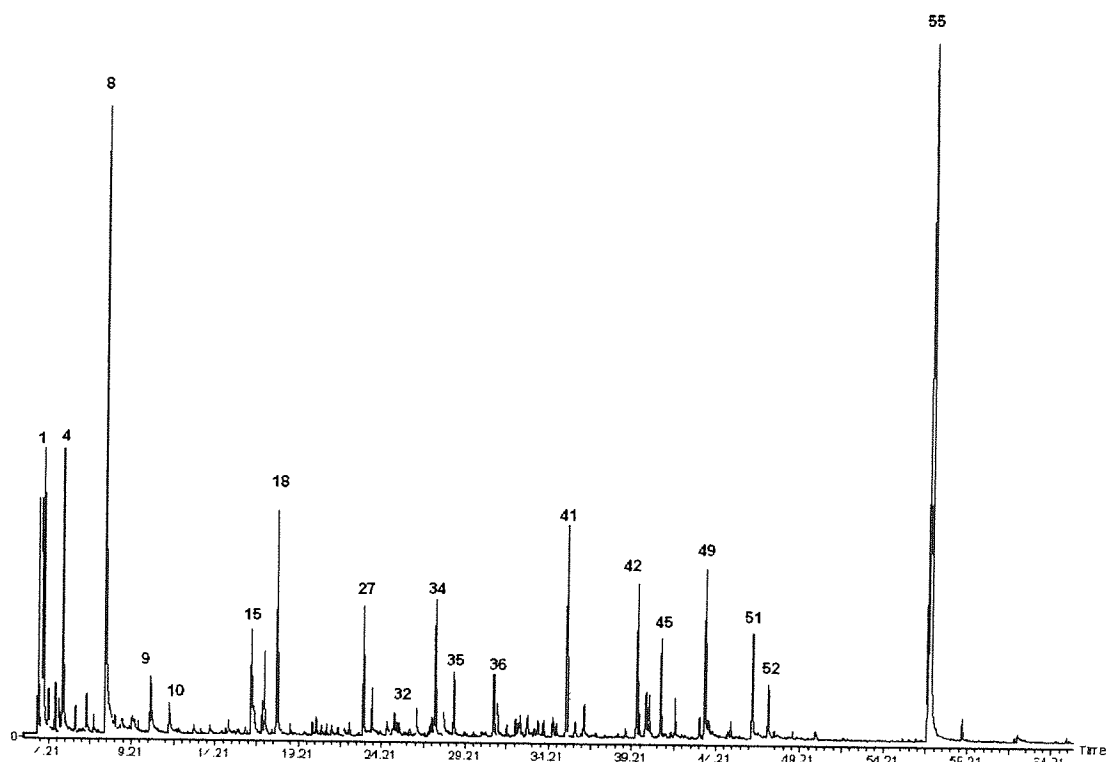


Figure 4-5 - Pyrogram of Avicell cellulose derived compounds

The main peaks are: furan, propanal-2-one, 2, 3-butanedione, hydroxyacetaldehyde, 4-hydroxy-3-methyl-(5H)-furanone, 5-hydroxymethyl-2furaldehyde, levoglucosan

Cellulose derived products are produced in high yields within the pyrolysis-oils (excluding high molecular weight lignin tar). Fifty five compounds were identified along with there molecular weight distribution and GC retention time. Not all 104 compounds can be identified due to lack of compound amount and interference from the column bleed on the molecular weight distribution of the compounds.

The compounds from the programs (pyroprobe-GC/MS) were identified by comparing the mass spectra via the Perkin Elmer NIST computer library with literature data to obtain the highest likelihood of compound identification. The key markers were selected by confidence and abundance levels on compound peaks from the pyrogram, and the number times of specific compounds shown up on literature data.

Table 4-1 - Assignment of compound composition and gas chromatographic retention times of cellulose [Avicell 99%] derived compounds.

PEAK	Compound	Mz	RT
1	Acetaldehyde	29/43/44	4.2
2	Furan	39/58/68	4.62
3	2-propanal	29/55/56/58/66	4.872
4	propanal-2-one	43/72	5.0631
5	2 methyl furan	39/53/82	5.816
6	2,3 Butanedione	43/86	6.51
7	3-pentanone	53/57/86	6.92
8	Hydroxyacetaldehyde	31/42/60	7.63
9	Acetic acid	15/43/60	10.364
10	Hydroxypropanone	43/74	10.98
11	1,2- di hydroxyethene	31/42/60	11.45
12	Propane 2,2 di-methyl	29/31/57	12.01
13	3-methylfuran	39/53/82	12.94
14	2-propenoic acid methyl ester	32/44/55/58	13.903
15	3-hydroxypropanal	43/73	15
16	furan2-one	32/55/84	15.584
17	furan-3-one	54/84	16.374
18	Butanedial	58/43/29	17.02
19	2 hydroxy-3-oxobutanal	43	17.189
20	2-furaldehyde	39/95/96	17.93
21	Propylfuran	43/81/110	18.72
22	A-angelicalactone	43/55/98	20.052
23	2-furfuryl alcohol	53/69/81/98	20.274
24	1-acetyloxypropane-2-one	43	20.6
25	tetrahydro-4-methyl-3-furanone	43/72	20.9
26	Di-methyl-dihydro-furan	55/69/83/98	21.2
27	2-acetylfuran	95/110	21.6
28	4-cyclopentene 1,3-dione	42/68/96	22.7
29	2 hydroxy-butanedial	43/44	23.126
30	Butanal 3 methyl	29/43/44/57	23.51
31	dihydro-methyl-furanone	42/55/69/98	23.61
32	dihydro-methyl-furanone	39/42/70/98	24.5
33	5 methyl-2 furaldehyde	53/110	24.96
34	2,3-dihydroxyhex-1-ene-4-one	43/57	25.27
35	(5H)-furan -2-one	55/84	26.3
36	beta lactose derivative	39/68/82/110	27.22
37	4 Hydroxy-5,6-Dihydro-(2H)-pyran-2-one	29/57/58/114	27.45
38	2-Hydroxy-1-methyl-1-cyclopententene-3-one	55/69/84/112	28.55
39	OH-methyl-dihdropyranose	43/72/128	30.92
40	3-methyl-terahydrofuran, 2,4-dione	43/114	31.16
41	overlapping spectra: unknown	39/53/81/82	31.73
42	2-furanoic acid methyl ester	39/95/126	32.25
43	methyl-butyraldehyde derivative	57/85/116/126	32.91
44	Unknown	41/58/70/98	40.02
45	Unknown	55/71/97	40.2
46	1,4:3,6 dianhydro-(alpha)glucopyranose	57/69/98/114	40.92
47	Unknown	43/44/57/85/103/116	41.8
48	furan derivative	60/69/97	43.23
49	5-hydroxymethyl-2-furaldehyde	41/69/97/126	43.58
50	Unknown	43/70/98/116	45.13
51	2 hydroxymthyl-5hydroxy-,2,3-dihydro-	57/87/97/144	46.39

52	(4H)-pyran-4-one	57/73/86/114	47.34
53	anhydro-pento-furanose: unknown	42/70/116	48.72
54	overlapping spectra: unknown	32/44/60/70	55.36
55	1,6-anhydro B-D mannopyranose	57/60/73	56.98
	levoglucosan		

Hemicellulose in comparison to cellulose is chemically unstable as it is exposed to high temperatures $>240^{\circ}\text{C}$ [6]. It was stated earlier in Chapter 2 Section 2.2.3 of this thesis that hemicellulose consists of hexosans and pentosans, however no product analysis has been carried out on unmodified hemicellulose, but products can be identified by difference from the complete biomass taken away from its cellulose/lignin compound derivatives. Hemicellulose compounds are thought to produce lower molecular weight compounds, with lower yields. Hemicellulose main compounds are: acetic acid, furfural, furan, butanedial, 2-furaldehyde, 2,5-dimethoxytetrahydrofuran, 2-hydroxy-1-methyl-1-cyclopentene-3-one, 4-hydroxy-5, 6-dihydro (2H)-pyran-2-one, 3- butenal-2-one, (2H) furan-3-one/3 furfural and 2 hydroxy-3-methyl-2-cyclopenten-1-one.

4.3.4.2 Lignin derived compounds

Lignin can also be analysed, however there is no universal standard which can be used but it is suggested that more than 82 chemical compounds can be given off in one type of lignin [39], and often occurs from side chains of the lignin structure, since the majority of the lignin molecule is retained through pyrolysis. The pyrogram of lignin is shown in Figure 4-6, and the assigned compound peaks can be found in Table 4-2.

The higher molecular organic species [which can not be analysed in GC/MS] are known as pyrolytic lignin. The main S and G type lignin compounds are: phenol, catechol, syringol, guaiacol, 4-methyl guaiacol, vanillin, syringol, eugenol, acetosyringone, syringaldehyde, and o/m/p-cresol. The less abundant H-Type lignin are; phenol, 2 methyl phenol, 4 ethylphenol, 4 vinyl phenol. Forty three compounds were identified along with there molecular weight distribution and GC retention time [refer to Figure 4-6 and Table 4-2]. Not all 92 compounds can be identified due to lack of compound amount/height and interference from the column bleed on the molecular weight distribution of the compounds.

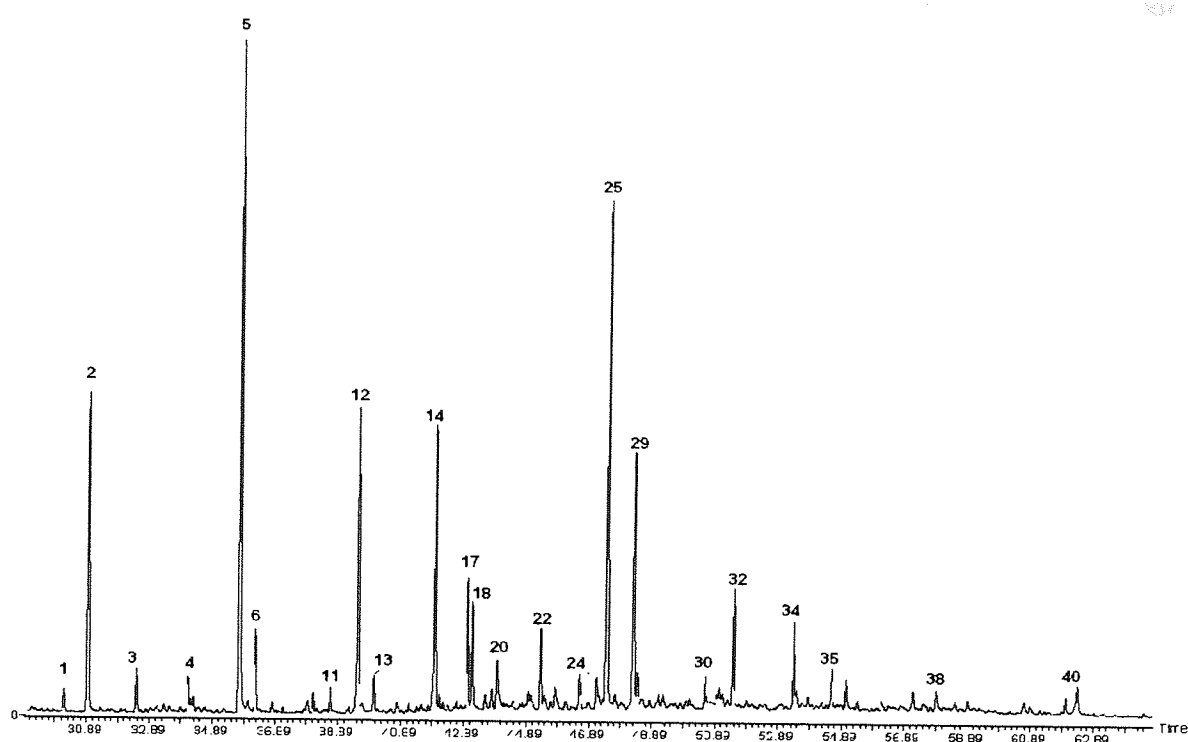


Figure 4-6 - Pyrogram of Pyrolytic Spruce Lignin Derived compounds

The compounds from the programs (pyroprobe-GC/MS) were identified by comparing the mass spectra's via the Perkin Elmer NIST computer library with literature data to obtain the highest likelihood of compound identification. The key markers were selected by confidence and abundance levels on compound peaks from the pyrogram, and the number times of specific compounds shown up on literature data.

It has to be stated that these contained of Table 4-2 are the main compounds in spruce lignin and cellulose, and may not be the case for other biomass lignin, as some compounds such as syringol or guaiacol can be more abundant than others from other feedstocks depending on conditions and variables from fast pyrolysis. These compound markers have the largest peaks, in which the area obtained by integration of the produced graph is proportional to the number of ions present for that particular specie which correspond to the quantity of that specie compound.

Table 4-2 - Assignment of compound composition and gas chromatographic retention times of Lignin [Spruce pyrolytic lignin] derived compounds.

PEAK	Compound	Mz	RT
1	Phenol	39/66/94	30.18
2	Guaiacol	53/81/109/124	30.94
3	o-cresol	51/77/90/108	32.48
4	guaiacol, 3 ethyl	77/91/109/137/152	34.127
5	m/p cresol	51/77/107	35.768
6	guaiacol-4 methyl	55/67/95/123/138	37.954
7	Phenol, 2 methyl	108/107/90/79/51	36.27
8	phenol, 2 ethyl	77/107/122	36.797
9	phenol, 2,3-dimethyl	77/91/107/121/122	37.16
10	phenol, 3 ethyl	77/107/123	38.12
11	anisol, 3,4 methyl	77/91/121/136	38.66
12	Phenol, 4 ethyl	122/107/91/77/65	39.01
13	guaiacol, 4 ethyl	79/91/109/137/152	39.52
14	anisol, 2,4/2,5-dimethyl	77/91/121/136	39.87
15	guaiacol 4 vinyl	77/107/135/150	40.01
16	phenol, 4 vinyl	120/91/65/39	40.04
17	Eugenol	77/91/103/131/149/164	41.98
18	guaiacol 4-propyl-	137/166	42.13
19	Catechol	64/81/92/110	42.68
20	Syringol	111/139/154	43.04
21	phenol, 4 propenyl (cis)	77/91/105/133/134	43.18
22	Unknown	55/77/107/138	43.785
23	phenol, 4 propenyl (trans)	51/77/105/115/134	43.98
24	Iso-eugenol (cis)	77/91/103/131/149/164	44.962
25	Iso-eugenol (trans)	77/91/103/131/149/164	45.83
26	Syringol, 4-methyl	125/153/168	45.35
27	Vanillin	81/109/123/151/152	46.59
28	C ₁₀ H ₁₀ O ₂	91/119/147/162	46.64
29	Homovanillin	94/122/137/166	46.9
30	Acetoguaiacone	108/123/151/166	47.21
31	Syringol 4 vinyl	137/165/180	47.73
32	guaiacyl acetone	94/122/137/180	48
33	coniferyl alcohol	115/137/144/180	48.31
34	guaiacol 4-(oxo-allyl)-	91/103/131/149/164/178	50.591
35	Propioguaiacone	108/123/151/180	51.05
36	4-Propenyl syringol (trans)	167/179/194	51.94
37	dihydroconiferyl alcohol	137/137/182	52.68
38	Syringaldehyde	167/181/182	53.39
39	coniferyl alcohol (cis)	108/123/151	54.59
40	Acetosyringone	153/181/196	55.05
41	Coniferaldehyde	103/131/146/178	55.41
42	unknown	115/145/173/188	57.886
43	Sinapaldehyde	137/165/180/208	60.68

4.3.5 Pyroprobe-GC/MS repeatability

The pyroprobe-GC/MS unit is a well defined system of analysis for samples and vapours for qualitative and quantitative assessment for a given homogenous sample. Biomass is heterogeneous and large standard deviation can be obtained by analytical equipment, due to the fact that sampling issues can arise from different parts of the plant when a sample is taken for analysis.

An experiment was carried out to investigate the effect of sample sizes with different split ratios. The sample size of 0.1 mg (1:25 split ratio), 0.5 mg (1:125 split ratio) and 1 mg (1:250 split ratio) were investigated. The samples were pyrolysed at a fixed temperature and a heating rate of 0.4°C/ms. The experiments were conducted three times for reproducibility [136], in which it was found that larger mass samples with higher split ratios gave better repeatability with a 5 % standard deviation from the three runs. However it must be noted that larger sample sizes can give rise to heat and mass transfer.

4.4 **Conditions for analytical pyrolysis**

Analytical trials were conducted and analysed to obtain reliable data for characterisation. Each study was repeated three times under conditions as suggested by literature.

4.4.1 Thermal analysis experiments

A Perkin Elmer Pyris-1 TGA thermobalance was used to carry out pyrolysis under dynamic heating for both treated and untreated biomass samples (1-3 mg) at a heating rate of 10 K/min heating from ambient temperatures to 600 °C in a nitrogen flow of 50 ml/min. TG and DTG graphs are usually produced for each sample.

4.4.2 Pyrolysis-GC/MS experiments

The pyroprobe [Chemical Data Systems (CDS), USA] is an analytical scale pyrolysis unit which consists of an inductive heated coil to heat samples. A fire polished quartz tube was used to load 500 µg (0.5mg) of the feedstock using a Perkin Elmer Micro balance sensitive to 0.001mg. The sample was placed in the centre of the inductive coil with an isothermal setting of 600°C at a heating rate of 0.4 ms (due to a specified temperature difference of 100°C between the coil and the sample temperature) with a pyrolysis time of 10 seconds.

A gas chromatograph with a split ratio of (1:125) was used for compound separation. Both the injector and detector temperatures were at 280°C and the carrier velocity was at 38cm/s. Separation was achieved using a semi polar column PP1701 or DB 1701 (60 m by 25 µm with a 0.025 µm film thickness) with a chemical composition of 14% cyanopropyl-phenyl 86% dimethylpolysiloxane which shows a different selectivity to (phenyl) dimethylsiloxane phases because of the functional cyano groups. In order to give good product separation, the temperature program began at 45°C for 4 minutes, followed by a heating rate of 4 °C /min to 240°C and 39 °C /min to 280°C (MeierPersonal communication). Electron impact mass spectra were obtained by Perkin Elmer MS GOLD (UK) at 70eV. The mass range from m/z 28-600 was scanned with a speed of 1.0 s/decade. Data processing was done by Perkin Elmer Turbo mass spectrometer version 6.0. The compounds from the chromatograms were identified by comparison of the mass spectra with the Perkin Elmer NIST computer library, together with literature data to obtain the highest likelihood of compound identification.

The GC/MS were calibrated for 10 compounds which are commonly found in the pyrolysis of biomass, and retention times were obtained. The compounds were then calibrated to obtain peak sensitivity, by taking the 10 compounds and creating mixtures with acetone to produce three different concentration levels for the 10 compounds (0.1%, 0.5 % and 1 % in acetone).

Peaks from the pyrogram were identified and separated as either lignin derivative compounds or cellulose derivative compounds from pyrolysis. The most abundant peaks were taken as the key markers to represent the lignin and cellulose constituents.

4.5 Pyrolysis reactor system

4.5.1 Overview

All the energy crops used within this project was subjected to pyrolysis-oil production by the use of Aston's 150ghr^{-1} or 1kg hr^{-1} fast pyrolysis fluidised bed reactor [Figure 4-7].

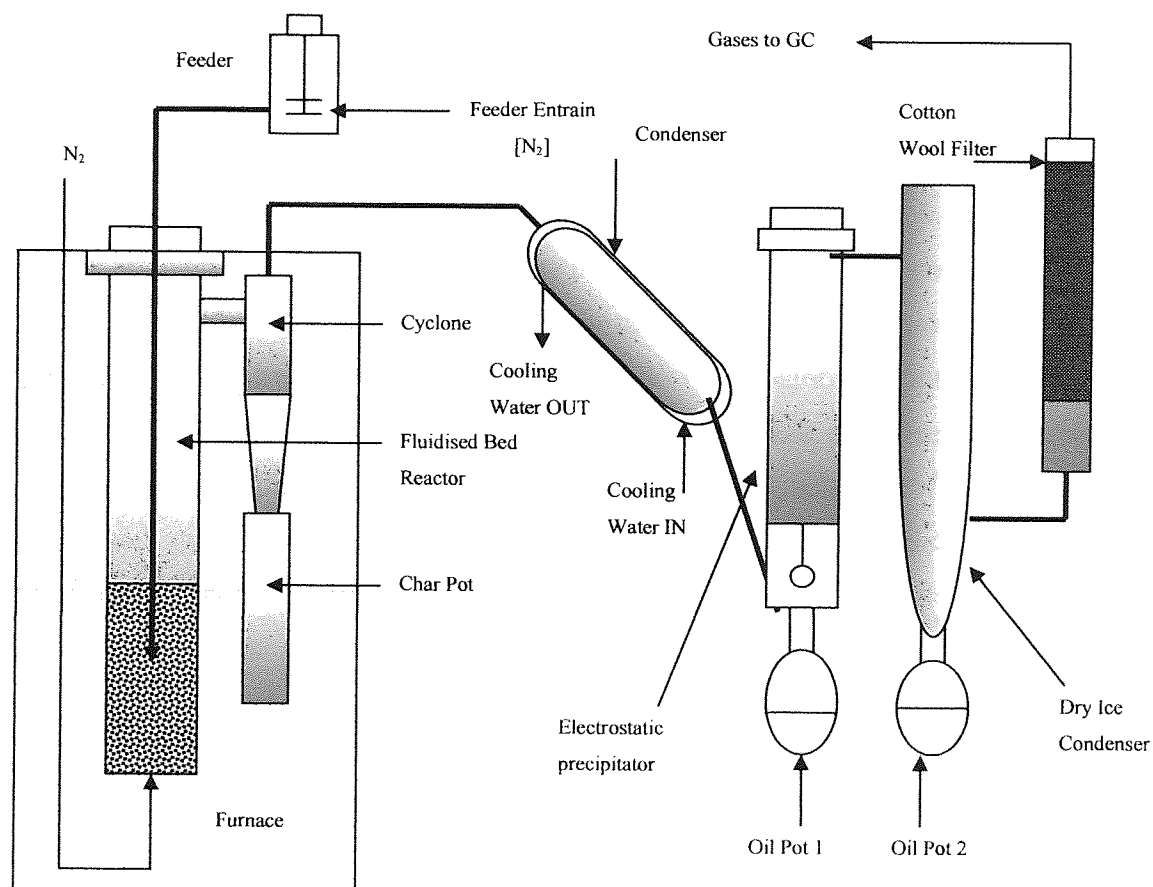


Figure 4-7 - Aston's 150ghr^{-1} fluidised bed fast pyrolysis rig

Nitrogen was used as the inert gas throughout the process and was supplied to the reactor, the feeder entrain and top. The reactor fluidising gas passes through a porous distributor before coming in contact with heat transfer medium [quartz sand].

The feeder entrain is a flow of nitrogen which passes through a pipe, located at the bottom part of the feeder. It consists of a small hole to allow the particles of biomass to get sucked in and carried away into the fluidised bed, by the means of a flexible tube. The feeder top is used to push the biomass down the feeder into entrain hole. The feeder is assembled from clear perspex, which possesses the advantage of seeing the biomass as it is being fed into the

reactor. The feedstock used was in the particle size range of 250-355 μ m, and was placed in the feeder. The pneumatic paddle stirrer allows the particle in the feedstock to be distributed evenly and prevent bridging or blocking in the entrain hole to achieve an accurate continuous steady flowrate. The aim of the feeder top is to pressurises the biomass and apply a force from the top to push the biomass down and into the hole of the entrain tube. The fluidising medium used is quartz sand. Four thermocouples were placed round the process to measure the temperature at the centre of the reactor, the temperature of the top of the reactor, the out let temperature after the cyclone and the temperature of the transition pipe.

The rig ran at approximately 500⁰C with a vapour residence time of 0.4-1.5 seconds. The pyrolysis products which are produced in the pyrolysis reactor [organic volatiles, gases, chars, aerosols, nitrogen and sand] passes through a primary cyclone to separate the char by the use of gravitational pull by a tangential velocity to collect the majority of the char in a char pot which is located below the cyclone. The cyclone and the char pot were also placed in the furnace so that an isothermal temperature consistency could be achieved. The organic vapours, aerosols and gases are then passed into a glass transition pipe which is maintained at approximately 400⁰C then into a water condenser. The condenser drops the temperature from 400⁰C to 30⁰C in order to condense the organic vapours into the pyrolysis-oil.

The electrostatic precipitator is used to improve the efficiency of collecting the organics and aerosols (which are a mixture of low and high molecular weight compound vapours). It supplies a charge to the mixture of vapours leaving the condenser to nucleate and form the first heavy tarry liquid in oil pot 1.

The remaining vapours travel into the dry ice/acetone condenser where it is maintained at approximately -30 ⁰C. The lower organic compounds which have lower molecular weights are condensed into oil pot 2 which is located below the dry ice condenser. The acetone acts as a heat transfer medium between the dry ice and vapours entering the inner wall of the condenser. The non condensable gases produced from fast pyrolysis of biomass are CO, CO₂, H₂, CH₄, C₂H₄, and C₂H₆. The gases pass into a cotton wool filter which has a temperature of -4 to - 8⁰C to condense and absorb any remaining condensable vapours by the wool, while the incondensable gases which leave the cotton filter, are split between the vent & the online GC unit for analysis.

Astons 1 kg hr^{-1} rig has similar principles to that of the 150 g hr^{-1} rig, but had a screw feeder which can feed particle size ranges from 0.1-2 mm.

4.5.2 Feed rate Determination

Before conducting an experimental run on the 150g hr^{-1} pyrolysis reactor, a feedstock calibration had to be carried out to obtain the best conditions to obtain a constant and suitable flowrate. The feedrate should be set at 50-100 [g hr^{-1}] to ensure consistency and accuracy otherwise processing problems will be encountered i.e. using a low flowrate can cause the sand bed to agglomerate and a poor gas analysis, while using a high flowrate can cause blockages within the feeding tube of the reactor and downstream of the process.

The pyrolysis reactor is capable to run at higher and lower feedrates, however it is not recommended due to possible blockages. The flowrate of the feedstock is completely dependent on the nature of the feedstock [particle size, sphericity etc], the stirrer speed, entrain flow and the feeder top. These four variables have an impact on the flowrate, but from previous studies [6, 10, 92] it has been shown that the entrain flow and the nature of the feedstock have the major influencing factor on the feedstock flowrate. It was observed that as the height of the biomass in the feeder fell, so did the flowrate. Thus for mass balance purposes the feedrate result used are calculated by the difference in mass of the feedstock used measured before and after the experiment, at which the result is divided by the total run time to obtain an average flowrate. Data readings are collected every five minutes at which an average was taken for each temperature reading, and then averaged again to give an average temperature of the reactor.

The amount of feedstock used in each experiment was based on the difference in weight of the feeder before and after the experiment divided by the total run time. The dry mass feed stock used in each experiment can be calculated by the amount of the wet feedstock used subtracted from the weight of the moisture content of the feedstock used.

4.5.3 Fluidised bed reactor

The fluidised bed reactor is made of 3/16 stainless steel with a length of 26 cm and a 4 cm diameter. The top of the cylinder was threaded allowing the reactor to be removed for cleaning and maintenance as well adding and removing the quartz sand. The reactor top consists of

three units, a thermocouple unit, the feed input and an air cooling pipe. The thermocouple unit is a K type which measures the internal bed temperature. The air cooling pipe allows the feedstock to enter at ambient temperature, without preheating [risking pre-pyrolysis] due to the radiation and convection of heat from the fluidised bed.

150 grams of quartz sand [particle size range of 355-500 μ m] is placed into the reactor so that a good distribution can occur in the bed [with an appropriate nitrogen fluidising velocity] to act as the fluidising medium. This allows the char and vapours to leave the bed and enter the cyclone. The sand approximately takes 8cm of the height of the reactor and reaches a height of 12cm once fluidised.

The fluidising medium nitrogen enters the bottom of the bed at a rate of 6-9 l/min and passes a perforated distributor plate of a 100 μ m pore size. The fluidising rate is approximately 3 times the minimum fluidising velocity [U_{mf}]. The fluidising velocity was sufficient to carry the vapours out the bed, while the sand remains in the bed. This was reasonable since the density of the char is one tenth to that of the density of the quartz sand; however some sand particles can be entrained from the bed if fluidising velocity is slightly higher to that which is stated.

The entire reactor is placed in a furnace which is heated to 20-30°C higher than the fluidised bed. The furnace uses a proportional controller which is linked to a thermocouple (placed 100mm from the top), in which a manual set point is entered, and the temperature of the furnace will overshoot and then come within 10 % of its desire set point. The biomass enters from the feeder and instantaneously being pyrolysed with a residence time of 0.4-1.5 seconds. The vapours are formed in the reactor and pass into the cyclone in addition to char, at which the char has similar dimensions to that of the particle, but only having approximate 10 % of its original weight.

The reactor temperature can be inconsistent e.g. for 30 minutes it can read 450°C and 30 minutes it can read 550 °C, thus this methodology can gain an average temperature for this run to be 500 °C [10] so an average temperature is calculated by the summation of the temperature of the reactor readings measured by the number of readings. The entire reactor, cyclone and char pot are placed in the furnace as mentioned, but are insulated at the top of the reactor to prevent any heat loss. The outlet pipe from the cyclone and the transition pipe are heated via a trace heating tape and intensively insulated to maintain a temperature of 400°C. If this was not

carried out vapour condensation can occur and blockages can build up, making the overall trial unsuccessful.

4.5.4 Residence Time

A residence time is calculated from the run, which is also known as hot space residence time. This is the exposure time of heat to a single thread of particle entering the fluidised bed [time spent in the reactor]. This would give an insight to the amount of secondary reactions occurring in the bed. However if an average feedrate and bed temperature are taken, then a less inaccurate residence time is calculated.

Two methodologies can be used in calculating the residence time, one only considering the reactor duration, and the other being the complete time it spends in the “hot zone” which includes the reactor, cyclone and exit pipe from the cyclone. The hot zone is referred to as the complete assembly in the furnace, suggesting that vapours and char are at constant temperature and there is no temperature gradient across the assembly.

The reactor residence time is a calculation only measuring the vapour time only in the fluidised bed, and disregarding the other units which are also present in the furnace i.e. cyclone. A more realistic value for residence time is using the total hot zone residence time, because vapours leaving the reactor are still subjected to the same temperature in the cyclone and exit pipe. The residence time is calculated using the following formulae:

$$ResidenceTime_{TotalHotSpace} = \frac{(Volume_{TotalHotSpace} - \frac{W_{Sand}}{\rho_{Sand}}) \times T_{Measurement} \times Time}{1000 \times T_{Reactor} \times Volume_{TotalThru-put}}$$

$Volume_{TotalHotSpace}$ = Volume of reactor, cyclone and exit tube in cm^3 [377.86 cm^3]

W_{Sand} = Weight of sand used in trial in grams [150g]

ρ_{Sand} = Particle density of sand in g/cm^3 [2.67 g/cm^3]

$T_{Measurement}$ = Ambient temperature in Kelvin [273 K]

$T_{Reactor}$ = The average temperature of the reactor in K [873 K]

$Time$ = The total run time of experiment in seconds [3600 s]

$Volume_{TotalThru-put}$ = Total volumetric output of trial in litres [300 l]

The volume and the density of the sand in the bed remain constant throughout the experimental trial, however the mass of the sand is to ± 0.01 g accuracy, but is likely to cause a significant effect on the calculation. The average temperature of the reactor, the volume throughput of gas and the run time are the significant variable which will effect the residence time calculation that is stated above.

All the trials were conducted at a temperature of around 500°C , but it is quite difficult to maintain the same average temperature for all the trials, and a tolerance of $\pm 10^{\circ}\text{C}$ was hypothesised thus a major potential for deviation for residence time. The gas inlet and outlet can also be hotter or colder than any other trials as it is passing through the reactor, condenser, EP and dry ice condenser. Blockages can interrupt the time of the trial and the level of accuracy for the average temperature and volume thru-put.

4.5.5 Liquid collection systems

Liquid formation throughout the pyrolysis system begins from the condenser and carries onto the cotton wool filter in which the non-condensable gases pass through. The majority of the pyrolysis-oil is collected from two main location points, one being the flask underneath the electrostatic precipitator and the other being the dry ice condenser, these are oil pots 1 and 2 respectively. Oil pot 1 collects the higher molecular weight compounds/aerosols which are cellulose/lignin derived and are high in viscosity, while oil pot 2 consists of approximately 60 % water and 40 % lower molecular weight compounds. The behaviour of organic vapours to pyrolysis-oil can be observed through out the system as all the liquid collection units were constructed out of glass. The liquid collection system consists of four units which is the condenser, electrostatic precipitator, a dry ice/acetone condenser and a cotton wool filter. Each unit is described below.

4.5.5.1 *Condenser*

A typical heat exchanger condenser is used and is often referred to as the “Davies” double surface water condenser. The condenser is mounted at a 60° angel to direct and aid the liquid to the EP while minimising liquid build up in the condenser. The condenser operated with a continuous water coolant from the mains tap to condense the organic vapours from 400°C to 30°C . The heavy organic fractions built up on the walls of the condenser and runs down into the EP.

4.5.5.2 *Electrostatic precipitator*

The electrostatic precipitator is made out of glass with stainless steel plate [50mm diameter] surrounding the circumference of the glass wall. The use of the stainless steel plate acted as a positive electrode, in which at the centre of the EP a thin wire hangs which ends up in a glass housing where an external magnet is placed. The wire acts as a negative electrode and carries a voltage of 15 kV. The organic vapours pick up charges as it passes the electrodes due to the presence of ions present between the electrodes. The negative charged vapours are collected to the positive plate on the wall of the EP, in where it is accumulated and runs down the EP into the collection pot [oil pot 1].

4.5.5.3 *Dry ice/acetone condenser*

The dry ice/acetone condenser allows the light organic vapours to be condensed by the use of dry ice and acetone which produces a temperature of -30°C , allowing the light organic vapours to be condensed as it leaves the EP which has a temperature of approximately 30°C . The light organic vapours and water condense on the walls of the inner glass condenser, and runs down in the collection pot [oil pot 2].

4.5.5.4 *Cotton wool filter*

The cotton wool filter is used to collect any condensable oils, if the EP and dry ice/acetone condenser did not operate efficiently and acted as a fail safe unit to prevent the gas meter and GC. The cotton wool filter is a cylindrical column which is packed with dry wool in which it was mounted horizontally. The organic vapours which did not condense upstream in the process is condensed on the wool, and allowed only the non-condensable gases to pass through. Only a small fraction of the total liquids was actually collected in the cotton wool filter as experiments are carried out. The condensable gases are still at an extreme cold temperature before entering the cotton wool filter. The dry ice condenser and the entrance of the cotton wool filter condense the water in the air on the outskirts of the units. This would only produce a small amount of volatiles and too little for liquid analysis.

4.5.5.5 *Gas meter and Gas chromatography*

Once the non-condensable gases leave the cotton wool filter they pass through a gas meter which records the total volumetric throughput. The gas stream is then split between the vent and the gas chromatography, at which only a small amount of the volumetric gas is analysed.

The gas chromatography unit is a well established technique, which is used to identify and quantify gas composition streams. The gas composition is analysed for fixed intervals of time, and three columns are used to identify the compound stream, which are:

Molecular Sieve column: H₂, O₂, N₂, CO

Poropak Q column: CO₂

Picric acid column: C₁-C₄ compounds

Before any data can be recorded, a calibration is to be set and saved as a method in the program by the use of known compound standards. A known concentration is passed through the GC so that a calibration can be set for quantification purposes, but also to obtain specie residence time. The standard compounds are the same to those gases which are produced from pyrolysis, and then the peak areas are recorded for different concentrations to produce a “set” to allow for quantification analysis.

4.5.6 Limitations of 150 ghr⁻¹ pyrolysis rig

The Fractionation of biomass to different particle sizes would result in different pyrolysis characterises and product yields. This is due to:

1. Ash content and composition can vary with particle size
2. The cellulose/lignin ratio can vary with particle size

Since the ash and alkali metals content has a dominant effect on fast pyrolysis which leads to secondary reactions, the differences in ash content/composition between particle sizes for pyrolysis would affect the volatile product yields and compositions. If the small particles [<200 micron] are not sieved out then there will be a tendency towards more ethanol/methanol insoluble solids in the pyrolysis-oil (char) [137]. The reason for this is that there is only a single cyclone on the rig and this is optimised to remove the majority of the large particles without too much pressure drop.

In addition, attempting to pyrolyse larger fractions [i.e. a particle size range greater than 0.5mm] could lead to process difficulties such as feeder blockages and excessive char levels in the oil [due to poor cyclone separation of the smaller fractions] produced in the 150 ghr⁻¹ rig. Fast pyrolysis of larger particles [usually 355-500 micron range] can be fed however

encountering problems such as binding in the feeder or blockages in the feed tube. These phenomena often occur with needle-like particles which seem to be a fairly common problem with grasses. Agglomeration of the bed is unusual and has only occurred with a few feedstocks over the history of pyrolysis at Aston. It seems to occur for high ash feedstocks with particular inorganic elements present [perhaps a particular combination of K, Na and Ca].

4.6 Mass balance

A mass balance is usually conducted over a process to estimate its efficiency, and to make any improvements to optimise the system. Justified assumptions are usually associated with a mass balance to simplify calculations, however the fewer assumptions made the more complex the mass balance becomes, but resulting in a more realistic commercial scale process.

Biomass fast pyrolysis, produce three main products which are organics [high and low molecular weight volatiles], char and gas which will be the outputs for the mass balance, while the inputs are the weight of the biomass feedstock used. The experimental run to be expressed in percentage terms [on dry mass basis] for the amount of organic, char and gas produced. A good closure on the mass balance would be approximately 90-100 %. It is extremely difficult to duplicate runs with the same bed temperature, thus an average bed temperature is calculated, by manually recording the bed temperature every five minutes throughout the entire run and taking the average.

The products of fast pyrolysis have been separated into three categories, liquids, char and gas. The procedures for each category are described below as they define on how the mass balance was constructed. All parts of the complete system were weighed before and after the experimental run, to ensure a superior mass balance closure with an accuracy of ± 0.01 grams. The parameters measured include the furnace and reactor temperature, flow rates, volume of gas and composition.

4.6.1 Liquids

The two main liquids from fast pyrolysis are organics and reaction water, and together they are referred to as the total liquid yield.

The principle of weighing before the experiment and after the experiment is adopted to all the liquid collection systems. This is done since a small proportion of liquids and solids remain in units after the experiment and are not collected in the main oil pots. The amount of oil which remains in the condenser and EP are high in molecular weight and viscosity while being low in water content. Substantial amounts of these oils are left in the units and do not run down into oil pot 1.

In order to obtain the deposits of oil in these units a solvent such as methanol is used to remove the additional liquids from the condenser and electrostatic precipitator. These washings are kept and analysed. If a known amount of methanol [grams] is applied to wash the condenser and electrostatic precipitator, thus the additional weight after washing can be assumed to be organic liquid, water and char. The subtraction of the weight of washing from the original amount of methanol applied gives the amounts of organics, char, and water. Once this is carried out the remains in the condenser and EP will be assumed to be the char residue which will be included to the total char yield calculation.

The washings from the condenser and EP, once analysed will undergo vacuum filtration to remove the methanol and to obtain the original oil which was present in each unit. This is done so that a ratio of the oils produced in the condenser, EP and oil pot 1 can be mixed together for an overall oil which is representative of the biomass used from the pyrolysis experiment. Once the water and char content for each of the different oil fractions have been determined [chapter 5], it can be incorporated into the mass balance. Water in pyrolysis-oils is produced from dehydrating reactions during pyrolysis but also from its original moisture content from its feedstock. The reaction water produced will be calculated by subtracting the mass of the water content which is present in the total liquid yield from the original moisture content [mass] of the biomass.

4.6.2 Char

The total char yield is calculated from six parts of the process and are listed below:

1. Charpot
2. Deposits on transition pipe
3. Char coating the surface of quartz sand
4. Deposits of condenser
5. Deposits of EP

6. Char present in the pyrolysis-oil.

The char present on the coating of the sand, in the charpot and on the transition pipe can be easily calculated by the difference in weight between each of the units at the beginning of the run and after the run. This is done since it is assumed that these units remain at constant weight throughout the run, so any increase will be due to the char addition.

However char can also be blown and end up downstream of the process in the condenser and electrostatic precipitator especially on the walls and this can be calculated after washing with methanol [6]. The calculations of the char deposits which remain in the condenser and EP are found in section 4.5.1.

The organic liquid collected from all parts of the system also consists of smaller micro fine char [less than 20 microns]. A char content analysis on the oils is carried out using Whatman No.1 filter paper which has a 11 μm pore size. The filter papers are pre-dried in the oven at 105°C before analysis. They are then weighed in a microbalance and placed in a vacuum filtration unit, where it is washed with methanol. A known amount of pyrolysis-oil is injected on the methanol wet filter paper, where it is washed intensively with methanol again, until a non-coloured washing observed and collected in the beaker below. The filter paper is then replaced in the oven at 105°C for six hours and then cooled in desiccators. It is then re-weighed for the additional weight due to the char, and a percentage of char from the pyrolysis-oil can be calculated. An average percentage of char present in the pyrolysis-oil is approximately 0.1- 2 % wt.

4.6.3 Gas

Manual data readings are taken every five minutes from the total volumetric gas meter [Schlumberger total gas meter] which has units of cubic meters. This enables to calculate the total amount of gas produced throughout the run. From this line it is transported by a gas pump and divided into two streams, one stream leading to a gas chromatographic system known as the “line stream”, while the other line leads to a vent.

The GC analyses the gas for its gas contents which are nitrogen, carbon monoxide, carbon dioxide, methane, C₂ [ethane and ethylene] , C₃ [propane and propylene], n-butane and n-butylenes. The residence time from the GC corresponds to that particular gas under the

specific conditions. From the results of the GC it can then be determined how much each compound specie is present [grams] by multiplying the percentage volume for each specie by the total volume of gases [in m³] along with each compound density. This is then incorporated into the mass balance as weight percentage of dry feedstock basis.

Nitrogen will also be analysed, since the majority of the gas composition is nitrogen passing through the system. Since 6-18 l/min of nitrogen is used to keep the sand fluidised, as well as an additional 2-5 litres/minute for the feeder top and entrain flow. Due to this an increase of sensitivity must be carried out to identify the low concentration of gases ranging from 1% of CO₂ [total gas volume base] to 0.02 % for the n-butane and n –butylenes. All gas yields are reported as a weight percent of dry feed basis, which is calculated by dividing the weight of each gas with the weight of the dry feedstock.

4.6.4 Summary

Table 4-3 below summarises the analysis required out for an accurate mass balance.

Table 4-3-Smmary of methods for mass balances

Run Number	Experimental run number
Feedstock	Feedstock used
Reactor temperature[°C]	Average fluidised bed reactor temperature
Hot vapour residence time [s]	Average total hot space residence time
Feedrate in wet basis [ghr⁻¹]	Average feedrate of biomass entering reactor
Moisture content [mf wt%]	Moisture content of feedstock [chapter 5]
Ash [mf wt%]	Ash content of feedstock [chapter 5]
Particle size [mico meters]	Feedstock particle size range [chapter 5]
Run Time [minutes]	Run time of experiment
Wet Feed [g]	Weight of feedstock in wet basis
Dry Feed [g]	Weight of feedstock in dry basis
Water in Feed [g]	The amount of moisture in the feedstock
Organics (%)	Analysis method described in section 4.5.1
Char (%)	Analysis method described in section 4.5.2
Gas (%)	Analysis method described in section 4.5.3
Reaction Water (%)	Analysis method described in section 4.5.1
Total Liquids (%)	The sum of organics and reaction water
Closure (%)	The accuracy of mass balance (in=out)
Methane (%)	Yield of methane produced
Carbon dioxide (%)	Yield of carbon dioxide produced
Carbon monoxide (%)	Yield of carbon monoxide produced
Hydrogen (%)	Yield of hydrogen produced
Ethylene (%)	Yield of ethylene produced
Ethane (%)	Yield of ethane produced
Propane (%)	Yield of propane produced
Propylene (%)	Yield of propylene produced

4.7 Pyrolysis-oil background

Pyrolysis-oils derived from biomass are an alternative source of fuels producing a renewable source of energy, suitable for the applications of transport fuels, heat, and power generation. However it is still a relatively new technology and its research knowledge lags behind, in comparison to that of combustion and gasification. Pyrolysis-oil quality and quantity depends on five major variables: two being process variables and three being feedstock variables. The process variables are heating rate and final reactor set point temperature, while the feedstock variables are alkali metal content, organic composition and particle size [after processing] [6]. It is speculated by researchers that reducing lignin content in biomass would produce a more stable pyrolysis-oil by reducing the chances of phase separation by increasing solubility, stability and increase homogeneity [130, 142], however this is still not proven. Pyrolysis-oil problems such as fuel quality, phase separation, stability and fouling issues are potential limitations on thermal processes. The majority of heavier molecular weight derived compounds present in pyrolysis-oil tend to originate from the lignin monomers. Thus a biomass with lower lignin content could help reduce the heavier molecular weight compounds present in pyrolysis-oil and produce a more homogenous liquid. Pyrolysis-oils made from biomass contains a wide range of derived compounds, and is thought as a micro emulsion of pyrolytic lignin dispersed in aqueous solution of anhydrosugars and light oxygenated hydrocarbon such as organic acids and aldehydes [143]. The level of nitrogen content will contribute to the colour of the pyrolysis oil from blackish reddish to a dark green tinge [144]. Traditional pyrolysis-oil is a black liquor, with a density of 1200 kg/m^3 and a viscosity between 20-1000 cP depending on the water quantity in the suspension [1]. The oil also possesses polar charges even though it has no presence of metal/sulphur elements, and does not mix easily with hydrocarbons. Composition of pyrolysis-oil is a mixture of acids, alcohols, aldehyde, esters, ketenes, sugars, guaiacol's, syringol's, furans and multi functional compounds [86].

4.7.1 Pyrolysis-oil uses

Pyrolysis liquids which are derived from biomass can be used for different applications such as for transport fuels for diesel engines, heat and power generation, gas turbine, combustion engines, adhesives, chemical generation and food flavouring [144]. Electricity production of over 500 hours has been achieved by the use of pyrolysis-oil including 1.4 MW energy, and

now large companies are modifying gas turbines to use pyrolysis-oil as a feedstock [144]. Fine compounds such as levoglucosan, resins and slow release fertilisers have been produced from pyrolysis-oil, making it an attractive renewable source of chemical production for future sustainability plants. The quality level for pyrolysis-oils for each application varies to the needs of the commercial process. An example of this is, the chemical industry [bio-refineries] for chemical generation requires high yields of certain chemicals present in the pyrolysis-oil, while for combustion applications the level of char and ash content in the pyrolysis-oil must be as low as possible.

4.8 Pyrolysis-oil analysis

10 quality parameters are known for the assessment of pyrolysis-oil quality, and they are used to relate to nature of the biomass, and the process parameters. A number of quality parameters have been investigated and compared by producing the pyrolysis-oil for all the feedstocks, by holding the process parameters as constant as possible. A commercial pyrolysis-oil maintains its stability in terms of its chemical composition, viscosity, molecular weight, the number of different molecules and its water content. This would be only achieved if the oil had a low heterogeneity of compounds, and having lower molecular weight compounds present. A number of indices were used to understand how the oil changes with respect with time to understand its stability behaviour.

The quality parameters assessed in this work are:

1. Molecular weight of pyrolysis-oil
2. compound identification and quantification
3. Yields of char and pyrolysis-oil and water content
4. pH
5. Elemental content
6. Viscosity analysis

The final oil used for analysis is a mixture of the oils produced in the condenser, EP and oil pot 1 from the end of the experiment. Mixing the liquid product meant that an oil was obtained which was representative of the feedstock [as fractions are deposited through out different parts of the equipment]. The entire analysis will be carried out within a few days after the pyrolysis-oil is made, as well carrying out rapid ageing tests by putting the oil in a closed vessel and

heating it to 80°C for 24 hours [145] allowing for rapid aging of pyrolysis liquids and by repeating the analysis tests.

4.8.1 Molecular weight: Gel Permeation Chromatography

Gel permeation chromatography [GPC] measures the molecular weight distribution of the oil. The GPC column was calibrated before trials on polystyrene having a molar mass of 161-72200 g/mol by detectors with a UV photometer range of 280 nm [10]. The GPC was set up at a temperature of 40°C with a column of 300 and 600mm with a pore size of 50 and 100 Å. The pyrolysis-oil was diluted in THF [HPLC grade: Tetrahydrofuran, Aldrich 99.5 %] to make a solution of 5 mg/ml. The pyrolysis-oil with the THF solution was first filtered from its char content by using filter paper of 0.2 µm. The pyrolysis-oil/THF solution was then added to toluene to act as a flow marker standard. Approximately 100 µl were injected to the column. Curves and calculations processing were conducted on Cirrus GPC software, where [Mn] is the number of average molar mass, [Mw] molecular weight at highest peak [Mp] and polydispersity index [PD=Mw/Mn] calculated from refractive index [RI].

The higher molecular weights present in the pyrolysis-oil will increase the average molecular weight. Therefore molecular weight stability was used to gain insight on how the molecules present in the pyrolysis-oil changes with respect to time.

The GPC stability is stated as:

$$Mw_{STABILITY} = \frac{Mw_{AGED} - Mw_{FRESH}}{Mw_{FRESH}}$$

This was calculated for each sample to determine how much the oil changed after aging, using digit indicators where 0 being no change and 1 being doubled in average molecular weight.

4.8.2 Compound identification and quantification: liquid GC/MS

Compound identification of biomass and pyrolysis-oil has been covered in Chapter 4 Section 4.2. A number of compound calibrations can be used to quantify compounds, but more commonly used in the bio-energy communities is to dilute the pyrolysis-oil in acetone to act as a transport fluid and reducing contamination of the column and of the detector [145]. The oils produced on the 150 ghr⁻¹ and 1 kghr⁻¹ rig were subjected to liquid injection in the GC/MS in

order to correlate the composition and amounts of cellulose/derived compounds to that which was produced from solid biomass pyrolysed in the pyroprobe-GC/MS. Three oils were produced from the 150 ghr -1 rig which, oil pot 1 (possessing the majority of the organic fractions), oil pot 2 (the lighter organic fraction with high quantity of water) and the evaporated washings of the EP and condenser (consisting aerosols, and much higher molecular weight compounds similar to that of oil pot 1) in which all were subjected to characterisation. Approximately 0.20 ml of the pyrolysis-oil was measured and mixed with 0.8 ml of high grade [HPLC] acetone; this gave a 20 % concentration of pyrolysis-oil in the pyrolysis-oil/acetone solution. For viscous oils which were not able to be filled by the pipette, an average pyrolysis-oil density of 1.2 kg/litre [1.2 g/ml] was used to measure the mass of pyrolysis-oil needed to obtain the same concentration using the equation:

$$\rho_{BIO-OIL} = \frac{MASS(grams)}{Volume(ml)}$$

This gave a mass of approximately 0.25 grams of pyrolysis-oil in 0.8 ml of acetone to obtain the same concentration. The solution of pyrolysis-oil/acetone was then filtered through a Millipore millex-GW nylon filter of 0.2 μm filter, to remove char and tars from the solution, to reduce any risk of blocking or deposits on the GC column.

A gas chromatography with a split ratio of (1:25) was used for compound separation. The injector temperature: 280 °C with a detector temperature: 280 °C. The carrier velocity is at 38cm/s, and the temperature program begins with 45°C for 4 minutes, and using a heating rate of 4°C/min to 240°C; 39°C to 280°C. GC column: The semi polar column PP1701 or DB 1701 (60 m by 25 μm with a 0.025 μ film thickness) with a chemical composition of 14% cyanopropyl-phenyl 86% dimethylpolysiloxane which shows a different selectivity to (phenyl) dimethylsiloxane phases because of the functional cyano groups. The GC-eluted part of pyrolysis liquid is typically 25-40 wt % of wet liquid, about 70-90% of the eluted fraction can be identified [48].

4.8.3 Yield determination and water content analysis: Karl Fischer Coulometer

Organic yield, char and gas yields have been discussed in detail in Chapter 4 Section 4.5. However water content was only mentioned briefly. Karl Fischer coulometer enables to identify [in percentage] the amount of water present in pyrolysis liquids. A Metrohm model

758 KFD coulometer was used to analyse the pyrolysis-oil pots and washings. The system was first calibrated with HPLC water to ensure a reading of greater than 99 % was achieved, this was repeated twice to gain a higher level of accuracy and reliability with a standard deviation of less than 1 and an accuracy of ± 0.01 mf wt %. If the reading was less than 99 % for HPLC water, then a factor was computed into the program to ensure that future readings would give a reading result of greater than 99 % for the HPLC water. A known amount of pyrolysis-oil from the different fractions was injected in the KFC, and this was repeated three times for reliability purposes with a standard deviation of less than 0.5 % being acceptable. Oil pot one gives a reading of 10-30 %, while oil pot two gives a reading of 50-60 %.

4.8.4 PH- Metrohm PH meter

A Metrohm model 713 Ph meter was used to test the acidity of the pyrolysis-oil.

4.8.5 Elemental method

ICP and CHN analysis were carried out by Rothamstead research to determine metals [ppm] and elements (%). Metals and other inorganic components were determined by digestion, and carried out by Accuris ICPES [Induced coupled plasma emission spectrometer] using the following procedure: The plant materials was dried for four hours at 80°C in an oven and cooled by a desiccator. 0.250 g of the oven dried material was placed in a 25 ml digestion tube, while 5 ml of nitric or perchloric acid are added around the side of the tube ensuring the sample is washed down into the tube. It was then mixed by swirling and held at room temperature for 2 hours [140] prior to heating overnight. 5ml of 25 % of HCl was then added and the mixture heated to 80°C. After cooling the samples were subjected to ICP analysis.

4.8.6 Viscosity- viscometer

Fluid dynamics books often refer viscosity as the fluids internal resistance to flow and can be measured by measuring the distance travelled or by applying a force [stress] until the liquid breaks down. Viscosity is an important in the oil industry as it needs to be transported by pumps and injected into chambers.

A Gebr Haake GmbH rotovisco1 viscometer is used to determine viscosity. 5 ml of the pyrolysis-oil is injected into the viscometer at ambient conditions and heated to 40°C. The device measures the dynamic viscosity of the liquid at 25°C, by the use of double gap cylinder

sensor. Prior to the measurement the rotor is turned to a distance of 0.5 mm from the bottom of the measurement cylinder in order to zero and to obtain a set point. This procedure is also repeated after the oil was injected. The shear is applied and a number of peaks are produced, and displayed on the RheoWin pro software. The degassing step allowance gives an opportunity to remove gas/air bubbles are emulsified in the pyrolysis-oil. Once this is carried out the shear velocity is increased within 90 s up to the test shear velocity, followed by a decrease at the same ramp. The final temperature at which viscosity is measured is 40°C, as it is found to be the optimum temperature where less deviation occurs within oil viscosity analysis [146].

Viscosity index [VI] is calculated by:

$$VI = (\mu_F - \mu_i / \mu_i)$$

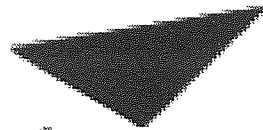
Where μ_F is the final viscosity (80°C for 24 hours)

And μ_i is the initial viscosity (25°C for 24 hours)

The lower the VI number the more stable is the pyrolysis liquid, and if 0 is achieved it would be completely stable liquid. The stability of the pyrolysis-oil is strongly linked to the viscosity of the pyrolysis-oil, and a term known as viscosity index [VI] measures the change in viscosity with time to gain an insight of stability.

4.9 Stability theory

Pyrolysis-oils made from biomass are a single phase, low viscosity with high conversion yields. During storage of pyrolysis-oil, the oil becomes more viscous due to chemical and physical changes due to volatile loss and reactions. This is due to the reactions occurring from the degradation of biomass within the pyrolysis reactor during pyrolysis. The volatiles produced do not allow the products within the vapours to reach thermodynamic equilibrium, as they are condensed to form the oil. These phenomena would allow the products in the pyrolysis-oil to react with each other within the oil, until product stability is formed. Figure 4-8 shows the increase in viscosity of three different hardwoods over 90 days demonstrating pyrolysis oil instability with ageing



Aston University

Illustration removed for copyright restrictions

Figure 4-8 - The effect of aging on pyrolysis-oil [86]

Aging tests have been developed [86, 146-148] to predict the rate of aging, if the pyrolysis-oil is stored up to one year. Diebold concluded that the aging of the pyrolysis-oil occurs much faster at higher temperature [86, 149], but can be reduced by storing the pyrolysis-oil in a cool place to slow reaction mechanisms and kinetics. Figure 4-9 from [86] shows that the viscosity increases with molecular weight, suggesting that the lower the average molecular weight, the



Aston University

Illustration removed for copyright restrictions

Figure 4-9 - Average molecular weight vs. viscosity of pyrolysis-oil [86]

Aging the pyrolysis-oil increases the average molecular weight and viscosity, this implies that the compounds present in the pyrolysis-oil moves to thermodynamic equilibrium, and can result in the oil separating into two phases. The phase separation produces a tarry liquor [high in molecular weight and viscosity] and the other being an aqueous solution. This suggests that water influences the homogeneity of the pyrolysis oil.

4.9.1 Factors that determine quality and quantity of pyrolysis-oil

The variables [feedstock and process] which effect pyrolysis-oil composition, quality and yield have been well cited in literature [8, 10, 26, 27, 33, 54, 92, 151, 152]. It is well established that yield and composition of the pyrolysis-oil is a complex interrelation between many of the feedstock and process variables which include:

- Biomass specie (organic and inorganic specie)
- Heating rate and temperature of pyrolysis
- Residence time of vapours in the hot space
- Secondary cracking vapours passing through char
- Efficiency of cyclone to remove char
- Efficiency of condenser to condensate volatiles
- Water content of pyrolysis-oil
- Length and temperature of pyrolysis oil storage
- Chemical composition and amounts in pyrolysis-oil.

4.9.2 Inorganic species in pyrolysis-oil

Metals present in the char depend on the efficiency of cyclones, the quantity of char produced and the inorganics which end up in vapour downstream of the process. Diebold's review on pyrolysis-oil chemical and physical properties showed that inorganic species like char, Ca, Cl, Fe, Mg and Zn promotes catalytic reactions during aging.

4.9.3 Chemical mechanisms within pyrolysis-oil

Pyrolysis-oil consists over 180 compounds [153] and as much as 400 organic compounds in some literature [38, 40]. The different types of reactions which could possibly proceed are many to state, however Diebold's review [86] stated that 9 major reactions take place and which all agree with literature findings [52, 53, 101, 102, 154].

5 INVESTIGATION OF REFERENCE FUELS ON FAST PYROLYSIS AND PYROLYSIS-OILS

This chapter explores the relationship between the different biomass composition and its yields as predicted by analytical pyrolysis, against the actual organic yield from fast pyrolysis and the quality of the oil produced. This chapter also investigates the oil composition via liquid GCMS to gain an insight into how the pyrolysis-oil changes during aging and at different parts of the pyrolysis equipment.

5.1 Introduction

The six reference fuels [defined in Chapter 1] are willow, straw, switchgrass 2004, Reed Canary grass 2004, switchgrass 2005 and Reed Canary grass 2005. These reference fuels were used to correlate predicted yields [and derived compounds] from analytical pyrolysis, and relate it to the organic yield composition obtained from Aston's 150 ghr⁻¹ fast pyrolysis reactor as well as to act as a bench mark to the rest of the work carried out in this research.

The temperature of analytical pyrolysis and Aston's 150 ghr⁻¹ reactor was at 500°C [$\pm 10^\circ\text{C}$], with all the reference fuels having the same particle size range [see chapter 5]. A reference temperature of 500°C was used, since this is the temperature that maximum liquid yields are achieved in fast pyrolysis for a wide range of biomass samples.

5.2 Experimental

The reference fuels were subject to TGA, pyroprobe-GC/MS and fast pyrolysis rig trials. The oils produced from Aston's 150 ghr⁻¹ fluidised bed reactor were collected and analysed. The fast pyrolysis rig used for conversion of the reference fuels was Aston 150 ghr⁻¹ fluidised bed reactor rig [see Chapter 4 Section 4.6]. Mass balances were conducted with a closure level of 90 % or above so that feedstocks can be compared.

5.2.1 Reference fuel characterisation and analytical pyrolysis conditions

The feedstock characterisation has been described in Chapter 5, Section 5.1. The TGA and pyroprobe methods and conditions have been described in previous Chapter 4, Section 4.3.

5.3 Results & Discussion

5.3.1 Reference fuel characterisation

The elemental analysis of the six reference fuels and their ash content were described in Chapter 5 Section 5.1 and are summarised in Table 5-1 and Table 5-2 below.

Table 5-1 – Chemical analysis of reference fuels

Sample	C _{DAF} (%)	H _{DAF} (%)	N _{DAF} (%)	O _{DAF} (%)	Moisture (%)	Lignin (%)	ASH (%)	HHV (MJ/KG)
Willow	47.78	5.90	0.31	45.92	7.76	19.62	1.34	18.86
Switchgrass 2004	44.77	5.79	0.31	49.03	8.30	8.56	4.30	17.30
Reed canary grass 2004	45.36	5.81	0.34	48.39	7.86	9.33	5.07	17.57
Straw	44.94	5.75	0.47	48.75	9.14	7.51	6.29	17.29
Switchgrass2005	46.35	5.93	0.31	47.31	2.92	8.20	4.26	18.04
Reed canary grass 2005	46.11	5.89	0.36	47.54	3.85	9.10	4.45	18.31

Table 5-2 - ICP analysis of reference fuels [ppm]

Sample	Ca (ppm)	K (ppm)	Mg (ppm)	Na (ppm)	Total Alkali metals (ppm)
Willowchip	3132	1956	385	58	5532
Switchgrass 2004	6173	716	542	158	7590
Reed canary grass 2004	2783	1455	598	74	4911
Wheat straw	5332	9621	902.3	101	15957
Switchgrass 2005	8847	880	1204	161	11093
Reed Canary Grass 2005	1342	1725	664	109	3840

5.3.2 TGA and pyroprobe-GC/MS results

Table 5-3 shows the results of the TGA analysis on a dry mass feed basis, where the char residue was measured at 500°C, and the temperature at which maximum rate of volatilisation of cellulose [T_{max}]. The TG volatile and gas yield was calculated by subtracting the char residue at 500°C from 100 percent. The TGA plots are found in APPENDIX I.

Table 5-3 - TGA results of reference fuels

Sample	TGA char at 500°C yield [%]	TGA Volatile & gas yields [%]	Temperate of maximum rate of cellulose volatilisation [°C]
Willowchip	19.3	80.70	354.87
Switchgrass 2004	21.61	78.39	359.36
Reed canary grass 2004	24.45	75.55	360.85
Wheat straw	29.86	70.14	336.05
Switchgrass 2005	19.3	80.70	364.6
Reed Canary Grass 2005	25.28	74.72	359.84

It can be seen that as T_{max} increased the ash content decreased, which overall resulted in the shifting of the maximum rate of volatilisation to higher temperatures. This suggests that metals influence the yields, rates, and temperatures of maximum yields. This has been described further in chapter eight.

Table 5-4 shows the key compounds derived from fast pyrolysis for the reference fuels, and the percentage distribution as determined by pyroprobe-GC/MS. The selected markers have been summated together to make a total area, at which each individual compound was divided by the sum of the total to give a percentage contribution.

Table 5-3 and Table 5-4 are in agreement, suggesting that the yields of volatiles increase as the lignin increase while decreasing in ash. Willow had the highest yield from analytical pyrolysis and the lowest char residue, while the worst reference fuel was the straw which gave a high char content and low volatile yield which agrees with reference [159].

Table 5-4 - Pyroprobe-GC/MS results of reference fuels

Name of compound	CODE	Willow chip	Switch 2004	RCG 2004	Straw	Switch 2005	RCG 2005
2,3-Butandione	Cellulose	2.10	2.05	2.05	4.36	2.26	2.10
Hydroxyacetaldehyde	Cellulose	20.07	17.89	24.35	23.61	24.13	22.07
Hydroxypropanone	Cellulose	6.51	6.27	7.82	18.90	7.53	7.94
2-Furaldehyde, 2-Furfural	Cellulose	3.95	6.26	6.26	6.38	6.97	5.32
2 FURANMETHANOL	Cellulose	1.58	1.20	1.18	1.90	1.26	1.60
(5H)-Furan-2-one	Cellulose	2.63	1.36	1.99	2.48	1.79	2.23
4-Hydroxy-5,6-dihydro-(2H)-Pyran-2-one	Cellulose	6.08	15.81	14.10	3.66	25.11	13.21
Phenol	Lignin	0.89	0.58	0.50	1.15	0.56	0.64
Guaiacol	Guaiacol	2.23	2.69	2.70	4.82	3.18	2.69
4-Vinyl guaiacol	Guaiacol	27.97	17.85	18.85	14.31	14.38	23.33
Eugenol	Guaiacol	0.60	0.48	0.44	0.24	0.55	0.43
5-Hydroxymethyl-2-furaldehyde	Cellulose	1.46	1.99	2.75	0.87	2.40	2.09
Pyrocatechol	Lignin	0.38	0.21	0.26	1.03	0.23	0.35
Syringol	Syringol	5.13	0.94	1.86	4.21	1.16	2.85
Vanillin	Guaiacol	0.75	1.08	1.21	1.09	1.26	1.14
4-Vinyl syringol	Syringol	5.66	0.80	1.52	2.79	1.00	2.13
Levoglucozan	Cellulose	3.47	17.37	5.22	1.76	0.27	3.71
4-Propenyl syringol (trans)	Syringol	4.71	0.83	1.39	1.41	0.15	2.02
Syringaldehyde	Syringol	1.36	0.21	0.26	0.41	0.15	0.45
Acetosyringone	Syringol	0.45	0.18	0.29	0.67	0.22	0.31
Coniferyl alcohol	Guaiacol	0.66	0.50	0.72	1.54	0.56	0.66
Guaiacyl 4 ethyl	Guaiacol	1.36	3.47	4.26	2.44	4.88	2.75
		100.0	100.0	100.0	100.0	100.0	100.0
Cellulose derived compounds		47.86	70.20	65.72	63.91	71.72	60.25
Guaiacyl groups		33.57	26.08	28.19	24.43	24.81	30.99
Syringyl groups		17.31	2.95	5.32	9.48	2.68	7.77
Unknown lignin compounds		1.26	0.78	0.76	2.18	0.79	0.99
TOTAL LIGNIN		52.14	29.81	34.27	36.09	28.28	39.75

5.3.3 Fast pyrolysis experiments on reference fuels

5.3.3.1 *Mass balance results*

The mass balance methodology has been discussed in Chapter 4 Section 4.5. Table 5-5 shows the mass balance closure for the reference fuels on the 150 ghr⁻¹ fast pyrolysis reactor on a dry mass feed basis.

Table 5-5 - Mass balances of fast pyrolysis experiments on the reference fuels on Aston's 150 ghr⁻¹ fast pyrolysis rig

Run Number	141-06	139-06	102	142-06	143-06	157-158
Feedstock	Willow 2004	Switchgrass 2004	RCG 2004	Straw 2004	Switchgrass 2005	RCG 2005
Reactor temperature[°C]	507	500	502	509	508	505
Hot vapour residence time [s]	0.75	0.91	0.73	0.82	0.76	0.34
Feedrate in wet basis [ghr ⁻¹]	62.59	72.07	34.30	42.56	26.48	60.60
Moisture content [mf wt%]	7.76	8.30	7.86	9.14	2.92	3.85
Ash [mf wt%]	1.34	4.30	5.07	6.30	4.26	4.45
Particle size [micro meters]	250-350	250-350	250-350	250-350	250-350	250-350
Run Time [minutes]	60.00	85.00	85.10	95.00	100.00	60.00
INPUT						
Wet Feed [g]	62.59	102.10	54.36	67.39	44.14	60.60
Dry Feed [g]	54.83	93.63	50.09	61.23	42.85	58.27
Water in Feed [g]	8.30	8.47	4.27	6.16	1.29	2.34
YIELDS [mf wt %]						
Char	20.92	24.73	22.03	31.92	20.75	23.70
Organics	52.93	51.49	47.18	24.85	50.70	41.31
Gas	9.29	7.92	11.13	15.62	11.31	13.69
Reaction water	15.93	12.35	13.08	25.67	11.32	15.46
Total Liquids	68.86	63.84	60.26	50.52	62.02	56.77
Closure (%)	98.31	96.49	93.43	98.24	94.08	90.54
GAS YIELDS [%]						
Methane	5.71	6.40	2.44	4.58	6.60	6.46
Carbon dioxide	60.26	45.11	60.62	65.67	30.98	37.20
Carbon monoxide	25.21	43.86	32.40	25.65	53.57	50.38
Hydrogen	0.76	1.04	0.47	0.47	1.04	0.93
Ethylene	1.68	2.77	1.27	0.63	2.67	2.75
Ethane	5.61	0.60	2.35	2.47	3.24	0.58
Propane	0.10	0.11	0.11	0.13	0.93	0.10
Propylene	0.67	0.11	0.34	0.39	0.97	1.58

It can be seen from Table 5-5 that the results from each reference fuel are comparable to each other, since reactor temperature and the hot vapour residence time are within a good standard deviation of each other as well as having a mass balance closure of greater than 90 %. The ash and moisture results were taken from Table 5-1, and incorporated into Table 5-5 to calculate the actual mass feed in dry weight and ash contribution in the biomass fed. The minimum runtime used from these experiments was sixty minutes, to ensure an accurate mass balance closure, with enough oil produced for all analysis which is mentioned in section 5.3. The results show that the total liquid yield [mf wt%] increases as lignin increases, while the ash content decreases. This has been suggested in the past by previous researchers [6, 10, 26] as well as agreeing with the results from analytical pyrolysis results. An overview of the table and the methods used for calculations can be found in section 4.6.5. Figure 5-1 shows that as ash content decreases, the total liquid yields increases at the expense of the char and gas in reference to Table 5-5, as well as the *Lolium & Festuca* grasses data found in Chapter 7.

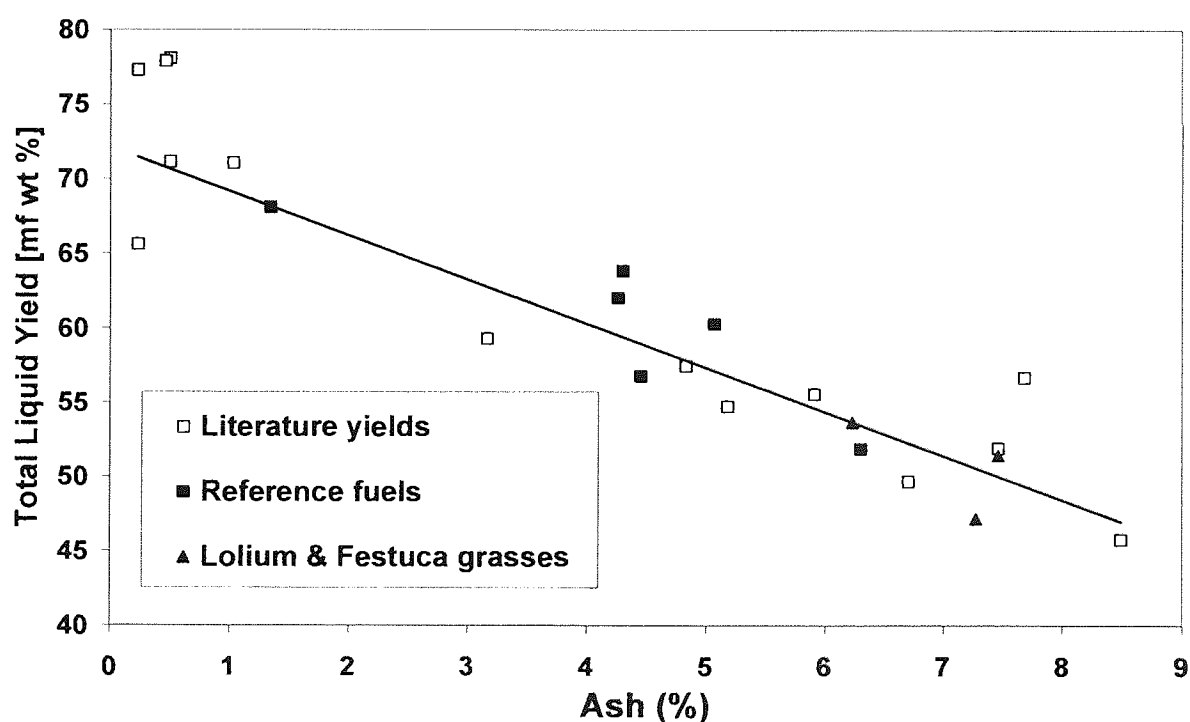


Figure 5-1 - Comparison of Total liquid yields from the reference fuels and other feedstocks used in this research in comparison to literature results.

This is due to the alkali metals present in the biomass having the dominate effect on fast pyrolysis as shown in Figure 5-2, where the main alkali metals sodium and potassium are plotted against pyrolysis product yields. The ash consists of the majority of the metals as oxides and usually ends up in the char. It is well stated in the literature that the char and alkali metals possess a catalytic effect on the thermal degradation of biomass during fast pyrolysis, and having the ability to shift yields and optimum temperatures to lower degradation temperatures and affecting the yields [refer to chapter eight for a more comprehensive analysis]. The total liquid yields for the reference fuels and the *Lolium* and *Festuca* grasses [refer to chapter 7] were compared to results from literature [6, 10, 92, 160, 161] for total liquid yields. The results from this study and that of the literature are shown in Figure 5-1. It shows that the results of the reference fuels and the *Lolium* and *Festuca* grasses on Aston's 150 ghr⁻¹ fluidised bed reactor are in good agreement to researchers published data.

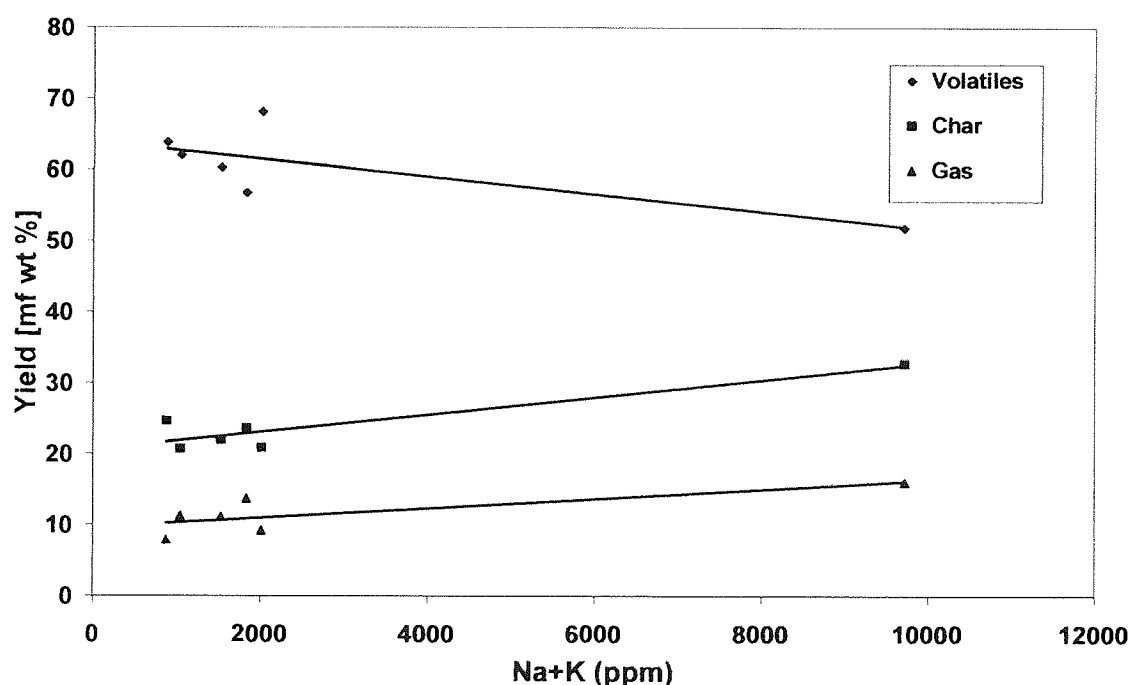


Figure 5-2 - The effect of Na and Potassium on total pyrolysis product yields

It can be seen in Figure 5-2 that more data is needed from feedstocks which have a sodium and potassium content of 2000<10,000 to ensure that a linear relationship exists and statistically correlated.

5.3.3.2 Oil pot 1 and Evaporated washings composition

The heavy organic oil fraction found in oil pot 1 and the evaporated washings of the condenser and EP were subjected to liquid-GC/MS for oil characterisation. This was done to investigate how the oil composition varies from different types of biomass and different parts of the equipment. The heavy organic oil fraction [oil pot 1 and the evaporated oils] had similar composition; Figure 5-3 shows oil pot 1 of the willow oil produced, while Table 5-6 shows compounds identification for the willow oil.

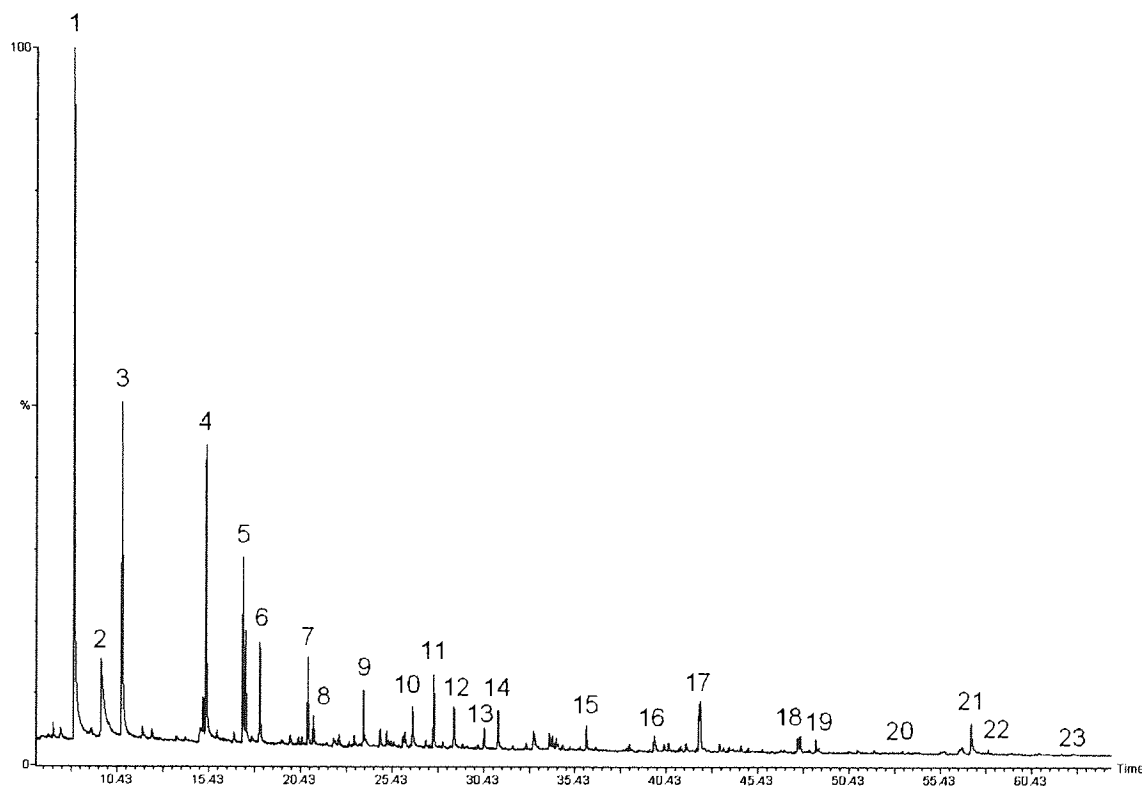


Figure 5-3 - Chromatogram of oil pot 1 from Willow

Table 5-6 – Typical compounds found in oil pot 1 and evaporated oils

Peak No.	Name	RT (min)	Mz	Origin
1	Hydroxyacetaldehyde	8.07	15/31/60	Cellulose
2	Acetic acid	9.67	32/43/45/60	Cellulose
3	Hydroxypropanone	10.72	32/43/74	Cellulose
4	unknown	15.277	43/73/74	Cellulose
5	Butanedial	17.28	29/43/57/58/86	Cellulose
6	2-Furaldehyde	18.239	32/39/82/95/96	Cellulose
7	1-Acetyloxypropane-2-one	20.904	32/43/86/116	Cellulose
8	Tetrahydro-4-methyl-3-furanone	21.13	32/43/72	Cellulose
9	Dihydro-methyl-furanone	23.864	32/55/69/98	Cellulose
10	(5H)-Furan-2-one	26.56	32/55/84	Cellulose
11	4-Hydroxy-5,6-dihydro-(2H)-Pyran-2-one	27.69	32/58/114	Cellulose
12	2-Hydroxy-1-methyl-1-cyclopentene-3-one	28.82	32/69/112	Cellulose
13	Phenol	30.46	32/66/94	Cellulose/ Lignin
14	Guaiacol	31.22	81/109/124	Lignin –G
15	4-Methyl guaiacol	36.05	32/44/123/138	Lignin –G
16	Guaiacol, 4-ethyl	39.771	137/152	Lignin –G
17	4-Vinyl guaiacol	42.29	107/135/150	Lignin –G
18	Isoeugenol (trans)	47.473	131/149/164	Lignin –G
19	Vanillin	48.621	109/151/152	Lignin –G
20	4-Vinyl syringol	53.36	137/165/180	Lignin-S
21	Levoglucosan	57.13	57/60/73/98	Cellulose
22	Acetosyringone	60.90	153/181/196	Lignin-S
23	Coniferyl alcohol	62.38	91/124/137/180	Lignin-G

5.3.3.3 Oil pot 2 composition (low molecular weight compounds)

The light organic oil fraction produced in oil pot 2 was also subjected to liquid-GC/MS analysis for all the oils produced from the reference fuels. Figure 5-4 shows the light organic oil fraction of oil pot 2 while Table 5-7 shows the compounds identified for the light organic oil fraction. It is shown that the light oil fraction consists of only light organic compounds, and due to the fact that the oil comprises of approximately 60 % water as measured by KFC. It can be concluded that the light organic oil fraction is made of low molecular weight compounds which are soluble in water as the oil did not phase separate.

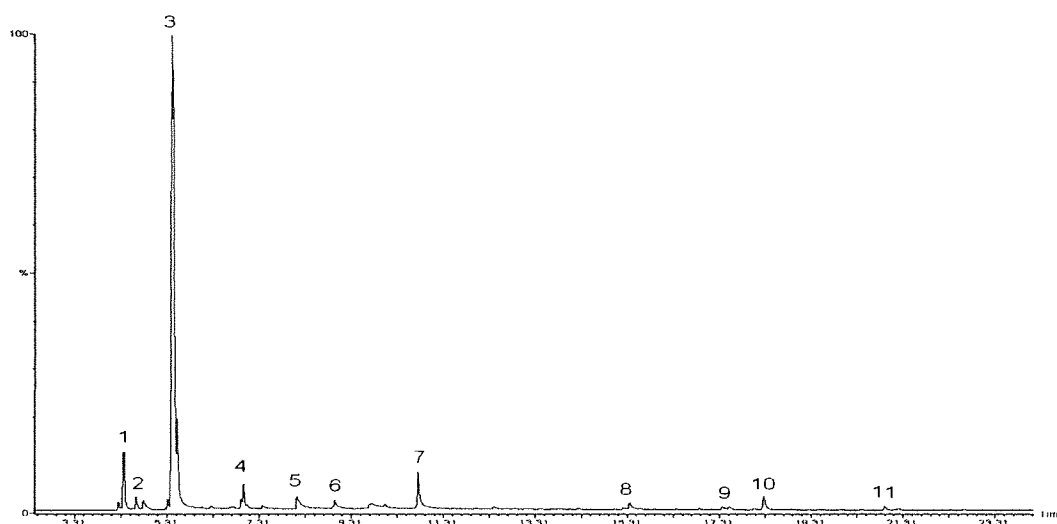


Figure 5-4 - Chromatogram of oil pot 2 from Willow

Table 5-7 – Typical compounds found in oil pot 2

Peak No.	Name	RT (min)	Mz	Origin
1	Methanol	4.383	29/30/32/44	Cellulose
2	Acetaldehyde	4.63	29/32/42/43/44/69	Cellulose
3	Acetone	5.42	29/41/44/57/59	Cellulose
4	2,3 Butanedione	6.98	43/86	Cellulose
5	Hydroxyacetaldehyde	8.14	31/42/60	Cellulose
6	2-butenal (cis or trans)	8.96	39/41/69/70	Cellulose
7	Hydroxypropanone	10.760	43/74	Cellulose
8	3-Hydroxypropanal	15.364	43/73	Cellulose
9	unknown	17.523	32/43	Cellulose
10	2-Furaldehyde	18.29	32/3982/95/96	Cellulose
11	1-Acetyloxypropane-2-one	20.904	32/43/86/116	Cellulose

5.3.3.4 Relating total liquid yield to pyroprobe-GC/MS yield

The total liquid yield results for the reference fuels were compared to the hypothetical yields [area] from the pyroprobe-GC/MS and are shown in Figure 5-5.

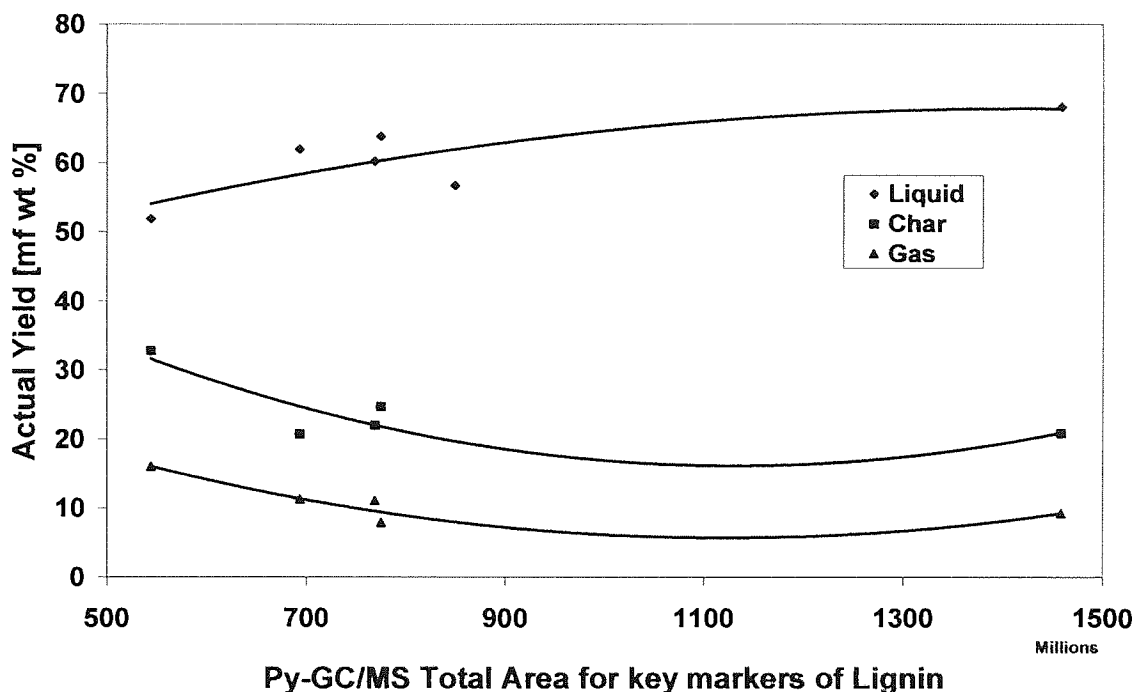


Figure 5-5 - Relationship between pyroprobe-GC/MS yields to laboratory scale total pyrolysis liquid yields

The relationship between the predicted analytical pyrolysis results against the total liquid yield from fast pyrolysis are in agreement with each other; however more feedstocks are needed to create a greater picture of this relationship. This relationship however is not absolute, but only acts as an indicator to predict total liquid yields between biomasses. This is due to the high standard deviation between runs of the same feedstock using analytical pyrolysis, which results from sample inhomogeneity of the raw biomass. This relationship indicator can demonstrate a screening methodology for different types of biomass to predict total liquid yields and composition. In the case of the reference fuels, willow had the highest area of compounds from analytical pyrolysis analysis to that of any other reference fuels, thus suggesting that it will possess the highest total liquid yield to that of any other standards.

5.3.3.5 Oil quality analysis of reference fuels

The oils produced from the fast pyrolysis experiments [fluidised bed reactor] were subjected to analysis to investigate their quality and stability [methodology found in Chapter 5 Section 5.3]. It can be seen from Table 5-8 that as the water content in the oil increases, the heating value decreases. This is due to the level of ash content of the biomass as suggested by literature [162] resulting in catalytic cracking of the vapours to produce a high yield of reaction water.

Table 5-8 - Oil quality analysis of reference fuels

	Willow 2004	Switchgrass 2004	Switchgrass 2005	RCG 2004	RCG 2005	Straw 2004
Water content, [mf wt %]	17.41	24.70	16.90	23.20	16.32	47.40
Char content, [mf wt %]	0.40	0.77	0.81	0.22	0.56	0.62
Elemental analysis [mf %]						
C	43.17	38.30	42.62	38.42	43.35	28.2
H	7.15	7.42	7.11	7.89	6.98	8.78
N	0.10	0.10	0.10	0.10	0.10	0.095
S	0.10	0.10	0.10	0.10	0.10	0.1
O	49.49	54.08	50.08	53.49	49.48	62.83
HHV [MJ/kg]	18.35	16.43	17.98	17.07	18.14	13.56
LHV [MJ/kg]	16.79	14.81	16.43	15.34	16.62	11.64
GPC analysis [g/mol]						
Average Mw	517	468	438	470	455	468
Average Mw of aged oil	689	597	580	635	605	575
Mw Difference	172	129	142	165	150	107
Mw Index	0.33	0.28	0.32	0.35	0.33	0.23
Mn	350	328	305	322	326	300
Aged oil Mn	409	380	368	387	345	337
Mp	243	243	238	309	274	238
Aged oil Mp	485	356	243	356	302	249
Polydispersity	1.47	1.43	1.44	1.46	1.34	1.56
Aged oil Polydispersity	1.68	1.57	1.58	1.65	1.61	1.71
Viscosity@40°C, cp	53.24	34.18	34.67	31.60	35.50	17.21
Aged oil viscosity@40°C, cp	91.86	57.64	56.88	51.15	58.37	26.00
Viscosity index	0.73	0.69	0.64	0.62	0.64	0.51
pH	2.68	2.87	2.92	3.01	2.84	3.45
Homogeneity	Single phase	Single phase	Single phase	Single phase	Single phase	phase separated*

* phase separation within 3 months after analysis.

The GPC results were plotted against the pyroprobe-GC/MS total areas, and the total liquid yields from the mass balances [Figure 5-6 and Figure 5-7 respectively]. The figures are seen to have linear trends for the average molecular weight and the number of different molecules as compound yields and liquid yields increase.

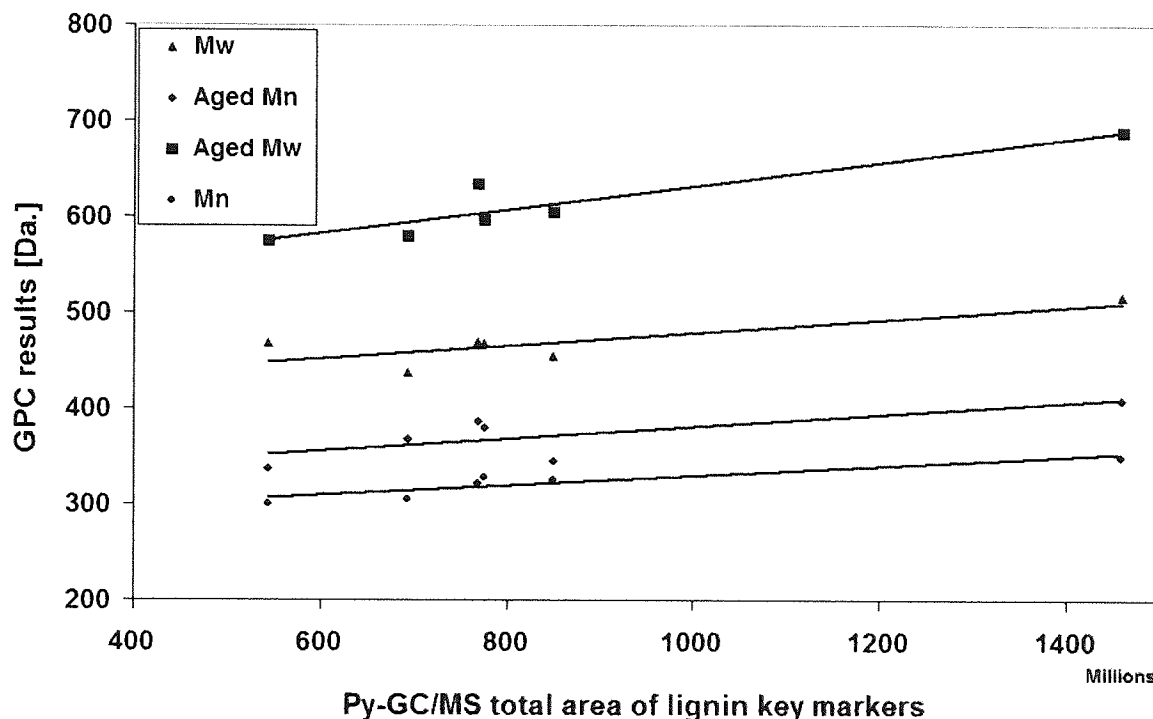


Figure 5-6 - Pyroprobe-GC/MS total area yields of key marker yields Vs. GPC results

The aged oil which was placed in an oven for 80°C for 24 hours [section 5.3] also exhibited similar linear trends, however increasing in molecular weight [Mw] and the number of different molecules [Mn], suggesting that condensation reaction is taking place for the loss of water and the remaining molecules bonding together to form higher molecular weight compounds while taking place in the oven, thus giving an increase in molecular weight for the aged oils, and a increase in the number of different molecules.

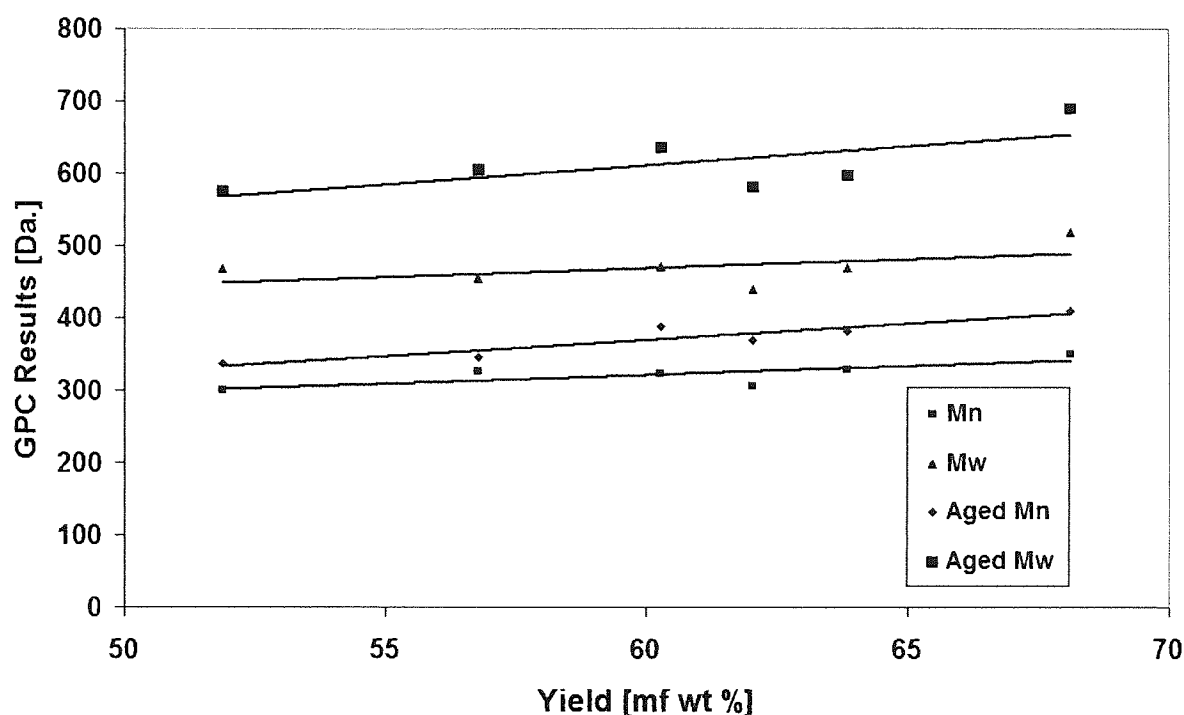


Figure 5-7 - Total pyrolysis liquid yields vs. GPC results

The linear trend suggests that higher lignin content biomass produces a higher organic yield which consists of higher molecular weight derived compounds. This is due to the aromatic structures of the lignin monomers [syringyl, guaiacyl and hydroxylphenyl], however there is no direct correlation between viscosity and higher heating value, as viscosity and heating value are dependant on water content [145].

The average molecular weight and viscosity results are in agreement with each other according to Table 5-8. This shows that as the lignin content increases, the oil is subjected to a greater change [differences in fresh and aged oil] as well as having lower water content. This in turn impacts the viscosity and molecular weight index. However having lower lignin content reduces the average molecular weight, the number of molecules and viscosity, but increasing in water content due to the catalytic effect from the ash. These findings agree with other results shown in chapter seven.

The only oil which phase separated after three month of analysis was the straw fuel, as it had the highest level of water content and having the highest ash content from any of the reference fuels. The oil which changed the most was the willow making it unstable in its characteristics,

but producing the highest yield than any other reference fuel. The energy crops possessed the greatest results in oil analysis which was balanced with a good production yield and satisfying fuel criteria for application of pyrolysis-oil.

The pH of the pyrolysis-oil shows the indicative amount of acid compounds present in the oil, such as acetic acid, formic acid and propanoic acid which are holocellulose derived. Table 5-8 indicates that as the lignin content decreases pH of the oil increases due to a lower level of derived acids from the polysaccharide components (and possibly the increase of total metal content which favours ring opening and low yields of molecular weight acidic compound production). Figure 5-8 shows that as the yield increases, the level of the pH decreases. This suggests that the highest yield was from the willow which had the highest lignin content, and lowest metals present among the rest of the reference fuels, thus producing high acids and having a lower pH.

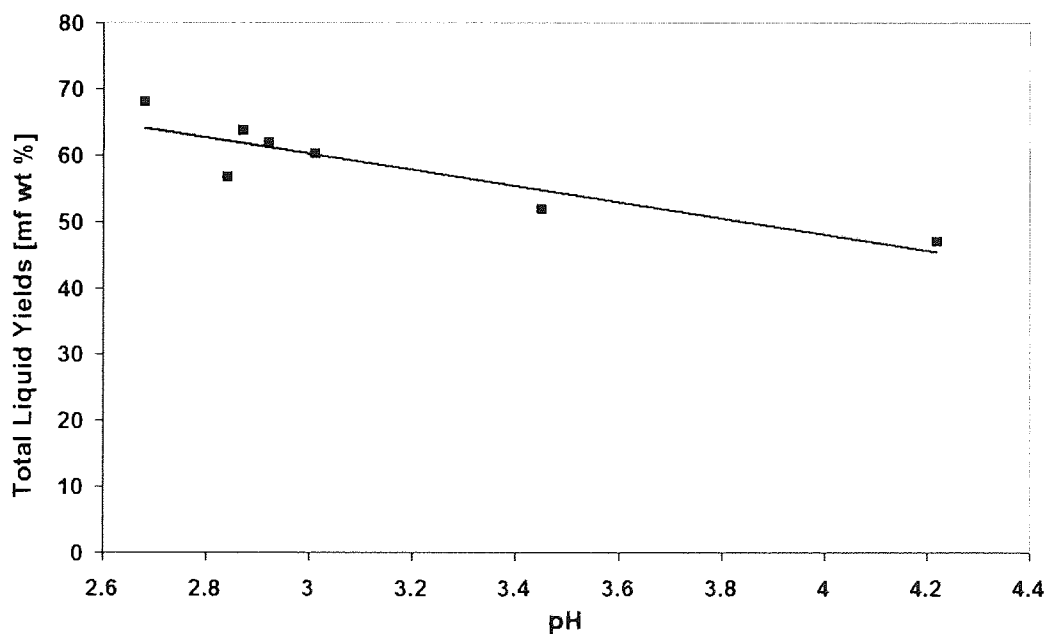


Figure 5-8 - Total liquid yields vs. pH

The results represent data from a single experiment. Statistical validation is required with replicates.

5.3.3.6 Relating organic composition (Liquid-GC/MS) to organic constituents

Pyrolysis-oil quality and quantity depends on five major variables: two being process variables and three being feedstock variables. The process variables are heating rate and final reactor set point temperature, while the feedstock variables are alkali metal content, organic composition and particle size [after processing]. The organic liquid made from the reference fuels, were subjected to liquid-GC/MS to identify key chemicals and to relate the wet chemistry lignin of the feedstocks to gain a deeper insight of organic liquid composition. The GC/MS measures molecular weight compounds from 30-600. Pyrolysis-oil are not directly injected into the GC but diluted in a solution of acetone to prevent any polymerisation occurring in the column, thus preventing blockages and dirtying the lens of the mass spectroscopy detector [refer to chapter 5].

Figure 5-9, shows the relationship between the sum of the calibrated lignin compounds present in the pyrolysis-oil [lignin derived compounds are broken into there monomers] against their wet chemistry lignin content [%].

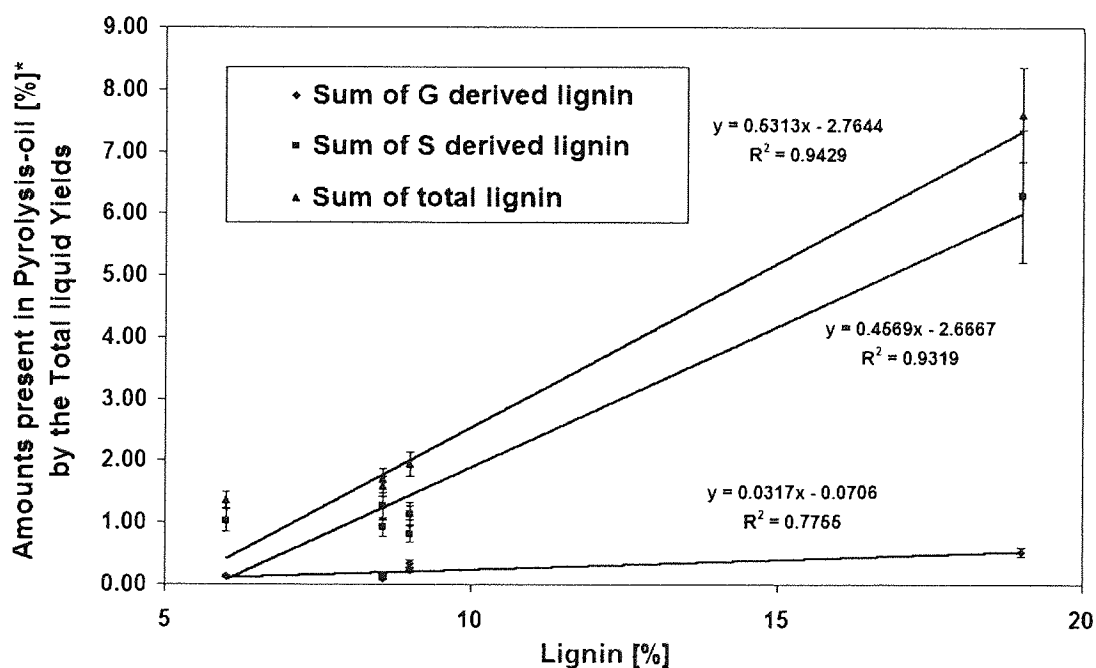


Figure 5-9 - The relationship between pyrolysis-oil lignin derived compounds found in oil pot 1 vs. wet chemistry lignin content [%]

This figure illustrates that a linear relationship for lignin can be established for the organic liquids, which possess a similar trend to that pyroprobe-GC/MS results for the reference fuel. It is shown that the summated calibrated compounds for S and G all possess a linear trend. However individual compounds such as guaiacol, syringol and vanillin plots versus wet chemistry lignin produce non linear trends. This is due to the thermal degradation mechanisms which take place during fast pyrolysis and the effect of the alkali metals [or the coating of char on the sand] which crack the vapours. Due to these phenomena individual compounds are faced with further degradation which makes it difficult to quantify the level of further cracking or the concentration of the product evolved as it leaves the biomass in the reactor.

To relate the organic liquid composition to the biomass constituents, the group of compounds present in the pyrolysis-oil must be quantified and summated together to obtain a more realistic representation of the pyrolysis-oil composition, as individual compounds can be subjected to further degradation by secondary reactions making it difficult to relate and quantify then. The aged oils have a higher organic composition than the fresh oil, and are in agreement to that of the GPC results [Figure 5-10].

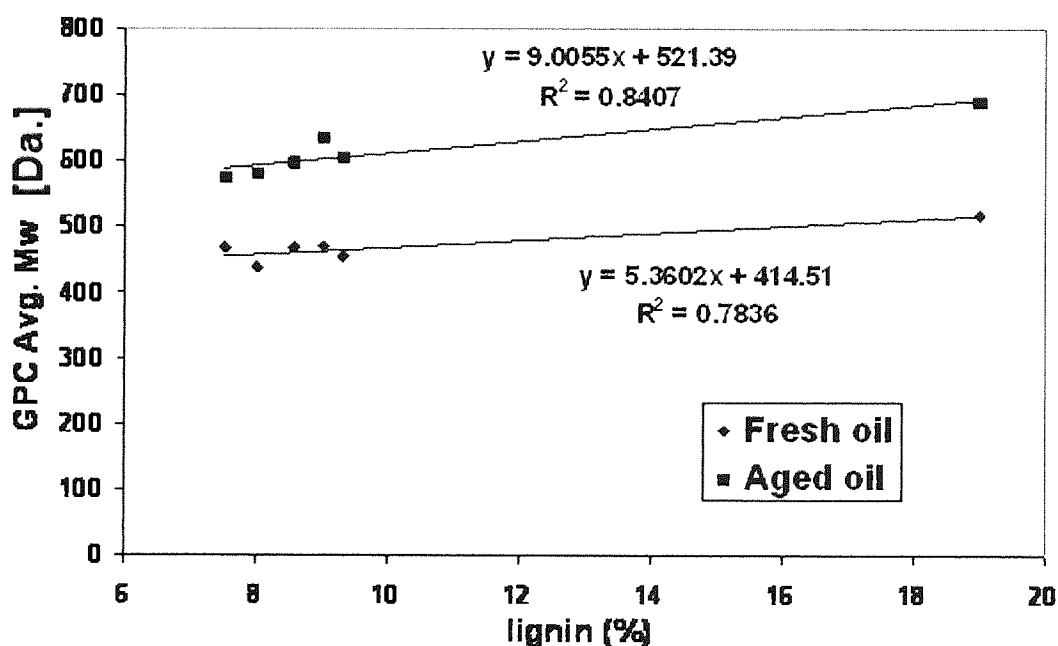


Figure 5-10 - GPC results of fresh and aged oils vs. wet chemistry lignin content [%]

This is due to condensation reactions occurring during ageing, thus reducing the lower molecular weight compounds, as molecules bond together to produce larger molecular weight compounds. The GPC results show that aged oils have a higher average molecular weight of around 530, thus suggesting that molecules averaging above 600 (which the GC/MS cannot read). The results so far show that a higher lignin biomass is more susceptible to changes to that of a lower lignin content biomass.

Figure 5-11 shows the total area of all the compounds present in oil pot 2 [dry ice condenser] as measured by the liquid-GC/MS against its lignin content as determined by wet chemistry. It is clear that as the lignin decreases, the concentration of the light organic fractions increases, suggesting that secondary reactions due to catalytic effects from the high level of alkali metals to produce a higher yield of a lighter organic fractions which is in agreement with Oasmaa [147].

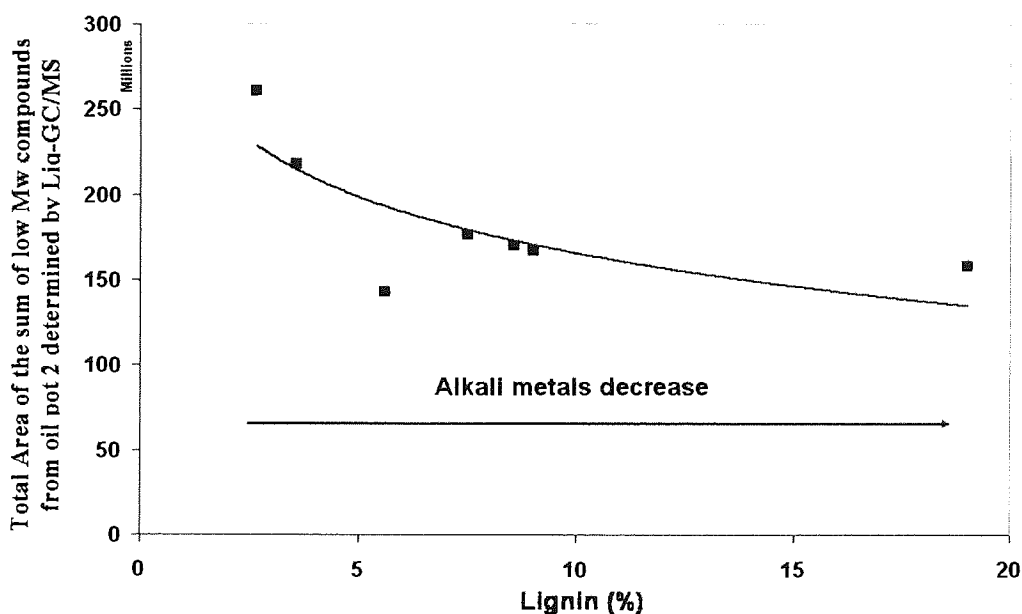


Figure 5-11 - The relationship between the total area for the low molecular weight compounds found in oil pot 2 vs. actual lignin content as measured by wet chemistry [%]

5.3.3.7 Oil fractions of EP and condenser

The heavy organic liquid which does not end up in oil pot 1 are left on the walls of the EP and condenser due to their high viscosity making it extremely “sticky”. They are considered to be

higher in organic fractions and low in water content in comparison to the pyrolysis-oil produced in oil pot 1. The washing of the EP and condenser was placed into a vacuum rotary evaporator at 37.5°C to remove the methanol, to retain the original organic liquid which was present in the units. The evaporated washings were injected into the liquid-GC/MS and compared to the oils produced in oil pot 1. Figure 5-12 shows the comparison of the oils from oil pot 1 and the evaporated washings.

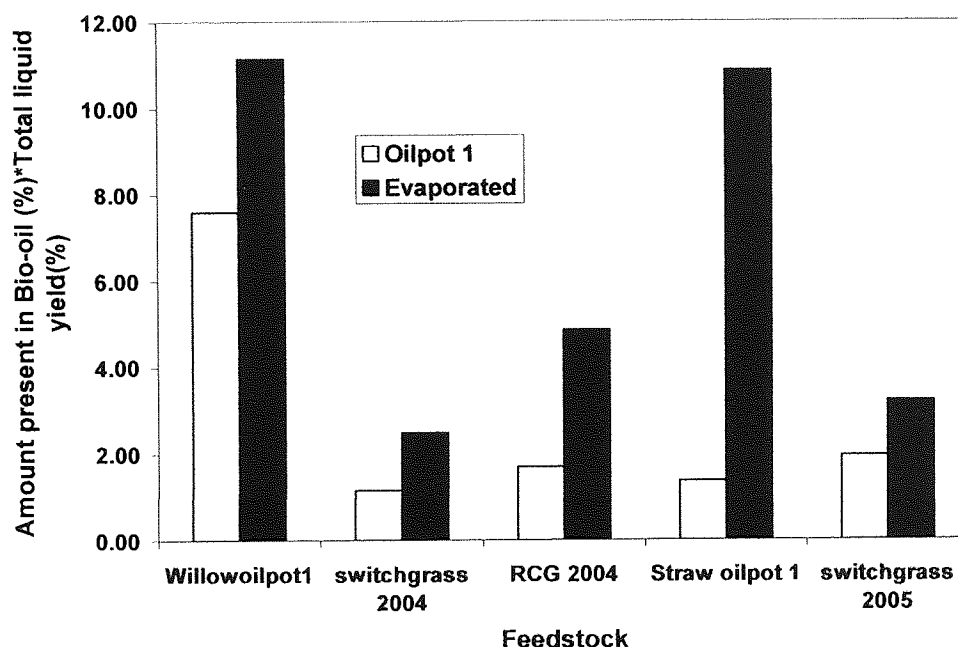


Figure 5-12 - Comparison of oil pot 1 composition and methanol evaporated EP/condenser oil composition

It is noticeable that the evaporated oils have a higher organic yield composition to that of the oil pot 1 and is especially evident with the straw oil. The organic oil compositions are shown to be different at different stages of the process, and questions if the oil composition produced in oil pot 1 is a true composition to that of other commercial rigs.

5.3.3.8 *The effect of aging on pyrolysis-oil composition*

Aging tests were conducted to investigate if the pyrolysis-oil remains the same after a period of time [stability]. Rapid ageing tests were conducted by putting pyrolysis-oil into an oven at 80°C for 24 hours which is equivalent to leaving the oil on a bench for one year [chapter 5]. The reference oils produced were subjected to rapid aging tests and then injected into the

liquid-GC/MS and compared to the original oil produced. It was found that the organic liquid changes with time as shown in Figure 5-13 and Figure 5-14.

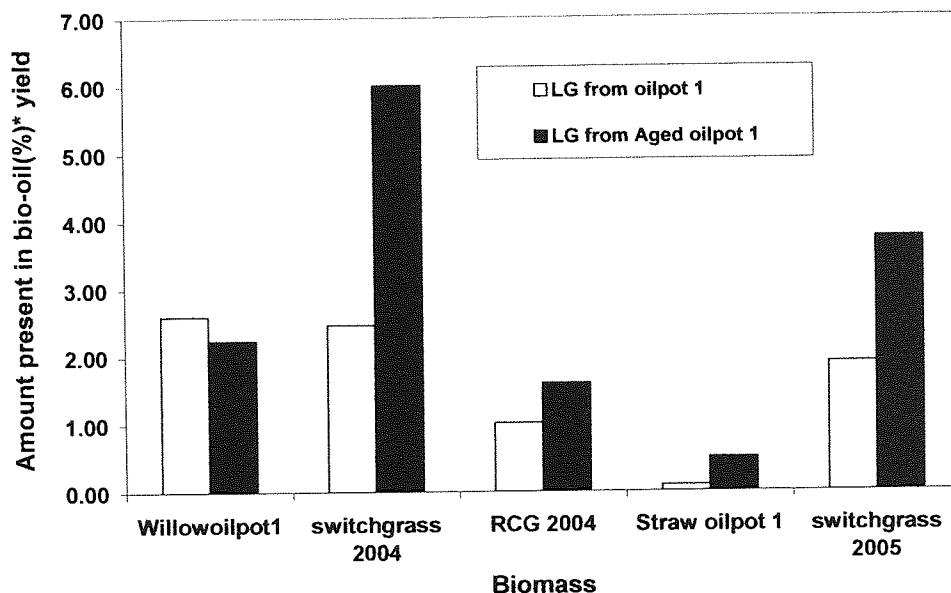


Figure 5-13 - The effect of aging on Levoglucosan

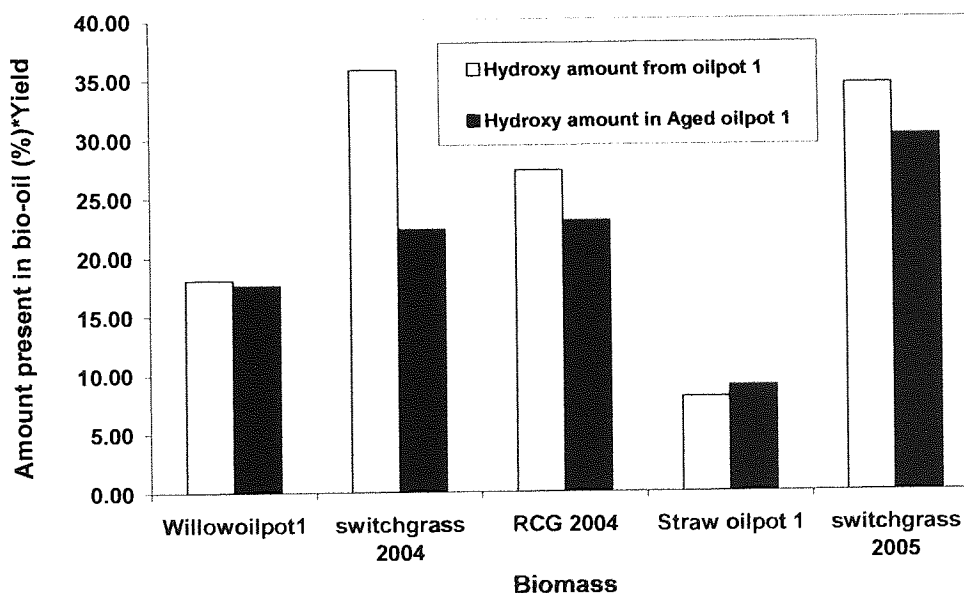


Figure 5-14 - The effect of aging of hydroxyacetaldehyde

The aged oils increased in levoglucosan for the majority of the feedstocks, at the expense of hydroxyacetaldehyde. This suggests re-polymerisation of the scission molecules from the glucose monomers are recombining together to form more ring compounds of higher

molecular weight. Oasmaa and Kuoppala [148] speculated a decrease in hydroxyacetaldehyde and an increase in levoglucosan during aging tests, and stated it was due to acid hydrolysis of the sugars and re-polymerisation or lower molecular weight compounds. It can be concluded that the oils composition changes during aging, and their compound concentrations/yields within the oil varies substantially. This suggests that the oil undergoes reactions of an uncontrollable manner while aging occurs. The number of reactions occurring in the pyrolysis-oil and their pathways are still relatively unknown in this field, however further work needs to be conducted to gain a deeper insight into pyrolysis-oil chemistry.

5.4 Conclusion

This chapter investigated the effect of organic and inorganic composition on fast pyrolysis and pyrolysis-oil quality [stability] for the reference fuels. The results clearly show that ash has a dominant effect on fast pyrolysis in comparison to that of lignin in terms of pyrolysis yields for organics, char and gases. However, the higher molecular weight compounds present in the pyrolysis-oil is due to the lignin derived compounds according to GPC and liquid-GC/MS. The light organic fraction also increases in yield, and reduces in water content as ash increases at the expense of the lignin content. The results based on the reference fuels clearly show that a higher lignin content biomass is susceptible to a greater change during aging than a lower lignin content biomass. The results revealed that energy crops show the most potential for producing a stable pyrolysis-oil more than any other types of feedstocks. A relationship exists between the results from the GPC/liquid GC/MS and the fast pyrolysis-oils produced using Astons 150 ghr⁻¹ reactor in terms of their yield and quality.

It is also found that the evaporated oils from the EP and condenser are different to the oil produced in oil pot 1. It was shown that the oils which remain in the condenser and EP are higher in molecular weight and viscosity due to their low water content, thus resulting in higher compound intensities as identified in the liquid-GC/MS.

The aged oils in comparison to the fresh oil have different compound intensities, due to a large number of reactions occurring while the oil ages day by day. This agrees with previous studies [86, 146, 147, 163]. A large amount of re-polymerisation occurs during the aging of the oil as the results show the increase of levoglucosan yields at the expense of smaller compounds such as hydroxyacetaldehyde.

6 EXPERIMENTAL DETERMINATION OF BIOMASS LIGNIN IN *LOLIUM* & *FESTUCA* GRASSES USING PYROPROBE- GC/MS AND WET CHEMISTRY LIGNIN METHODS

Lolium and *Festuca* grasses genes which give rise to a variation of lignin content of 2-4%. These *Lolium* and *Festuca* grasses were grown in a green house in which they were all exposed to the same environmental conditions (sunlight, water content, humidity etc). The results obtained have been used to relate analytical scale pyrolysis to lignin composition as measure by wet chemistry.

6.1 Introduction

Lolium and *Festuca* grass consists of stems and leaves [refer to chapter two]. Each plant component consists of lignin and holocellulose, and varies in its metal content. These grasses have been exposed to the same environmental conditions, and were grown in 6" pots in polytunnels under natural daylight between April 2003 and October 2004. They were sequentially cuts by hand and combined, following an oven drying period at 80 °C for 24 hours.

Pyroprobe-GC-MS was used to validate a rapid screening method for determining biomass lignin content in comparison to traditional methods of lignin analysis [Klason/ADF]. The screen methodology is based on relating the lignin derived products from fast pyrolysis to the wet chemistry lignin content. Pyrolysis of three *Lolium* and *Festuca* grass was also conducted to investigate whether lower lignin can produce a stable pyrolysis-oil.

Fifteen *Lolium* and *Festuca* grasses samples were subjected to pyroprobe-GCMS, in which the pyrogram was analysed. The key markers for lignin were then added together to obtain a total area. A calibration was then determined between the total area and the wet chemistry lignin.

6.2 Experimental

The characterisation of the *Lolium* and *Festuca* grasses have been described and presented in previous chapters [Chapter 5 Section 5.1], while the TGA and pyroprobe methods and conditions have been described in previous Chapter 4 Section 4.3.

The total ion count [TIC] traces from 3 machine replicates of the 15 samples representing the full range of chemically pre-determined lignin were subjected to a number of Multivariate Eigenvector quantification methods. First the data was base line corrected with a linear correction factor using a least squares line fit. To remove the offset from the data before mathematical decomposition, each chromatograph was mean centred by calculating the overall average spectrum along with the mean concentration value before subtraction from the concentration of each sample. Principle Component Regression [PCR] and Partial Least-Squares [PLS 2] analysis were performed on the corrected data. PLS is a spectral decomposition technique that uses the known concentrations [lignin values] to correlate with the spectral data, while PCR is a multivariate analysis method. This cross validate method was chosen primarily due to the size of the data set available.

6.3 Results & Discussion

Table 6-1 show the elemental and calorific value analysis [CHNO and CV value] of the fifteen samples. Oxygen content was calculated by difference. It can also be noticed in Table 6-2 that the alkali metals decrease as lignin content increases for the grasses.

Table 6-1 – Chemical and calorific value analysis of *Lolium* and *Festuca* grass samples.

Sample identification	C (%)	H (%)	N (%)	O (%)	C.V. (kJ/kg)	Moisture (%)
<i>F.boissieri</i> -2x	43.75	5.94	2.10	48.22	17632.75	5.79
<i>F.scariosa</i> -4x	43.86	5.93	1.77	48.45	17632.04	7.03
<i>F.drymeja</i> -2x	43.94	6.02	2.33	47.72	17736.9	6.99
<i>F.glaucescens</i> -4x	44.08	6.03	2.06	47.84	17813.5	5.7
<i>F.atlantagena</i> -8x	44.08	6.08	2.48	47.37	17813.5	6.92
<i>L.multiflorum</i> -2x	44.13	5.94	1.83	48.11	17747.6	5.54
<i>L.multiflorum</i> -2xi	44.15	6.08	1.89	47.90	17765.3	6.36
<i>L.perenne</i> -2x	44.17	6.01	1.89	47.93	17775.12	5.87
<i>L.multiflorum</i> -4x	44.30	6.00	2.24	47.48	17869.87	5.82
<i>F.pratensis</i> -2x	44.31	5.96	1.91	47.83	17830.48	6.47
<i>F.arundinacea</i> -6x	44.55	6.05	1.40	48.01	17865.51	6.8
<i>F.apennina</i> -4x	44.63	6.17	1.10	48.11	17864.69	5.36
<i>F.mairei</i> -4x	44.95	6.07	1.59	47.39	18057.12	6.14
<i>F.donax</i> -4x	44.98	6.05	1.61	47.36	18070.68	5.95
<i>F.pratensisxglaucescens</i> -4x	45.38	6.06	1.40	47.17	18206.85	5.83

Table 6-2 - Lignin content and ICPES metal analysis in ppm.

Sample identification	Lignin (%)	Cellulose (%)	Ca (PPM)	K (PPM)	Mg (PPM)	Na (PPM)
<i>F.donax</i> -4x	2.1	24.8	7113	28007	2270	224
<i>F.boissieri</i> -2x	2.2	25.5	7989	27481	1392	160
<i>L.perenne</i> -2x	2.4	16.9	6209	28138	1695	903
<i>F.pratensis</i> -4x	2.4	17.32	3617	29502	1416	139
<i>F.arundinacea</i> -6x	2.5	19.3	2694	28985	1548	785
<i>F.pratensisxglaucescens</i> -4x	2.5	22.6	2793	32130	1511	191
<i>L.multiflorum</i> -2x	2.8	15.5	3894	37022	1343	217
<i>F.drymeja</i> -2x	2.8	18.2	2008	18426	1159	200
<i>L.multiflorum</i> -6x	2.8	21.6	6554	30214	1653	1210
<i>F.pratensis</i> -2x	2.9	19.4	1953	19049	829	131
<i>F.apennina</i> -4x	2.9	20.8	4420	36805	1993	302
<i>F.atlantagena</i> -8x	3.0	20.4	3034	24382	1667	127
<i>F.glaucescens</i> -4x	3.2	17.7	2868.3	25984	1944	364
<i>F.scariosa</i> -4x	3.2	18.9	1873	22957	831	191
<i>F.mairei</i> -4x	3.7	19.65	1366	21645	1353	87

Figure 6-1 shows the wet chemistry lignin content plotted against the sum of the total metal content in ppm for the *Lolium* and *Festuca* grasses. It can be seen that as the lignin content increases the sum of the total metals decrease.

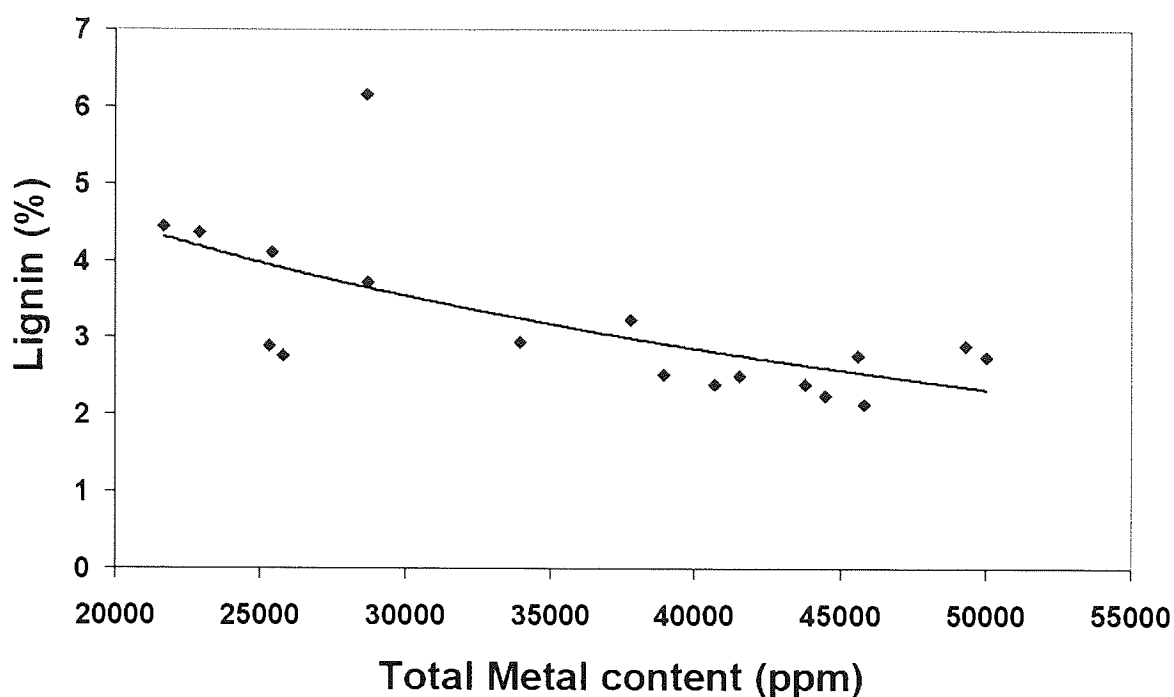


Figure 6-1 - Relationship between lignin and total metals for *Lolium* and *Festuca* grass

In order to ensure that there was a relationship between the wet chemistry lignin and the total metal content, the six reference fuels and the first sampling of the agronomical *Miscanthus* [refer to chapter 9] was plotted along side the *Lolium* and *Festuca* grasses [Figure 6-2]. Figure 6-2 shows a broader relationship between lignin and total metal content, and it can be seen that there is an inverse exponential relationship between the lignin and the sum of the total metals. A linear trend can also be noticed for the non-woody reference fuels, as well as the *Miscanthus* species used for the agronomical study. The results clearly indicate that there is a relationship between the lignin present in the leaves, and the metals it uptakes in order to achieve its function. This is once again showed in the PCA analysis in Chapter 7 Section 8.3.4. This might be due natural senescencing of the leaves which results in cell death and the accompanying withdrawal of nutrients back in to the main body of the parent plant.

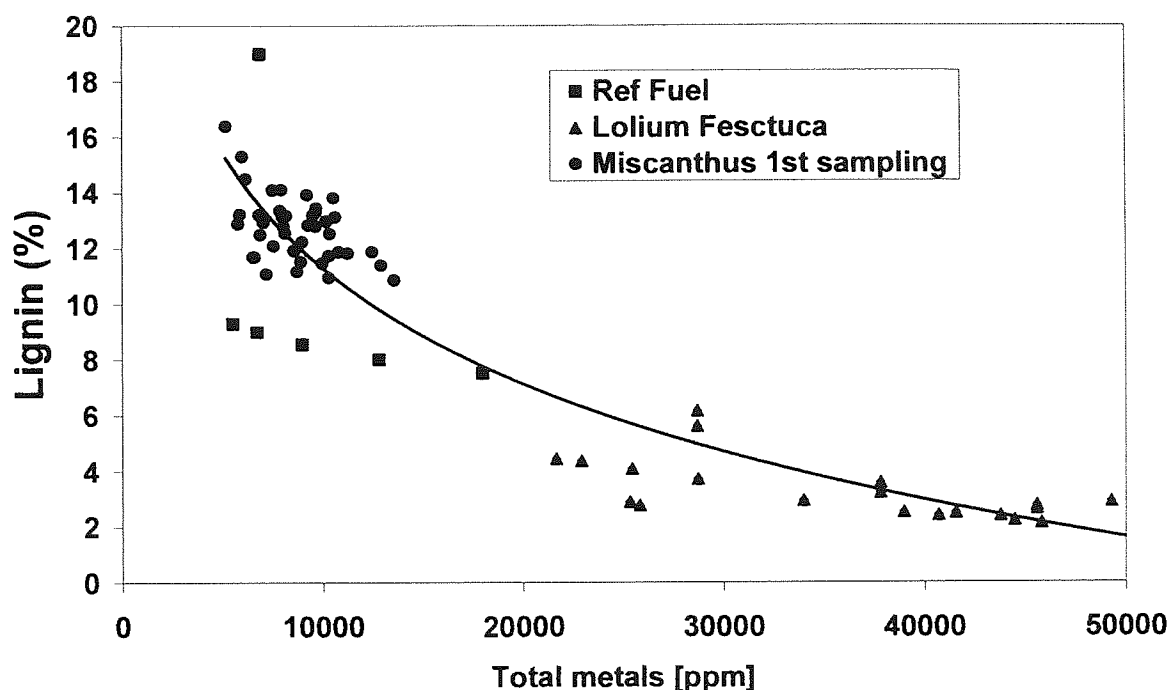


Figure 6-2 - Relationship of lignin and total metals for species used in this investigation

Cellulose and hemicellulose analysis was also determined for the *Lolium* and *Festuca* grasses by the use of wet chemistry [via acid digest refer to Section 5.1.7]. The sum of the cellulose and hemicellulose content present in the biomass [%] was referred to as holocellulose, Figure 6-3 shows the percentage present of wet chemistry lignin, cellulose and hemicellulose [as measure by wet chemistry] for the 15 species of *Lolium* and *Festuca* grasses. It can be seen that as the lignin increases; the cellulose content also increases, this might be due to the cross linkage between the lignin and cellulose within the leaf. However the hemicellulose decreases due to a result of the cellulose and lignin increasing. Figure 6-4 shows the relationship between lignin and the holocellulose content as measured by wet chemistry.

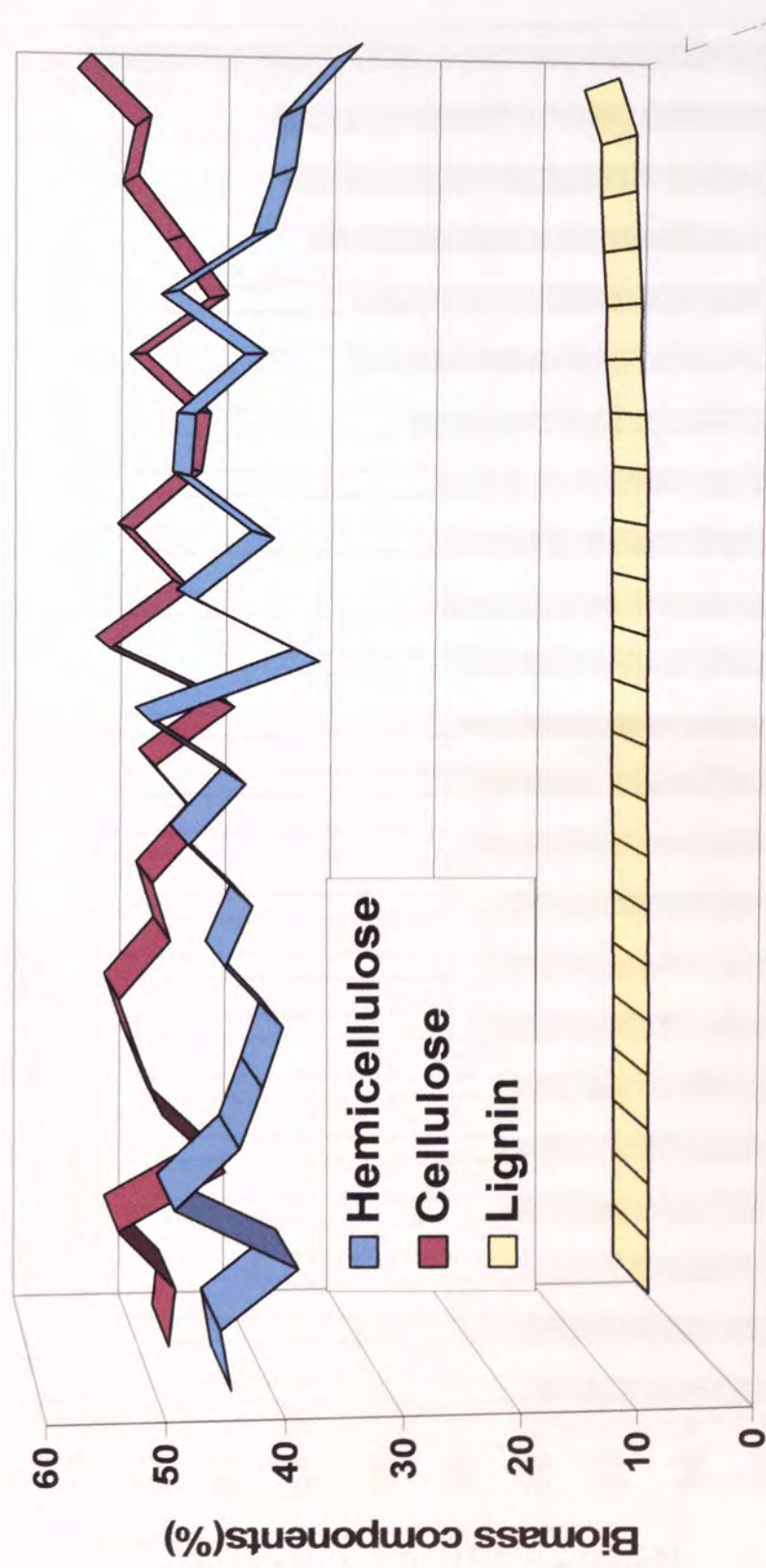


Figure 6-3 - Relationship between biomass components in *Lolium* and *Festuca* samples

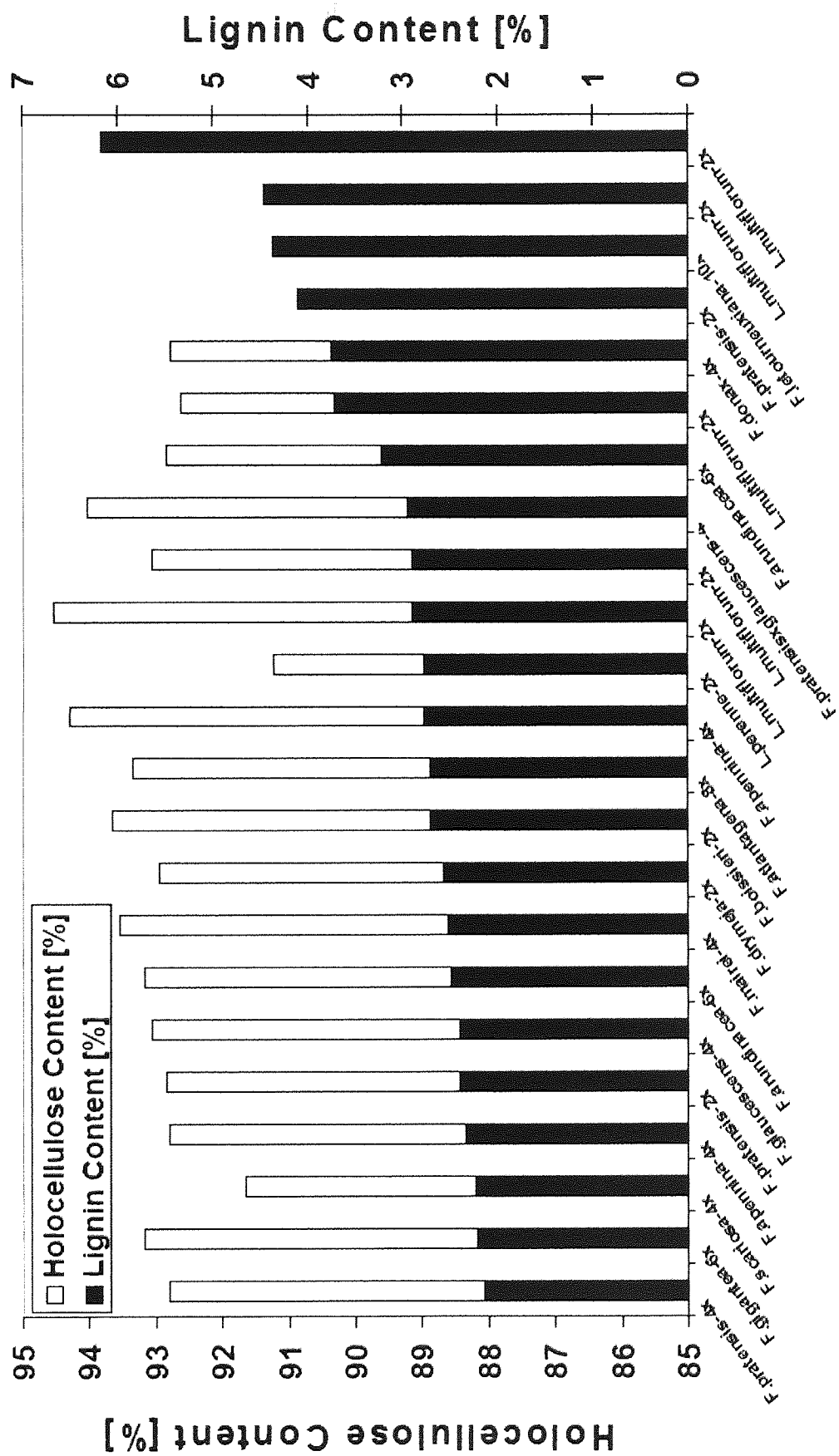


Figure 6-4 - Relationship between lignin and holocellulose content in *Lolium* and *Festuca* grasses

From Figure 6-4 it clearly shows that there is an inverse relationship between the holocellulose and lignin content present in the *Lolium* and *Festuca* grasses. From the characterisation of the *Lolium* and *Festuca* grasses it can be clearly stated that there is a complex relationship between the total metals present in the leaf material and the holocellulose/lignin contents of the species.

6.3.1 Pyroprobe-GC/MS analysis

The key markers for lignin and cellulose compounds were identified by comparing the mass spectra fragmentation pattern to the Perkin Elmer NIST library and with existing published data to obtain the highest likelihood of compound identification. Fig. 7.5(a) shows a typical pyrogram of a grass sample and a list of compounds identified can be found in chapter 4.4. The compounds identified were derived from cellulose, hemicellulose and lignin structures. The lignin compounds could be further separated into syringyl, guaiacyl and hydroxylphenyl type monomers. A total of 39 main compounds were identified, and key markers were selected on the basis of abundance. The key markers for syringyl lignin derived compounds were syringol, 4-vinyl syringol, 4-propenyl syringol [trans], syringaldehyde, and acetosyringon. The key markers for guaiacyl lignin were guaiacol, guaiacol 4 ethyl, 4-vinyl guaiacol, eugenol, vanillin, and coniferyl alcohol cis. The key markers for hydroxylphenyl were 2 methyl phenol, 4 ethyl phenol and 4 vinyl phenol. The unassigned lignin peaks were phenol and pyrocatechol.

The grass leaves were found to vary in lignin content from 2.1 to 3.7 % using the Klason/ADF methods. In order to efficiently test if there was any linear relationships within the total ion count data to the known lignin values for the sample sets, a Partial Least-Squares PLS analysis was performed on the data set using cross validation. The results of this modelling produced a predicted lignin [%] vs. wet chemistry lignin values with a relationship shown in Figure 6-6. The optimal model estimated from the PRESS value was fitted at factor 9 with $R^2=0.757586$. The Factor Loadings (FLs) [Fig. 7-5(b)] were then plotted along the same time axis as the Total Ion Count [TIC] data and aligned to it. The larger the positive peak values for the FLs, the greater the contribution that can be attributed to the TIC values at the same point in the linear model fitting process undertaken to calibrate the data to the wet chemistry lignin values. The largest FL peak values were then used to mine the original Mass Spectra [MS]

fragmentation pattern data files at that point of the TIC chromatogram. By an iterative process of comparing these candidates to known standards and standard libraries a total of 20 key markers likely to be attributable to lignin thermal decomposition were identified and validated. A further 17 likely markers of cellulose were also identified.

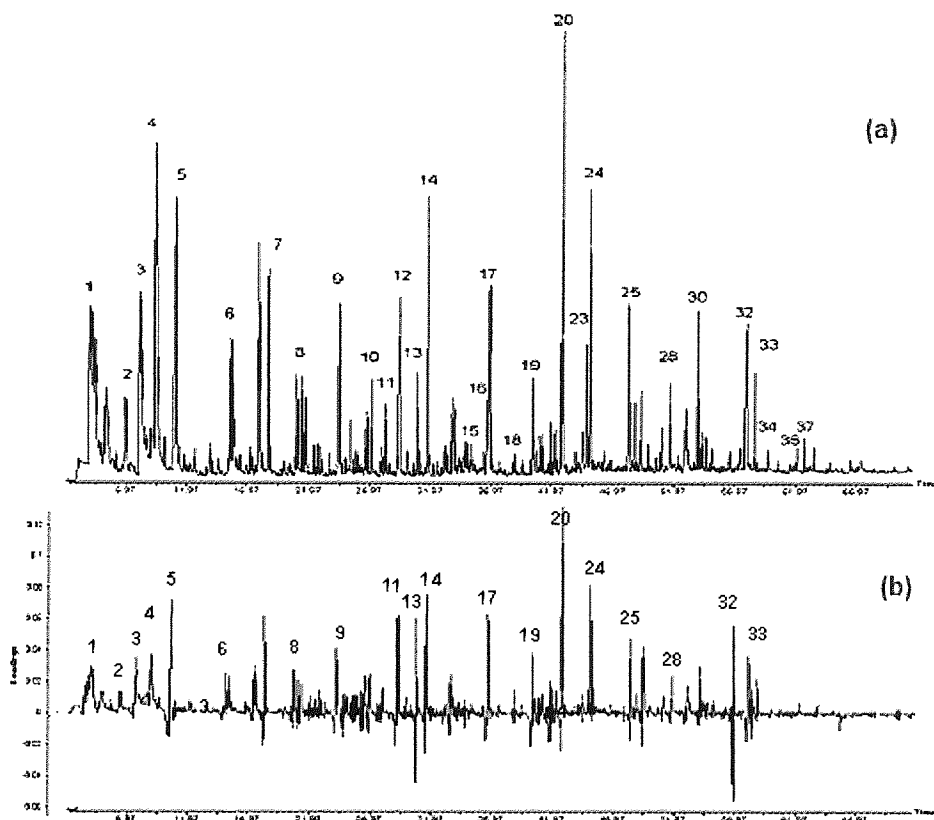


Figure 6-5 - (a) Py-GC/MS Chromatogram of a representative grass sample; (b) Partial Least-Squares Factor Loadings.

In total 16 key lignin markers were selected for their correlation to the wet chemistry lignin values. The relative peak areas were calculated for each sample and an average was taken from the three pyrogram replicates, after standardisation. The total peak area for the lignin markers [S, G, H units and the unassigned lignin peaks] were combined to produce a total area value for all the grasses and its repeats at which they were then plotted against the lignin [Figure 6-6]. G-lignin was the most abundant form in all samples over the range of lignin values and did appear to increase somewhat in proportion to the total lignin value. However, as a proportion of the lignin key markers could not be assigned specifically to a lignin type, a

definitive estimation of compositional changes within the overall lignin value will require further analysis.

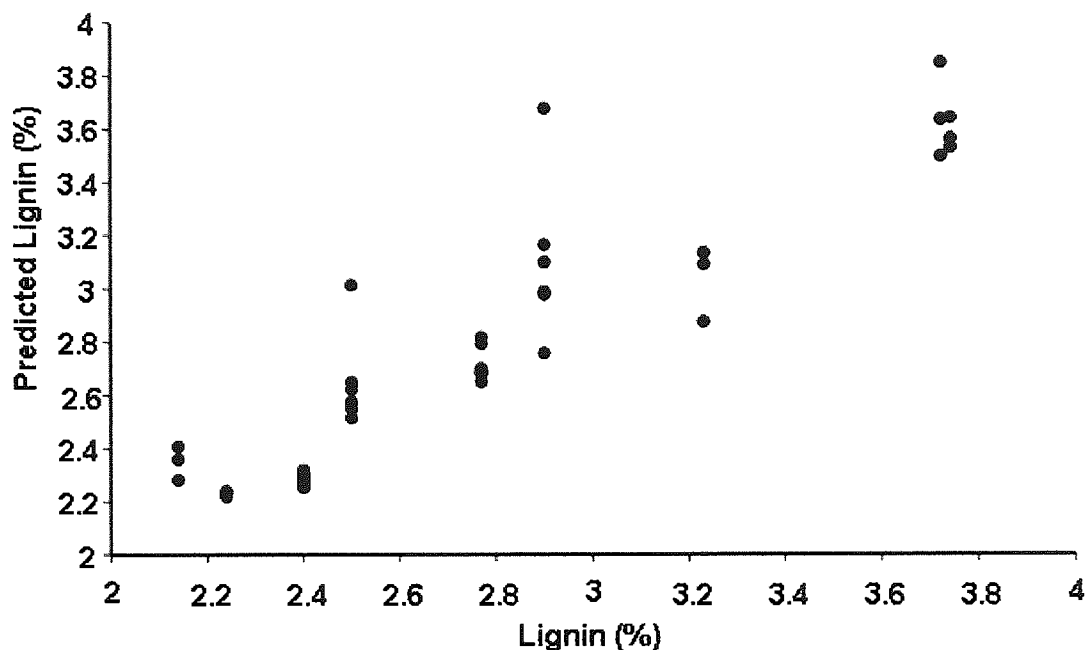


Figure 6-6 - Pyroprobe-GC-MS predicted vs. actual lignin content [%] as measured by wet chemistry

Figure 6-7 shows the break down of the total lignin area into its sub units, and it can be seen that the lignin sub units increase as lignin [as determined by wet chemistry] increases. There was though a positive relationship between the lignin as measured by wet chemistry and the total peak area for lignin markers, with a correlation of 0.88 as shown in Figure 6-8.

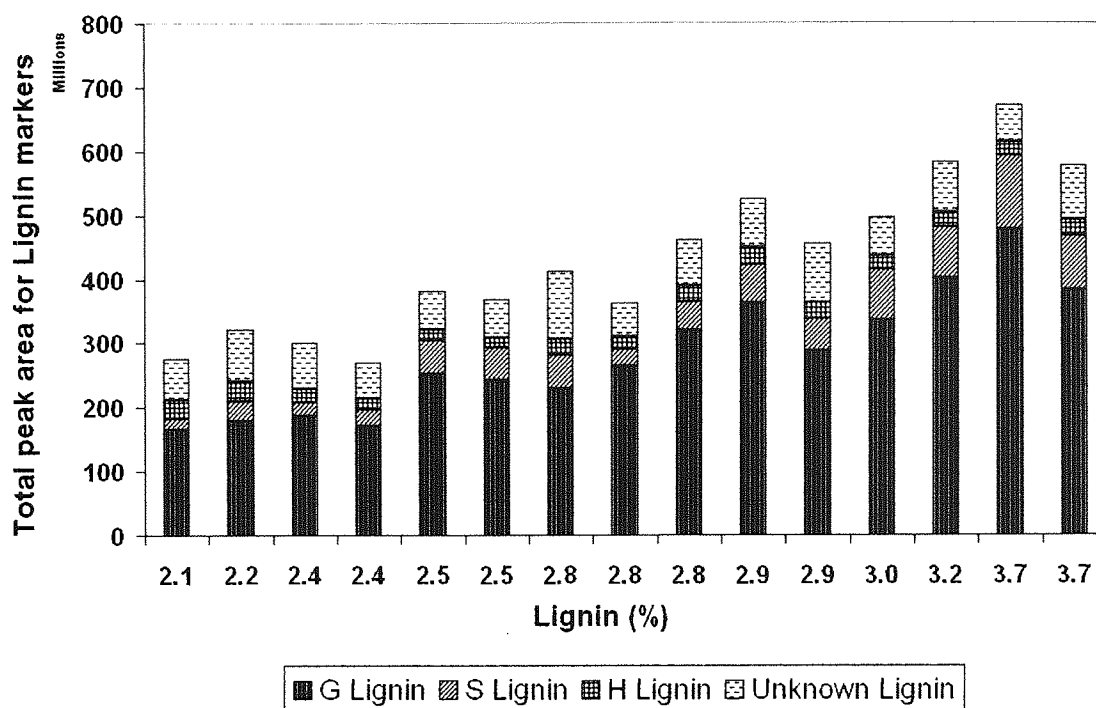


Figure 6-7 - Relationship of subunits in *Lolium* & *Festuca* samples

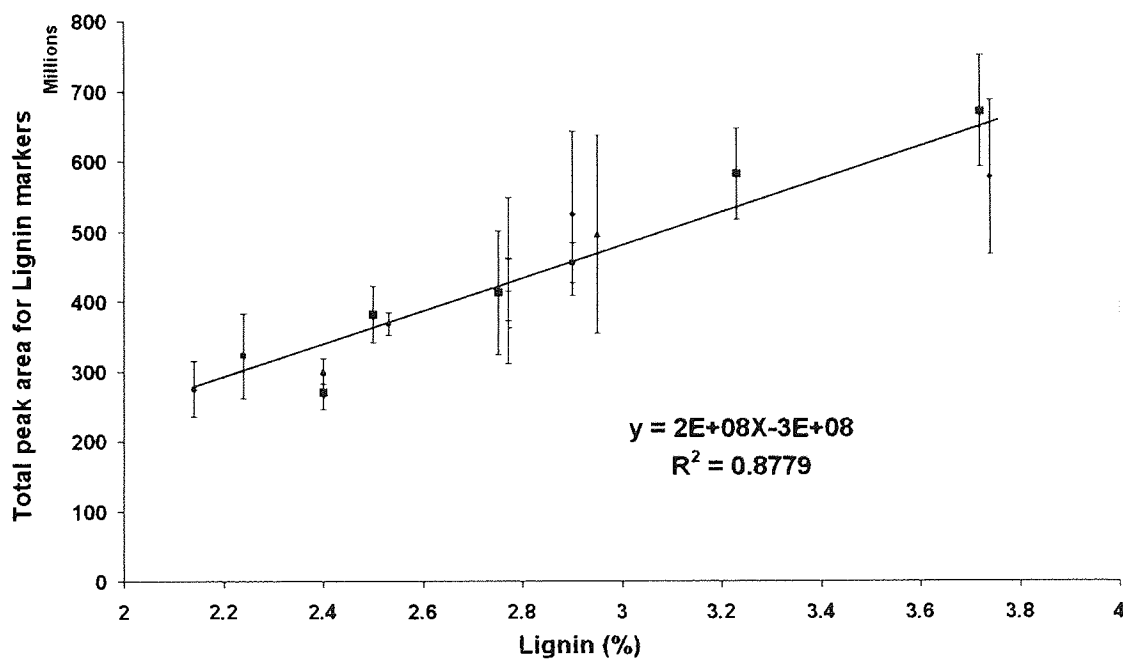


Figure 6-8 - Relationship between Pyroprobe-GC/MS lignin vs. actual lignin [%] as measured by wet chemistry

Although the fragmentation patterns of markers previously assigned to cellulose in the literature and from pure standards could be identified in the chromatograms; there was no simple correlation to cellulose as measured by wet chemistry [ADF minus lignin]. A significant correlation was achieved by PLS-2 analysis [data not shown] and the identification of candidate key markers for these will be the subject of further work in the field. It has also been reported [59] that cellulose and hemicellulose are responsible for volatile products while lignin is responsible for the contribution to char. Raveendran et al [60] reported that the main alkali metals in biomass such as potassium, sodium and silicon increasing the maximum rate of devolatilisation and initial decomposition temperature. The results are in agreement with this. It has previously been determined that in fast pyrolysis specific mineral content [potassium, sodium, magnesium and calcium] introduces catalytic affects on the degradation of biomass [6, 10, 28, 60, 131]. The removal of metals by a pre-treatment such as washing can remove the majority of the metals and reduce the ash content by 70 % [10, 151]. This would therefore decrease the char content, and increases the amount of volatiles released from the biomass during fast pyrolysis. However the degradation mechanism would move towards depolymerisation rather than fragmentation reduction and would be predicted to increase the cellulose derived compounds shown by Scott et al [28].

Figure 6-9 shows the *Lolium* and *Festuca* leaves and stems along with the reference fuels used in this project. The linear slope is plotted through origin of the graph and shows that the reference fuels also follows the linearity of the line, suggesting that the pyroprobe-GC/MS is appropriate for screening feedstock's for their lignin content by using this sort of relationship where the actual lignin content is plotted against the total grouped key marker compound areas of lignin derived products to obtain an approximation for lignin content.

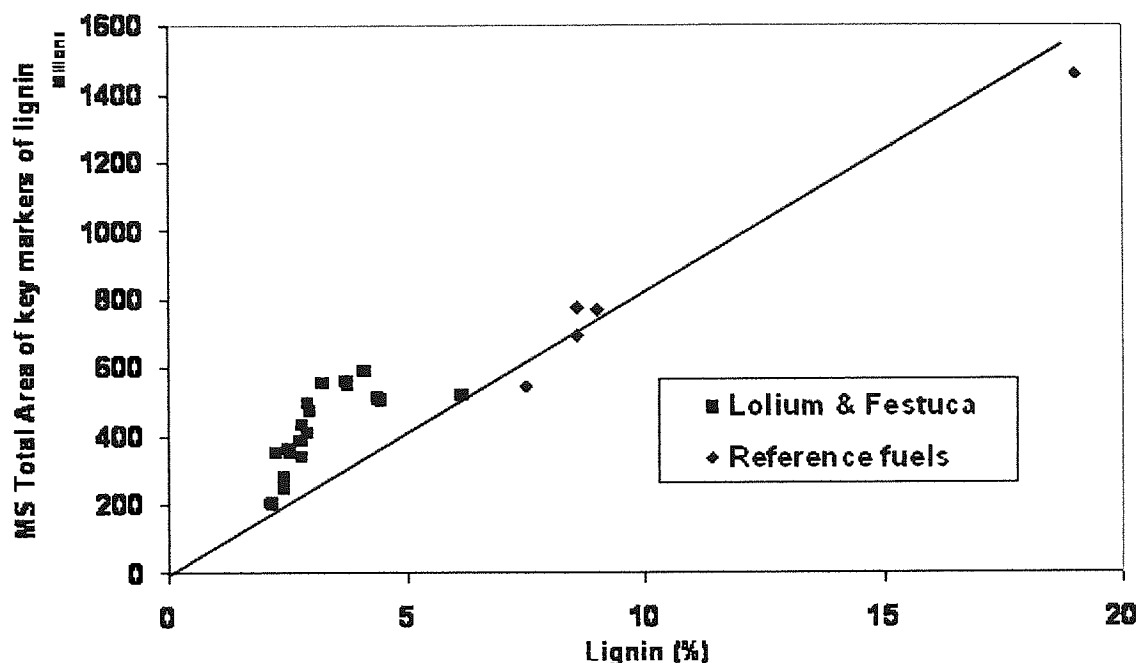


Figure 6-9 – The screening of other feedstocks by the use of pyroprobe-GC/MS

The linear relationship gives an $R^2 = 0.7$. The R^2 value gives an appropriate fit for analytical equipment taking into consideration the level of standard deviations between samples on a day to day comparison as well as the biomass inhomogeneity which leads to sampling errors.

If each Syringyl and guaiacyl derived compound [for the reference fuels and the *Lolium* and *Festuca* grasses] was plotted against the lignin content, no linear relationship can be established due to the different levels of degradation of each compound due to the catalytic effect of the metals promoting secondary reactions agreeing with the findings from Chapter 6 Section 6.3.3.6. However, if the Syringyl and guaiacyl sub units were plotted for the *Lolium* and *Festuca* grasses plotted against the lignin content, a linear trend would emerge.

6.4 Fast pyrolysis experiments on selected *Lolium* & *Festuca* grasses

6.4.1 Introduction to rig experiments

Three large batches of *Lolium* and *Festuca* grasses which have a known lignin content of 2.66, 3.59 and 5.61% [which have been grown in 2004-2005] have been selected and subjected to fast pyrolysis investigation on the 1 kg fluidised bed pyrolysis rig. The aim of the trial is to investigate if a natural lower lignin biomass is capable of producing a stable pyrolysis-oil by reducing chemical reactions, which maintains its viscosity with respect to storage time from date of production. Analytical analyses by TGA and pyroprobe-GC/MS have been conducted to gain an early indication of thermal degradation and possible yield results which could be expected for large scale fast pyrolysis trials, as well as the elemental analysis and HHV as described in chapter five.

6.4.2 Experimental

6.4.2.1 *Lolium and Festuca characterisation*

Refer to Chapter 5 Section 5.1 for detailed methodology.

6.4.2.2 *TGA and Pyroprobe-GC/MS conditions*

The TGA and pyroprobe methods and conditions have been described in previous Chapter 4 Section 4.3.

6.4.2.3 *Pyrolysis reactor set up and methodology*

The mass balance methodology has been discussed in Chapter 4 Section 4.5.

6.4.3 Results & Discussion

6.4.3.1 *Lolium and Festuca characterisation*

Table 6-3 shows the elemental analysis of the *Lolium* and *Festuca* grasses which were used for fast pyrolysis trials [oxygen calculated by difference] while Table 6-4 shows the alkali metal content.

Table 6-3 - Elemental analysis of *Lolium* and *Festuca* grasses with heating values

Name	C (%)	H (%)	N (%)	S (%)	O (%)	ASH (%)	H.H.V. (MJ/kg)
Dactylis glomerata (5.61 %)	42.96	5.7	1.9	0.1	49.34	7.46	16.83
Festuca arundinacea (3.59 %)	42.22	5.63	1.5	0.1	50.25	7.27	16.36
Lolium perenne (2.66 %)	43.12	5.80	1.3	0.1	49.40	6.24	17.00

Table 6-4 - Alkali metal content of *Lolium* and *Festuca* grasses

Sample	Ca (ppm)	K (ppm)	Mg (ppm)	Na (ppm)	Total Alkali metals (ppm)
Dactylis glomerata	4505	26710	1100	2821	40830
Festuca arundinacea	4334	24026	1136	1346	35653
Lolium perenne	4156	20127	886	933	30467

6.4.3.2 TGA and pyroprobe-GC/MS results

Figure 6-10 shows the TG results of the three *Lolium* and *Festuca* grasses while Figure 6-11 shows the DTG results. It can be seen that *Lolium perenne* had a different degradation pathway in comparison to the other two species, which resulted in a lower char content. The DTG results show the rate of thermal degradation increases with higher lignin content, thus suggesting the rate increases with lower ash content. Figure 6-12 once again demonstrates that yield of volatiles and gases increase due to lower ash content while the char yield have an opposite effect as shown in [6, 28].

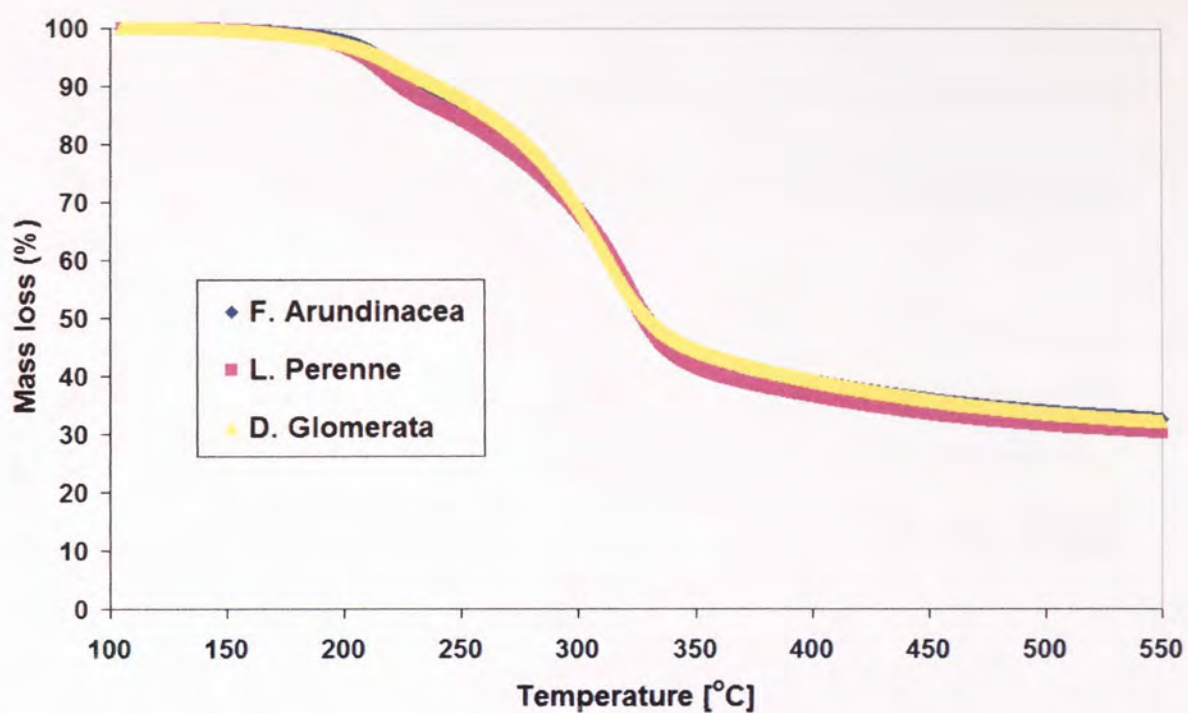


Figure 6-10 - TG of *Lolium* and *Festuca* grass

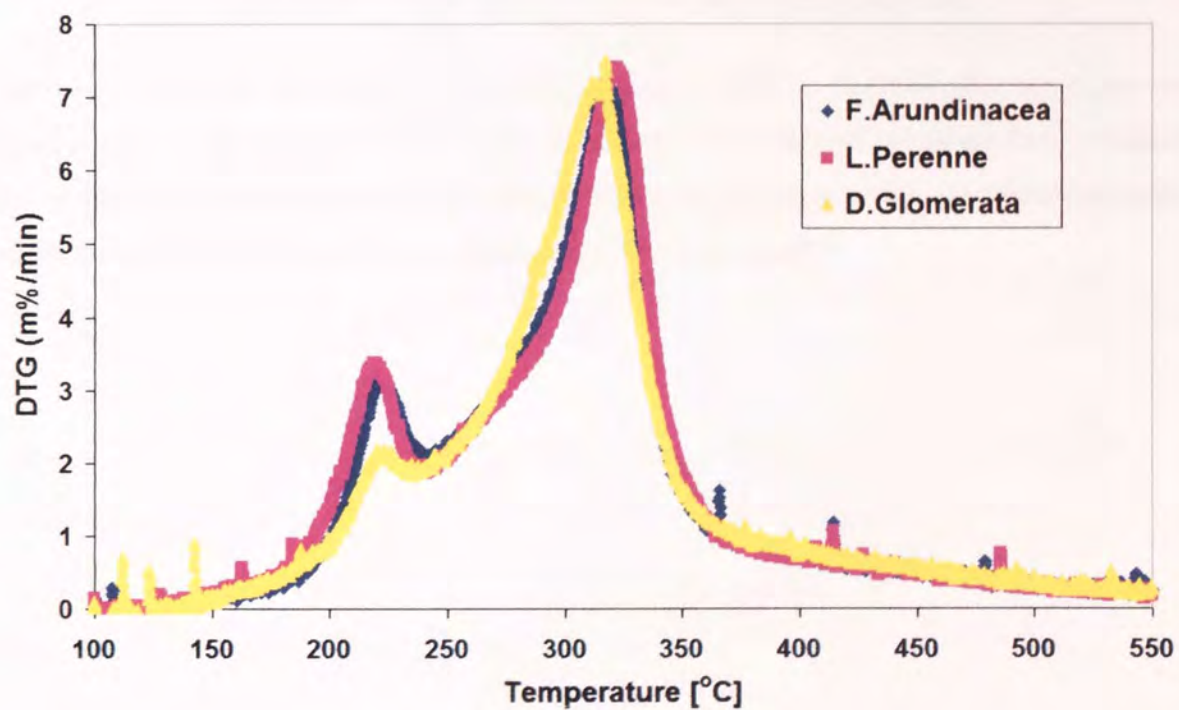


Figure 6-11 - DTG of *Lolium* and *Festuca* grass

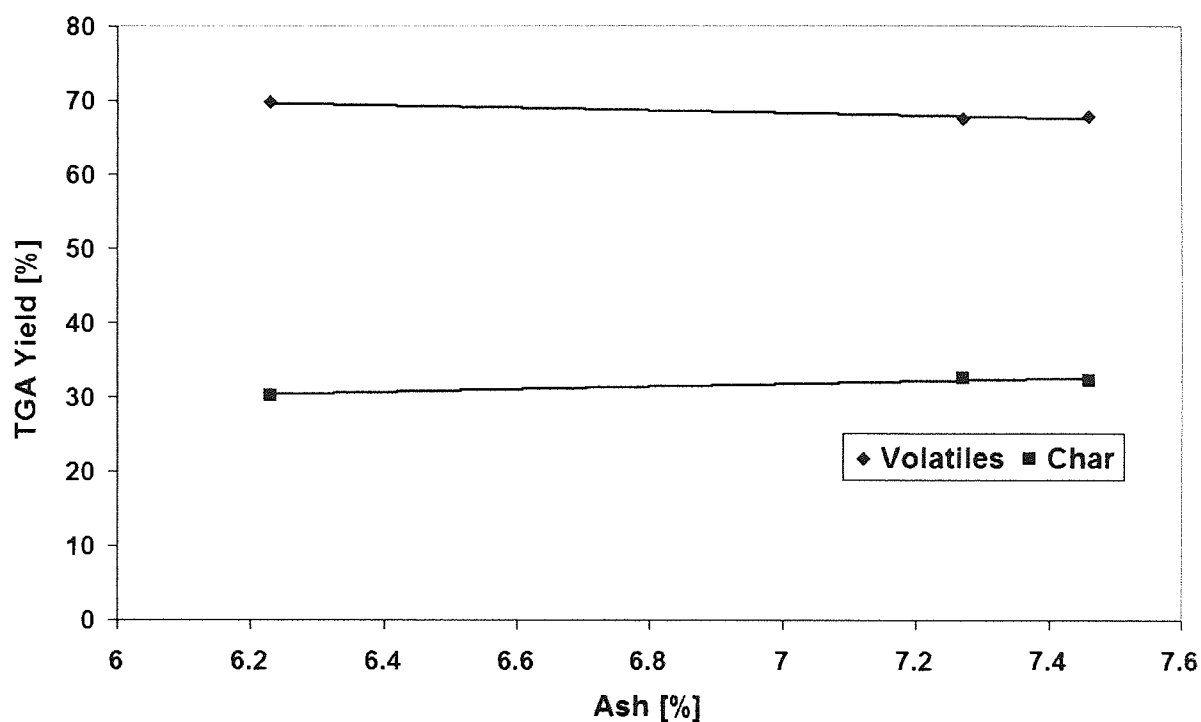


Figure 6-12 - TGA results of *Lolium* and *Festuca* grasses

Table 6-5 shows the areas of the compounds scaled to 100 %. It shows that the higher the lignin content in the specie, the higher the amounts of lignin derived compounds are produced, this is due to the low level of metals present within the biomass which contribute secondary reactions and effects the quantity of lignin compounds produced.

Table 6-5 - Key markers present in *Lolium* and *Festuca* samples scaled to 100 %

Name of compound	CODE	Dactylis glomerata	Festuca arundinacea	Lolium perenne
2,3-Butandione	Cellulose	3.667	4.156	5.837
Hydroxyacetaldehyde	Cellulose	24.891	22.720	29.502
Hydroxypropanone	Cellulose	13.583	15.208	16.010
2-Furaldehyde, 2-Furfural	Cellulose	6.671	6.883	6.330
2 FURANMETHANOL	Cellulose	4.079	4.097	3.920
(5H)-Furan-2-one	Cellulose	2.344	2.314	2.059
4-Hydroxy-5,6-dihydro-(2H)-Pyran-2-one	Cellulose	1.773	1.793	1.454
Phenol	Lignin	2.958	2.703	2.759
Guaiacol	Guaiacol	3.080	4.223	4.373
4-Vinyl guaiacol	Guaiacol	15.271	13.688	12.535
Eugenol	Guaiacol	0.000	0.000	0.000
5-Hydroxymethyl-2-furaldehyde	Cellulose	13.069	12.150	6.449
Pyrocatechol	Lignin	1.191	1.323	1.418
Syringol	Syringol	1.707	2.095	1.894
Vanillin	Guaiacol	0.463	0.555	0.486
4-Vinyl syringol	Syringol	0.844	0.982	0.579
Levogluconan	Cellulose	1.386	2.298	1.940
4-Propenyl syringol (trans)	Syringol	0.684	0.594	0.328
Syringaldehyde	Syringol	0.205	0.208	0.165
Acetosyringone	Syringol	0.085	0.132	0.097
Coniferyl alcohol	Guaiacol	0.175	0.122	0.130
Guaiacyl 4 ethyl	Guaiacol	1.876	1.757	1.735
		100.0	100.0	100.0
Cellulose derived compounds		71.46	71.6	73.50
Guaiacyl groups		20.86	20.35	19.26
Syringyl groups		3.52	4.01	3.06
Unknown lignin compounds		4.17	4.03	4.18
TOTAL LIGNIN		28.54	28.38	26.50

Figure 6-13 shows the sum of the derived lignin and cellulose compound [percentage], from the compounds analysed. The figure also incorporates on the x axis the lignin content and ash content.

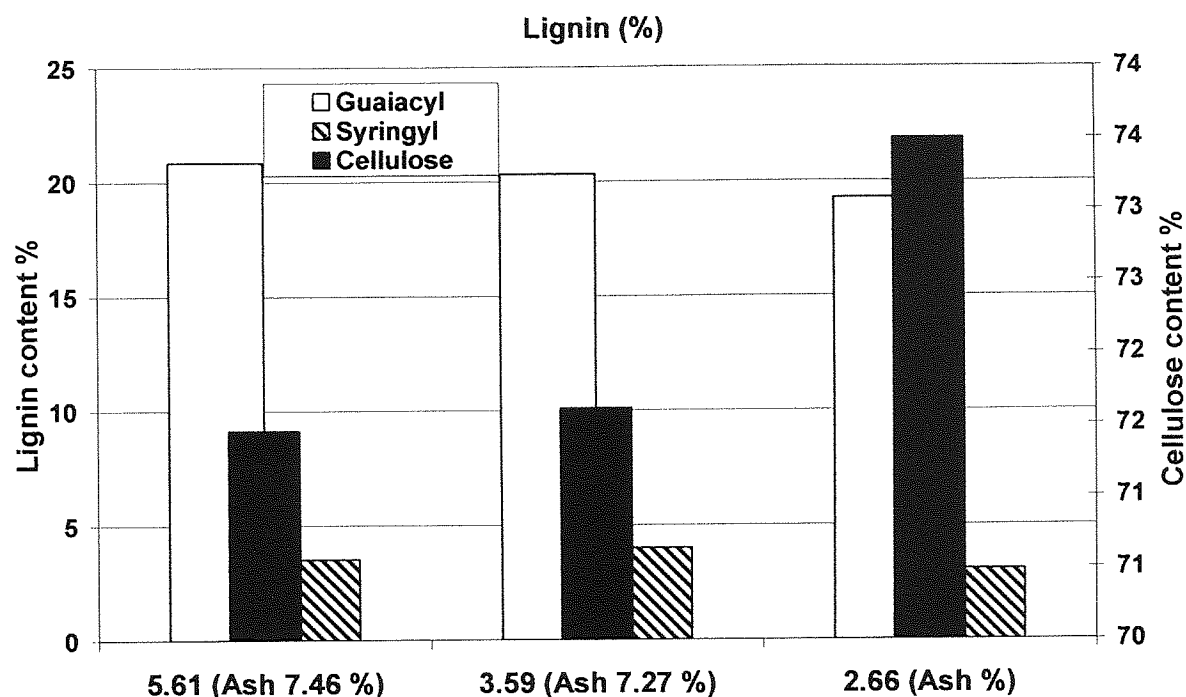


Figure 6-13 – The comparison of organic composition on grouped compounds in *Lolium* & *Festuca* grasses based on Pyroprobe-GC/MS results

The results clearly show the complex matrix of the degradation results as mentioned in chapter 6.3.1 that as lower lignin species are pyrolysed a greater yield of cellulose compounds are derived with lower yields in syringyl and guaiacyl derived compounds. The two higher lignin grasses show an increase in lignin derived compounds, with lower yields of cellulose derived compounds.

6.4.3.3 Mass balance results

The mass balance methodology has been discussed in Chapter 4 Section 4.5. Table 6-6 shows the results of the fast pyrolysis trials which was conducted on the 1 kg hr⁻¹ fluidised bed rig [methodology and description can be found in chapter 4]. It also shows the ash and moisture content for the *Lolium* and *Festuca* grasses as conducted according to the ASTM standard. The results presented in Table 6-6 are on dry basis. The results are in agreement with the early results as indicated by the analytical equipment, that the yields increase with higher lignin content, due to the reducing level of ash. The ash content is within a 0.5 % standard deviation.

Table 6-6 - Mass balance results on *Lolium* & *Festuca* grasses on Aston's 1 kghr⁻¹ fast pyrolysis rig

Run Number	175-06	169-06	172-06
Feedstock	<i>Lolium perenne</i> [2.66 %]	<i>Festuca arundinacea</i> [3.59 %]	<i>Dactylis glomerata</i> [5.61 %]
Reactor temperature[°C]	503	510	500
Hot vapour residence time [s]	0.93	0.84	0.88
Feedrate in wet basis [ghr ⁻¹]	506.44	55.67	762.82
Moisture content [mf wt%]	4.76	4.69	5.06
Ash [mf wt%]	6.23	7.27	7.46
Particle size [micro meters]	250-355	250-355	250-355
Run Time [minutes]	50.00	75.00	70.00
INPUT			
Wet Feed [g]	506.44	69.59	762.82
Dry Feed [g]	482.35	66.33	724.22
Water in Feed [g]	24.08	3.264	38.6
YIELDS [mf wt %]			
Char	32.12	33.79	34.86
Organics	29.46	30.81	30.62
Gas	14.19	15.37	13.70
Reaction water	24.21	16.37	20.81
Total Liquids	53.67	47.18	51.43
Closure (%)	92.48	96.51	93.56
GAS YIELDS [%]			
Methane	9.9	19.8	6.3
Carbon Dioxide	58.4	40.2	39.4
Carbon Monoxide	26.5	37.5	51.9
Hydrogen	0.22	1.04	0.92
Ethylene	0.61	0.05	0.50
Ethane	3.58	0.87	0.58
Propane	0.34	0.18	0.15
Propylene	0.45	0.36	0.25

The table shows that approximately 30 % of organics are produced from all the three species with a high yield of reaction water in comparison to other biomass feedstocks [1, 6, 10]. These oils would lower the viscosity and making it a more watery pyrolysis-oil, however allowing the risk of phase separation. The fresh oil and the aged oil did not phase separate when the oils were analysed. Aging was carried out on all the oils produced and the method is mentioned in Chapter 6. The mass balance closures exceeded 90 %, allowing the results of each of the

specie to be compared. It can be seen from Table 6-6 that the char and gas yields increase as ash content increases and as lignin decrease as suggested by literature [6, 10, 151].

6.4.3.4 Oil quality analysis

The oils produced from the fast pyrolysis experiments [fluidised bed reactor] was subjected to analysis to investigate its quality and stability [methodology found in Chapter 5 Section 5.3]. Table 6-7 shows the heavy oil fraction analysis, while Table 6-8 shows the elemental analysis of the light fraction oil.

Table 6-7 - Oil analysis of *Lolium* & *Festuca* grasses

	Dactylis glomerata [5.61 %]	Festuca arundinacea [3.59 %]	Lolium perenne [2.66 %]
Water content, [mf wt %]	43.53	34.14	48.04
Char content, [mf wt %]	0.42	0.14	0.28
Elemental analysis [mf %]			
C	36.75	32.05	30.64
H	8.82	9.76	9.63
N	1.88	1.41	0.77
S	0.10	0.10	0.10
O	52.46	56.69	58.86
HHV [MJ/kg]	17.62	16.65	15.82
LHV [MJ/kg]	15.69	14.52	13.72
GPC analysis [g/mol]			
Avg Mw	448	430	441
Avg Mw of aged oil	487	511	458
Mw Difference	39	81	17
Mw Index	0.09	0.19	0.04
Mn	345	340	313
Aged Mn	354	350	326
Mp	288	281	288
Aged Mp	288	281	281
Polydispersity	1.59	1.65	1.41
Aged Polydispersity	1.27	1.75	1.37
Viscosity@40°C, cp	9.23	10.86	6.53
Aged Viscosity@40°C, cp	12.06	12.81	7.87
Viscosity stability	0.31	0.18	0.21
pH	3.12	3.18	3.16
Homogeneity	phase separated*	phase separated*	phase separated *

*phase separation within 3 months after analysis.

Table 6-8 - Elemental analysis on *Lolium* and *Festuca* oil pot 2

Name	C (%)	H (%)	N (%)	S (%)	O (%)	H.H.V. (MJ/kg)
Dactylis glomerata [5.61 %]	7.74	10.9	0.1	0.1	81.15	7.02
Festuca arundinacea [3.59 %]	11.17	10.64	0.1	0.1	77.99	8.09
Lolium perenne [2.66 %]	11.06	10.47	0.1	0.1	78.27	8.98

Figure 6-14 and Figure 6-15 show the relationship between the average molecular weight against viscosity and lignin for the fresh and aged oils respectively for all the biomass samples which were subjected to pyrolysis-oil production for this project. It can be shown that as the lignin content decreases, so does the average molecular weight of the compounds present in the oil, thus lowering the viscosity, due to the level of reaction water present in the oil.

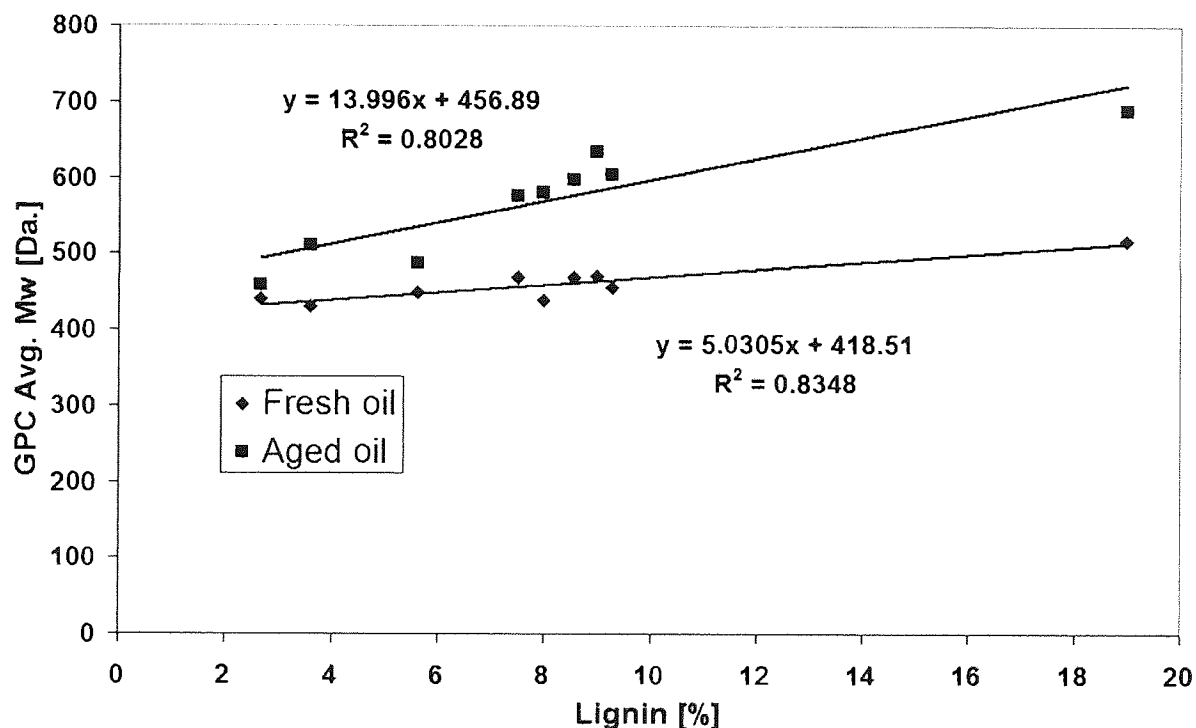


Figure 6-14 - Average molecular weight of pyrolysis-oil vs. actual lignin content [%] determined by wet chemistry

The average molecular weight for the aged oil increases dramatically as the lignin content increases, suggesting that the oil changes thermodynamically and increases in viscosity as aging occurs making the oil unstable [163].

Figure 6-14 results are in agreement with Figure 6-15, in which the viscosity does not change dramatically at lower lignin content [which gives a lower molecular weight] in comparison to the fresh and aged oils for the *Lolium* and *Festuca* and reference fuels [162, 164, 165].

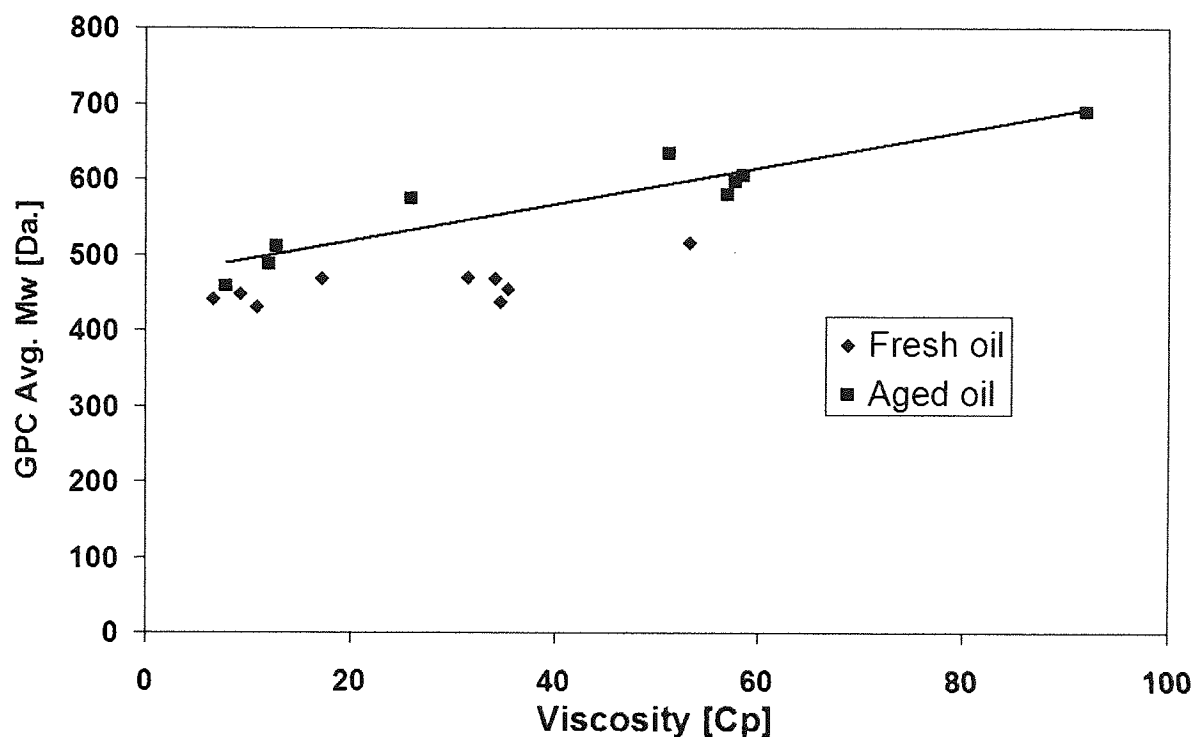


Figure 6-15 - Average molecular weight of pyrolysis-oil vs. viscosity

The viscosity method has been mentioned in chapter 5 Section 5.3, and results were analysed at 40°C to reduce any major deviations in viscosity according to a round robin analysis by Osama and Meier [146]. Viscosity analysis is influenced by the water content present in the oil [145], and is suggested that viscosity is one of the best analytical analyses to determine stability.

These results conclude that lowering the lignin content reduces the chemical change of the oil and making it more stable as aging occurs to the oil due to the lowering deviation in molecular weight. Figure 6-16 show relationship between viscosity and lignin for the fresh oil, while Figure 6-17 shows the relationship between the water content against viscosity, which include the reference data found in Chapter 6.

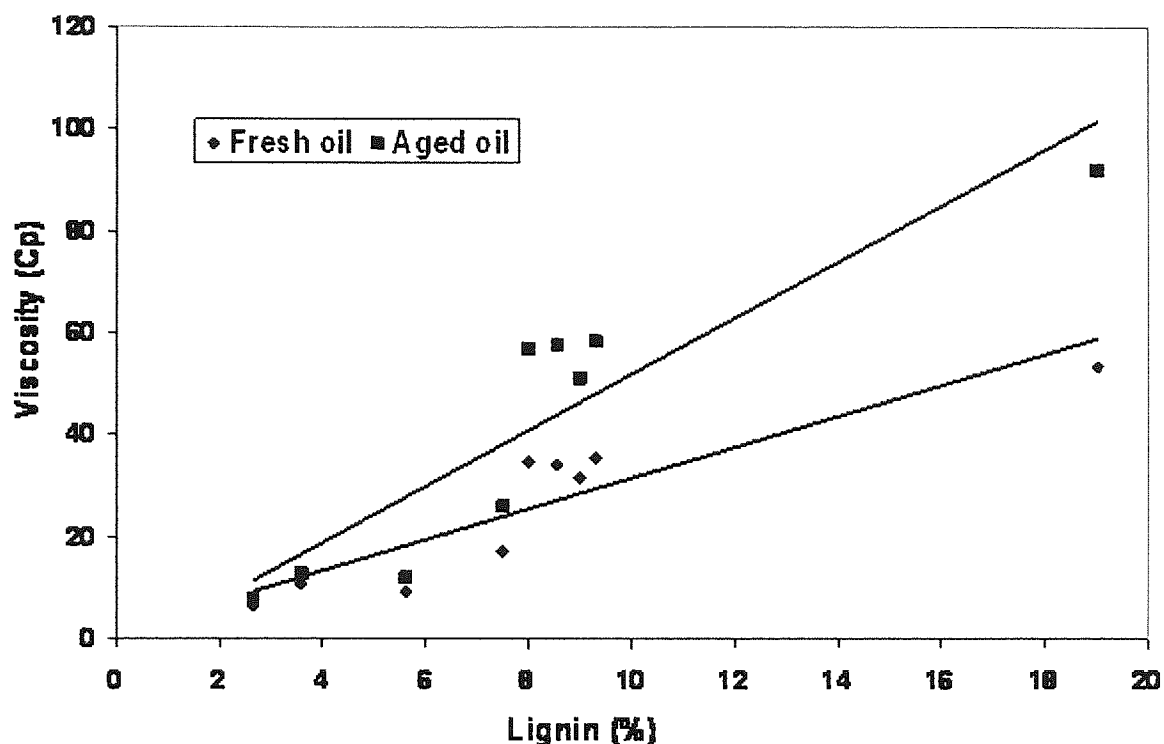


Figure 6-16 - Viscosity of pyrolysis-oil vs. actual lignin content [%] as determined by wet chemistry

It shows that the viscosity decreases while the organic yield also decreases, however the higher viscosity indicates lower water content which is present in the oil. Figure 6-16 is in agreement with the GPC results showing a clear relationship between the viscosity and the lignin content for producing stable oil with lower lignin feedstocks [similar trends were found for the average molecular weight as analysed by the GPC as shown in Figure 6-14 and Figure 6-15]. Figure 6-16 shows the viscosity results of all the reference fuels and *Lolium* and *Festuca* biomass plotted against the lignin content. The results suggest that the lignin present in the biomass contributes to the stability of the pyrolysis-oil, along side with the metal content of the raw biomass. The higher the lignin content within the biomass, the less stable the derived pyrolysis-oil becomes as it increases in viscosity as the aging progresses, while a lower lignin biomass can possess greater stability as the aging occurs. The lowering of molecular weight compounds can also be produced if excessive pyrolysis reactor temperatures were used allowing the vapours to undergo secondary and tertiary cracking as well as furthering depolymerisation to the lignin monomer [166].

Figure 6-17 show the relationship between the viscosities of the pyrolysis-oil against the water content for the fresh oil, for the *Lolium* & *Festuca* grasses and reference fuels. It can be seen that as the water content in the pyrolysis-oil decreases, the more viscous the pyrolysis-oil becomes; which agrees to the findings of Peacock and Bridgwater [145, 164].

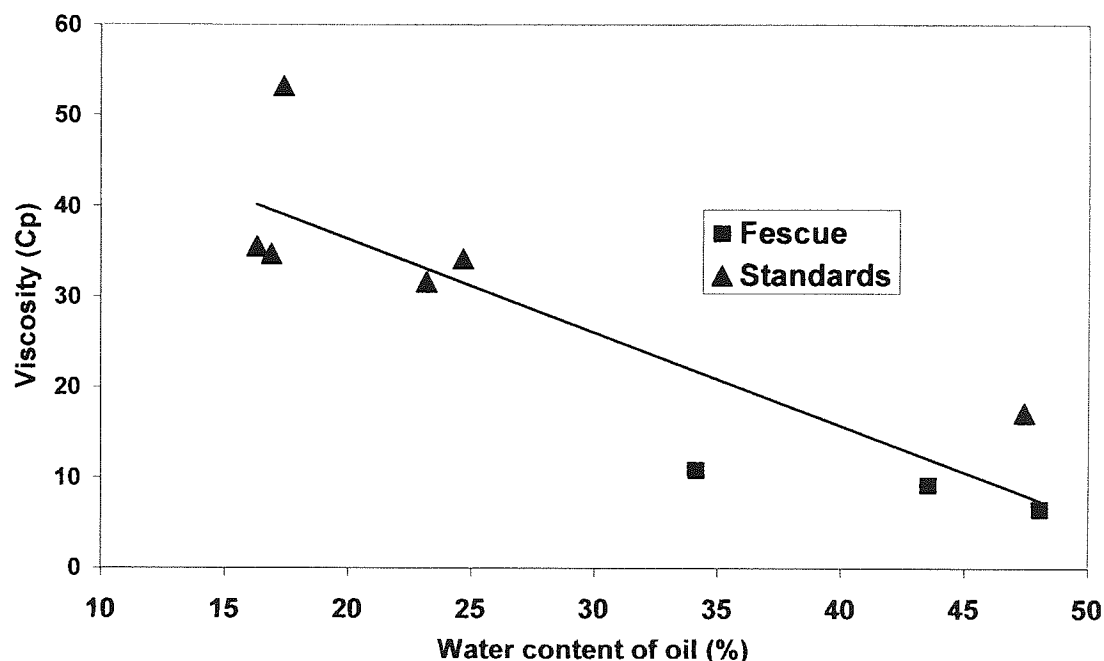


Figure 6-17 – Pyrolysis-oil viscosity vs. pyrolysis-oil water content

The three *Lolium* and *Festuca* oils produced were subject to liquid-GC/MS analysis along with its aged counterparts, in order to investigate how the chemical composition change with respect to time.[method is described in chapter 5]. Table 6-9 shows the results of the liquid-GC/MS of the *Lolium* and *Festuca* oils. It can be shown that the compound quantities do not change dramatically agreeing with the viscosity and GPC results. Oil pot 2 were also analysed from the trials [data not shown]. The results show that there is an increase in lower molecular weight compounds present in the dry ice condenser oils as ash increases [lower lignin content]. Thus increasing the oil yield and composition produced in the dry ice condenser which agrees with findings of the mass balance.

Table 6-9 - Chemical composition present in *Lolium* and *Festuca* pyrolysis-oils

Genotype	Chemical	Fresh Oil (% yield present in oil)	Aged Oil (% yield present in oil)
<i>Lolium perenne</i> Lignin 2.66 % Ash 6.23 %	2,3-Butandione	0.220	0.220
	Hydroxyacetaldehyde	5.671	5.940
	Phenol	0.318	0.674
	Guaiacol	0.098	0.012
	Eugenol	0.196	0.196
	5-Hydroxymethyl-2-furaldehyde	0.355	0.196
	Pyrocatechol	0.857	0.950
	Syringol	0.600	0.404
	Levogluconan	0.159	0.269
Total % present in yield		8.476	8.862
<i>Dactylis glomerata</i> Lignin 5.61% Ash 7.47 %	2,3-Butandione	0.259	0.222
	Hydroxyacetaldehyde	2.588	4.880
	Phenol	0.530	0.222
	Guaiacol	0.086	0.012
	Eugenol	0.062	0.062
	5-Hydroxymethyl-2-furaldehyde	0.246	0.148
	Pyrocatechol	0.863	0.875
	Syringol	0.764	0.678
	Levogluconan	0.407	0.592
Total% present in yield		5.805	7.690
<i>F. Arundunaces</i> Lignin 3.59 % Ash 7.27 %	2,3-Butandione	0.130	0.118
	Hydroxyacetaldehyde	1.284	2.263
	Phenol	0.330	0.542
	Guaiacol	0.012	0.035
	Eugenol	0.035	0.047
	5-Hydroxymethyl-2-furaldehyde	0.141	0.118
	Pyrocatechol	0.825	0.848
	Syringol	0.742	1.237
	Levogluconan	0.518	0.660
Total % present in yield		4.018	5.868

Figure 6-18 shows the results of the PCA analysis on how lignin affects pyrolysis-oil quality for all the *Lolium* and *Festuca* grasses and reference fuels. L-19, L-8, L-7.5 etc are abbreviation of lignin followed by the Klason [with ADF] values for each of the feedstocks as measured by wet chemistry. The results clearly show that there is a clear positive effect on low lignin fuels on metals, ash, char and reaction water. While the higher lignin contents like the energy crops and woody biomass affects greatly the molecular weight, viscosity, heating value

and organic yield by increasing its value. The data also shows that the lower lignin feedstocks have a negative effect on molecular weight, viscosity, heating value and organic yield which agrees from the findings of this chapter.

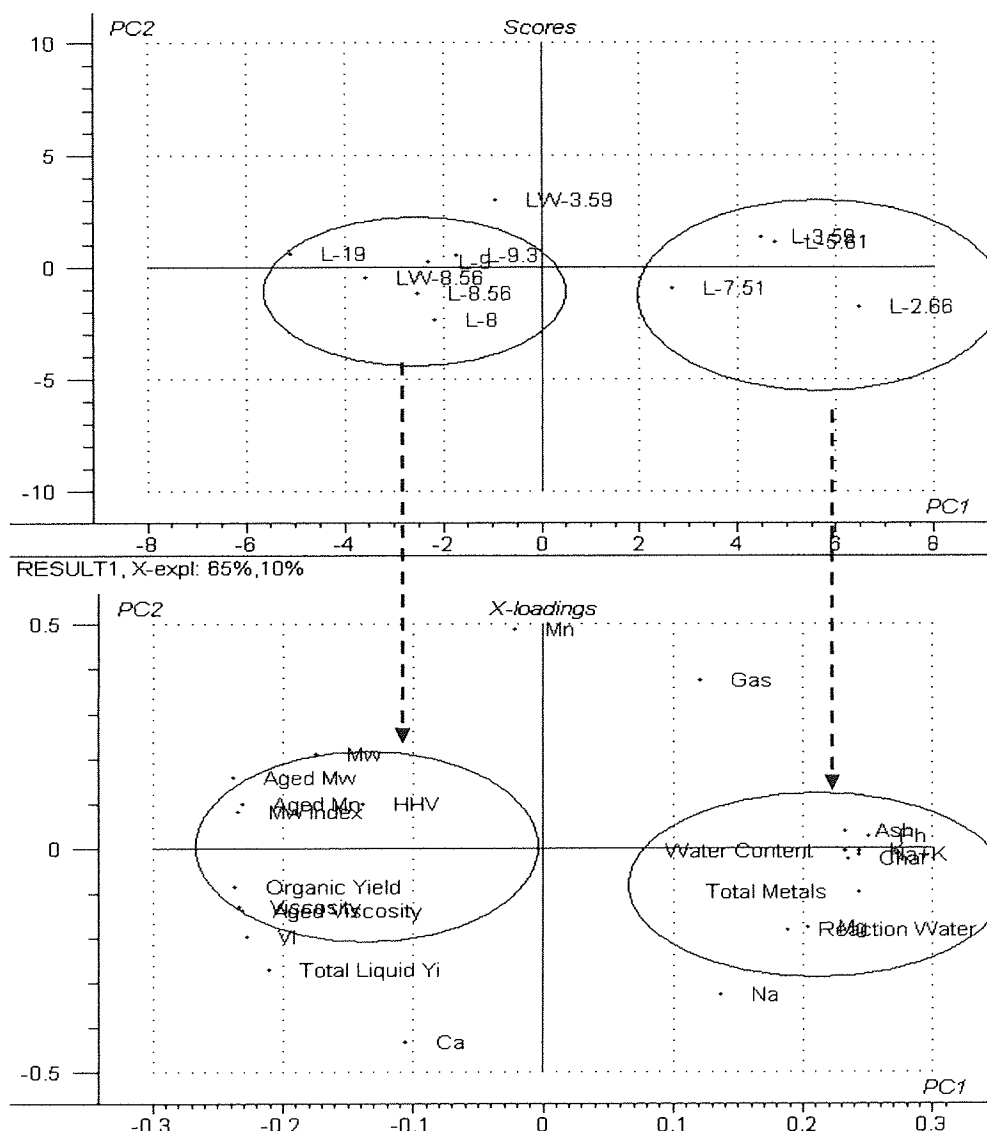


Figure 6-18 - PCA analysis of lignin and pyrolysis-oil qualities

From Figure 6-18 it can be seen that lower lignin content on the score plot [i.e. L-7.51, L-2.66, L-3.58 etc] has a clear relationship between reaction water, ash, char and total metals as found on the loading plot. Towards the left hand of the score plot the higher lignin content such as the energy crops have a strong relationship between the organic yield, molecular weight, heating value and viscosity as found on the loading plot.

6.5 Conclusions

This study showed that pyroprobe-GC/MS can be used as an analytical technique to assess the lignin content of grasses and other biomasses by the use of key markers found from the pyrograms, then summated together and plotted against the lignin content as determined by wet chemistry. A collection of *Lolium* and *Festuca* grasses with a lignin range from 2.1 to 3.7 % were used to validate this technique with the use of partial least squares to obtain a correlation of $R^2 = 0.88$.

The biological relationship between the different components of the biomass has also been investigated in this chapter. It shows that there is a relationship between the lignin content and the total metal content of the species, as well as the lignin having an inverse relationship with the holocellulose content of the plant.

The pyroprobe-GC/MS can qualitatively predict the yields of the pyrolysis-oil; however the chemical composition for individual compounds for the raw feedstocks and its pyrolysis-oil could not be derived. This is due to vapours undergoing so many reactions and secondary reactions during fast pyrolysis [due to the metal content] and as they are condensed to form the pyrolysis-oil. The results show that low lignin feedstocks would produce a lower molecular weight which has high water content. It also shows that the *Lolium* and *Festuca* grasses gave low organic yields and high char content. It can be seen from the PCA results [Figure 6-18] that all the energy crops have a positive effect on the molecular weight [Mw], and the number of different molecules [Mn], viscosity, organic liquid and total liquid yield, as well as having an effect on its aged counterpart by increasing its quality traits. However it can be seen that the L-19 [willow] has the greatest positive effect on Mw, Mn and heating value than any other of the feedstocks. However using a lower lignin feedstock gave a negative effect on the oil characteristics; by having a clear relationship on ash, char, metals, and water content. The gas content and certain alkali metals such as Na and Ca have no effect on any of the feedstocks. The PCA result agrees with the other findings in this work, suggesting that higher lignin biomasses can cause a greater instability in the oil in comparison to that of a lower lignin.

The results shown in this chapter strongly indicate that a stable pyrolysis-oil can be produced if a lower lignin biomass is used but not to a lignin region as for the *Lolium* and *Festuca* grasses as phase separation occurs. This was hypothesised by researchers in the past that if the

lignin was reduced or depolymerised further a stable oil can be produced [130, 166]. However this would affect the yield produced by lowering the organic yield due to the high level of metal content and high yield of reaction water which also reduces the oils heating value. This in turn would result in phase separation. The results of this would imply further investigation on a trade off analysis between yield and oil stability. However feedstock limits for metals, ash and lignin need to be identified and addressed in order to obtain and produce a commercial oil which can be used for applications, which does not change considerably with time, but still consists of an acceptable yield with a good heating value.

An investigation on the effect of the removal of these metals and its effect on pyrolysis-oil traits will be investigated and discussed in Chapter 7.

7 THE EFFECT OF METALS ON PYROLYSIS AND WASHING TREATMENTS FOR ENHANCING PYROLYSIS CHARACTERISTICS

This chapter investigates the effect of alkali metals on pyrolysis for *Lolium* and *Festuca* grasses. Two main reference fuels [switchgrass 2004 and willow chip] were also investigated to examine the effect and impact of washing biomass on pyrolysis and oil stability.

7.1 Introduction

This study involves a collection of *Lolium* and *Festuca* hybrids, in which some chromosome segments of *Lolium perenne* were substituted by the homologous region from *Festuca pratensis*, thus providing a variation in low lignin content. The *Lolium* and *Festuca* samples were separated into leaves making a total of 15 samples. Two reference fuels, switchgrass 2004 and willow, were also used to act as comparative standards in order to examine the effect of different washing conditions and study the overall impact of removing alkali metals, at which the optimum washing treatment was applied to the selected *Lolium* and *Festuca* grasses. The chapter also investigates the effect on pyrolysis-oil production from two washed feedstocks, Switchgrass 2004 and *F. Arundinacea*. Washing is a technique used to either reduce the amount of ash [in the form of metals oxides] or to remove the hemicellulose by using hot water, or acid washing to hydrolyse the hemicellulose component.

7.2 Experimental

7.2.1 *Lolium* and *Festuca* characterisation

The feedstock characterisation has been described in Chapter 5 Section 5.1. The TGA and pyroprobe methods and conditions have been described in previous Chapter 4 Section 4.3.

7.2.2 Principle component analysis

Principle component analysis method was used to analyse both the washed and unwashed *Lolium* and *Festuca* grasses as well as the reference fuels. The analysis was carried out to discriminate different feedstocks which were grown differently, and to investigate if a true

relationship exists between the lignin content and the metal content. The principle component analysis [PCA] technique and method has been described in Chapter 5 Section 5.5.

7.2.3 Washing techniques

The willowchip and switchgrass 2004 was subjected to three types of washing:

1. A continuous stirred washing for two hours using de-ionised water
2. A continuous stirred washing for twenty four hours using de-ionised water
3. A continuous stirred washing for two hours using de-ionised water at 60°C

While the *Lolium* and *Festuca* grasses were subjected to condition one only.

7.3 Results & Discussion

7.3.1 Characterisation results for *Lolium* and *Festuca* grasses

Lolium & *Festuca* hybrids and the reference fuels have been analysed for its elements, as well as for its moisture and ash content in Table 6-1, Table 6-2, Table 5-1, Table 5-2, Table 7-1 and Table 21. Table 7-1 shows the ICP analysis of the unwashed feedstocks while Table 8-2 shows the ICP analysis of the washed feedstocks.

It was found previously in chapter seven that as the lignin decreases the levels of the metals [especially sodium and potassium] increases. The most significant metal present was potassium, with levels of up to 3.7 % wt of dry biomass, and comprising up to 91 % of the total metals analysed. Magnesium, phosphorus, sulphur and calcium were also present in relatively high quantities. The *Lolium* and *Festuca* grasses were harvested green for maximum yield and thus the content of the essential nutrients are high. By comparison, the metal contents of the switchgrass and willow, which were winter harvested after senescence, were much lower. The metal analysis was also carried out on the washed samples [Table 8-2]. It was apparent that the different washing treatments were capable of reducing the content of water-soluble metal salts, although some individual metal contents were still relatively high. Metal contents could be further reduced by carrying out alternative washing treatments and identifying the optimum level of removal for each metal. However water washing treatment 1 was sufficient to remove 71-79 % of the metals, and the other more intensive washing techniques only removed an additional 0-12 % of the metals.

Table 7-1 - ICP analysis of unwashed *Lolium* & *Festuca* grasses [ppm]

Sample Code	Ash (%)	Al (ppm)	Ca (ppm)	Cu (ppm)	Fe (ppm)	K (ppm)	Mg (ppm)	Mn (ppm)	Mo (ppm)	Na (ppm)	P (ppm)	S (ppm)	C.V. (kJ/kg)
<i>L. multiflorum</i> -2x	3.38	37	1678	3	25	14606	804	46	1	1014	2459	942	18032
<i>L. multiflorum</i> -2xi	3.70	33	1699	3	22	16669	956	48	2	212	2142	1092	18116
<i>F. leytourneuxiana</i> -10x	4.07	33	2410	4	26	17405	1288	83	2	164	2925	1058	17691
<i>F. pratensis</i> -2x	4.43	163	1953	8	70	19049	828	35	10	131	1867	1184	17632
<i>F. mairei</i> -4x	5.12	165	1366	8	97	21645	1353	31	9	87	1652	2269	18057
<i>F. donax</i> -4x	5.34	137	1873	11	88	22957	831	69	13	191	2144	1442	18070
<i>F. boissieri</i> -2x	4.69	36	1261	4	25	22745	826	20	1	49	2444	1236	18194
<i>F. glaucescens</i> -4x	6.62	112	2868	6	65	25984	1944	35	9	364	3721	2634	17760
<i>F. apennina</i> -4x	8.58	45	4420	7	63	36805	1993	28	6	302	3368	2179	17864
<i>F. atlantigena</i> -8x	5.88	97	3033	5	69	24381	1667	52	8	127	2012	2452	17813
<i>F. drymeja</i> -2x	4.63	157	2007	11	90	18425	1159	48	10	200	2140	1550	17736
<i>F. pratensis</i> x <i>glaucescens</i> -4x	6.68	39	2793	5	60	32130	1510	30	4	191	2540	2194	18206
<i>L. multiflorum</i> -6x	7.84	82	6554	6	93	30214	1653	40	12	1210	2732	2926	18206
<i>F. arundinacea</i> -6x	6.94	75	2693	6	60	28985	1548	35	6	785	2538	2178	17865
<i>F. pratensis</i> -2x	6.71	42	3617	6	64	29501	1416	33	4	139	3698	2118	17830
<i>L. perenne</i> -2x	7.18	67	6208	8	80	28138	1695	55	3	902	3056	3499	17775
<i>L. multiflorum</i> -4x	7.73	69	7989	7	97	27480	1392	41	7	160	3519	3656	17747
<i>F. gigantea</i> -6x	7.93	61	7113	8	93	28007	2270	39	5	224	4038	3891	17869
<i>L. multiflorum</i> -2x	8.09	107	3894	8	87	37022	1343	44	14	217	3707	3539	17632
Switchgrass	4.30	102	6173	2	113	717	542	41	0	158	494	615	17305
Willow	1.34	60	3133	4	74	1957	385	32	0	58	804	301	18861

Table 7-2 - ICP analysis of washed *Lolium* & *Festuca* grasses and other biomass [ppm]

Sample Code	Al (ppm)	Ca (ppm)	Cu (ppm)	Fe (ppm)	K (ppm)	Mg (ppm)	Mn (ppm)	Mo (ppm)	Na (ppm)	P (ppm)	S (ppm)
<i>L. multiflorum</i> -4x (W)	50	922	3	44	686	293	25	0	67	466	533
<i>L. multiflorum</i> -2x (W)	67	1340	2	67	702	433	44	1	19	585	623
<i>F. apennina</i> -4x (W)	33	633	1	33	943	268	8	0	9	299	402
<i>F. mairei</i> -4x (W)	102	968	4	52	859	557	18	3	18	389	784
<i>F. arundinacea</i> -6x (W)	102	1857	5	155	966	690	19	3	30	1084	1382
<i>L. multiflorum</i> -6x (W)	199	8036	11	466	3227	1256	58	21	248	3181	4352
<i>L. perenne</i> -2x (W)	99	3955	5	168	612	862	23	6	18	1381	1957
<i>F. boissieri</i> -2x (W)	62	2817	4	68	1114	772	16	3	24	1097	1565
Willow Method 1	79	3054	4	56	419	349	53	0	23	186	302
Willow Method 2	77	3198	4	52	340	349	55	0	24	139	279
Willow Method 3	59	2933	3	34	264	328	51	0	15	147	256
Switchgrass Method 1	106	5409	3	122	78	422	30	2	32	213	500
Switchgrass Method 2	86	4604	8	96	116	306	23	2	28	182	460
Switchgrass Method 3	92	4996	4	123	69	345	26	1	30	185	446

7.3.2 Pyroprobe-GC/MS Results

Even though the alkali metal contents were still relatively high in the washed *Lolium* and *Festuca* grasses, the levoglucosan [analysis residence time typically 57-58 min] formed by pyrolysis increased after washing as indicated for the *Festuca mairei*-4x sample [Figure 7-1 and Figure 7-2]. However some lignin derived compounds decreased in concentration, such as phenol, and guaicol, which have residence times of 30.81 mins and 31.62 mins respectively, but coniferyl alcohol [which is also lignin derived] increased [Table 7-3]. The mechanisms behind the variable results are not clear, but future investigations should be carried out.

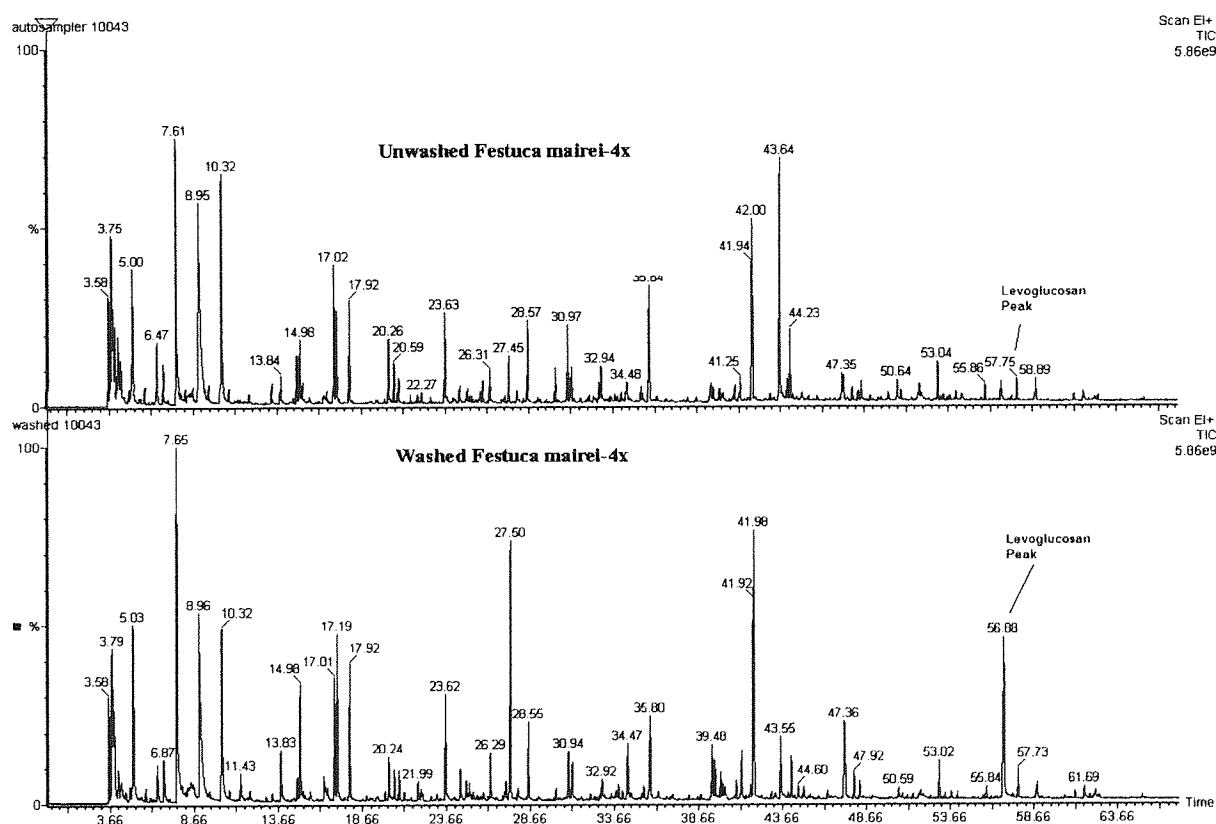


Figure 7-1 - Unwashed and washed *Festuca mairei*-4x

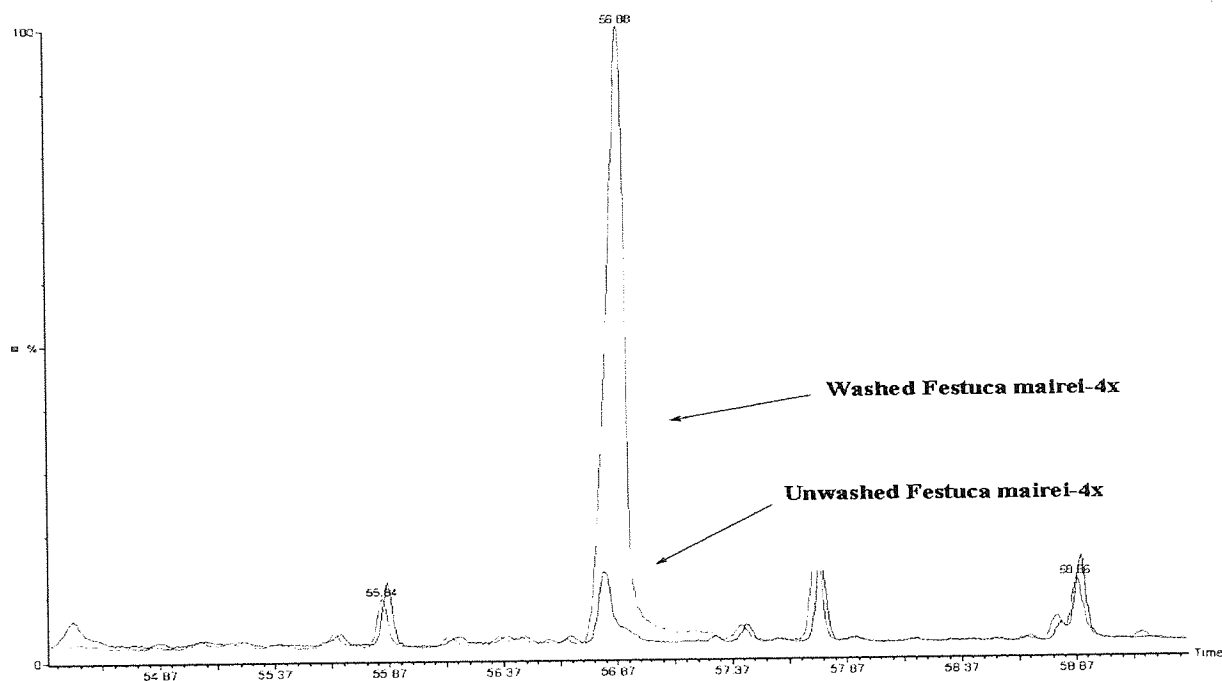


Figure 7-2 - The effect of washing on Festuca mairei-4x levoglucosan peak

The trends observed for the percentage change in degradation products for *Festuca mairei-4x* were before and after washing were representative of other feedstock samples. Levoglucosan exhibited the biggest change [a 900% increase] between samples [Table 7-3] due to the cellulose depolymerisation fragmentation pattern being most affected by the removal of the alkali metals. Lower alkali metal concentrations result in less fragmentation [ring scission] and are expected to reduce the hydroxyacetaldehyde yields. However the results in this study [Table 7-3] showed an increase in hydroxyacetaldehyde yields which were believed to be due to the only partial removal of alkali metals, resulting in higher yields of levoglucosan without reducing hydroxyacetaldehyde. Complete removal of alkali metals would be predicted to give very low yields of hydroxyacetaldehyde.

Table 7-3 - The overall effect of washing on pyrolysis products from unwashed/washed F. Mairei-4x [concentration reported as weight per volume]

Name of compound	Pre-cursor	Unwashed	Washed	Status	Concentration variation %
		Calibrated Conc. (g/l)	Calibrated Conc. (g/l)		
2,3-Butandione	Cellulose	0.96	0.82	decrease	15
Hydroxyacetaldehyde	Cellulose	8.48	17.81	increase	110
5-Hydroxymethyl-2-furaldehyde	Cellulose	3.21	0.7	decrease	78
Levogluconan	Cellulose	0.78	7.8	increase	900
Phenol	Lignin	0.63	0.2	decrease	68
Guaiacol	Guaiacol	0.59	0.38	decrease	36
Eugenol	Guaiacol	0.09	0.1	increase	11
Syringol	Syringol	7.48	4.69	decrease	37
Vanillin	Guaiacol	1.9	1.88	decrease	1
Syringaldehyde	Syringol	0.04	0.08	increase	100
Acetosyringone	Syringol	0.16	0.17	increase	6
Coniferyl alcohol	Guaiacol	0.45	0.53	increase	18

For the lignin derived compounds, some products increased in concentration, such as phenol and 2-methoxy-4-vinyl phenol, but others decreased. The influence of alkali metals and temperature on the fragmentation pattern of lignin is less well studied than cellulose, but it is clear that the mechanism of lignin decomposition is also modified by the presence of metals.

These results also support the finding that reduced alkali metal contents, especially of potassium, moves the degradation mechanism from fragmentation to de-polymerisation. Interestingly, a reduction in some lignin derived products was observed for more vigorous washing at higher temperature, suggesting that there may be a comparable mechanism for lignin degradation pathways as for cellulose.

7.3.3 The effect of washing time on willow chip

Washing has three types of parameters which can be varied independently. These are; the length of the washing treatment, the temperature of washing and the liquid solution used to wash the feedstock [de-ionised, distilled, or acid washing].

Willowchip and switchgrass 2004 was used to investigate the different duration times for washing at two hours and 24 hours and compared it back to its original untreated feedstock. Figure 7-3 show the concentration of products from willow on the y axis while on the x axis shows the washing condition as well as the potassium level in parts per million. The area were obtained from pyrograms and then calibrated to that specific chemical to give a concentration in g/l. Figure 7-3 shows the reduction of hydroxyacetaldehyde as washing periods increase, but an increase in levoglucosan. This suggests that the lower alkali metals especially potassium moves the degradation mechanism from fragmentation to de-polymerisation as suggested in the past by Broido Shafizadeh and Scott. Based on the data in Table 7-3 a similar principle can be applied to lignin compounds where compounds such as phenol, guaiacol, syringol and vanillin decrease while larger molecular weight compounds such as eugenol and syringaldehyde increase. This suggests a similar mechanism to that of the depolymerisation and fragmentation of cellulose compounds previously observed by researchers, due to the alkali metals present in the biomass. However there is not enough data in the table to support this theory, and the effect of alkali metals on lignin degradation due to alkali metals is poorly understood and will be the subject of future research.

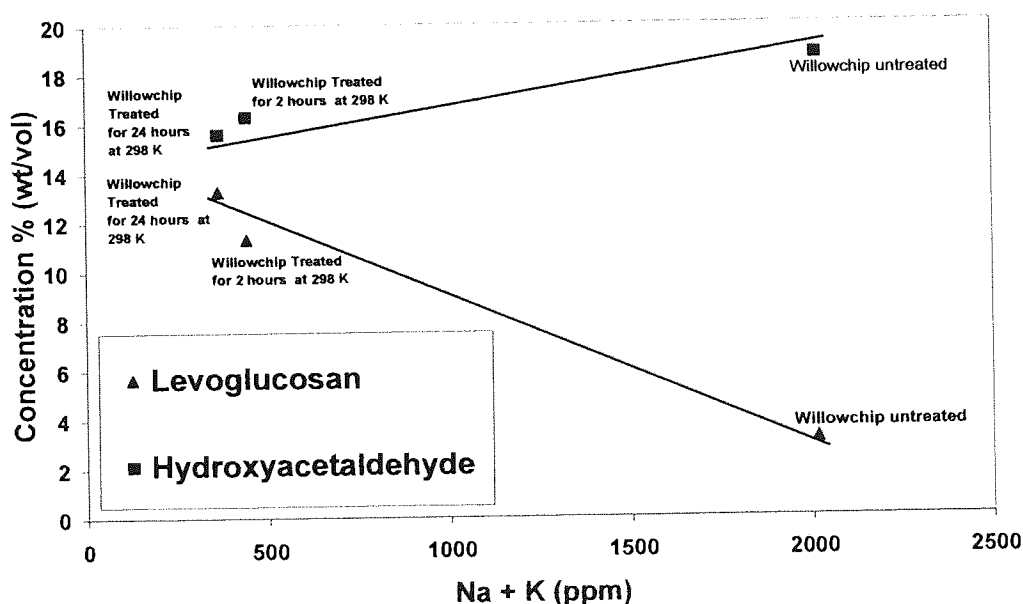


Figure 7-3 - The effect of washing time on Hydroxyacetaldehyde and Levoglucosan from willow chip

The relationship between levoglucosan and hydroxyacetaldehyde with sodium and potassium content in washed and unwashed willow was plotted [Figure 7-3]. This data strongly supports the mechanism proposed by previous authors [8, 27] whereby the degradation via depolymerisation and fragmentation can produce more or less of one product depending on the amount of metals present [especially alkali metals]. Similar trends were seen for the *Lolium* and *Festuca* grasses and switchgrass samples, with a reduction in hydroxyacetaldehyde concentration as washing period increased, but an increase in levoglucosan.

7.3.4 TGA results

Pyrolysis studies were undertaken using TGA for all the washed and unwashed samples, as described in the following sections. For the *Lolium* and *festuca* grasses, significant changes in the pyrolysis characteristics were observed after washing such as the degradation pattern of the biomass, char contents, and rate of degradation. Similar trends in DTG traces were seen for the unwashed versus washed willow and switchgrass 2004 samples [not shown]. These samples had much lower initial alkali metal contents and hence, while still easily detected, treatment has a less pronounced effect on the pyrolysis behaviour as investigated by the TGA. The unwashed *Festuca mairei* DTG curve [Figure 7-4] has two clearly defined peaks with a third peak tailing throughout and towards the end of the DTG curve.

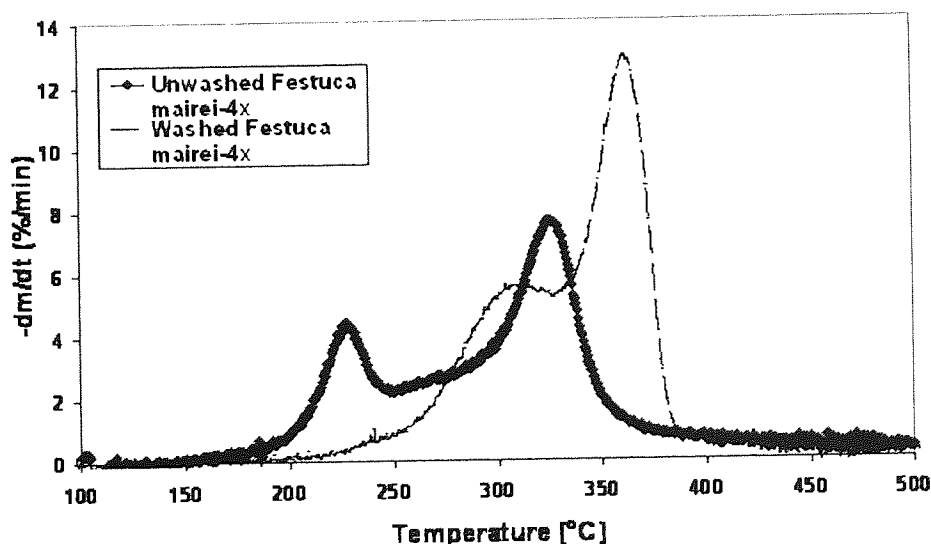
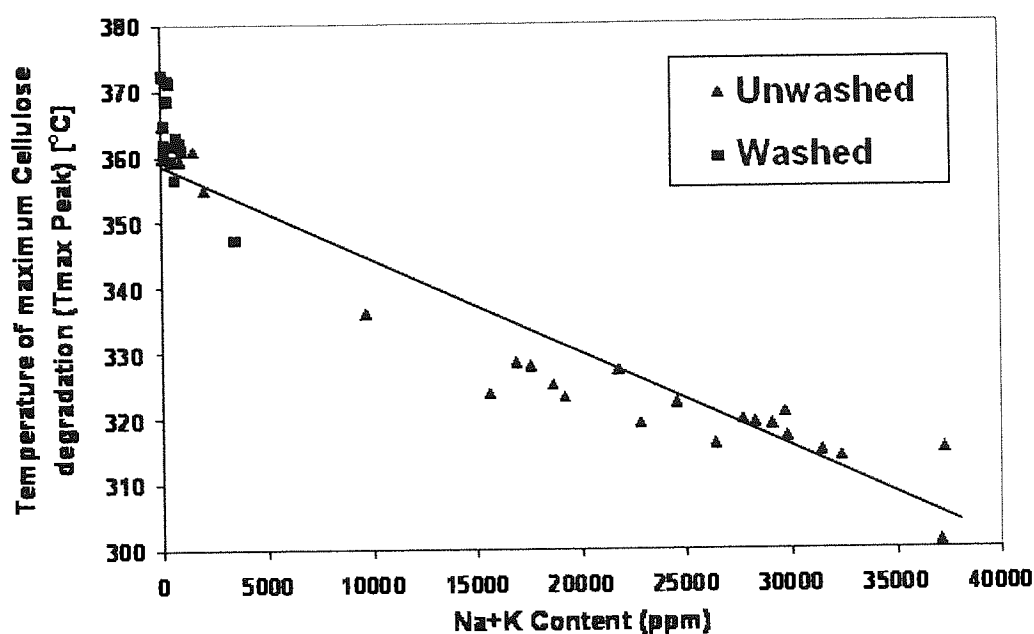


Figure 7-4 - DTG of temperature programmed pyrolysis of unwashed and washed Fescue Sample F.mairei-4x

The first peak at 230°C is usually attributed to hemicellulose decomposition, because of its less stable structure. The second major peak at 325°C corresponds to cellulose decomposition, and the greater peak height is indicative of the greater concentration of cellulose in the biomass. Lignin degrades over a wide temperature range and there is no clear maximum, because of its cross-linked structure and aromatic nature, the polymeric lignin matrix is capable of withstanding temperatures greater than 500°C [3, 65, 131, 167]. Pyrolysis of the washed *Festuca mairei* sample is also shown in Figure 7-4 as a DTG curve in comparison to the unwashed sample, and this indicates that the hemicellulose and cellulose apparently degrade at higher, and at closer, temperatures to produce a single peak with a shoulder. The shoulder is usually considered to arise from hemicellulose decomposition, while the main peak is considered to be mainly due to cellulose degradation.

Figure 7-5 depicts the shift in the temperature of pyrolysis of the main (cellulose) peak as a result of washing of samples. As well as shifting temperature, the washing to reduce alkali metals also changes the relative intensities of the decomposition ranges, indicating changes in decomposition pathways together with changes in product distributions as shown in [168]. The influence of metals on char yield in pyrolysis is illustrated in Figure 7-6. These results, together with those from the previous section show that the effect of washing was to reduce the amount of char and improved the yield of the organic vapours produced. This helps in the prediction of the quality and quantity of pyrolysis-oil from a larger scale process.



7.3.5 PCA analysis on the effect of lignin on metals

Figure 7-7 shows the results of the PCA analysis of the effect of lignin on the metals for all the biomass used in this project. It can be seen that the lignin content varied the quantity of metals present in the biomass, as well as showing that lower lignin biomass are enriched with sodium and potassium content which have a catalytic effect on pyrolysis. The higher lignin *Lolium* and *Festuca* grasses began to reduce on alkali metals and began to develop relationships with Ti, Fe Pb and Zn while reducing in P, Mg, Mo, S and K. The energy crops and woody biomass had a slight impact on certain metals such as Zn and Pb, but having a clear negative effect on certain metals such as Na, Cu, Mg and K. Overall the PCA gave a confidence level of 60 % on the relationship between lignin and metal content. It can be seen on the score plot that all the biomass follow a linear trend from low to high lignin content, as well as its clear relationship on the mineral uptake found on the loading plot. However the *Lolium & Festuca* grass which has a lignin content of 2.22% [*F.boissieri*-2x] does not follow the trend. From the loading plot it can be seen that the *lolium Festuca* grass which has a lignin content of 2.22% has a strong relationship with cadmium and aluminium [Cd and Al respectively] suggesting that this particular genotype is enriched with these metals and that it does not follow the same metal uptake and trend as the rest of the *Lolium Festuca* genotypes.

months of analysis as well as reducing its heating value. This finding concluded that the oils produced from low lignin feedstocks produce pyrolysis-oils which are low in viscosity and unsuitable for any application.

7.4.2 Experimental

7.4.2.1 *Washed feedstock characterisation*

The characterisation of the washed feedstocks has been described in Chapter 5.1. The TGA and pyroprobe methods and conditions have been described in previous Chapter 4.3.

7.4.2.2 *Pyrolysis reactor set up and methodology*

The mass balance methodology has been discussed in Chapter 4 Section 4.5.

7.4.3 Results & Discussion

7.4.3.1 *Washed feedstock characterisation*

F.Arundinacea and switchgrass 2004 exhibit a lignin content range of 3.59 % to 8.56 % respectively, and were washed in a continuous stirred washing for two hours using de-ionised water. The samples were selected based on molecular weight and viscosity results, as both being the best grasses within its grass specie. Table 7-4 and Table 7-5 show the elemental analysis and the alkali metals of the washed F. arundinacea and switchgrass 2004 respectively.

Table 7-4 - Elemental analysis of washed Festuca arundinacea and washed Switchgrass 2004

Sample	C _{DAF} (%)	H _{DAF} (%)	N _{DAF} (%)	S _{DAF} (%)	O _{DAF} (%)	ASH (%)	HHV (MJ/KG)
Washed switchgrass 2004	47.14	6.08	0.07	0.1	46.12	3.37	18.73
Washed F. arundinacea	45.20	5.98	0.87	0.1	47.86	4.38	17.77

Table 7-5 - Alkali metal content of washed grasses [ppm]

Sample	Ca (ppm)	K (ppm)	Mg (ppm)	Na (ppm)	Total Alkali metals (ppm)
Washed Switchgrass 2004	5409	78	422	32	6945
F. arundinacea Washed	3209	1605	757	47	8436

7.4.3.2 Pyrolysis rig results

7.4.3.2.1 Mass balance results

The mass balance methodology has been discussed in Chapter 4 Section 4.5. It was found early in the chapter that the *Lolium* and *Festuca* range have a low molecular weight with little chemical change after aging, even though the oil has no suitable application. Table 7-6 shows the mass balance of the washed feedstocks on Aston's 150 ghr⁻¹ fast pyrolysis reactor in comparison to the unwashed feedstocks extracted from Table 5-5 and Table 6-6. The washing with de-ionised water decreased the metals present in the biomass as well as reducing the ash content.

Table 7-6 - Mass balance of washed *Lolium Festuca* grass and switchgrass 2004 on Aston's 150 ghr⁻¹ fast pyrolysis rig

Run Number	169-06	195-w1	139-06	195-w2
Feedstock	Unwashed <i>Festuca</i> <i>arundinacea</i>	Washed <i>Festuca</i> <i>arundinacea</i>	Unwashed switchgrass 2004	Washed switchgrass 2004
Reactor temperature[°C]	510	504	500	509
Hot vapour residence time[s]	0.84	0.89	0.91	0.76
Feedrate in wet basis [ghr ⁻¹]	55.67	84.05	72.07	84.96
Moisture content [mf wt%]	4.69	5.0	8.30	5.0
Ash [mf wt%]	7.27	4.38	4.30	3.37
Particle size [micro meters]	250-355	250-355	250-350	250-355
Run Time [minutes]	75.0	60.0	85.0	50.0
INPUT				
Wet Feed [g]	69.59	70.0	102.10	77.34
Dry Feed [g]	66.33	66.50	93.63	70.8
Water in Feed [g]	3.264	3.50	8.47	7.0
YIELDS [mf wt %]				
Char	33.79	19.86	24.73	20.17
Organics	30.81	41.72	51.49	55.23
Gas	15.37	21.65	7.92	10.54
Reaction water	16.37	8.71	12.35	11.9
Total Liquids	47.18	50.43	63.84	67.13
Closure (%)	96.51	91.94	96.49	97.84
GAS YIELDS [%]				
Methane	19.8	15.26	6.40	14.32
Carbon Dioxide	40.2	64.04	45.11	60.01
Carbon Monoxide	37.5	18.64	43.86	21.71
Hydrogen	1.04	0.33	1.04	0.63
Ethylene	0.05	0.56	2.77	1.47
Ethane	0.87	0.39	0.60	1.46
Propane	0.18	0.36	0.11	0.37
Propylene	0.36	0.42	0.11	0.03

Fast pyrolysis was carried out to a similar temperature to that of its unwashed counterpart. The table shows that the organic yield increased for both samples, but had a higher impact on *F. arundinacea* rather than on the Switchgrass 2004. This is due to the optimum level of removing the metals from the water washing. This is shown by the switchgrass 2004, which the ash content only decreased by 25 % in comparison to the *Lolium Festuca* grass which was 43 %.

Due to the removal of metals from the water washing, the thermal degradation pathway was different to that of its unwashed counterpart as shown previously in this chapter. This resulted in a lower char, gas and water content, while the organic content increased as well as the total liquid yield.

7.4.3.2.2 Oil quality

The oils produced from the fast pyrolysis experiments [fluidised bed reactor] was subjected to analysis to investigate its quality and stability [methodology found in Chapter 5 Section 5.3]. The analysis of the oil produced from the fast pyrolysis of the washed *F. arundinacea* grass and switchgrass 2004 was analysed using the methods described in chapter five. Table 7-7 shows the oil analysis of the washed pyrolysed samples in comparison to the unwashed samples extracted from Table 6-7 and Table 5-8. It can be seen that the oil quality improved slightly in the case of the switchgrass 2004 and increased dramatically for *F. arundinacea* grass.

However similar trends can be seen in both of the feedstocks. The water content and viscosity of both washed species was improved, as well as its char content. Both of the oils produced from the washed feedstocks increased in the average molecular weight compound [Mw] and increased in the number of different molecules present in the oil [Mn] as measured by the GPC. The average molecular weight and the number of different molecules of the aged oils on both washed feedstocks increased greater than its unwashed counter part. This is probably due to the reduction in gas and char yield, thus allowing the degradation during pyrolysis to produce a greater yield of medium/high molecular weight compounds with a greater number of molecules present in the oil. Another explanation is due to the evaporation of water in the pyrolysis oil which increases the level accuracy of analysis of the higher viscous aged oil when the oil is analysed in the GPC. This concludes that the removal of metals increased the number of different molecules present in the oil, at which the majority of the molecules

produced are of a high molecular weight. These results agree with the area intensity of larger molecular weight derived compounds for cellulose and lignin as measured by liquid-GC/MS [Data not shown]. The data overall shows that water washing can improve the quality of the pyrolysis-oil, however is dependant on the feedstock, as a greater oil instability can be occur if the unwashed counter part oil has already a high Mw and Mn.

Table 7-7 - Oil quality analysis on washed F. arundinacea and washed Switchgrass 2004

	Festuca Arundinacea unwashed	Festuca Arundinacea washed	Switch grass 2004 unwashed	Switch grass 2004 washed
Water content, [mf wt %]	34.14	29.21	24.70	17.2
Char content, [mf wt %]	0.14	0.09	0.77	0.27
Elemental analysis [mf %]				
C	32.05	44.82	38.30	39.42
H	9.76	9.18	7.42	6.73
N	1.41	1.09	0.10	0.1
S	0.10	0.1	0.10	0.1
O	56.69	44.82	54.08	53.65
HHV [MJ/kg]	16.65	21.7	16.43	16.02
LHV [MJ/kg]	14.52	19.70	14.81	14.55
GPC analysis [g/mol]				
Average Mw	430	490	468	480
Average Mw of aged oil	511	645	597	624
Mw Difference	81	155	129	144
Mw Index	0.19	0.316	0.28	0.30
Mn	340	339	328	317
Aged oil Mn	350	383	380	387
Mp	281	316	243	337
Aged oil Mp	281	316	356	347
Polydispersity	1.65	1.44	1.43	1.39
Aged oil Polydispersity	1.75	1.68	1.57	1.55
Viscosity@40°C, cp	10.86	13.51	34.18	33.25
Aged oil viscosity@40°C, cp	12.81	18.27	57.64	52.11
Viscosity index	0.18	0.35	0.69	0.57
pH	3.18	3.01	2.87	2.8
Homogeneity	phase separated*	Single phase	Single phase	Single phase

* phase separation within 3 months after analysis.

7.5 Conclusions

Comparing Table 6-7, Table 5-8 and Table 7-2 [unwashed and washed samples], it was observed that the washing treatment reduced the majority of the metal contents by a factor of 60-80 % of the original metal content. Pyroprobe-GCMS of the untreated and treated *Festuca mairei* sample shows the same compounds, but the intensities of certain compounds generally increase, of which the most significant is levoglucosan.

It has been shown previously that the yield of organic volatiles for pyrolysis-oil increased after washing at the expense of char and gas [54, 60]. In this study where the TGA results of char yield were plotted against alkali metal contents, there was a negative linear relationship [Figure 7-6]. It can be seen that the washed feedstocks all produce less char than the unwashed feedstocks. The results show the same trend of evolution of volatiles in the pyroprobe-GCMS as suggested by other researchers even though char and gases were not measured [6, 8, 131]. The compounds from degradation of the feed materials can be quantified from the pyroprobe-GCMS by calibrating the spectra areas with known standards. As for willow, in the grasses levoglucosan increased with lower alkali metal contents at the expense of hydroxyacetaldehyde [Figure 7-3], suggesting ring scission is occurring at lower alkali metal levels instead of defragmentation of the glucose monomer in cellulose. The TGA pyrolysis of unwashed and washed *Festuca* [Figure 7-4 and Figure 7-5], indicated that the maximum rate of degradation for the washed grass sample moved to higher temperatures in comparison to the unwashed biomass. This suggests that metals increase the rate of degradation as well as lowering the temperature of degradation. Noticeable features of this data are that the hemicellulose peak merges with the cellulose peak in the washed *Festuca* sample unlike the unwashed sample. This is due to limiting the temperature region where hemicellulose and cellulose degrade together even though the degradation temperature for hemicellulose and cellulose has increased. It has been shown that as lignin increases the level of metals decrease, but feedstocks of low lignin content with high metals content can be improved by treating the feedstock by water washing and removing up to 70 % of the alkali metals.

PCA was carried out on the effect of lignin on metals for the *Lolium* and *Festuca* grasses as shown in Figure 7-7. The findings of the PCA agree with Figure 6-2, that the lignin has an effect on metals in general. It can be seen that as higher lignin values are used the alkali metals

are reduced significantly but increases in Zn, Mn and Pb according to the PCA analysis. Lower lignin content would increase the main alkali metals such as K and Na as well as Cu, P and Mo. However the *Lolium* and *Festuca* grass with a lignin content of 2.22 % increased in Cd and Al. Thus the major alkali metals such as sodium, potassium, calcium and magnesium have a significant effect on pyrolysis, as shown by effects on temperature of maximum degradation, rate of degradation, chemical degradation mechanisms and yields of products. It is well stated in literature that the effect of metals, lower/increases the temperature at which maximum pyrolysis liquid is produced, as well as effecting its oil characteristics [166, 169-171].

The catalytic effects of metals on pyrolysis are similar and are applicable to any type of biomass. The catalytic effects tend to lower yields, reduce degradation temperatures and change the reaction pathways and decomposition mechanisms [172, 173]. Previous researchers [28] have obtained relationships for the mechanisms of the degradation of cellulose and how it can determine the fragmentation [ring scission] or depolymerisation route and its dependence on the alkali metal content. This can increase certain derived compound concentrations while reducing other compounds of lower molecular weight. The same principle can be applied to lignin compounds [Table 7-3] where compounds such as phenol, guaiacol, syringol and vanillin decrease while larger molecular weight compounds such as eugenol and syringaldehyde increase. This suggests that a similar mechanism to the depolymerisation and fragmentation of cellulose compounds previously observed due to the alkali metals present in the biomass. However the actual mechanism of lignin degradation due to the alkali metals is unknown and should be the subject of future research.

The pyrolysis-oils produced from the washed *Festuca arundinacea* and switchgrass 2004 improved the oil quality in comparison to that of its unwashed counterpart and did not phase separate within three months. The water content and char content of the oil decreased due to the reduction of catalytic cracking of the vapours, resulting also in a lower gas and water yields during fast pyrolysis. The average molecular weight compound [Mw] increased for both washed species, as well as the number of compounds present in the oil [Mn]. This suggests that a slightly increased number of molecules were produced within pyrolysis at which a large proportion of the vapors were of a higher molecular weight. This is likely due to the reduction of the metals resulting in a different thermal degradation fragmentation [i.e. in the case of

cellulose depolymerisation rather than ring scission], and reducing cracking and secondary reactions of the vapours. This has been speculated in literature that secondary reactions may be of importance in producing an oil [166]. This can either improve oil stability or reduce it, depending on the biomass and its organic and inorganic composition. However due to the increase of the number of molecules, and in molecular weight; the oil was improved substantially but caused a greater change during aging unlike its unwashed counterpart, as shown in the molecular weight difference and viscosity index.

However it was shown that the switchgrass 2004 has reached its optimum metal and ash reduction [Figure 7-5], and the oil qualities only improved slightly in comparison to its unwashed counterpart [Table 7-7], suggesting that all biomass have a threshold in the removal of the metals, which will result on the impact of the level of improvement in the oil quality.

8 AGRONOMICAL EFFECTS ON MISCANTHUS FEEDSTOCK QUALITY

This chapter reports on the effect of different fertiliser treatments of Miscanthus to optimise yield and fuel qualities for producing a commercial pyrolysis-oil by fast pyrolysis. The biomass production work using different fertilisers was carried out by Rothamsted Research which is a partner in the SUPERGEN Bioenergy project. Three different fertilisers were used: nitrogen and potassium as chloride and sulphate. The Miscanthus that was produced under the different fertilisation conditions was subjected to characterisation and analytical pyrolysis investigation in order to establish a relationship between pyrolysis products, Miscanthus and the growing conditions.

8.1 Introduction

The optimum agronomical practices for Miscanthus have yet to be established to identify conditions and treatments which optimise feedstock characteristics for fast pyrolysis conversion. The results of such a study would enable chemists, engineers and farmers within the bio-energy community to gain a deeper understanding in how the feedstock grows as well as how much the feedstock can be modified to reach optimum Miscanthus yield and pyrolysis-oil yield and fuel quality.

The energy crop used in this study was Miscanthus [*Miscanthus x giganteus*] which was planted in 2003 and sampled three times throughout the growing season. The first sampling of growth was carried out on 3/11/05, the second sampling was conducted on 19/12/05, and the last sampling on 1/02/06 at Rothamsted. Miscanthus *giganteus* was separated into leaves and stems to understand how the plant varies throughout the growing season from the effects of different fertiliser treatments.

Three fertilisers have been used in this study, nitrogen, potassium as muriate of potash [KCl] and potassium as sulphate of potash [K₂SO₄], in which their rates of application varies from plot to plot. Overall 14 experimental treatments were carried out and repeated three times to give 42 samples for stems and leaves. This has enabled identification of key fertiliser

treatments and harvesting periods which give the maximum yield and optimum feedstock characteristics for producing a good fast pyrolysis yield and oil quality.

8.1.1 Fertiliser treatments and plots

The field used for the experiments at Rothamsted was made up of an 84 meter by 82 meter to investigate the effect of fertiliser treatments on Miscanthus. The field area was divided into 42 plots with a size of 120m² [0.012 ha]. Table 8-1 shows the 14 different experiments with the field plot numbers which have been assigned to from its treatment number.

Table 8-1 - Treatments for Miscanthus

Treatment number	Treatments			PLOTS
	Nitrogen (kg/ha)	KCl (kg/ha)	K ₂ SO ₄ (kg/ha)	
1	0	50	0	2,15,33
2	50	100	0	1,19,41
3	50	0	0	3,22,38
4	50	0	50	4,26,36
5	50	50	0	5,24,29
6	50	0	100	7,21,39
7	100	50	0	13,27,42
8	150	100	0	6,18,31
9	150	0	100	9,16,32
10	150	0	0	10,17,37
11	150	50	0	11,23,35
12	150	0	50	12,20,34
13	200	50	0	14,28,40
14	250	50	0	8,25,30

Each treatment was repeated in three different plots to replicate conditions. It has been suggested that soil types, amount of sunlight and rainfall would change nutrient levels for the same treatment in each of the three different plots [2].

8.1.2 Grouped fertiliser treatments

8.1.2.1 *Nitrogen*

The effect of nitrogen fertiliser and its application rate on Miscanthus was investigated throughout the growing period. Five nitrogen treatments were investigated in which a fixed level of KCl [50 Kg/ha] was also applied to compensate for the lack of fertiliser in order to aid the establishment and growth of the plant. The five treatments for nitrogen were:

- Treatment 3:- Nitrogen 50 kg/ha 0 kg/ha KCl & 0 kg/ha KS
- Treatment 7:- Nitrogen 150 kg/ha 0 kg/ha KCl & 0 kg/ha KS
- Treatment 10:- Nitrogen 100 kg/ha 50 kg/ha KCl & 0 kg/ha KS
- Treatment 13:- Nitrogen 200 kg/ha 50 kg/ha KCl & 0 kg/ha KS
- Treatment 14:- Nitrogen 250 kg/ha 50 kg/ha KCl & 0 kg/ha KS

8.1.2.2 *Potassium Chloride*

The effect of potassium as potassium chloride was also investigated on Miscanthus. A fixed amount of nitrogen of 50 kg/ha and 150 kg/ha [high land low levels] was used to help the plant be established when varying the potassium chloride rate. The treatments was selected based on practical agronomical practices, however to obtain a realistic result, nitrogen should remain constant with vary levels of potassium chloride, to investigate the effect of potassium chloride on Miscanthus metals, yield and pyrolysis characteristics. The five potassium chloride treatments which were used to investigate the effect of chloride are:

- Treatment 1:- Nitrogen 0 kg/ha 50 kg/ha KCl & 0 kg/ha KS
- Treatment 2:- Nitrogen 50 kg/ha 50 kg/ha KCl & 0 kg/ha KS
- Treatment 5:- Nitrogen 50 kg/ha 100 kg/ha KCl & 0 kg/ha KS
- Treatment 8:- Nitrogen 150 kg/ha 50 kg/ha KCl & 0 kg/ha KS
- Treatment 11:- Nitrogen 150 kg/ha 100 kg/ha KCl & 0 kg/ha KS

8.1.2.3 *Potassium Sulphate*

The effect of potassium as potassium sulphate [rather than as potassium chloride] was the last fertiliser treatment to be investigated in the field experiments. A fixed amount of nitrogen of 50 kg/ha and 150 kg/ha [high land low levels] was used to help the plant to be established when varying the potassium sulphate rate. The treatments was selected based on practical agronomical practices, however to obtain a realistic result, nitrogen should remain constant with vary levels of potassium sulphate, to investigate the effect of potassium sulphate on Miscanthus metals, yield and pyrolysis characteristics. Four sulphate treatments were used to investigate the effect of sulphate which is:

- Treatment 4:- Nitrogen 50 kg/ha 0 kg/ha KCl & 50 kg/ha KS
- Treatment 6:- Nitrogen 50 kg/ha 0 kg/ha KCl & 100 kg/ha KS
- Treatment 9:- Nitrogen 150 kg/ha 0 kg/ha KCl & 50 kg/ha KS
- Treatment 12:- Nitrogen 150 kg/ha 0 kg/ha KCl & 100 kg/ha KS

8.1.2.4 *Samples*

14 sets of samples were provided by Rothamsted Research for each treatment method, separated into leaves and stems, with three replicates.

8.1.3 Miscanthus yield reports per sampling

The yield results are based on the height of Miscanthus, and the average changes in yield, on a per stem basis [dry wt per “tiller”] for each of the three replicates. A factor can be applied to convert the results into [ton/ha]. The analysis on average took 15 stems from the selected area, at which it was sampled again along the plot. The stem has been cut at approx 5 cm above the soil surface using secateurs and placed into a labelled bag. This method allowed an accurate yield assessment without damaging the crop and limiting the amount of material taken off the field.

8.2 **Experimental**

The Miscanthus feedstock was subject to moisture and ash analysis to characterise the biomass, and methods are explained in Chapter 5.4. ICP analysis for the main alkali metal contents was also conducted on all the samples throughout the different sampling periods and its methodology can be found in Chapter 5 Section 5.1.6. The average standard deviation percentage of each of the alkali metal content varies from 5-20 % for leaves and 15-35 % for stems.

8.2.1 Miscanthus characterisation

Please refer to Chapter 4 Section 4.5 for a description of the detailed methodology.

8.2.2 TGA and Pyroprobe-GC/MS conditions

Please refer to Chapter 4 Section 4.5 for a description of the detailed methodology. The PCA analysis [as described in Chapter 5 Section 5.5], for the compounds derived from Miscanthus and its treatments are included in APPENDIX II for leaves and stems.

8.3 Results and discussion

8.3.1 The agronomical effect of nitrogen fertiliser

8.3.1.1 *The effect on ash and metal content with respect to sampling time*

Figure 8-1 shows the average leaf ash content for the nitrogen fertiliser treatments for the three set of samples throughout the growing seasons, while Figure 8-2 shows the stem ash content for the different nitrogen treatments.

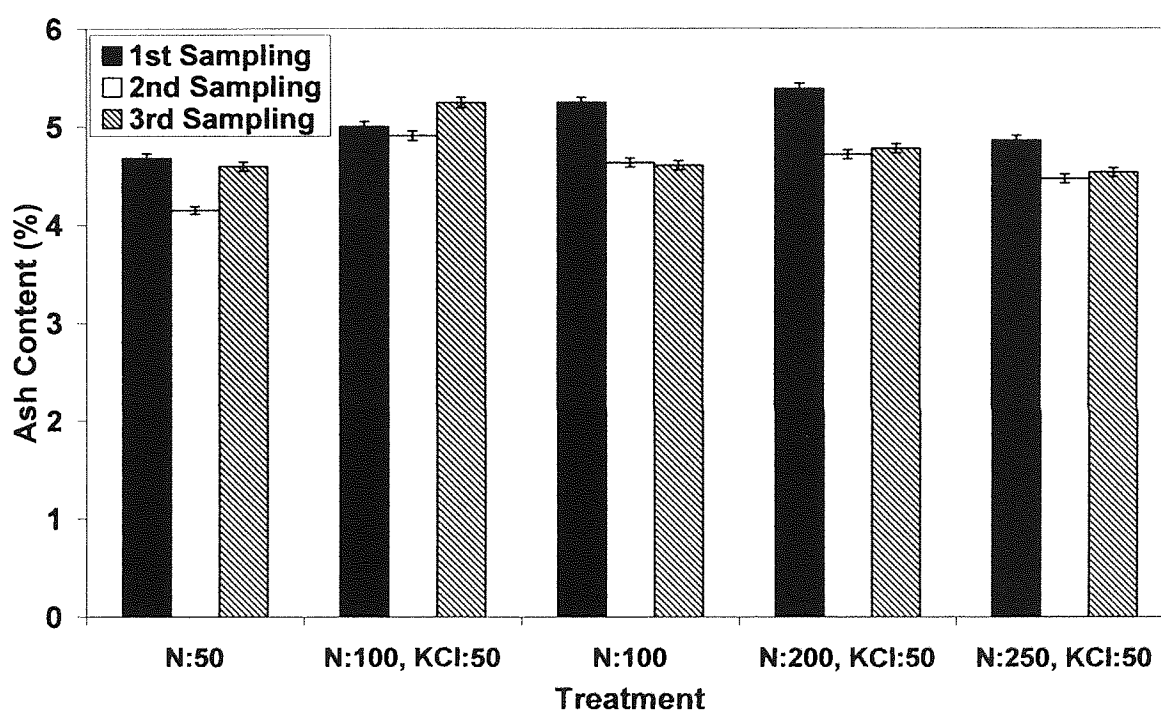


Figure 8-1 - The average ash content of nitrogen fertiliser treatments of the three sampling periods for leaves

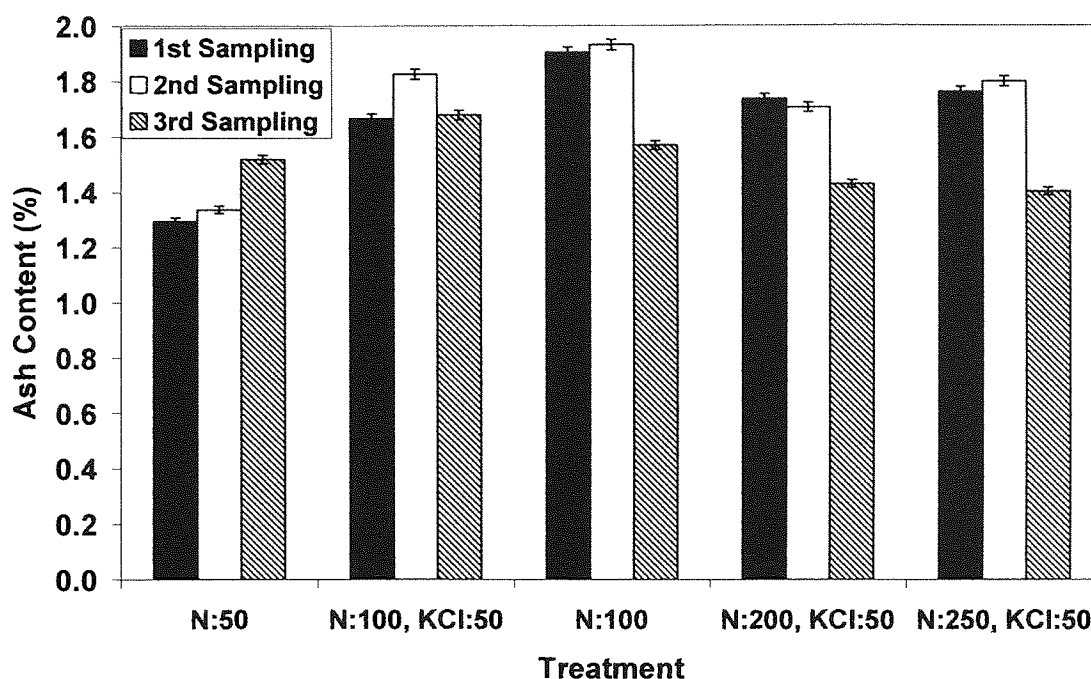


Figure 8-2 - The average ash content of nitrogen fertiliser treatments of the three sampling periods for stems

It can be seen from Figure 8-1 that while the average ash content for leaves varies during the growing period this is not significant, and is typically 4.2 to 5.5%wt. The stems [Figure 8-2] exhibit comparable behaviour over the growing cycle and have a lower ash content than that of the leaves, typically 1.2 to 1.9 %wt. The standard deviation percentage for each treatment [based on the average of three plot replicates], are shown for the leaves, and varies from 0.1-0.6 %. The average ash content for the stems has a standard deviation of below 0.8 %.

8.3.1.1.1 Leaf alkali metals

The total average alkali content present in the leaves for each of the different nitrogen treatments throughout the three sampling periods are shown in Figure 8-3. The treatments show that the total average alkali metal contents present in the leaves [the sum of Na, K, Mg and Ca] decrease throughout the sampling periods for all the nitrogen treatments. The results agree with the ash content for the leaves [for the majority of the treatments] showing that senescence occurs over the winter period, and higher level of metals are required in the beginning to establish the plant to grow. Approximately 30-35 % of the alkali metals present in the leaves is lost over the winter period, and becomes almost constant in February. Figure

8-3 suggests that senescence is complete by mid December [for this particular crop] and that little change occurs after this time.

Referring to APPENDIX II-Table 1 it can be seen that the level of potassium and magnesium contents [ppm] decrease, while the sodium content increases throughout the sampling periods for all the nitrogen treatments. This suggests that as the plant senesces, natural biological changes occur within the plant, and requires different mineral uptake in order for the plant to die.

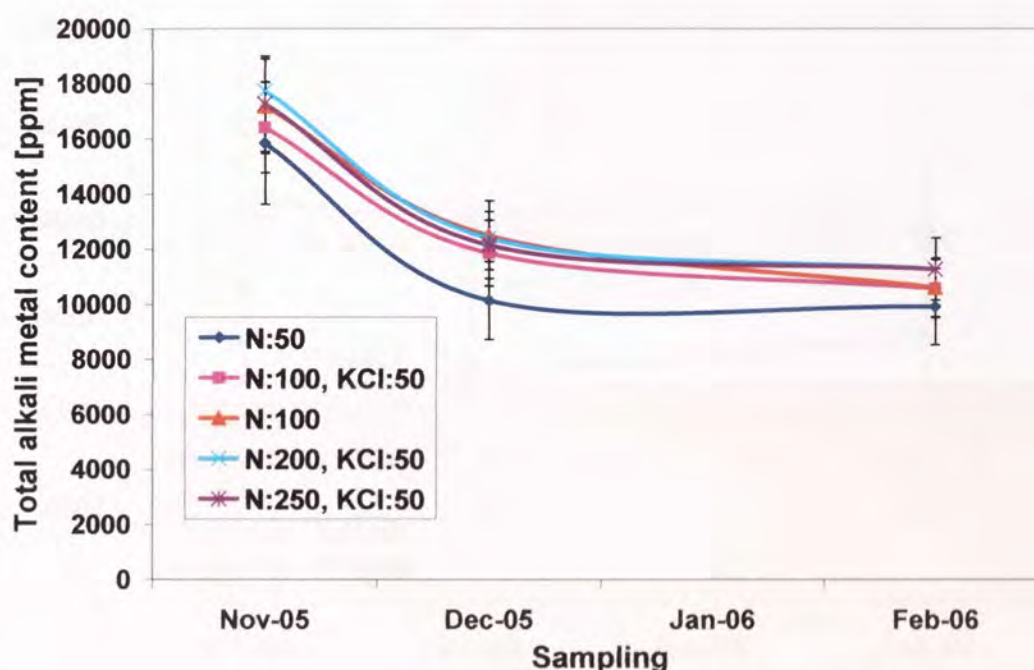


Figure 8-3 - The effect of nitrogen treatments and sampling on Miscanthus alkali metal content in leaves

8.3.1.1.2 Stem alkali metals

Figure 8-4 shows the total average alkali content present in the stems for each of the different nitrogen treatments throughout the three sampling periods. It can be seen that the majority of the results for stems are different to those of the leaves. In particular the senescence effects are quite different with little overall change in alkali metal content. The leaves indicated that the overall alkali content decreases for all the different nitrogen treatments, however the stems portray a different result at which only N:100 decreased uniformly throughout the sampling

periods. The remaining treatments suggest an increasing trend, but this is an unlikely effect and is within the experimental error of the results.

Due to the higher standard deviations for all the stem results, it can only be concluded that the majority of treatments increase the sodium content [refer to APPENDIX II- Table 4], similar to that of the leaves results throughout the sampling periods. The results clearly show that the stem alkali metal content is lower than that of the leaves, and the mechanism of metal loss and retention is different in different parts of the plant.

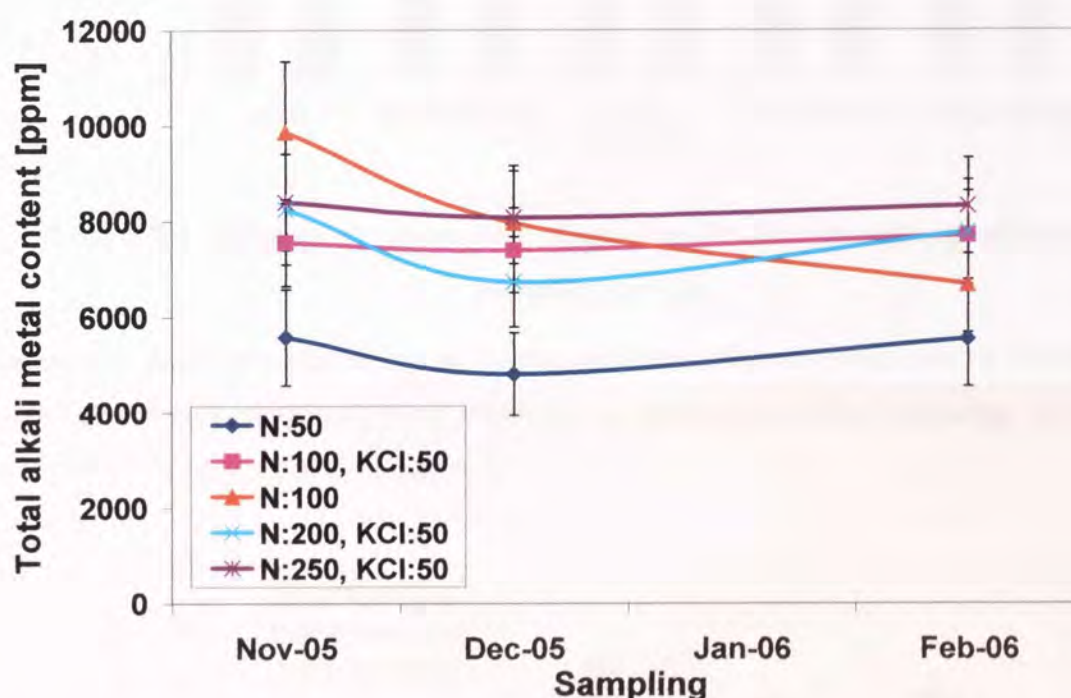


Figure 8-4 - The effect of nitrogen treatments and sampling on *Miscanthus* alkali metal content in stems

8.3.1.2 *The effect of nitrogen treatments on harvest yield with respect to sampling time*

The effect of different nitrogen fertilisers on the total harvest yield of *Miscanthus* has been investigated and the results are shown graphically in Figure 8-5 for the three sampling periods. This shows that yield harvest reduces during the growing season. Treatment N:100_KCl:50 consistently gave the highest yield. This suggests that this treatment is the most beneficial for farmers in terms of harvest yield. The lowest yield produced was N:50 as well as giving the greatest reduction in yield from the second to the third sampling period over winter.

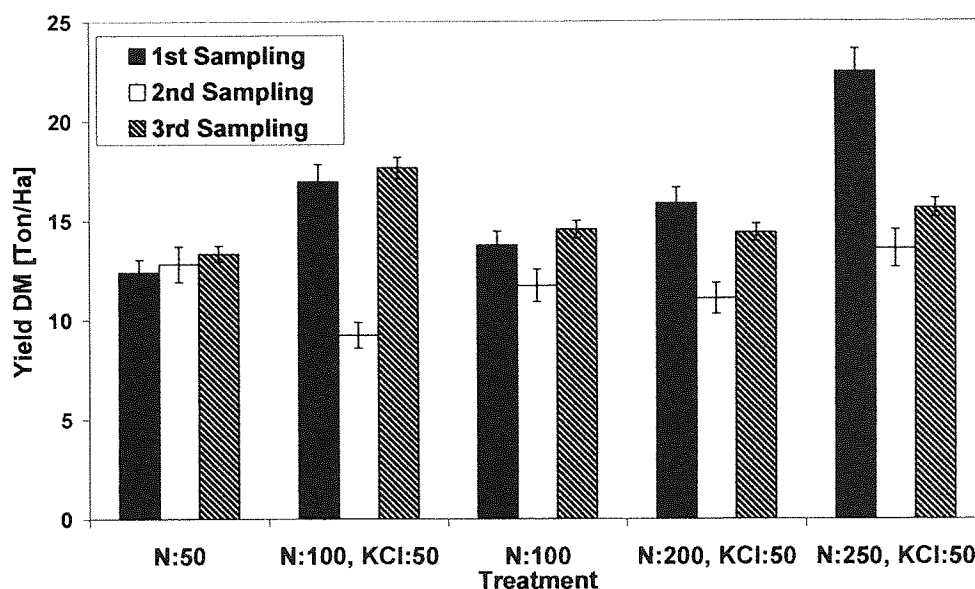


Figure 8-5 - Average dry mass yield of nitrogen fertiliser treatments of the three sampling periods

Figure 8-6 shows the percentage of leaves which contributed to the overall yield for each treatment for each sampling period, including the standard deviation percentage which varies from 0.5-10 % for each of the treatments.

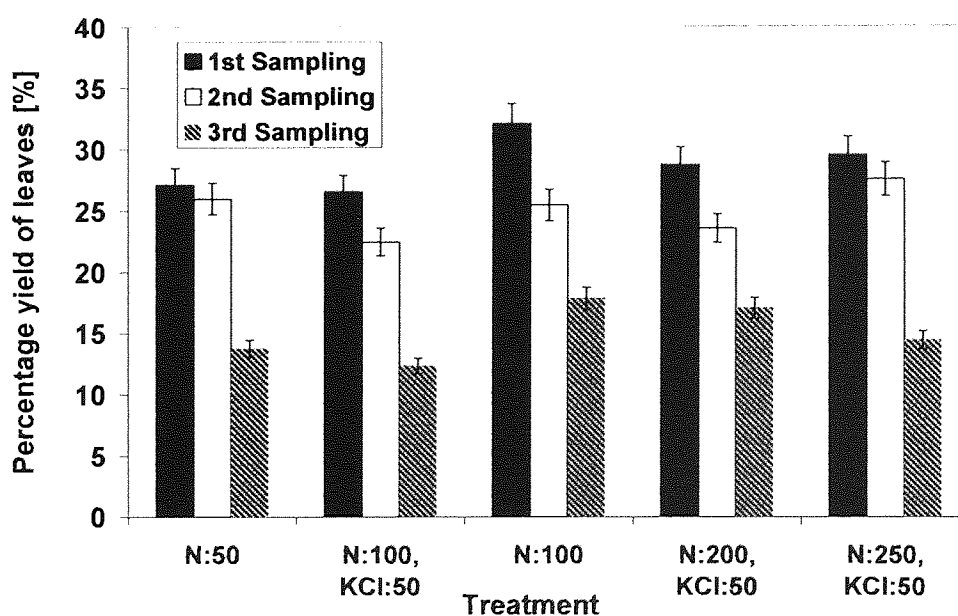


Figure 8-6 - Average percentage of leaves present in yields of the nitrogen fertiliser treatments of the three sampling periods

Figure 8-6 shows that all the nitrogen treatments throughout the sampling periods decreased the yield of harvest for leaves, resulting in an increase of stem content. The first sampling gave approximately 25-31 wt % of leaves which contributed to the overall harvest yield; however as sampling periods increased it fell to 12-17 %.

8.3.1.3 *The effect of nitrogen on TGA yields and product distribution with respect to sampling time*

Figure 8-7 shows the yields of volatiles (including gases) from TGA [dry mass feed basis] for the leaves throughout the different nitrogen treatments and sampling periods. Results for the stem results are shown in Figure 8-8. It is shown [Figure 8-7] that as the sampling time gets later, the volatiles for the leaves increase for the all the nitrogen treatments. This would be expected as the alkali metals decrease significantly over this period according to Figure 8-3, thus allowing the degradation of the biomass to be more effective giving a higher TG yield. Treatment 3 [50 kg/ha of nitrogen] gave the highest volatiles yield reaching 78-80%, in the second sampling. However by the third sampling it decreased significantly. Treatment N:100 was the only treatment which showed a steady increase throughout the sampling periods.

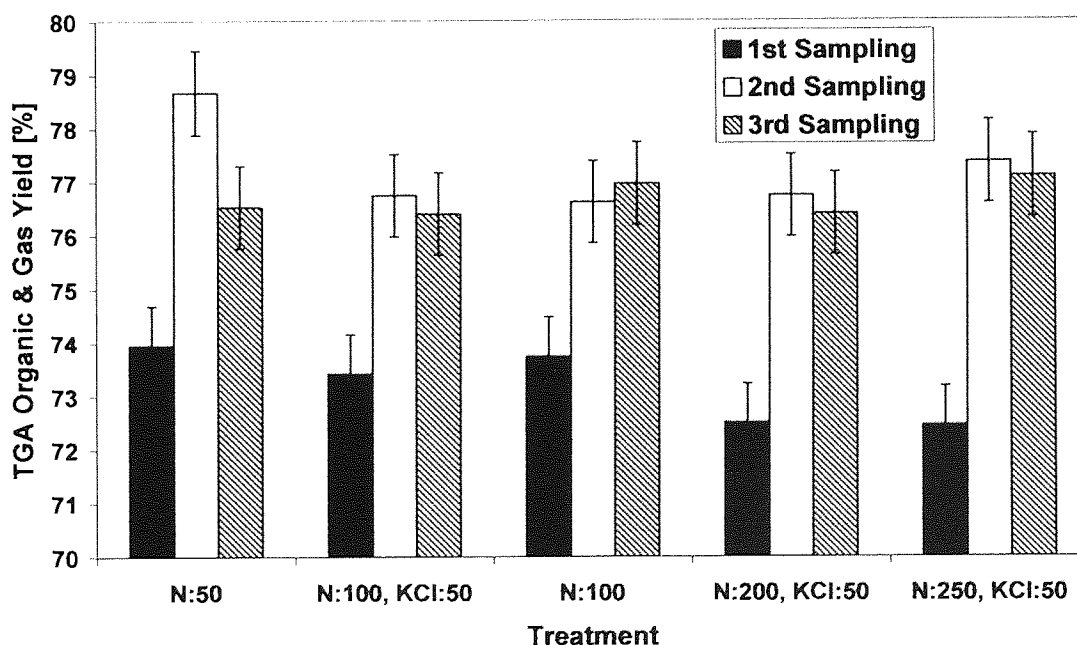


Figure 8-7 - Volatile and gas yields for leaf material determined by TGA for the nitrogen treatments over the three sampling periods

The TGA results for the stems [Figure 8-8], gave a wide range of results for the different treatments, with standard deviation reaching up to 5 %. Due to the high standard deviation no clear trends for each of the nitrogen treatments could be identified for the first and second samplings.

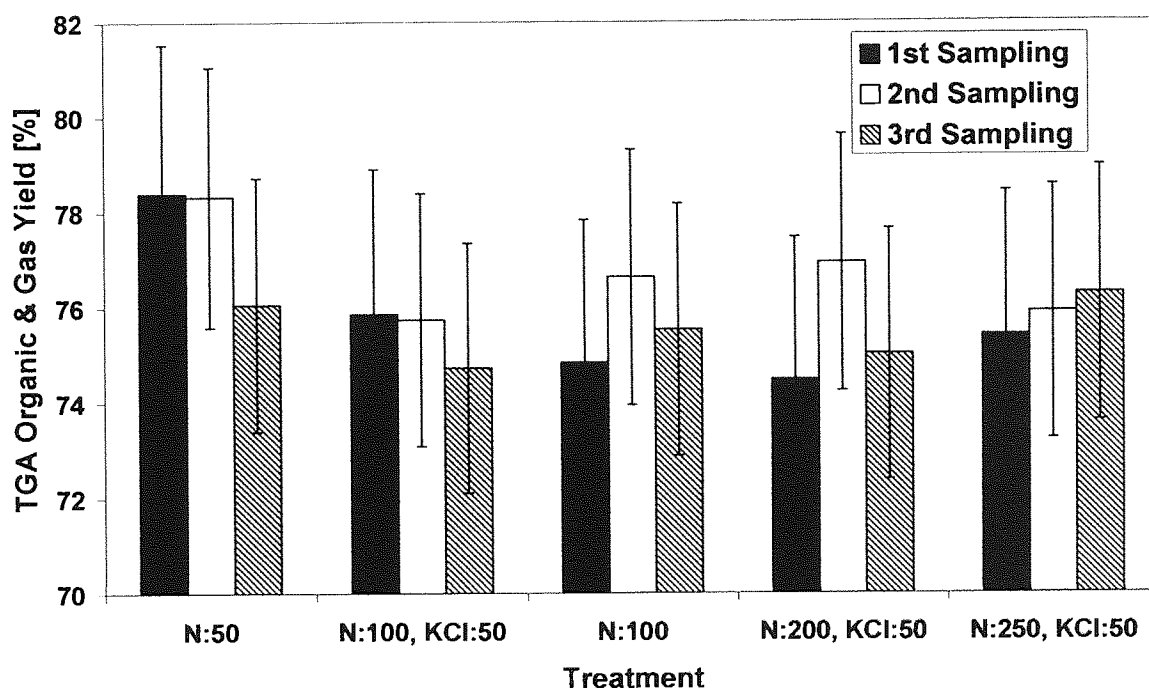


Figure 8-8 - Volatile and gas yields for stem material determined by TGA for the nitrogen treatments over the three sampling periods

8.3.1.4 PCA analysis on pyroprobe-GC/MS leaves and stems compounds:

A PCA Analysis has been carried out on the peak areas of the pyrograms of leaves and stems of the different treatments. These are reported in detail in APPENDIX II-13.3. A number of compounds responded to different nitrogen fertiliser treatments during the first sampling period. However as sampling time increased fewer compounds responded to the treatments until no relationship existed.

8.3.2 The agronomical effect of potassium chloride fertiliser

8.3.2.1 *The effect on ash and metal content with respect to sampling time*

Figure 8-9 shows the average leaf ash content for the potassium chloride fertiliser treatments during the three sampling periods, while the ash results for the stems can be found in Figure 8-10. The average ash contents for leaves and stems vary from 4.5-4.7 % and 1.4-2.0 % respectively with standard deviations below 0.5 % for both leaves and stems. All the ash contents for leaves and stems for the potassium treatments gave different results, suggesting that the ash content is dependant on the different potassium fertiliser rates. During the third sampling it can be seen that the ash content reaches its lowest value for the majority of the treatments except for KCl:50 which showed all showed a decrease. The treatments which decreased in a uniform pattern was N:50_KCl:100, N:150_KCl:100 and N:150_KCl:50 in which the ash content dropped from 4.9 to 3.9 %.

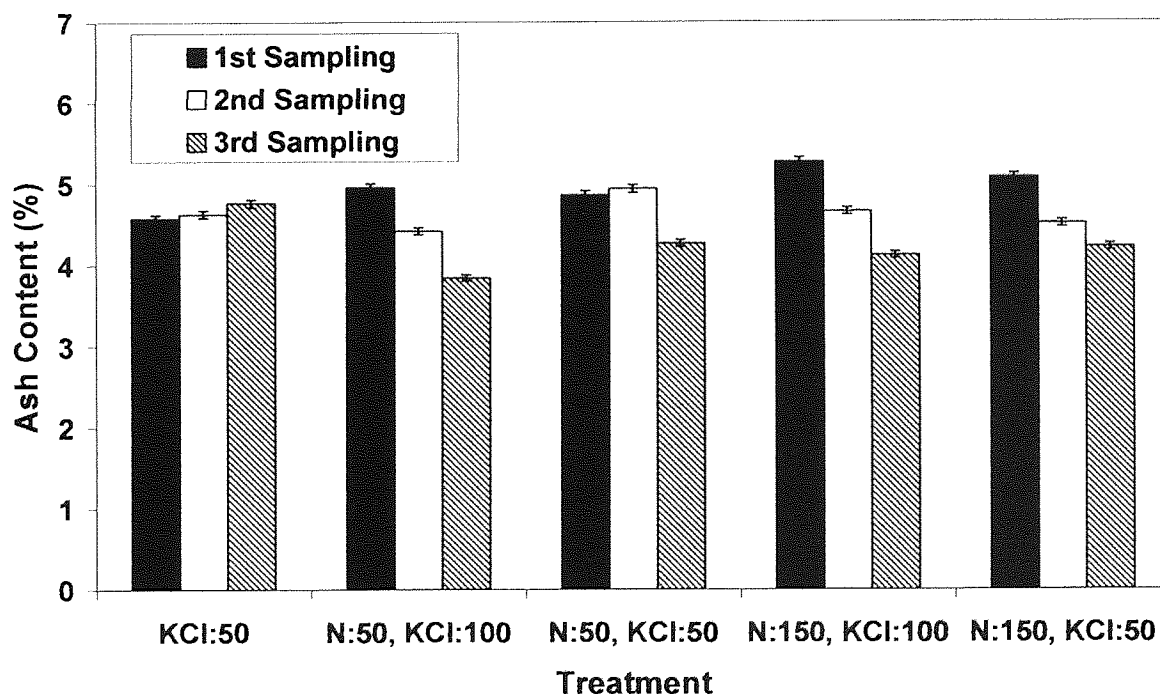


Figure 8-9 - The average ash content of potassium chloride fertiliser treatments of the three sampling periods for leaves

A similar trend is noticed for the stems [Figure 8-10] as most of the ash content reached its lowest level during the third sampling. The only exception was for N: 150_KCl:50 which showed a positive trend as the sampling time gets later.

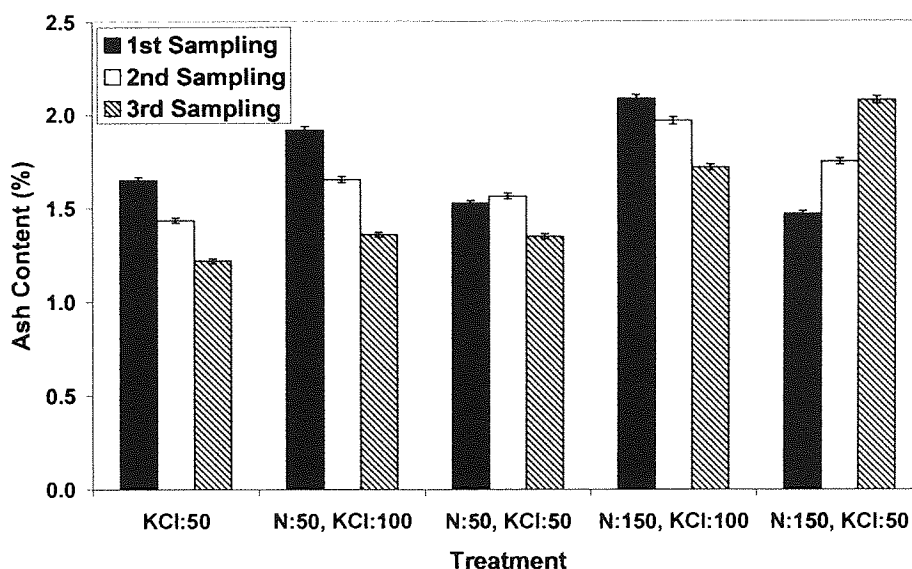


Figure 8-10 - The average ash content of potassium chloride fertiliser treatments of the three sampling periods for stems

8.3.2.1.1 Leaf alkali metals:

Figure 8-11 shows the total average alkali content present in the leaves for each of the different potassium chloride treatments throughout the three sampling periods.

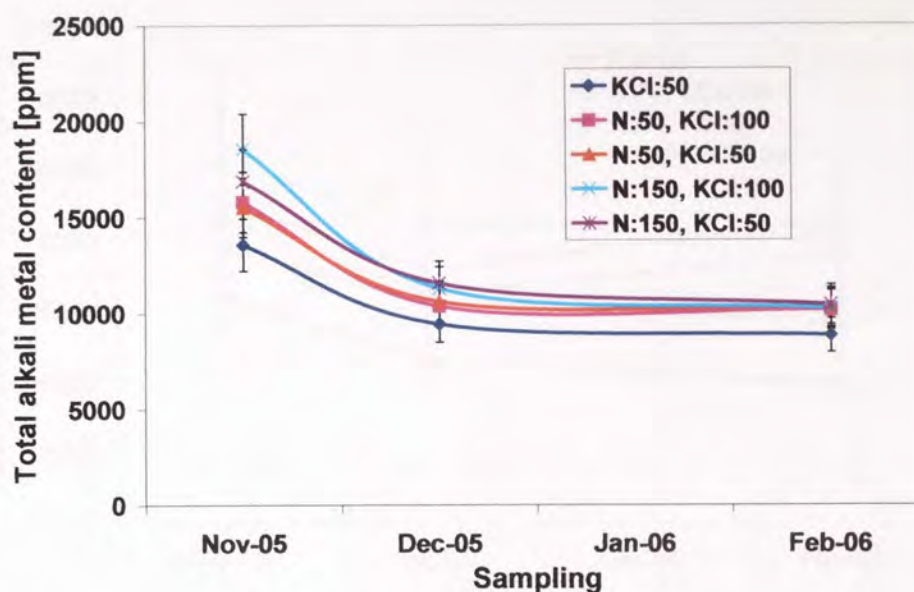


Figure 8-11 - The effect of potassium chloride treatments and sampling on Miscanthus alkali metal content in leaves

The results are similar to that of the nitrogen fertilisers at which all the treatment decrease in alkali metal content throughout the sampling periods. This can be identified for most of the treatments by the ash content in Figure 8-9, at which the alkali metals reduce by 28-35 % from November 05 to February 06. Referring to APPENDIX II –Table 2 it can be seen that the potassium and magnesium content decrease throughout the sampling periods, while the sodium content increases. The results show a similar trend to that of the nitrogen fertiliser results, and may be a function of senescence rather than agronomical practices.

8.3.2.1.2 Stem alkali metals:

The total average alkali content present in the stems for each of the different potassium chloride treatments throughout the three sampling periods are shown in Figure 8-12.

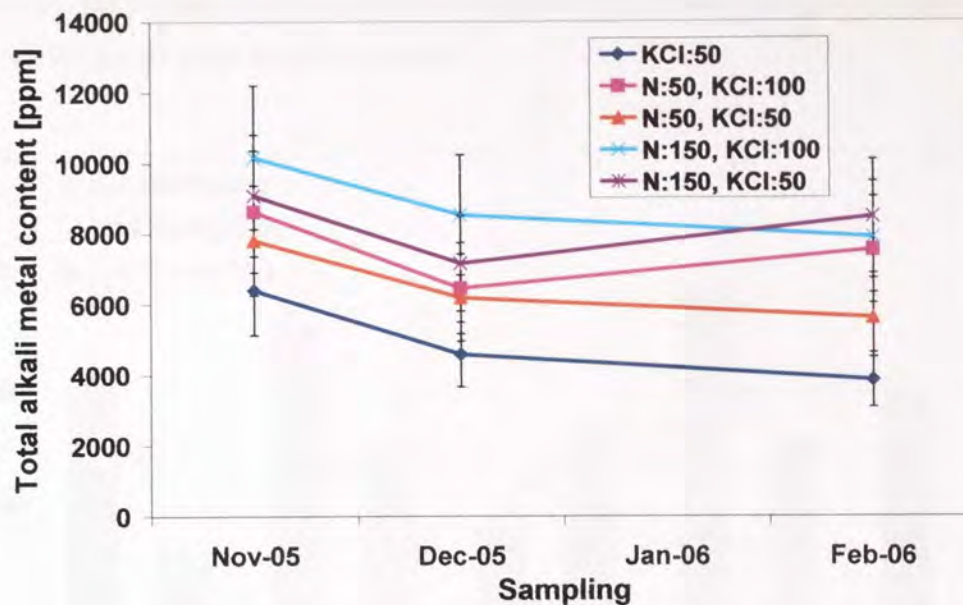


Figure 8-12 - The effect of potassium chloride treatments and sampling on *Miscanthus* alkali metal content in stems

The stems results in Figure 8-12 show a similar result to that of Figure 8-4, at which three of the potassium chloride treatments decreased in its alkali metal content uniformly throughout the sampling periods and agrees with the results from their ash content for each of the treatments in Figure 8-10. The treatments which decreased in alkali metal content are KCl:50, N:50_KCl:50, and N:150_KCl:100 which all show a negative trend with similar standard deviations. The remaining treatments show a dip in alkali metal content in December.

The results show that the stems are lower in alkali metal content [ppm] to that of the leaves and agree with the ash content results at which they also reduced in its alkali metal content. The only alkali metal content which showed a trend in APPENDIX II was magnesium which showed a decrease as the sampling time gets later.

8.3.2.2 *The effect on harvest yield with respect to sampling time*

Figure 8-13 and Figure 8-14 show the average harvest yield for each potassium chloride treatment throughout the three sampling periods and the percentage of leaves contributed to the overall harvest yield respectively. It can be seen that the overall impact on harvest yield for the potassium chloride treatments on *Miscanthus* crops tends to decrease. Most of the treatment harvest yields are comparable in yield, but treatment N:50_KCl:100 clearly stands

out from the rest by having the highest harvest yield. Treatment N:50_KCl:50 gave the lowest harvest yields for all three sampling periods.

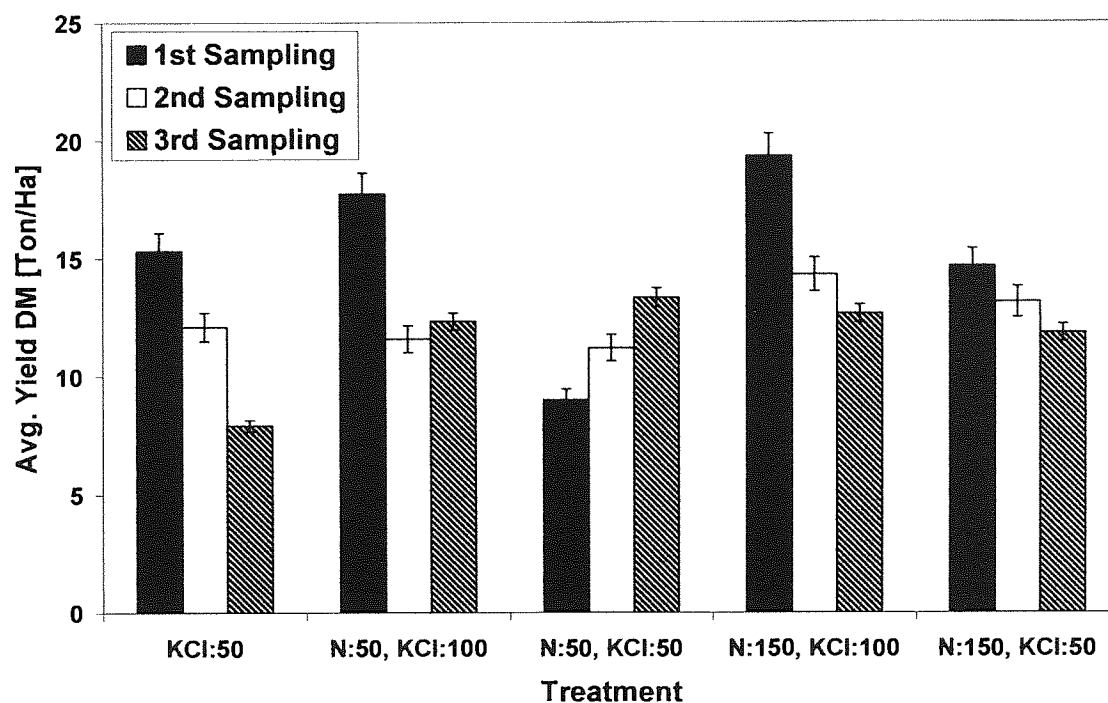


Figure 8-13 - Average dry mass yield of potassium chloride fertiliser treatments of the three sampling periods

Figure 8-14 shows the results of the percentage of leaves contributed to the overall yield for each KCl treatment for each sampling period.

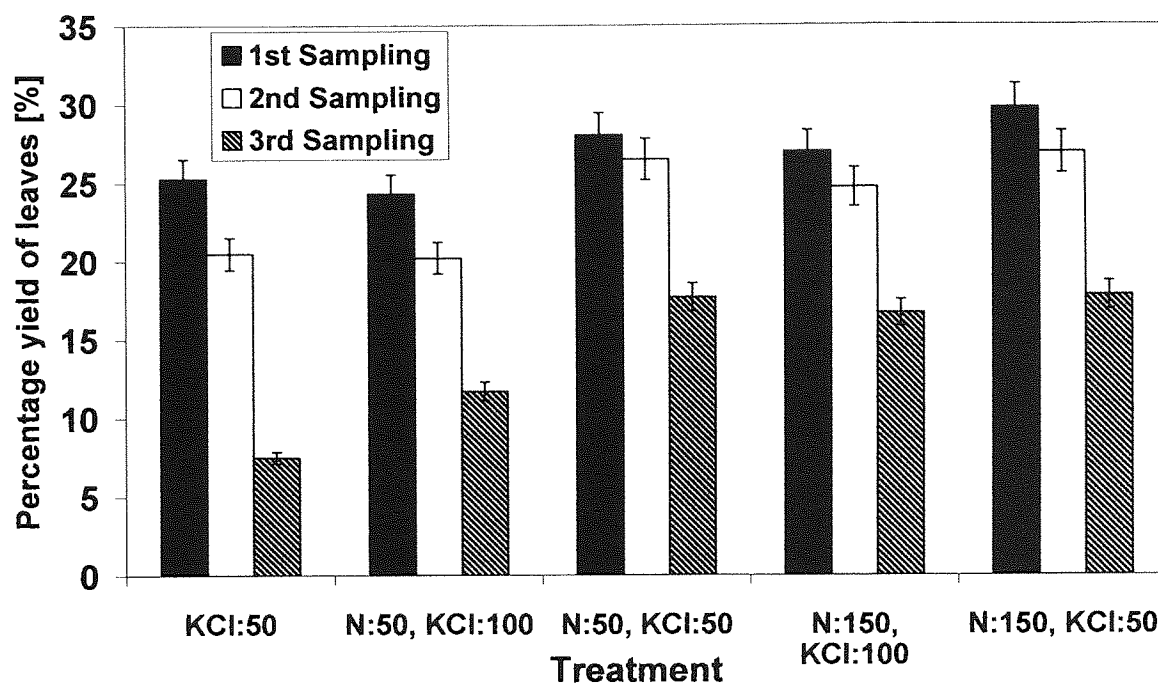


Figure 8-14 - Average percentage of leaves present in yields of the potassium chloride fertiliser treatments of the three sampling periods

They show a similar result to that of the nitrogen fertiliser results, that as the sampling periods increase, a decrease in the weight of leaves occurs. This once again suggests that the leaves die, as they are being changed biologically and impacting on its weight as senescing occurs. Treatment 1 was most effected by it the most, by losing 80 % of its weight from the first sampling period to the third sampling period.

8.3.2.3 *The effect of potassium chloride on TGA yields and product distribution with respect to sampling time*

Figure 8-15 shows the average TGA leaf volatile [and gas] yields for the different potassium treatments throughout the sampling periods, while Figure 8-16 show the TGA stems results for the potassium chloride treatments. All the potassium chloride treatments for the leaf material [Figure 8-15] gave similar TGA results to that of the nitrogen treatments, showing that greater TG volatile and gas yields are evolved throughout the first sampling to the second sampling periods. The third sampling results were similar to that of the second sampling with the exception of N:150_KCl:100 which showed an increase. This agrees with previous finding earlier in the chapter suggesting that as the growing seasons continues the level of metals

decrease [Figure 8-11], giving a greater TG volatile and gas yield due to a greater degradation of the biomass.

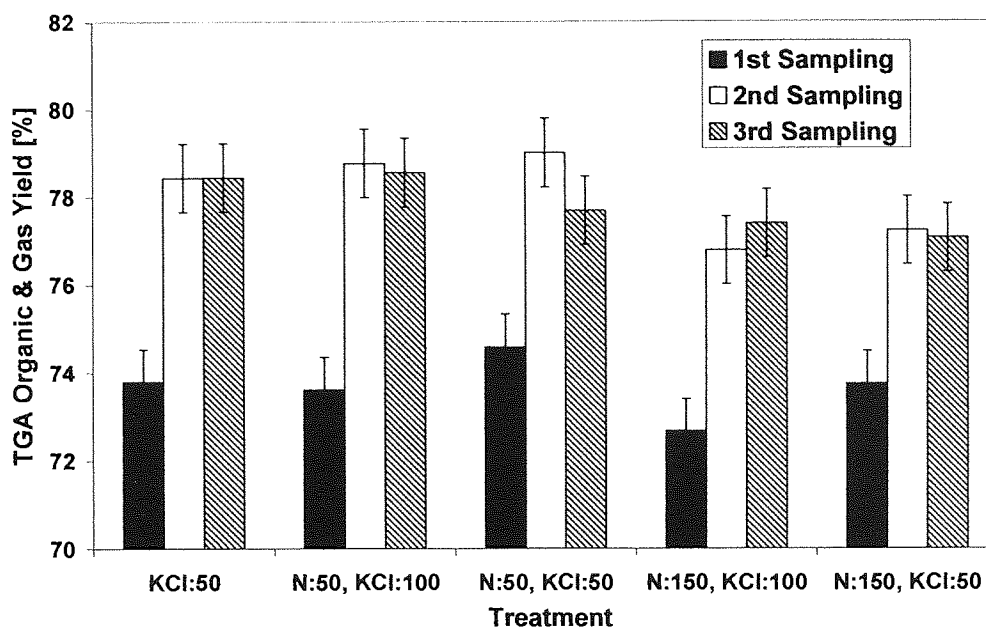


Figure 8-15 - Volatile and gas yields determined by TGA for the potassium chloride treatments over the three sampling periods for the leaf material

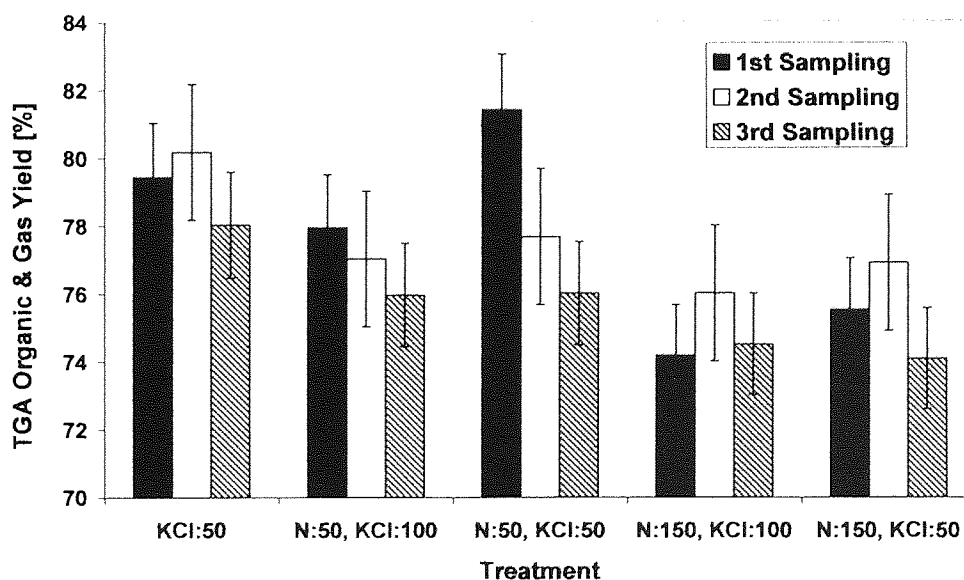


Figure 8-16 - Volatile and gas yields determined by TGA for the potassium chloride treatments over the three sampling periods for the stem material

Treatments 1, 8 and 11 for the stems [Figure 8-16] indicated a similar trend to that of the leaves, in which its alkali metals decreased, and allowing for a greater yield of volatiles and gases to be produced. However due to the larger standard deviations; an indication can only be made. Treatments 5 for the stems show a clear decrease in yield, unlike its counterpart for treatment 2. By the third sampling period all the potassium chloride treatments decreased in its TG yield substantially.

The standard deviation for the leaves vary from 1 -3 %, while the stems gave less than 5 %. Treatment 5 gave the highest TGA yield of 78.4 %. Treatments KCl:50 and N:150_KCl:50 show a steady increase in volatile yield during the sampling periods.

8.3.2.4 *PCA analysis on pyroprobe-GC/MS leaves and stems compounds:*

A PCA Analysis has been carried out on the peak areas of the pyrograms of leaves and stems of the different treatments. These are reported in detail in APPENDIX II-13.3. A number of compounds responded positively to different potassium chloride fertiliser treatments during the first sampling period. However as sampling time increased fewer compounds responded to the treatments.

8.3.3 The agronomical effect of potassium sulphate applications

8.3.3.1 *The effect on ash and metal content with respect to sampling time*

Figure 8-17 shows the average leaf ash content for the sulphate fertiliser treatments over the three sampling periods, while Figure 8-18 shows the ash content for the stems.

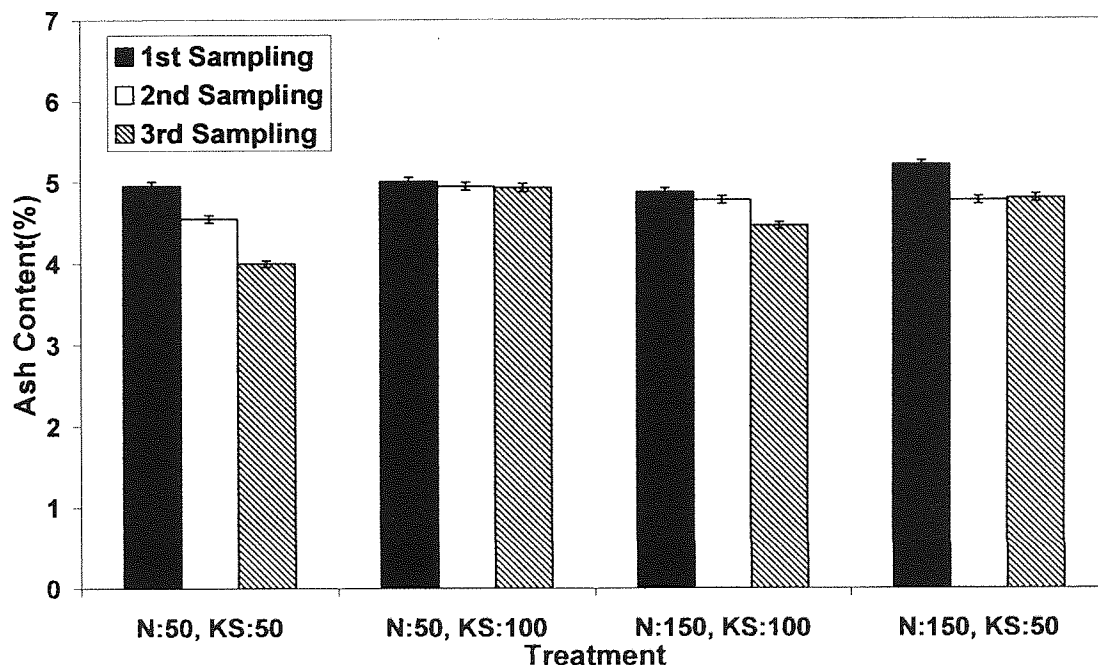


Figure 8-17 - The average ash content of potassium sulphate fertiliser treatments of the three sampling periods for leaves

The potassium sulphate ash results for the leaves [Figure 8-17] show the weakest trends to that of any of the different fertiliser applications. This is due to the close proximity of the ash results for the different treatments, thus no clear trend can be identified. The results also show that all the sulphate treatments have a slight decrease in ash content, but having the most influence on treatment 4 and 12 [N:50_KS:50 and N:150_KS:100].

The stems [Figure 8-18] showed a similar trend to that of the leaves with treatments 9 and 12 [N:150_KS:100 and N:150_KS:50] giving the greatest decrease. Treatment N:150_KS:50 is the only treatment which increased significantly in ash content by the third sampling. The standard deviation for leave and stems was less than 0.5 %.

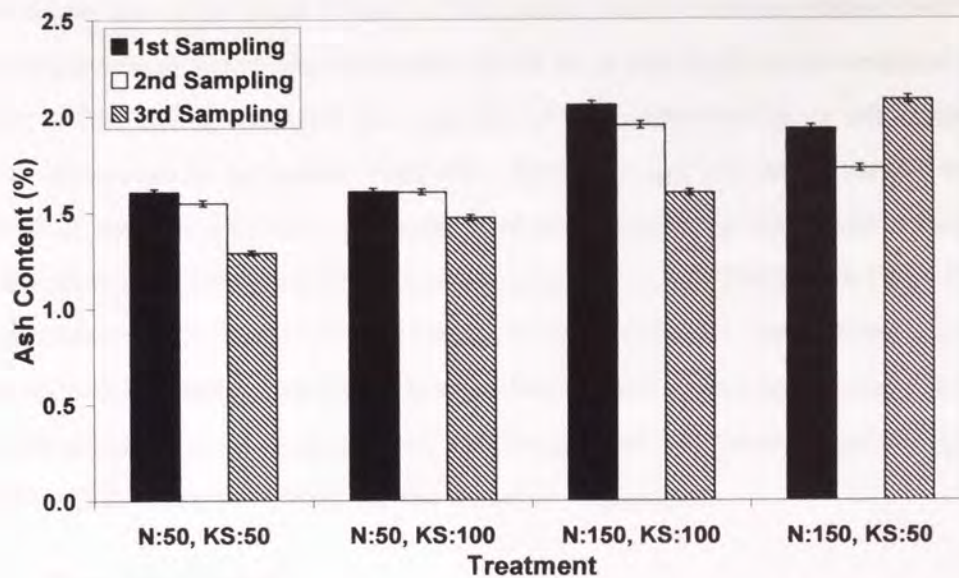


Figure 8-18 - The average ash content of potassium sulphate fertiliser treatments of the three sampling periods for stems

8.3.3.1.1 Leaf alkali metals:

Figure 8-19 shows the total average alkali content present in the leaves for each of the different potassium sulphate treatments throughout the three sampling periods.

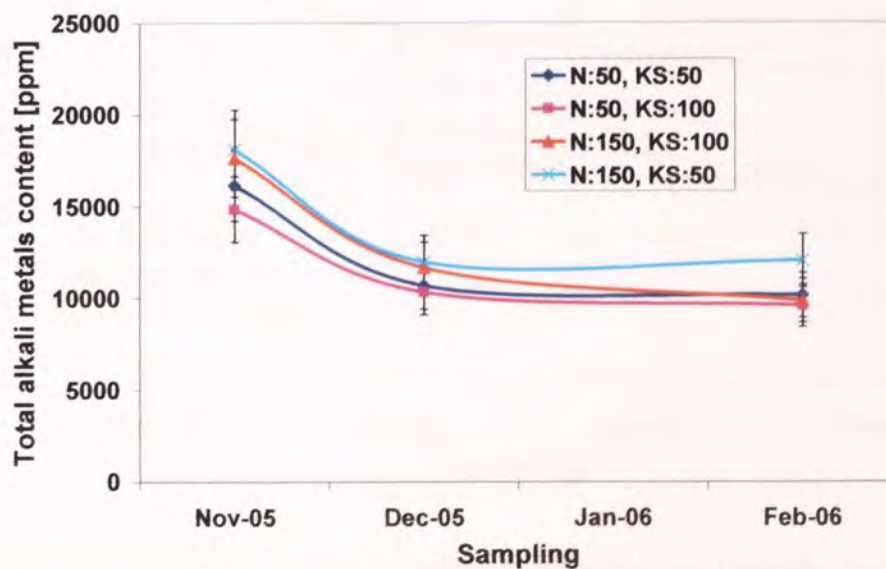


Figure 8-19 - The effect of potassium sulphate treatments and sampling on *Miscanthus* alkali metal content in leaves

The data shows the same trend to that of the leaves results for the nitrogen and potassium chloride treatments, at which approximately 25-35 % of the alkali metals reduced throughout the winter period and agrees with the majority of the treatments in its ash content [Figure 8-17]. The results are in agreement with other fertilisers and are shown clearly that the leaf reduce in alkali metal content due to natural plant senescing rather than fertiliser treatment, and is not a function of agronomical practice. The results from APPENDIX II-Table 3 also show that as sodium content increases, the levels of potassium and magnesium content [ppm] decreases over the sampling periods. This has been stated before in Section 9.3.1 and 9.3.2 that a relationship exists between sodium, magnesium and potassium as senescing occurs for all the different fertiliser treatments for the leaves in *Miscanthus*.

8.3.3.1.2 *Stem alkali metals:*

The total average alkali content present in the stems for each of the different potassium sulphate treatments throughout the three sampling periods are shown in Figure 8-20.

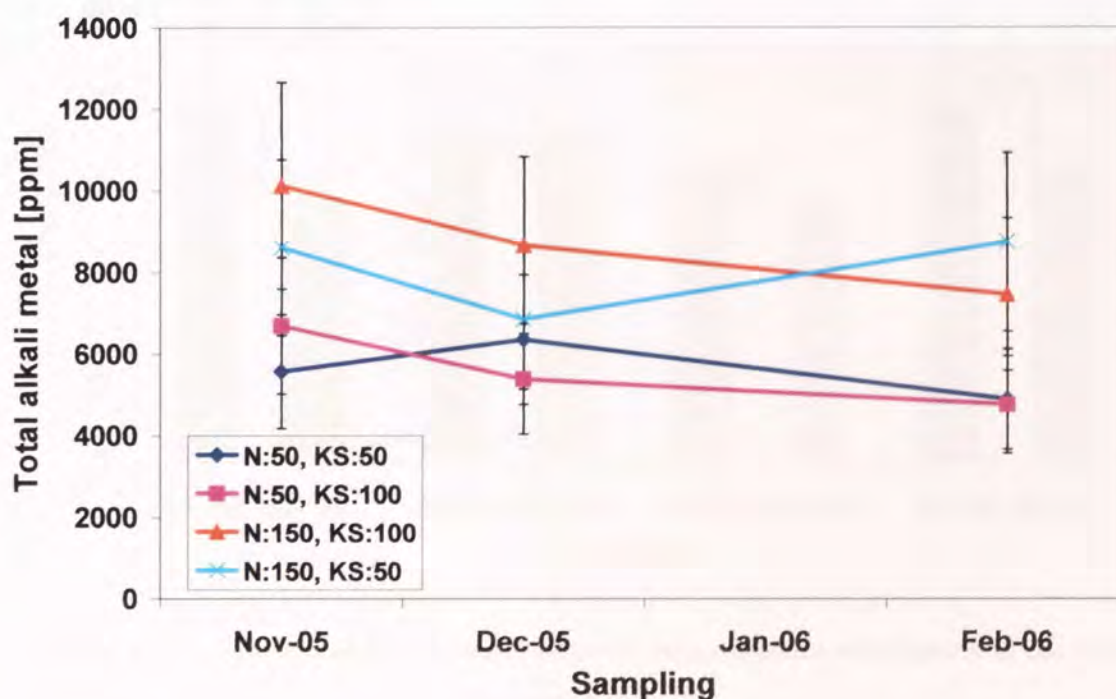


Figure 8-20 - The effect of potassium sulphate treatments and sampling on *Miscanthus* alkali metal content in stems

The results show that certain potassium sulphate treatments have a greater effect on the stem alkali metal content at which certain treatments aids in the reduction of alkali metal content. The treatments which reduced in alkali metal content uniformly are treatment N:50_KS:100 and N:150_KS:100. The remaining treatments either dips/shoots up during December and due to the standard deviation percentage no clear trend can be speculated. The result also agree with the ash content results for the stem, and also shows that the stems possess lower ash and alkali metals than in the leaves.

8.3.3.2 *The effect on harvest yield on with respect to sampling time*

Figure 8-21 and Figure 8-22 show the average harvest yield per fertiliser treatment throughout the three sampling periods and the percentage of leaves contributed to the overall throughout the sampling period respectively.

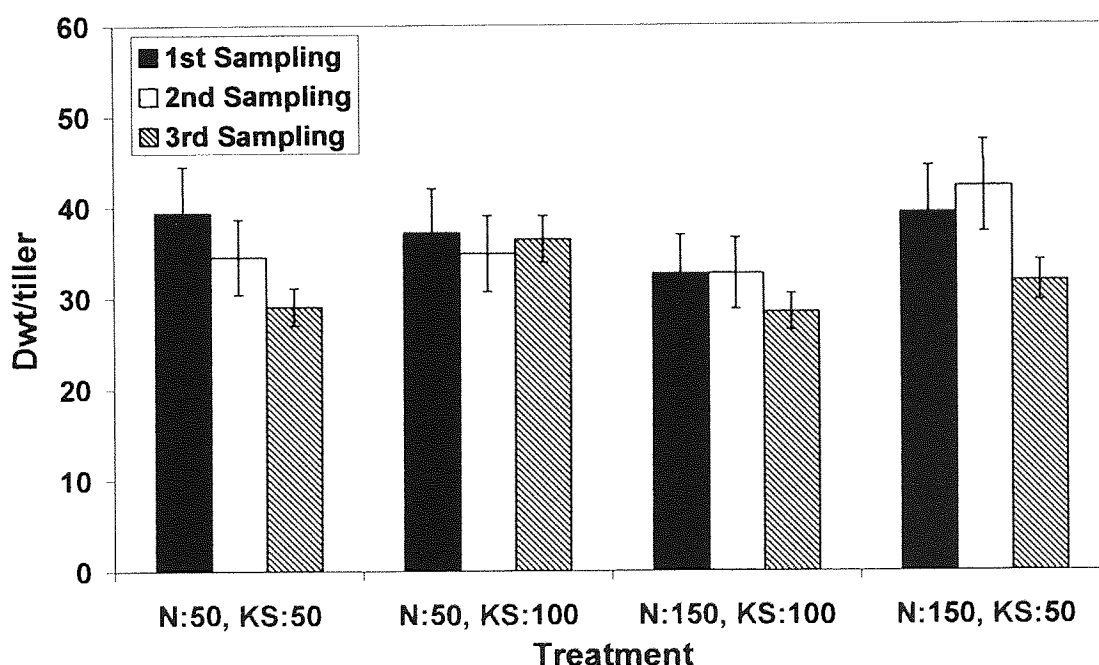


Figure 8-21 - Average dry mass yield of potassium sulphate treatments of the three sampling periods

It can be seen from Figure 8-21 that the effect on the average harvest yield throughout the sampling periods differs to each of the different treatment of the sulphate rates. The first and second sampling harvest yields were similar for all the treatments, at which the majority of the treatments then decreased in harvest yield during the third sampling period. However due to

the high level of standard deviation percentage, it is difficult to comment on the level of decrease as well as its trend. Treatment N:150_KS:50 gave the highest harvest yield of approximately 40 dw/til during the second sampling, but decreased severely in the third sampling. Treatment N:50_KS:100 maintained its harvest yield than any other treatment during all three sampling periods.

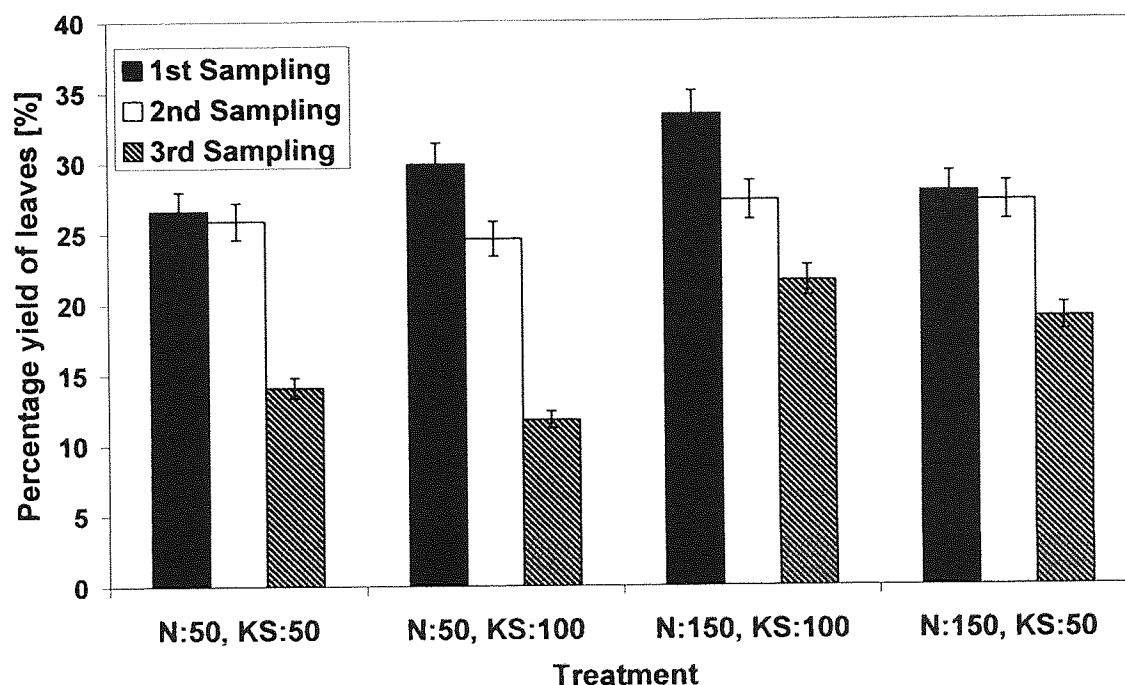


Figure 8-22 - Average percentage of leaves present in yields of the potassium sulphate fertiliser treatments of the three sampling periods

Figure 8-22 shows the decrease of the percentage of leaves to the overall harvest yield, for each treatment for each sampling period. The results follows the trends of the other fertiliser treatments in Section 9.3.1 and 9.3.2, in which the yield of leaves decrease substantially at which had an overall impact on its harvest yield [dw/tiller], suggesting that senescing is occurring to the plant over the winter period.

8.3.3.3 *The effect on potassium sulphate on TGA yields and product distribution with respect to sampling time*

Figure 8-23 shows the average TGA volatile and gas yields for the leaves for the different sulphate treatments throughout the sampling periods, while the TGA results for the stems are

shown in Figure 8-24. The potassium sulphate results showed different trends to any of the other fertiliser treatments [Sections 9.3.1 and 9.3.2] as shown in Figure 8-23. The results for leaves and stems show an increase in TGA volatile and gas yield for all the sulphate treatments as sampling periods increase. The standard deviation for leave and stems are in the region of 2 and 7 % respectively. This suggests that the potassium sulphate treatments can enhance the Miscanthus characteristics to increase in volatile and gas yield over the growing season, and can possibly improve pyrolysis-oil yields. This is due to the lowering of alkali metals and ash content which gives rise to an increase in biomass degradation and results in a higher yield in volatiles and gases.

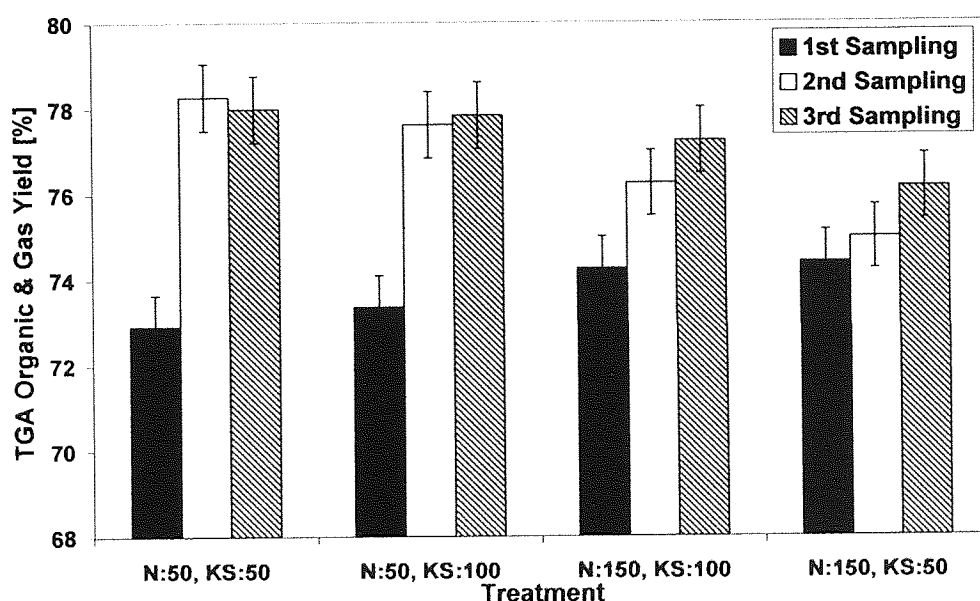


Figure 8-23 -Volatile and gas yields determined by TGA for the potassium sulphate treatments over the three sampling periods for the leaf material

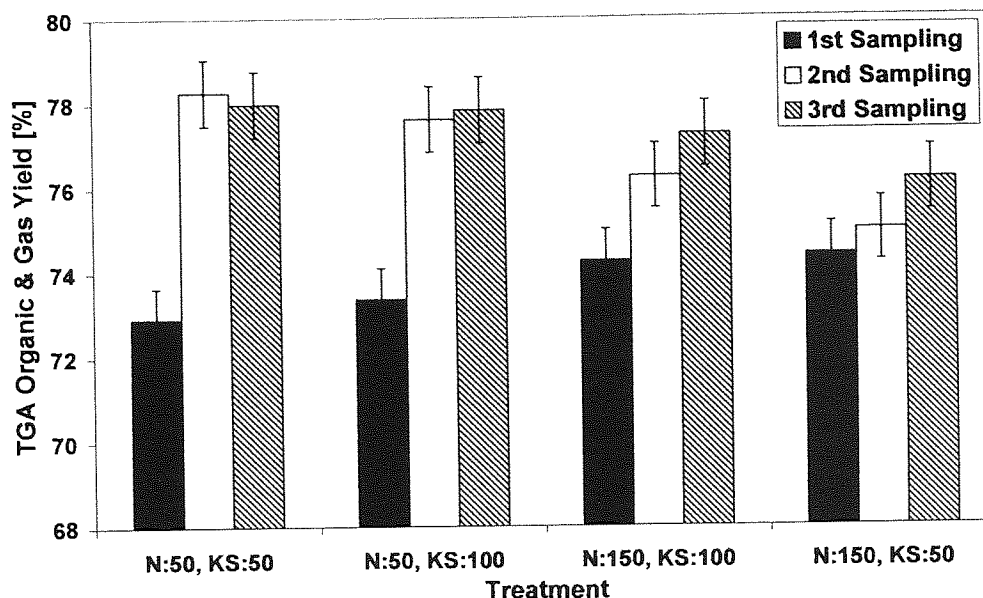


Figure 8-24 - Volatile and gas yields determined by TGA for the potassium sulphate treatments over the three sampling periods for the stem material

8.3.3.4 PCA analysis on pyroprobe-GC/MS leaves and stems compounds:

A PCA Analysis has been carried out on the peak areas of the pyrograms of leaves and stems of the different treatments. These are reported in detail in APPENDIX II-13.3. Overall there is no significant effect on any individual compound or family of compounds.

8.4 Fast pyrolysis experiments on Miscanthus samples studying the effect of fertiliser treatment

8.4.1 Introduction to rig experiments

The results produced from the agronomical study of Miscanthus, showed that nitrogen and nitrogen/chloride treatments were the most promising fertilisers that could be used to enhance pyrolysis-oil yields and characteristics based on an analytical scale. The yields from TGA in Section 9.3.3.3 of stems and leaves produced from the potassium sulphate experiments showed a steady increase in volatiles and gases. However due to the lack of knowledge in the percentage distribution of gases and organics in TGA, it is suggested that more gases would be produced than organic volatiles, based on other observations from the pyroprobe results and ash/metal contents. Five treatments from the final harvest of the first sampling period were selected [based on the results show in section 9.3], to carry out fast pyrolysis trials to produce

oils and to investigate if the effect of fertiliser has an impact on pyrolysis-oil quality and yield. The biomass consisted of a mixture of leaves and stems. The five selected feedstocks are shown below:

- [Treatment 1]: Potassium as muriate 50 kg/ha.
- [Treatment 10]: Nitrogen 150 kg/ha.
- [Treatment 11]: Nitrogen 150 kg/ha, Potassium as muriate 50 kg/ha.
- [Treatment 12]: Nitrogen 150 kg/ha, Potassium as sulphate 50 kg/ha.
- [Treatment 14]: Nitrogen 250 kg/ha, Potassium as muriate 50 kg/ha.

8.4.2 Experimental

The five *Miscanthus* feedstocks were subject to fast pyrolysis on the 150 ghr⁻¹ fluidised bed reactor. The pyrolysis system set up and method are described in Chapter 4 Section 4.5. Elemental and metal analysis were conducted as described in Chapter 5 Section 5.1, while the TGA and pyroprobe-GC/MS methodology was described in Chapter 4 Section 4.3

8.4.3 Results

8.4.3.1 *Miscanthus characterisation results*

Table 8-2 shows the elemental analysis of the five selected *Miscanthus* treatments, along with its ash and higher heating value content.

8.4.3.2 *TGA and Pyroprobe-GC/MS results*

Table 8-3 shows the TGA volatiles and char yields as reported at 500°C. The table indicates that treatment 1 gave the lowest ash content with the highest volatile and gas yield, while treatment 14 gave the highest ash content with the highest char yield. Figure 8-25 shows the TG results for the five selected treatments. Treatments 11, 12 and 14 have very similar degradation pathways suggesting that they possess similar metal qualities and quantities. Treatment 1 and 10 were alike in thermal degradation, however beyond 400°C treatment 1 undergoes a different degradation which is more favourable to pyrolysis and results in a lower char content and higher volatile TG yield.

Table 8-2 - CHNO analysis of Miscanthus plots. Oxygen calculated by difference

Name	C (%)	H (%)	N (%)	S (%)	O (%)	ASH (%)	H.H.V. (MJ/kg)
Treatment 1	43.61	5.265	0.1	0.1	50.93	1.27	18.06
Treatment 10	46.29	3.775	0.1	0.1	49.74	1.57	17.84
Treatment 11	48.13	3.06	0.1	0.1	48.61	1.53	17.73
Treatment 12	45.09	5.56	0.47	0.1	48.79	1.84	17.20
Treatment 14	45.48	3.62	0.1	0.1	50.71	1.91	17.25

Table 8-3 - The five selected treatments for pyrolysis analysis and pyrolysis-oil production

Treatment	Moisture [%]	Ash [%]	Char [%]	Volatiles & Gases [%]	Tmax [°C]
Treatment 1	3.58	1.27	15.45	84.55	343.11
Treatment 10	3.38	1.57	24.51	75.49	339.23
Treatment 11	3.38	1.52	23.80	76.2	351.74
Treatment 12	4.32	1.84	24.98	75.02	343.83
Treatment 14	2.71	1.91	25.17	74.83	347.86

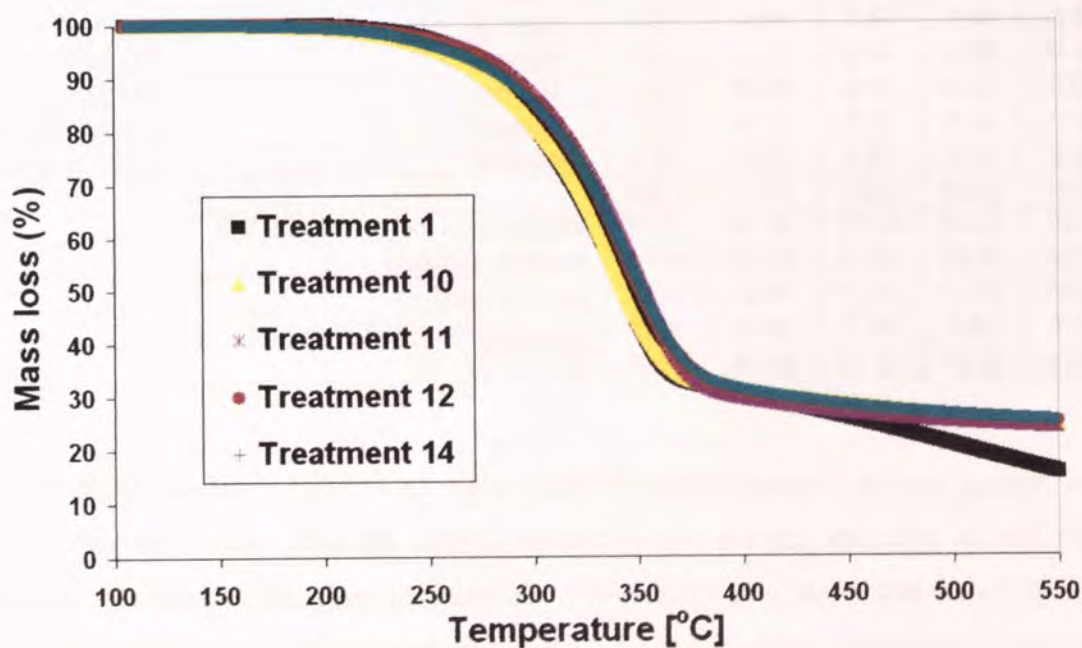


Figure 8-25 - TG results of the five Miscanthus batches of the five different treatments

Table 8-4 shows the compounds identified in the pyrograms and the percentage area that each compound selected as a key marker [Section 7.3] contributes to the overall grouped compound area. The values shown are the average of three repeats.

Table 8-4 - Pyroprobe-GC/MS of Miscanthus plots

Name of compound	CODE	Treat- ment 1	Treat- ment 10	Treat- ment 11	Treat- ment 12	Treat- ment 14
2,3-Butandione	Cellulose	3.07	3.39	3.42	3.25	3.13
Hydroxyacetaldehyde	Cellulose	24.31	23.22	25.06	25.37	25.83
Hydroxypropanone	Cellulose	8.99	10.13	11.41	9.22	11.02
2-Furaldehyde, 2-Furfural	Cellulose	4.42	4.75	4.75	5.00	5.31
2 FURANMETHANOL	Cellulose	3.31	3.33	3.69	3.10	4.46
(5H)-Furan-2-one	Cellulose	2.59	2.37	2.39	2.61	2.80
4-Hydroxy-5,6-dihydro-(2H)-Pyran-2-one	Cellulose	1.41	1.21	2.12	2.48	2.31
Phenol	Lignin	1.25	1.56	1.31	1.19	1.20
Guaiacol	Guaiacol	4.97	5.95	4.85	5.29	4.14
4-Vinyl guaiacol	Guaiacol	26.34	24.64	22.70	23.80	21.69
Eugenol	Guaiacol	0.35	0.37	0.47	0.46	0.44
5-Hydroxymethyl-2-furaldehyde	Cellulose	1.00	0.89	1.30	1.08	1.33
Pyrocatechol	Lignin	0.73	0.84	0.78	0.65	0.71
Syringol	Syringol	5.98	6.61	5.13	5.13	4.62
Vanillin	Guaiacol	0.96	0.96	0.77	1.04	1.04
4-Vinyl syringol	Syringol	3.65	3.46	2.86	3.22	2.81
Levogluconan	Cellulose	1.14	1.06	1.61	1.50	1.91
4-Propenyl syringol (trans)	Syringol	3.21	2.59	2.87	2.93	2.63
Syringaldehyde	Syringol	0.24	0.15	0.19	0.29	0.13
Acetosyringone	Syringol	0.15	0.09	0.11	0.13	0.08
Coniferyl alcohol	Guaiacol	0.15	0.17	0.10	0.15	0.19
Guaiacyl 4 ethyl	Guaiacol	1.79	2.27	2.12	2.10	2.20
		100.0	100.0	100.0	100.0	100.0
Cellulose derived compounds		50.24	50.35	55.74	53.62	58.11
Guaiacyl groups		34.56	34.35	31.01	32.84	29.71
Syringyl groups		13.22	12.90	11.15	11.70	10.28
Unknown lignin compounds		1.98	2.40	2.10	1.84	1.91
TOTAL LIGNIN		49.76	49.65	44.26	46.38	41.89

Figure 8-26 shows the evolution of compounds for each treatment plotted against its ash content. The data shows that the overall evolution of volatiles increases as ash content decreases, as stated in the previous chapters. The results also show that lower molecular weight compounds [i.e. hydroxyacetaldehyde and 5 hydroxymethyl-2-furaldehyde] increase in area as ash content increases. While having a lower ash content can increase the areas of larger

compounds such as 4-vinyl guaiacol and syringol. The data from Table 8-4 indicates that treatment 1 will have the highest organic/total liquid yield due to its low ash content and high compound areas in comparison to any other plot.

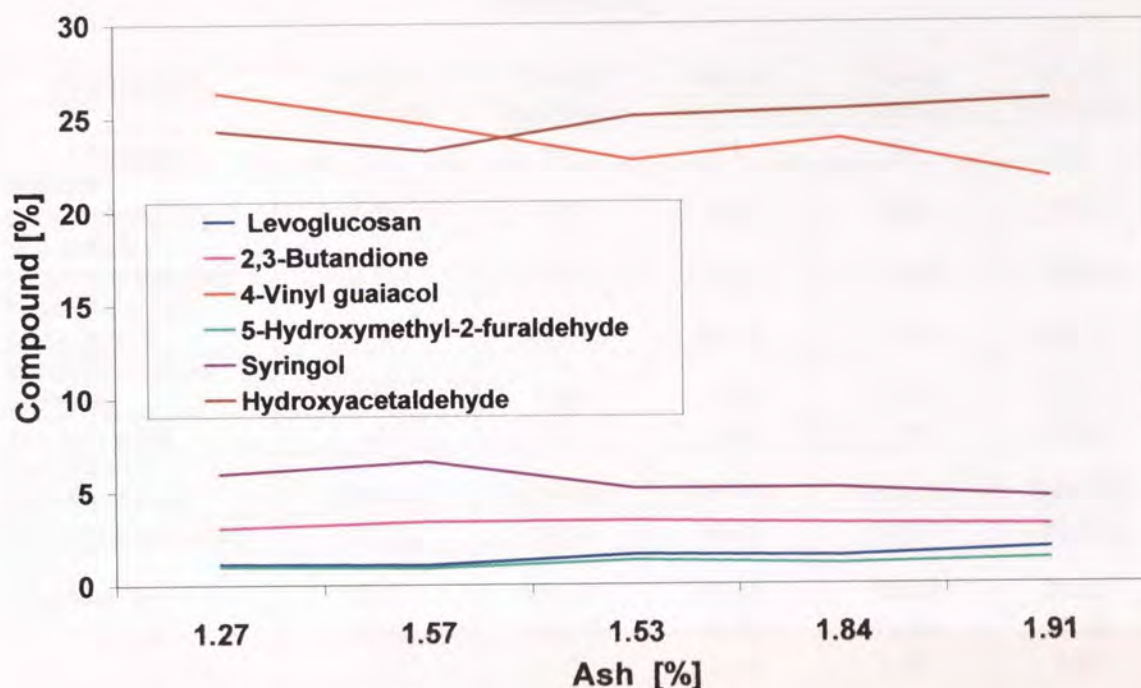


Figure 8-26 - The effect of ash on product distribution

8.4.3.3 Mass balance results

The mass balance methodology has been discussed in Chapter 4 Section 4.5. Table 8-5 shows the mass balance of experimental runs on a 150 ghr-1 rig, while Table 8-6 shows the analysis of the oil fraction. The fast pyrolysis trials were conducted at around 500°C, ± 10 °C and having similar hot vapour residence times. All the mass balance closures are above 90 % thus being able to be compared to each other. Treatment 12 gave the lowest organic yield and the highest char yield. This may be due to the high level of ash and alkali metals present in treatment which gave a rise to a build up of char in the transition pipe which catalytically cracks the vapours and reduce and results in an increase the char and gas content. The results agree with other findings from previous chapters showing that the ash content influences the yields of organics, char and gases from the fast pyrolysis of biomass. The analytical analysis [TGA/Pyroprobe-GC/MS] suggested that treatment 1 would produce the highest yield in

volatiles with the lowest in char content and the mass balances results [Table 8-5] agrees with this findings.

Table 8-5 - Mass balance of 1st sampling of Miscanthus on Aston's 150 ghr⁻¹ fast pyrolysis rig

Run Number	184-061	184-062	185-06	192-06	193-06
	Treatment	Treatment	Treatment	Treatment	Treatment
Feedstock	1	10	11	12	14
Reactor temperature[°C]	503	502	497	499	508
Hot vapour residence time [s]	0.72	0.72	0.70	1.83	0.92
Feedrate in wet basis [ghr ⁻¹]	94.97	85.00	88.18	75.88	64.33
Moisture content [mf wt%]	3.58	3.39	3.38	4.32	2.71
Ash [mf wt%]	1.27	1.57	1.53	1.84	1.91
Particle size [micro meters]	250-350	250-350	250-350	250-350	250-350
Run Time [minutes]	60.00	50.00	60.00	60.00	60.00
INPUT					
Wet Feed [g]	94.97	109.47	88.18	75.88	39.67
Dry Feed [g]	91.57	105.76	85.20	72.60	38.59
Water in Feed [g]	1.21	3.71	2.98	3.28	1.08
YIELDS [mf wt %]					
Char	19.17	22.79	24.11	27.75	25.57
Organics	52.38	43.32	36.57	34.47	39.27
Gas	11.10	13.65	12.25	16.21	16.01
Reaction water	8.93	13.65	16.99	17.42	15.02
Total liquids	61.31	56.97	53.56	44.89	54.29
Closure (%)	91.58	93.97	92.06	98.14	97.45
GAS YIELDS [%]					
Methane	3.75	3.82	4.24	4.71	17.90
Carbon dioxide	75.98	88.88	60.54	14.39	53.13
Carbon monoxide	18.24	4.97	32.77	80.25	27.49
Hydrogen	0.41	0.45	0.39	0.25	0.28
Ethylene	0.68	0.70	0.66	0.14	0.38
Ethane	0.47	0.53	0.73	0.13	0.44
Propane	0.11	0.12	0.17	0.03	0.10
Propylene	0.36	0.53	0.49	0.09	0.28

8.4.3.4 Oil quality analysis

The oils produced from the fast pyrolysis experiments [fluidised bed reactor] was subjected to analysis to investigate its quality and stability [methodology found in Chapter 5 Section 5.3]. Table 8-6 shows the analysis of the oil fraction along with the higher heating values. The oil produced from treatment 1 is rich in carbon and hydrogen which gave the highest heating value in comparison to the rest of the *Miscanthus* plots. The worst oil produced from the table is treatment 12 in terms of organic yield and high heating value [as it is rich in oxygen content]; this was due to a high water content or to a high level of low molecular weight oxygenated compounds. The reason treatment 12 produced low total liquid yield and a poor oil quality is due to its high ash content which decreased the temperature of maximum volatile evolution, and allowed the volatiles to crack further due to a higher temperature to produce a high level of char. The char build up around the process, allowed the vapours to crack further to produce high level of reaction water and gases. From Table 8-6 it can be seen that the oil which has the most changes, in terms of quality, was treatment 8, while the oil which had the least changes was treatment 14.

The oil produced from Treatment 14 had the least changes in its oil quality [defined Chapter 5 Section 5.4]. The oil only increased in its molecular weight by 91, while having the lowest GPC stability. However the oil phase separated within three months after the analysis. This agrees with Chapter 7 with the *Lolium* and *Festuca* grasses investigation, suggesting that the most stable oil is of a medium/high ash feedstock [with acceptable lignin contents], which allows the cracking of large molecular weight compounds to produce smaller molecular weight compounds which are soluble. It must be also stated that if the ratio between the reaction water and organic liquid is not balanced then phase separation can occur, as shown in the oils produced from treatments 12 and 14. However from Table 8-6 the most realistic stable oil produced were from treatments 1 and 10, which gave acceptable GPC results and possessing a good viscosity index. This suggests that nitrogen, nitrogen/potassium chloride and potassium chloride fertiliser's treatments are sufficient applications to enhance biomass characteristics to give a good yield of pyrolysis-oil with exceptional oil stability.

Table 8-6 - Oil analysis of Miscanthus treatments

	Treat- ment	Treat- ment	Treat- ment	Treat- ment	Treat- ment
	1	10	11	12	14
Water content, [mf wt %]	17.73	28.12	35.01	37.40	48.05
Char content, [mf wt %]	0.80	0.49	0.32	0.42	0.33
Elemental analysis [mf %]					
C	53.61	46.29	48.13	32.00	45.48
H	8.27	7.78	8.06	8.57	9.62
N	0.10	0.10	0.10	0.10	0.10
S	0.10	0.10	0.10	0.10	0.10
O	37.93	45.74	43.61	59.24	44.70
HHV [MJ/kg]	24.51	20.56	21.76	15.10	22.56
LHV [MJ/kg]	18.70	18.86	20.00	13.23	20.46
GPC analysis [g/mol]					
Average Mw	440	481	447	436	421
Average Mw of aged oil	538	584	580	530	512
Mw Difference	98	103	133	94	91
Mw Index	0.22	0.21	0.30	0.22	0.22
Mn	330	338	319	311	303
Aged oil Mn	371	382	370	355	339
Mp	302	309	201	302	197
Aged oil Mp	309	309	309	307	302
Polydispersity	1.33	1.42	1.40	1.40	1.39
Aged oil Polydispersity	1.45	1.53	1.57	1.54	1.51
Viscosity@40°C, cp	47.41	24.49	31.24	3.65	3.86
Aged oil viscosity@40°C, cp	73.51	39.87	71.69	17.50	10.70
Viscosity index	0.55	0.63	1.29	3.79	1.77
pH	2.80	2.77	2.91	3.22	3.13
Homogeneity	Single phase	Single phase	Single phase	Phase sep- arated *	phase sep- arated*

*phase separation within 3 months after analysis.

8.5 Conclusions

The chapter reviews the agronomical effects of fertiliser and harvesting times on *Miscanthus x giganteus* which was grown in 2003 in the UK. The 14 different fertiliser treatments allowed thorough evaluation of the effect that fertilisers have on biomass fuels and pyrolysis-oil properties. It was observed that fertiliser combinations and rates can affect how the plant grows in terms of metals, ash and harvesting yields; which in turn affects the pyrolysis liquid characteristics.

The results show that the alkali metals/ash content present in leaves are substantially higher than the stems, and a relationship exists between sodium and magnesium and potassium content for the leaves as senescing occurs, and is not a function of agronomical practice. However the metals decrease during the growing season, and can be indicated in most cases by the ash content, an explanation of this phenomena is that the plant requires a high level of metals to establish the first sampling, and as the plant grows over the growing season fewer minerals are required to maintain the plant [2, 125, 174]. It was found in most cases that during the growing period studied that the overall harvest yield and the percentage of leaves drops, confirming that natural senescing occurs over the winter period and is not a function of the fertiliser treatment. It can be seen that as the leaves are richer in metal and ash content compared to the stems, separation of stems and use of these as feed to a pyrolysis process will result in higher liquids yields of a higher quality, i.e. less propensity to phase separation.

The optimum yields for the TGA and product distribution from the pyroprobe-GC/MS varies with sampling for each of the 14 treatments, however it can be said that the maximum temperature for volatile evolution increases as sampling periods increase, due to the reduction in metals [APPENDIX II]. It can be seen that the yields for organics, char varies and is completely dependant on the ash/alkali metal content; however the pyrolysis-oil stability requires different fuel traits as indicated by previous chapters. To obtain the highest organic yield, a low ash/alkali metal content feedstock is required, while having the highest level of stability; acceptable ash content is required. However this would be at the expense of organic composition, yield, and higher heating value; further more the risk of phase separation.

From the pyrolysis experiments three major treatments were found to possess the most promising results for enhancing pyrolysis-oil quality and yield which were nitrogen, potassium

chloride and nitrogen/potassium chloride fertilisers. The results from the nitrogen treatments show a good yield for farmers, and a high conversion for volatile yields. It is shown that N:100_KCl:50 had the most significant results as well as influencing certain compounds to increase for leaves and stems. The effect of potassium chloride as a fertiliser showed similar yield results to that of the nitrogen fertiliser batches [for most of the sampling periods], however due to the increase of applications; certain metals [especially alkali metals] to be effected by increasing its quantity. However acceptable results were demonstrated from treatment N:50_KCl:50. The potassium sulphate fertiliser treatments had the worst results in comparison to that of any other treatments in terms of ash, yield and metals. However it is seen that as sampling periods increase, the yields of volatiles increase; this might be due to loss of nutrients, but still not reaching the level of yields to that of the nitrogen or nitrogen/potassium chloride treatments. Treatment N:50_KS:50 had the most promising result from the fertiliser treatments. From APPENDIX II it can be seen that the total yields for cellulose and syringyl derived compounds [based on the key markers used for PCA] reaches its optimum during the second sampling period for all 14 treatments. This yield then declines to its lowest yield during the 3rd sampling period for leaves and stems. The guaiacyl derived compounds on the other hand increases as sampling periods increase for the majority of the treatments for leaves and stems. The only treatments which did not show this trend is KCl:50 [stems], N:50_KCl:100, N:150_KS:100, N:200_KCl:50 and N:250_KCl:50 [leaves] which obtained an optimum yield in the 2nd sampling period. The results show that the yields of compounds are more influenced by sampling periods rather than fertiliser treatment. It also shows that the 2nd sampling period gives the highest yield for S-lignin and cellulose derived compounds and maybe beneficial for the bio-refinery industries. The yields of the majority of the compounds tends to decrease in the third sampling period due to the loss of the polysaccharides as senescing occurs within the biomass as leaves die which would lead to a less production of vapours produced during pyrolysis.

In general fertiliser treatments and harvesting times affects the feedstocks characteristics and in turn effects the pyrolysis degradation. This has been shown analytically and experimentally in this chapter. The fast pyrolysis results carried out on the 150ghr⁻¹ pyrolysis reactor showed that nitrogen, nitrogen/potassium chloride and potassium chloride fertilisers [treatment 1 and 10] had the most promising effect in reducing ash/metal content, giving rise to a high yield of

thermal conversion with good oil characteristics. The potassium chloride treatment [treatment 1] gave a total liquid yield of 61% with the average molecular weight of 440, at which the oil possessed good oil stability and only increasing by an average molecular weight of 91 during aging as well as a viscosity index of 0.55. However it must be stated that other treatments which used nitrogen/potassium chloride fertiliser applications gave poor organic yields and oil characteristics, which caused the oil to phase separate, due to its high ash/metal content [treatments 11 and 14]. The results clearly suggest that pyrolysis characteristics are completely dependant on the biomass fuel characteristics assuming that constant heating rates and reactor temperatures are set. A window for producing a stable pyrolysis-oil with good conversion yields has to be established by the bio-energy consortium; in order to set the upper and lower limits for ash and cellulose/lignin contents for the energy crops. This would allow for the continuous production of pyrolysis-oil [which is stable] on an industrial scale, as well as allowing the farmers to grow the biomass to the required quality specification.

9 CONCLUSIONS AND RECOMMENDATIONS

This chapter summarises the overall conclusions of the work in this thesis and makes recommendations for future investigation.

9.1 Conclusions

- Pyroprobe-GC/MS has been a useful technique to discriminate between different genotypes of grasses which possess a short range of lignin content. A relationship between the lignin content [as determined by wet chemistry] and the lignin derived compounds was established with a good linear trend. This suggests that screening of different types of biomass with different lignin content can be established by the use of analytical pyrolysis.
- A screening methodology based on all the feedstocks used in this research was established using TGA. The char yields and the temperature at which maximum degradation of cellulose occurs was plotted against the sum of Na and K present in the biomass, suggesting that metals has a dominant effect on pyrolysis and contributes to the rate, and temperature of cellulose degradation as well contributing to the yield of char.
- The effect of lowering the lignin due to agronomical preparation or genotypes tends to increase the metals present in the plant and thus increasing alkali metals. This was also evident in the relationship between lignin and ash content. It was shown that energy crops such as switchgrass and reed canary grass had the most positive influence on pyrolysis, by producing high yields, and good oil stability than on any other woody/non woody biomass.
- Low lignin feeds will tend to have high metal content. While low lignin feedstocks should reduce the propensity of aging, possible phase separation may occur due to the associated high metal content of the feedstock which accelerates the cracking of non-lignin derived components. Thus the resultant of this effect will reduce organic liquid yield, thus producing an overall more constant pyrolytic lignin content of liquids from most feedstocks [assuming phase separation does not occur. Ideally therefore, lignin

should be at least 7% but not more than 15% to give the most stable pyrolysis-oil product.

- The effect of water washing biomass results in reduction in metal content which thus reduces primary/secondary cracking during pyrolysis. The pyrolysis oil produced gives a higher average molecular weight than that of its unwashed counterpart, as this is due to the different degradation mechanism it undertakes. However the effect of metals on the lignin is significantly less than that on the holocellulose. Washing of biomass improves the oil quality and stability, but is dependant [varies] on each feedstock, as each feedstock has an optimum level of metal removal due to washing. Fast pyrolysis of washed biomass also increased the number of different molecules present in the pyrolysis oil and increases it's the viscosity index. However, some pyrolysis-oils produced from washed feedstocks can be more susceptible to aging and can jeopardise liquid stability. This suggests that the pyrolysis-oil produced and its stability varies from biomass to biomass and the levels of metals removed, and is clearly a complex phenomenon.
- The effect of aging on pyrolysis-oil changes the chemical composition in the organic liquid and tends to form larger molecular weight compounds, due to a number of reactions occurring while ageing. This includes an increase in levoglucosan and a decrease in hydroxyacetaldehyde, which gives an increase in viscosity and average molecular weight of the overall pyrolysis-oil.
- The 150 ghr⁻¹ fast pyrolysis rig produces different qualities of pyrolysis-oils at different stages of the rig. It was found that the condenser and EP oil quality had more organic content than that present in oil pot 1, as it had less water content making the oils more tarry and viscous. This suggests that the 150 ghr⁻¹ rig fractionates the pyrolysis-oil out and is not the same as from rigs that collect whole liquid by quenching.
- The analysis of the feedstocks from different agronomical practice of Miscanthus has been a useful research to discriminate between different farming practices and the influence on conversion. The Miscanthus grown in the UK tends to start off with high metals with high biomass yields. As the Miscanthus senescences over winter, the level

of metals decrease as well as lowering harvest yields partly from loss of leaves as the plant begins to die. This in turn affects the pyrolysis degradation and pyrolysis-oil quality. The best farming practices with regard to pyrolysis-oil yield and quality on *Miscanthus* was by the use of nitrogen or nitrogen/potassium chloride fertilisers. These treatments produced the lowest metal contents with relative high farming yields and giving the highest liquid yields and good quality. Other treatments had good effects but less pronounced.

9.2 Recommendations

Based on the outcomes of this study, the following recommendations are suggested for future investigation:

- Accurate sampling of *Lolium* and *Festuca* grasses and other biomass samples was found to be difficult, even though a sample divider was used to produce a homogenous sample size. It is difficult to originate which shard or particle came from what part of the plant [leaf or stem] as well as its subsystem. The advantage of resolving this issue would enable the identity of different regions of the leaf/stem and determine which region would give the highest organic yield, and giving a detailed insight to the pyrolysis analysis of leaf and stem.
- Trade off analysis of the *Miscanthus* grown under the different treatments and the impact on fuel quality needs to be established, so that customers can obtain the desired quality of biomass and at the same time allowing the producers to produce an acceptable yield which is profitable.
- It is recommended that greater number of repeats should be conducted on the pyroprobe-GC/MS to reduce standard deviation and to obtain an absolute representative result.
- Further investigation should be carried out on the effect of degradation on lignin for washed biomass in order to obtain a deeper understanding in lignin degradation, mechanisms and pathways. Also the technoeconomical assessment of effect of washing

biomass should be evaluated which takes into account pyrolysis liquid yields, quality, cost and energy efficiency.

- In this work a window has been identified showing that pyrolysis-oil can be produced by the use of energy crops within a certain lignin and ash range which can be modified by genotypes or agronomical practices. Pyrolysis oil quality is influenced by lignin and ash content within a defined range of values. However, a wider range of variables in these characteristics is required to understand the influence of these components on pyrolysis oil quality.
- A window for producing a stable pyrolysis-oil with good conversion yields has yet to be established by the bio-energy consortium; in order to set the upper and lower limits for ash and cellulose/lignin contents for the energy crops. This would allow for the continuous production of good quality pyrolysis-oil on an industrial scale, as well as allowing the farmers to grow the biomass to the required quality specification.
- The screening relationship for *Lolium* and *Festuca* grass by the use of pyroprobe-GC/MS was successful. However it is only valid for that particular feedstock with a lignin content of 2-4 %. To obtain a more universal screening relationship other biomass with a wider range of lignin content should be used and plotted with the existing *Lolium* and *Festuca* such as Switchgrass/RCG genotypes which also exhibit a wide range of lignin which falls in line with the *Lolium* and *Festuca* grasses.
- Further experiments are required to assess the impact of lignin on pyrolysis liquids and oil stability, as a short range of lignin contents was used [2.66-5.61 %]. A larger spectrum of lignin contents for the same species grown under the same conditions would be desirable to evaluate the effect of lignin and washing.
- At present there is no clear definition for standard “pyrolysis-oil quality”, due to the different applications it can be used for. Many literatures have suggested that good quality oil should have a good heating value, with a low char and a good viscosity index with a water content around 25 %. The stability of pyrolysis-oil is dependant on how fast reactions occur within the pyrolysis-oil. The reactions within the pyrolysis-oil during aging will continue until thermodynamic equilibrium is reached. The literature

suggests that the pyrolysis-oil can be used for application if 10 % of methanol is applied, in which the pyrolysis-oil becomes stable. Therefore a clear definition of pyrolysis-oil quality and stability must be determined [for each application] with higher and lower limits.

- Only 40 % of the pyrolysis liquid can be analysed by liquid GC/MS, this suggests that high molecular weight compounds are not passed through the column and not analysed by the mass spectrometer. Oil analysis should be investigated further on HPLC for a more comprehensive analysis and improving the amount of oil analysed.
- Fractionation of the pyrolysis-oil, and the possible applications for each fraction should be investigated to gain a deeper insight of other future products and markets.
- Pure cellulose and lignin should be pyrolysed and the oil produced should be characterised for its yield and quality. This would allow for a deeper insight of cellulose/lignin degradation and oil stability from biomass's main constituents.
- Oil quality and stability should be analysed with varying heat rates and pyrolysis set temperatures to optimise the finding found in this research, as process variables vary.
- The varying of ash content on a selected biomass should be investigated to obtain a clearer understanding on the effect of ash/metal on pyrolysis oil stability. This could be carried out by washing a particular biomass specie, and placing different ash quantities [%] in the pyrolysis reactor, and analysing the oil yield and quality which is produced.

10 REFERENCES

1. Bridgwater, AV, Czernik, S, and Diebold, J. *Fast pyrolysis of Biomass: A Handbook*. 1999. 1: p. 1-42.
2. Saijonkari-Pahkal, K. *Agricultural & food science in Finland*. The scientific agricultural society of Finland, 2001. 10 p.20-54.
3. Levitt, J. *Introduction to plant Physiology*. 1974 (2nd Edition) p. 5-32.
4. Goss, J.A. *Physiology of plants and there cells*. 1974. 1st Edition p. 7-22.
5. Gronli, M. *A theoretical and experimental study of the thermal degradation of Biomass*. PhD Thesis, 1996. p. 15-145.
6. Hague, RA. *The pre-treatment and pyrolysing of biomass for the production of liquids for fuel and speciality chemicals*. Aston university, 1998. PhD Thesis: p. 20-117.
7. Antal, J. *Biomass Pyrolysis: A Review of the Literature. Part 1-Carbohydrate Pyrolysis*. Advances in Solar Energy; K. W. Boer and J. A. Duffle, Eds.; Am. Solar Energy Soc.:N.Y, 1982: p. 61-100.
8. Bradbury, A, Sakai Y, and Shafizadeh F. *A kinetic model for pyrolysis of cellulose*. *Journal of Applied Polymer Science*. 1979. 23 (1): p. 3271-3280.
9. Antal, J. *A Review of the vapour phase pyrolysis of biomass derived volatile matter*. In *fundamentals of thermochemical biomass processing*. Elsevier Applied Science Publishers: London, 1985: p. 511-535.
10. Abdullah, N. *An assessment of pyrolysis for processing empty fruit bunches*. Aston university, 2005. PhD Thesis (1): p. 23-101.
11. Graboski M. *Properties of biomass relevant to gasification in a survey of biomass gasification*. SERI TR 33 239, 1979. 2(1): p. 22-66.
12. Yang, H. *Characteristics of hemicellulose, cellulose and lignin pyrolysis*. *Fuel*, 86, 12-13, 2007, p 1781-1788.
13. Oudia, A. *Pyrolysis-GC/MS and TG/MS study of mediated laccase biodelignification of Eucalyptus globulus kraft pulp*. *Journal of Analytical and Applied Pyrolysis*, 2007. 78(2): p. 233-242.
14. Bridgwater, A.V. *Biomass pyrolysis-oil*. Aston internal report, 2003: p. 1-18.
15. Bridgwater, AV. *Renewable fuels and chemicals by thermal processing of biomass*. *Chemical Engineering Journal*, 2003. 91(2-3): p. 87-102.
16. Wampler, T.P. *Applied Pyrolysis handbook*. 1990 p.1-60.
17. Uzun, BB, Putun AE, and Putun E. *Fast pyrolysis of soybean cake: product yields and compositions*. *Bioresource technology*, 2006. 97(1): p. 569-576.
18. Antal, J, Mok I, and Richards W. *Mechanism of formation of 2-furaldehyde from D-xylose*. *Carbohydr res*, 1991. 217: p. 71-101.
19. Tilman, D. *An overview of present technologies and programs*. *Fuels from wastes*, 1977: p. 17-40.
20. Mattucci E. *Technique de carbonisation dee pyrolysis*. Bio aletnatives SA, 1989: p. 205-220.
21. Milne, T. *Pyrolysis -The thermal behaviour of biomass below 600°C*. A survey of biomass gasification, 1979. 2: p. 95-132.
22. Graham RG, Mok LKS, and de Lasa HI. *Fast pyroysis (ultra pyrolysis) of biomass using solid heat carriers*. *Fundamentals of thermochemical biomass conversion*, 1985: p. 397-410.

23. Graham RG. *Fast pyrolysis of biomass*. Journal of Analytical and Applied Pyrolysis, 1984. 6: p. 95-135.
24. Graham, R. *A characterisation of the fast pyrolysis of cellulose and wood biomass*. PhD thesis, 1993. University of Western Ontario Canada: p. 20-137.
25. Gronli, M. *NTNU biomass and bioenergy principles lecture notes*. Trodehim Norway., 2003. 1(1): p. 1-50.
26. Bridge, SA. *Flash pyrolysis of biomass for liquid fuels*. MPhil Thesis, 1991. Aston University (1): p. 25-155.
27. Liden, A., Berruti F, and Scott D. *A kinetics model for the production of liquids from the flash pyrolysis of biomass*. Chem. Eng. Comm., 1998. 65(1): p. 207-221.
28. Scott, D, Radlein PJ, and Czernik S. *Liquid products from the fast pyrolysis of wood and cellulose" in Research in thermochemical biomass conversion*. Eds. A.V. Bridgwater and Kuester, Elsevier applied science, 1988: p. 557-571.
29. Piskorz J, Scott D, and Czernik S, *Liquid products from the fast pyrolysis of wood and cellulose in research in thermochemical biomass conversion*. Elsevier Applied Science Publishers: London & New York, 1988. 1(1): p. 557-583.
30. Hilland, G. and Holman J. *Chemistry in context*. 1998 (3): p. 45-69.
31. Hamann, C, Hamnett A, and Vielstich W. *Electrochemistry*. Wiley-VCH: Weinhem, 1998 p. 281-299.
32. Khadem, HSE. *Carbohydrate Chemistry*. Academic Press: New York, 1988: p .12-33.
33. Antal, J. *Biomass pyrolysis: A review of the literature. Part 2-Lignocellulose pyrolysis*. Advances in Solar Energy; K. W. Boer and J. A. Duffie, Eds.; Plenum Press: N.Y, 1985: p. 175-207.
34. Khadem, HSE. *Carbohydrate chemistry (Monosaccharide and their oligomers)*. The American university Washington DC, 1987: p1-25.
35. Antal, J. and Richards S. *Mechanism of formation of 5 hydroxymethyl-2- furdaldehyde from D-fructose and sucrose*. Carbohydr res, 1990. 199: p. 91-108.
36. Antal, J. *A review of cellulose degradations and similar reactions*. Advances in solar energy. 1: p. 81-100.
37. Faix, O, Fortmann I, and Meier D. *Thermal degradation products of wood*. Holzals Roh-und Werkstoff, 1991. 49 (1): p. 213-219.
38. Faix, O, Fortmann I , and Meier D. *Thermal degradation products of wood*. Holzals Roh-und Werkstoff, 1991. 49 (1): p. 299-301.
39. Faix, O, Fortmann I, and Meier D. *Thermal degradation products of wood*. Holzals Roh-und Werkstoff, 1990. 48 (1): p. 281-285.
40. Faix, O, Fortmann I, and Meier D. *Thermal degradation products of wood*. Holzals Roh-und Werkstoff, 1990. 48 (1): p. 351-354.
41. Bremer, J. *PhD thesis*. Quantification of polymers from lignocellulosics by analytical pyrolysis-GC/MS, 1991. 1 (1): p. 25-50.
42. Alves, A., *Analytical pyrolysis as a direct method to determine the lignin content in wood: Part 1: Comparison of pyrolysis lignin with Klason lignin*. Journal of Analytical and Applied Pyrolysis, 2006. 76 (1-2): p. 209-213.
43. Ohra-aho, T, Tenkanen M, and Tamminen T. *Direct analysis of lignin-lignin like components from softwood kraft by py-GC/MS*. Journal of Analytical and Applied Pyrolysis, 2005. 74 (1): p. 123-128.
44. Ververis, C. *Cellulose, hemicelluloses, lignin and ash content of some organic materials and their suitability for use as paper pulp supplments*. Bioresource technology, 2007. 98 (1): p. 296-301.

45. Rodrigues, J, and Meier D. *Determination of tree to tree variation in syringyl/guaiacyl ratio of Eucalyptus globulus wood lignin by analytical pyrolysis*. Journal of Analytical Applied Pyrolysis, 1999. 48 (2): p. 121-128.
46. Del Rio, J.C. *Py-GC/MS study of eucalyptus globulus wood treated with different fungi*. Journal of Analytical & Applied Pyrolysis, 2001. 58-59 (1): p. 441-452.
47. Franchini, J. and Gonzalez-Vila F. *Decomposition of plant residues used in no-tillage systems as revealed by flash pyrolysis*. Journal of Analytical & Applied Pyrolysis, 2002. 62 (1): p. 35-43.
48. Scholze, B. and Meier D. *Characterization of the water-insoluble fraction from pyrolysis-oil (pyrolytic lignin). Part I. PY-GC/MS, FTIR, and functional groups*. Journal of Analytical & Applied Pyrolysis, 2000. 60 (1): p. 41-54.
49. Meier, D, and Fortmann I. *Discrimination of genetically modified poplar clones by analytical pyrolysis GC and principle component analysis*. Journal of Analytical & Applied Pyrolysis, 2005. IN PRESS.
50. Fabbri, D, and Sangiori F. *Molecular characterisation of organic matter in air fine particles pyrolysis gas chromatography-mass spectroscopy*. Analytica Chimica Acta, 2005. 530: p. 253-261.
51. Henandez, M, and Hernandez-Coronado M, *Pyrolysis/gas chromatography/mass spectrometry as a useful technique to evaluate the ligninolytic action of streptomycetes on wheat straw*. Journal of Analytical & Applied Pyrolysis, 2001. 58-59 (1): p. 539-551.
52. Evans, R, and Milne T. *Molecular characterisation of the pyrolysis of biomass 1. Fundamentals*. Energy & Fuels, 1987. 1 (2): p. 123-137.
53. Evans, R, and Milne T. *Molecular characterisation of the pyrolysis of biomass 2. application*. Energy & Fuels, 1987. 1 (4): p. 312-319.
54. Shafizadeh, F. *Pyrolytic reactions and products of biomass*. wood chemistry laboratory, university of Montana, Missoula, Montana USA, 1989: p1-22.
55. Camarero, S. *Compositional changes of wheat lignin by a fungal peroxidase analyzed by pyrolysis-GC-MS*. Journal of Analytical & Applied Pyrolysis, 2001. 58-59 (2): p. 413-423.
56. Simkovic, I. and Francis B. *Pyrolysis-gas chromatography mass spectrometry analysis of starch-based ion-exchangers*. Journal of Analytical & Applied Pyrolysis, 1997. 43 (2): p. 145-155.
57. Tanczos, I., Pokol G, and Borsa J. *The effect of tetramethylammonium hydroxide in comparison with the effect of sodium hydroxide on the slow pyrolysis of cellulose*. Journal of analytical & applied pyrolysis, 2003. 68-69 (Conference issue): p. 173-185.
58. Szabo, P. *Thermogravimetric/mass spectrometric characterization of two energy crops, Arundo donax and Miscanthus sinensis*. Journal of Analytical & Applied Pyrolysis, 1996. 36 (2): p. 179.
59. Hsisheng T, and Wei YC. *Thermogravimetric studies on the kinetics of rice hull pyrolysis and the influence of water treatment*. Ind. Eng. Chem Res, 1998. 37 (1): p. 3806-3811.
60. Raveendran, K, Ganesh A, and Khilar KC. *Influence of mineral matter on biomass pyrolysis characteristics*. Fuel, 1995. 74 (12): p. 1812-1824.
61. Diaz, I. *Study of TG-MS of the oxidation of SH-MCM-41 to SO₃H-MCM-41*. Thermochemica acta, 2004. 413 (1): p. 201-207.

62. Lewandowski, I, and Heinz A. *Delayed harvest of Miscanthus—influences on biomass quantity and quality and environmental impacts of energy production*. European journal of Agronomy, 2003. 19 (1): p. 45-63.
63. Helsen, L, and Bulck EVD. *Kinetics of the low-temperature pyrolysis of chromated copper arsenate-treated wood*. Journal of Analytical & Applied Pyrolysis, 2000. 53 (1): p. 51-79.
64. Saade, R, and Kozinski JA. *Numerical modeling and TGA/FTIR/GCMS investigation of fibrous residue combustion*. Biomass & Bioenergy, 2000. 18 (5): p. 391-404.
65. Varhegyi, G. *Kinetic modeling of biomass pyrolysis*. Journal of Analytical & Applied Pyrolysis, 1997. 42 (1): p. 73-87.
66. Dogan, G. *Energy source*, 2003. 25: p. 753-765.
67. Gronli, M, Antal M Jr, and Varhegyi G. *Round robin study of cellulose pyrolysis kinetics by Thermogravimetry*. Ind. Eng. Chem, 1999. 38 (1): p. 2238-2244.
68. Jakab, E, Faix O, and Till F. *Journal of Analytical & Applied Pyrolysis*, 1997. 40-41: p. 171.
69. Kilzer FJ. *Speculation on the nature of cellulose pyrolysis, Pyrodynamics*. 1965. 2 (1): p. 151.
70. Shafizadeh, F. *Pyrolysis and combustion of cellulose materials*. Advances in Carbohydrate Chemistry, 1968. 23 (1): p. 419-474.
71. Avni, E, Davoudzadeh F, and Coughlin R. *Flash pyrolysis of lignin*. Fundamentals of thermochemical biomass conversion, 1985: p. 329-338.
72. Antal, J. *Mathematical modelling of biomass pyrolysis phenomena: Introduction*. Fuel, 1985. 64(11): p. 1483-1486.
73. Blasi, C. *Kinetics review-internal report*. 2004: p1-22.
74. Blasi, C. *Comparison of semi-global mechanisms for primary pyrolysis of lignocellulosic fuels*. Journal of Analytical & Applied Pyrolysis, 1998. 47 (1): p. 43-64.
75. Branca, C. and Blasi C. *Global intrinsic kinetics of wood oxidation*. Fuel, 2004. 83 (1): p. 81.
76. Blasi, C. *Heat, momentum and mass transport through a shrinking biomass particle exposed to thermal radiation*. Chemical Engineering Science, 1996. 51 (7): p. 1121-1132.
77. Blasi, C. *Influence of chemical changes of the isotropic matrix on physical properties of mesophase pitch*. Fuel, 1996. 75 (1): p. 58-66.
78. Blasi, C. *Drying characteristics of wood cylinders for conditions pertinent to fixed-bed counter current gasification*. Biomass and Bioenergy, 2003. 25: p. 45-58.
79. Blasi, C. *Multi-phase moisture transfer in the high-temperature drying of wood particles*. Chemical Engineering Science, 1998. 53: p. 353-366.
80. Blasi, C. *Modelling intra- and extra-particle processes of wood fast pyrolysis*. AIChE Journal., 2002. 48: p. 2386-2397.
81. Blasi, C. *The state of the art of transport models for charring solid degradation*. Polymer International, 2000. 49: p. 1133-1146.
82. Blasi, C. *Heat, momentum and mass transport through a shrinking biomass particle exposed in thermal radiation*. Chemical Engineering Science, 1996. 51: p. 1121-1132.
83. Gronli, M, Varhegyi G, and Blasi C. *Thermogravimetric analysis and devolatilisation kinetics of wood*. Ind. Eng chem. res, 2002. 41: p. 4201-4208.
84. Galgano T, and Blasi C. *Modelling the propagation of drying and decomposition fronts in wood, Combustion and Flame*. IN PRESS, 2006.

85. Gorton CW. *Oil from biomass by entrained flow pyrolysis*. Biotech and bio-energy, 1984. 14 (1): p. 14-20.
86. Diebold, J. *A review of the chemical and physical mechanisms of the storage and stability of fast pyrolysis bio-oils*. 2000. NREL (1): p. 3-42.
87. Ramiah, M. *Thermogravimetric and differential thermal analysis of cellulose, hemicellulose and lignin*. Journal of Applied Polymer Science, 1970. 14: p. 1323-1337.
88. Maggi, R, and Delmon B. *Characterization and upgrading of bio-oils produced by rapid thermal processing*. Biomass and Bioenergy, 1994. 7 (1-6): p. 245-249.
89. Varhegyi G, Szekely T, and Szabo P. *Kinetics of the thermal decomposition of cellulose, hemicellulose and sugar cane bagasse*. Energy & Fuels, 1989. 3: p. 329-335.
90. Simkovic I, Antal Jr MJ, Ebringerova A, Szekely T and Szabo P. *Thermogravimetric/Mass spectrometric characterisation of the thermal decomposition of (4-O-methyl-D-Glucurono)-D-xylan*. Journal of Applied Polymer Science, 1988. 36: p. 721-728.
91. Soltes, E, and Elder T. *Pyrolysis in organic chemicals from biomass*. Goldstein I.S., 1981: p. 63-100.
92. Peacocke, G.V.C. *Ablative Pyrolysis of Biomass*. PhD thesis, 1994: p.10-201.
93. Boerjan, W, Ralph J, and Baucher M. Lignin biosynthesis, Ann. Rev Plant Biology, 2003. 54: p. 519-46.
94. Choi, JW, Faix O, and Meier D. *Characterisation of residual lignin from chemical pulps of spruce and beech by analytical pyrolysis-GC/MS*. Holzforschung, 2001. 55(1): p. 185-192.
95. Kleen, M, and Gellerstedt G. *Influence of inorganic species on the formation of polysaccharide and lignin degradation products in the analytical pyrolysis of pulps*. Journal of Analytical & Applied Pyrolysis, 1995. 35 (1): p. 15-41.
96. Jakab, E, Faix O, and Till F. *The effect of cations on the thermal decomposition of lignin*. Journal of Analytical and Applied Pyrolysis, 1993. 25 (1): p. 185.
97. Milne T. *Pyrolysis -The thermal behaviour of biomass below 600°C*. A survey of biomass gasification, 1979. 2: p. 95-132.
98. Tang, W. *Effects of inorganic salts on pyrolysis of wood, alpha cellulose and lignin*. US forest service research paper FPL71, 1967.
99. Deglise, X, and Magne P. *Pyrolysis and industrial charcoal*. Biomass regenerable energy, 1987: p. 221-235.
100. Gorton, C, and Knight J. *Oil from biomass by entrained flow pyrolysis*. Biotech and bioener, 1984. 14 (1): p. 14-20.
101. Evans, R, and Milne T. *Applied mechanistic studies of biomass pyrolysis*. Biomass thermochemical conversion contractors, 1985: p. 57-67.
102. Evans R, and Milne T. *Applied mechanistic studies of biomass pyrolysis*. Biomass thermochemical conversion contractors, 1985: p. 57.
103. Avni E, and Coughlin RW. *Flash pyrolysis of lignin*. Fundamentals of thermochemical biomass conversion, 1985: p. 329.
104. Avni E, Solomon PR, and King H.H, *Mathematical modelling of lignin pyrolysis*. Fuel, 1985. 64: p. 1495-1511.
105. Goos, A. *The thermal decomposition of wood*. Wood chemistry, 1952. chapter 20: p.55-72.
106. Allan, G. and Matilla T. *Lignins: Occurrence, formation, structure and reactions*. 1971: conference report.

107. Sekiguchi Y. *Structure and formation of cellulosic chars*. Journal of Applied Polymer science, 1983. 28: p. 3515-3525.
108. Jegers, HE. *Primary and secondary lignin pyrolysis reaction pathways*. Ind. Eng. Chem. Process Des., 1985. 24: p. 173-183.
109. Iatridis B. *Pyrolysis of a precipitated Kraft Lignin*. Ind. Eng. Chem. Prod. Res, 1979. 2: p. 127-140.
110. Nunn TR, Longwell JP, and Peters WA. *Product composition and kinetics in the rapid pyrolysis of sweet gumhardwood*. Ind. Eng. Chem. Prod. Res., 1985. 24: p. 836-844.
111. Mok, W, Antal J, and Jones M. *Formation of Acrylic Acid from Lactic Acid in Supercritical Water*. J. Org. Chem, 1989. 54: p. 4596-4611.
112. Klein, M. and Virk P, *Primary and secondary lignin pyrolysis reaction pathways*. ind. Eng. Chem. Fundam, 1983. 22: p. 35-52.
113. Landau, R, Libanati C, and Klein M. *Monte carlo simulation of lignin pyrolysis: Sensitivity to kinetic parameters*. Research in thermochemical biomass conversion, 1988: p. 452-471.
114. Landau RN. *Monte carlo simulation of lignin pyrolysis: Sensitivity to kinetic parameters*. Research in thermochemical biomass conversion, 1988: p. 452-464.
115. King HH, Avni E, and Coughlin RW. *Modelling tar composition in lignin pyrolysis*. ACS Series, 1983. 2 8 (5): p. 319-333.
116. Smith, P, Powlson A, and Smith D. *Meeting Europe's climate change commitments*. Global change biology, 2000. 6 (1): p. 525-539.
117. Schwarz, H. *The effect of fertilization on yield and quality of Miscanthus sinensis 'Giganteus'*. Industrial Crops and Products, 1994. 2 (3): p. 153-159.
118. Clifton-Brown, JC, and Lewandowski I. *Screening Miscanthus genotypes in field trials to optimise biomass yield and quality in Southern Germany*. European Journal of Agronomy, 2002. 16 (2): p. 97-110.
119. Beale, C, and Long SP. *Seasonal dynamics of nutrient accumulation and partitioning in the perennial C4-grasses Miscanthus x giganteus and Spartina cynosuroides*. Biomass and Bioenergy, 1997. 12 (6): p. 419-428.
120. Danalatos, NG, Archontoulis SV, and Mitsios I. *Potential growth and biomass productivity of Miscanthusxgiganteus as affected by plant density and N-fertilization in central Greece*. Biomass and Bioenergy. In Press, Corrected Proof.
121. Jorgensen, U. *Genotypic variation in dry matter accumulation and content of N, K and Cl in Miscanthus in Denmark*. Biomass and Bioenergy, 1997. 12 (3): p. 155-169.
122. Foereid, B, de Neergaard A, and Høgh-Jensen H. *Turnover of organic matter in a Miscanthus field: effect of time in Miscanthus cultivation and inorganic nitrogen supply*. Soil Biology and Biochemistry, 2004. 36 (7): p. 1075-1085.
123. Arduini, I, Masoni A, and Ercoli L. *Effects of high chromium applications on Miscanthus during the period of maximum growth*. Environmental and Experimental Botany, 2006. 58 (1-3): p. 234-243.
124. Christian, DG, Yates N, and Riche A. *Establishing Miscanthus sinensis from seed using conventional sowing methods*. Industrial Crops and Products, 2005. 21 (1): p. 109-111.
125. Lewandowski, I. and Heinz A. *Delayed harvest of Miscanthus--influences on biomass quantity and quality and environmental impacts of energy production*. European Journal of Agronomy, 2003. 19 (1): p. 45-63.
126. Davidsson, K, Pettersson J, and Nilsson R. *Fertiliser influence on alkali release during straw pyrolysis*. Fuel, 2002. 81(1): p. 259-262.

127. Skrifvars, BJ. *Ash behaviour in a CFB boiler during combustion of coal, peat or wood*. Fuel, 1998. 77 (1-2): p. 65-70.
128. Baxter, L. *The behavior of inorganic material in biomass-fired power boilers: field and laboratory experiences*. Fuel processing technology, 1998. 54 (1-3): p. 47-78.
129. Lewandowski, I, and Kicherer A. *Combustion quality of biomass: practical relevance and experiments to modify the biomass quality of Miscanthus x giganteus*. European Journal of Agronomy, 1997. 6 (3-4): p. 163-177.
130. Czernik, S, and Bridgwater AV. *Overview of application of biomass fast pyrolysis-oil*. Energy fuels, 2004. 18: p. 590-562.
131. Teng, H, and Wei Y. *Thermogravimetric studies on the kinetics of rice hull pyrolysis and the influence of water treatment*. Ind. Eng, Res, 1998. 37 (1): p. 3806-3811.
132. Raveendran, K, Ganesh A, and Khilar KC. *Pyrolysis characteristics of biomass and biomass components*. Fuel, 1996. 75 (8): p. 987-998.
133. Elmer, P., *Perkin Elmer Pyris 1 TGA manual*. 2001. 1: p1-59.
134. CDS, *Pyroprobe manual*. 2005. 1: p1-25.
135. Elmer, P., *GC & MS spectroscopy manual*. 2000. 1: p1-74.
136. Fahmi, R. *PhD qualifying report*. 2004 (1): p. 7-21.
137. Bridgeman, TG. *Influence of particle size on the analytical and chemical properties of two energy crops*. Fuel, 2007. 86 (1-2): p. 60-72.
138. Acikgoz, C, and Kockar OM. *Flash pyrolysis of linseed (Linum usitatissimum L.) for production of liquid fuels*. Journal of Analytical and Applied Pyrolysis, 2007. 78 (2): p. 406-412.
139. *Chemical analysis & testing task Laboratory analytical procedure*. LAP-005.
140. Fundamentals, RRS. *Accurics ICPEs (Induced coupled plasma emission spectrometer)*. 2006.
141. Soest, HKG. *Forage fiber analysis: apparatus, reagents, procedures and some applications*. Agricultural Handbook. Agricultural Research Service, US Department of Agriculture, Washington, D.C., 1970. 379.
142. Fahmi, R., et al., *Prediction of Klason Lignin and lignin thermal degradation products by Py-GC/MS in a collection of Lolium and Festuca grasses*. Journal of Analytical and Applied Pyrolysis, 2007. IN PRESS.
143. Bridgwater, AV. *Fast pyrolysis of biomass: A handbook*. 2005. 2: p 19-43.
144. Bridgwater, AV. *Fast pyrolysis of biomass for liquid fuels and chemicals-A review*. Aston internal report, 2002: p. 1-21.
145. Bridgwater, AV. *Fast pyrolysis of biomass: A handbook*. 2005. 3: p. 19-43.
146. Oasmaa, A, and Meier D. *Norms and standards for fast pyrolysis liquids: 1. Round robin test*. Journal of Analytical and Applied Pyrolysis, 2005. 73 (2): p. 323-334.
147. Oasmaa, A. *Quality improvements of pyrolysis liquid: effects of light volatiles on the stability of pyrolysis liquids*. American Chemical Society, 2005 (IN PRESS).
148. Oasmaa, A, and Kuoppala E. *Fast pyrolysis of forestry residue 3. Storage stability of liquid fuels*. Energy & Fuels, 2003. 17: p. 1075-1084.
149. Ji-lu, Z. *Bio-oil from fast pyrolysis of rice husk: Yields and related properties and improvement of the pyrolysis system*. Journal of Analytical & Applied Pyrolysis. In Press, Corrected Proof.
150. Czernik, S, and Bridgwater AV. *Applications of Biomass Fast Pyrolysis-oil*. Energy & Fuels, 2004. 18 (1): p. 590-598.
151. Fahmi, R. *The Effect of Alkali metals on Combustion and Pyrolysis of Lolium and Festuca Grasses, Switchgrass and Willow*. Fuel (2007) Vol.86. Iss.1 p 1560-1569.

152. Piskorz, J. *Liquid products from the fast pyrolysis of wood and cellulose in research in thermochemical biomass conversion*. Elsevier Applied Science Publishers: London & Newyork, 1988. 1 (1): p. 557.
153. Meire, D, Moltran J, and Faix O. *Wood chemistry*. 2004. 1: p. 1-4.
154. Fratini, E. *SANS analysis of microstructural evolution during aging of pyrolysis-oils from biomass*. Langmuir, 2006. 22 (1): p. 306-312.
155. Fang, GC. *A study of polycyclic aromatic hydrocarbons concentrations and source identifications by methods of diagnostic ratio and principal component analysis at Taichung chemical Harbor near Taiwan Strait*. Chemosphere, 2006. 64 (7): p. 1233-1242.
156. Gokulakrishnan, P. *A functional-PCA approach for analyzing and reducing complex chemical mechanisms*. Computers & Chemical Engineering, 2006. 30 (6-7): p. 1093-1101.
157. Paasivirta, J, Tarhanen J, and Soikkeli J. *Occurrence and fate of polychlorinated aromatic ethers (PCDE, PCA, PCV, PCPA and PCBA) in environment*. Chemosphere, 1986. 15 (9-12): p. 1429-1433.
158. Statheropoulos, M, and Mikić K. *PCA-ContVarDia: an improvement of the PCA-VarDia technique for curve resolution in GC-MS and TG-MS analysis*. Analytica Chimica Acta, 2001. 446 (1-2): p. 351-368.
159. Worasuwannarak, N, Sonobe T, and Tanthapanichakoon W. *Pyrolysis behaviors of rice straw, rice husk, and corncob by TG-MS technique*. Journal of Analytical & Applied Pyrolysis, 2007. 78 (2): p. 265-271.
160. Sipila, K. *Characterization of biomass-based flash pyrolysis-oils*. Biomass and Bioenergy, 1998. 14 (2): p. 103-113.
161. Wang, C. *Direct conversion of biomass to bio-petroleum at low temperature*. Journal of Analytical & Applied Pyrolysis, 2007. 78 (2): p. 438-444.
162. Boucher, ME, Chaala A, and Roy C. *Bio-oils obtained by vacuum pyrolysis of softwood bark as a liquid fuel for gas turbines. Part I: Properties of bio-oil and its blends with methanol and a pyrolytic aqueous phase*. Biomass and Bioenergy, 2000. 19 (5): p. 337-350.
163. Oasmaa, A, and Kuoppala E. *Fast Pyrolysis of Forestry Residue. 3. Storage Stability of Liquid Fuel*. Energy & Fuels, 2003. 17: p. 1075-1084.
164. Das, P, Sreelatha T, and Ganesh A. *Bio oil from pyrolysis of cashew nutshell characterisation and related properties*. Biomass and Bioenergy, 2004. 27: p. 265-275.
165. Boucher, ME. *Bio-oils obtained by vacuum pyrolysis of softwood bark as a liquid fuel for gas turbines. Part II: Stability and ageing of bio-oil and its blends with methanol and a pyrolytic aqueous phase*. Biomass and Bioenergy, 2000. 19 (5): p. 351-361.
166. Bridgwater, AV. *Principles and practice of biomass fast pyrolysis processes for liquids*. Journal of Analytical & Applied Pyrolysis, 1999. 51 (1-2): p. 3-22.
167. Ghetti, P, Ricca L, and Angelini L. *Thermal analysis of biomass and corresponding pyrolysis products*. Fuel, 1996. 75 (5): p. 565-573.
168. Gani, A, and Naruse I. *Effect of cellulose and lignin content on pyrolysis and combustion characteristics for several types of biomass*. Renewable energy, 2007. 32 (1): p. 649-661.
169. Bridgwater, AV, and Peacocke G. *Fast pyrolysis processes for biomass*. Renewable and Sustainable Energy Reviews, 2000. 4 (1): p. 1-73.
170. Bridgwater, AV, Meier D, and Radlein D. *An overview of fast pyrolysis of biomass*. Organic Geochemistry, 1999. 30 (12): p. 1479-1493.

171. Muller-Hagedorn, M, and Bockhorn H. *Pyrolytic behaviour of different biomasses (angiosperms) (maize plants, straws, and wood) in low temperature pyrolysis*. Journal of Analytical & Applied Pyrolysis. In Press, Corrected Proof.
172. Nokkosmaki, Ml. *Catalytic conversion of biomass pyrolysis vapours with zinc oxide*. Journal of Analytical & Applied Pyrolysis, 2000. 55 (1): p. 119-131.
173. Demirbas, A. *Biodisel fuels from vegetable oils via catalytic and non catalytic supercritical alcohol transesterification and other methods: a survey*. Energy conversion and management, 2003. 44 (1): p. 2093-2109.
174. Chefetez, B, Tarchitzky J, and Deshmukh AP. *plant growth studies*. Soil science society, 2002. 66: p. 129-141.

11 APPENDIX I

11.1 Publications produced during the PhD course.

A list of publications which were submitted and accepted in journals during the work of the thesis is given below. The majority of the publications have been incorporated into the thesis as chapters, and others are finding carried out which have relevance to the thesis.

Main author

- Fahmi R, AV Bridgwater, L. I. Darvell, N. Yates, S. Thain. The Effect of Alkali metals on Combustion and Pyrolysis of Lolium and Festuca Grasses, Switchgrass and Willow. Fuel (2007) Vol.86. Iss.1 p 1560-1569
- Fahmi R, AV Bridgwater, S. Thain, I. Donnison, N. Yates. Prediction of Klason Lignin and lignin thermal degradation products by Py-GC/MS in a collection of Lolium and Festuca grasses. Journal of Analytical and Applied Chemistry (2007) Volume 80, Iss. 1, Pages 16-23
- Fahmi R, AV Bridgwater, I. Donnison, N. Yates, J. Jones. The Effect of Lignin and inorganic, on pyrolysis-oil yield, quality, and stability. Fuel (2007) – **IN PRESS**
ACCEPTED CORRECTED PROOF

Secondary author

- Bridgeman, T. G., Fahmi, R., Yates, N. Thain, S. C. Donnison, I. S. Influence of particle size on the analytical and chemical properties of two energy crops. Fuel (2007) Vol 86. Iss.1-2 p 60-72
- S. Thain, I. Donnison, Fahmi R, AV Bridgwater. Development of a method to predict the lignin content of energy grasses using Fourier-transform infrared and Fourier-transform Raman spectroscopy. New Phytologist (2007) **IN PRESS - ACCEPTED CORRECTED PROOF**



Available online at www.sciencedirect.com



ScienceDirect

Fuel 86 (2007) 1560–1569



www.fuelfirst.com

The effect of alkali metals on combustion and pyrolysis of *Lolium* and *Festuca* grasses, switchgrass and willow

R. Fahmi ^{a,*}, A.V. Bridgwater ^a, L.I. Darvell ^b, J.M. Jones ^b, N. Yates ^c,
S. Thain ^d, I.S. Donnison ^d



Aston University

Content has been removed due to copyright restrictions



Prediction of Klason lignin and lignin thermal degradation products by Py–GC/MS in a collection of *Lolium* and *Festuca* grasses

R. Fahmi^{a,*}, A.V. Bridgwater^a, S.C. Thain^b, I.S. Donnison^b, P.M. Morris^b, N. Yates^c



Aston University

Content has been removed due to copyright restrictions



ELSEVIER

Available online at www.sciencedirect.com

ScienceDirect

Fuel xxx (2007) xxx–xxx

www.fuelfirst.com

The effect of lignin and inorganic species in biomass on pyrolysis oil yields, quality and stability

R. Fahmi ^{a,*}, A.V. Bridgwater ^a, I. Donnison ^b, N. Yates ^c, J.M. Jones ^d



Aston University

Content has been removed due to copyright restrictions



Available online at www.sciencedirect.com



Fuel 86 (2007) 60–72



www.fuelfirst.com

Influence of particle size on the analytical and chemical properties of two energy crops

T.G. Bridgeman ^a, L.I. Darvell ^a, J.M. Jones ^{a,*}, P.T. Williams ^a, R. Fahmi ^b,
A.V. Bridgwater ^b, T. Barraclough ^c, I. Shield ^c, N. Yates ^c, S.C. Thain ^d, I.S. Donnison ^d

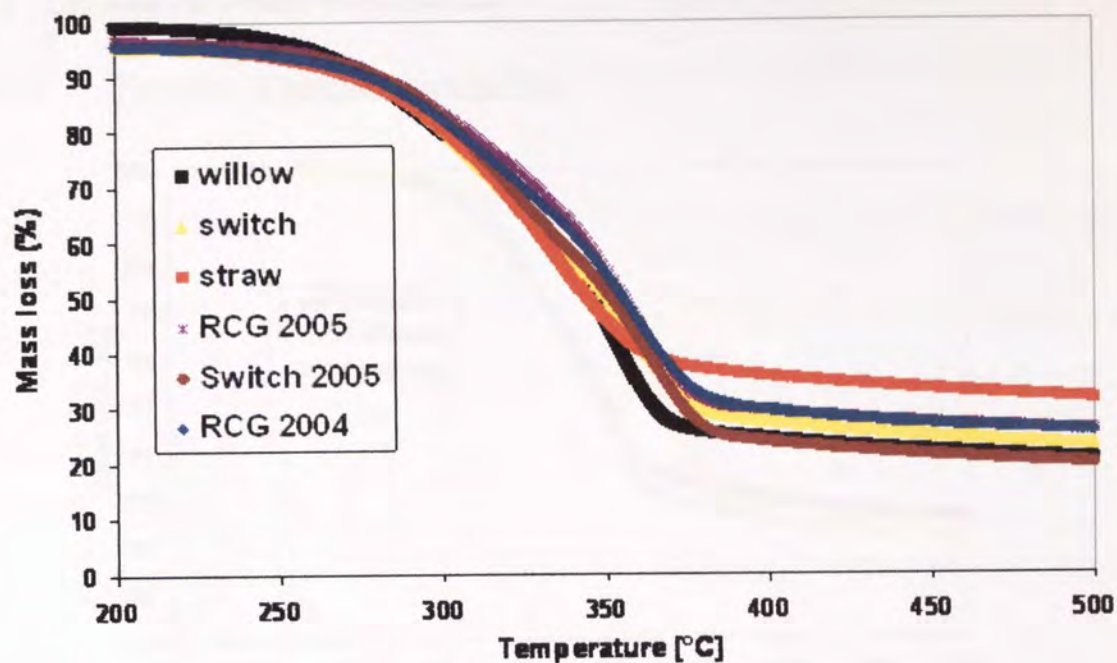
^a School of Chemical Engineering, Aston University, Birmingham, UK



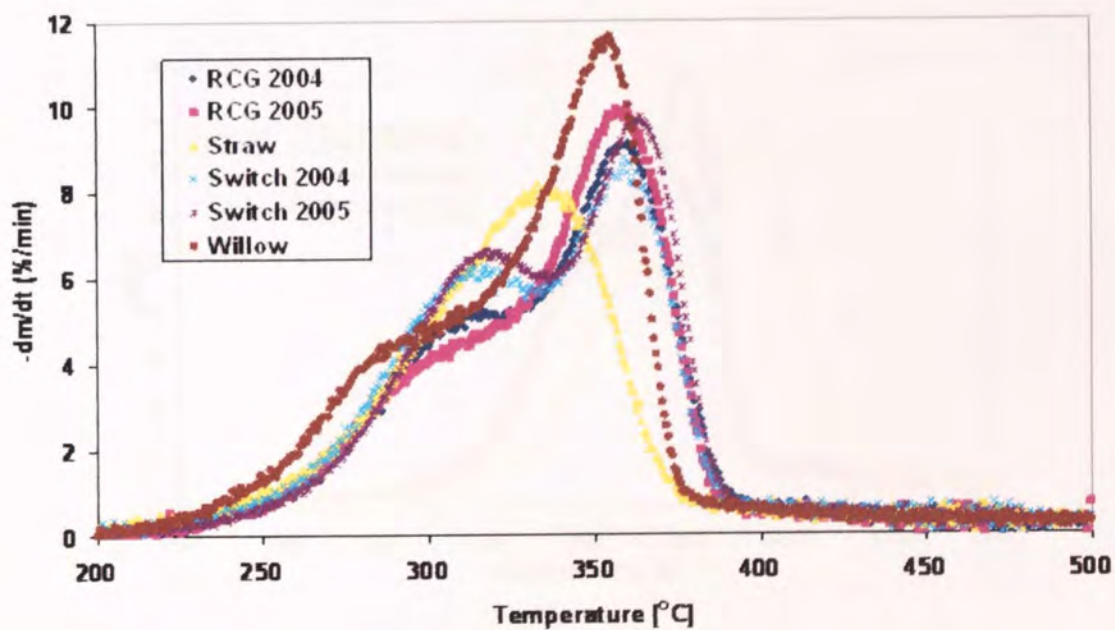
Aston University

Content has been removed due to copyright restrictions

11.2 Reference fuels TG & DTG data



APPENDIX I, Figure 1 - TG of reference fuels

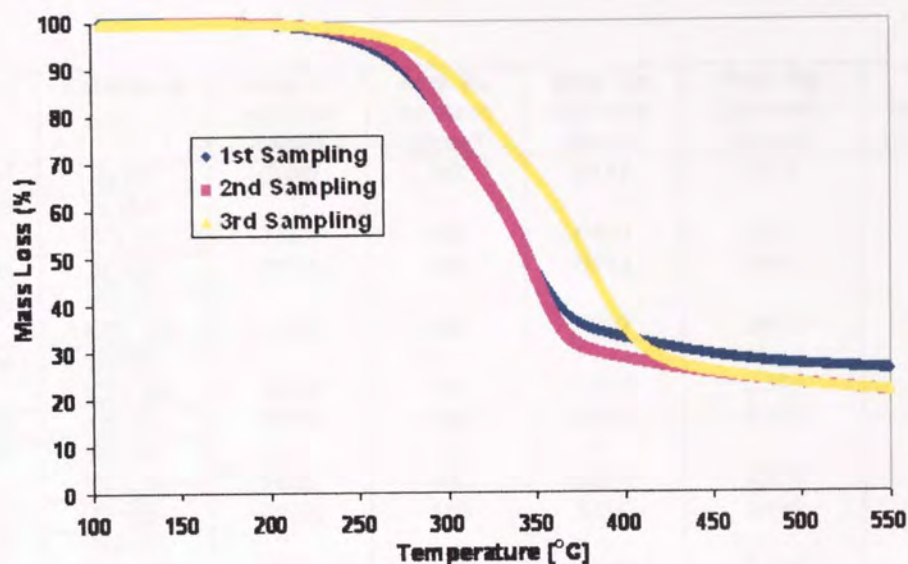


APPENDIX I, Figure 2 - TG of reference fuels

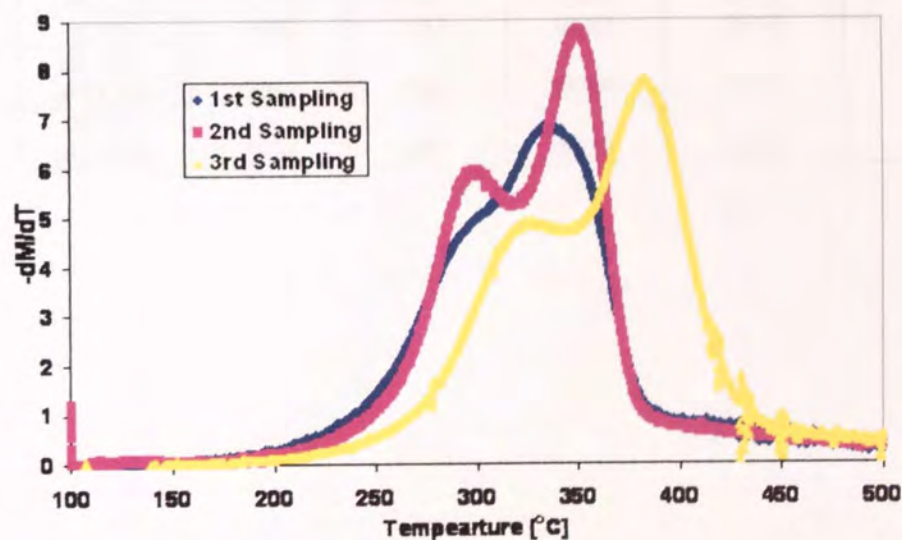
12 APPENDIX II

12.1 Agronomical results of Miscanthus

12.1.1 The effect of sampling time on TGA



APPENDIX II, Figure 1 - The effect of sampling on Miscanthus treatment 2 plot 1 on TG



APPENDIX II, Figure 2 - The effect of sampling on Miscanthus treatment 2 plot 1 on DTG

12.2 Alkali metal results of Miscanthus treatments

12.2.1 Nitrogen fertiliser treatments on the leaf content of Miscanthus

APPENDIX II 1 - Effect of Nitrogen application on the alkali metal content of Misacanthus leave

Sampling	Treatment	Avg. K content [ppm]	Avg. Na content [ppm]	Avg. Ca content [ppm]	Avg. Mg content [ppm]	Total alkali metal content [ppm]
1-Nov 05	N:50	6989	86	6111	2656	15843
1-Nov 05	N:100, KCL:50	7362	93	6440	2515	16412
1-Nov 05	N:100	7096	66	6713	3310	17187
1-Nov 05	N:200, KCL:50	7590	136	7357	2651	17735
1-Nov 05	N:250, KCL:50	8506	79	5937	2746	17269
2-Dec 05	N:50	2241	145	5608	2140	10136
2-Dec 05	N:100, KCL:50	2532	142	6875	2305	11856
2-Dec 05	N:100	3656	158	6189	2498	12503
2-Dec 05	N:200, KCL:50	3340	159	6737	2164	12401
2-Dec 05	N:250, KCL:50	3430	141	6189	2391	12152
3-Feb 06	N:50	1291	143	6356	2138	9930
3-Feb 06	N:100, KCL:50	1780	137	6478	2190	10586
3-Feb 06	N:100	1412	117	6683	2416	10628
3-Feb 06	N:200, KCL:50	2071	153	6904	2160	11289
3-Feb 06	N:250, KCL:50	1834	141	6972	2343	11292

12.2.2 Potassium chloride fertiliser treatments on the leaf content of Miscanthus

**APPENDIX II 2 - Effect of Potassium chloride application on the alkali metal content of
Misacanthus leave**

Sampling	Treatment	Avg. K content [ppm]	Avg. Na content [ppm]	Avg. Ca content [ppm]	Avg. Mg content [ppm]	Total alkali metal content [ppm]
1-Nov 05	KCL:50	5125	79	6371	2000	13576
1-Nov 05	N:50, KCL:100	7314	63	6186	2250	15815
1-Nov 05	N:50, KCL:50	5996	72	6676	2788	15534
1-Nov 05	N:150, KCL:100	8918	60	6600	2983	18564
1-Nov 05	N:150, KCL:50	7699	95	6277	2815	16888
2-Dec 05	KCL:50	1568	143	5891	1810	9412
2-Dec 05	N:50, KCL:100	2524	134	5918	1775	10352
2-Dec 05	N:50, KCL:50	1664	125	6519	2297	10606
2-Dec 05	N:150, KCL:100	2158	124	6761	2239	11283
2-Dec 05	N:150, KCL:50	2777	165	6338	2273	11554
3-Feb 06	KCL:50	1009	177	5986	1641	8815
3-Feb 06	N:50, KCL:100	1623	136	6478	1898	10136
3-Feb 06	N:50, KCL:50	958	111	7005	2203	10278
3-Feb 06	N:150, KCL:100	1415	120	6472	2200	10208
3-Feb 06	N:150, KCL:50	2029	137	6155	2090	10413

12.2.3 Potassium sulphate treatment fertiliser treatments on the leaf content of
Miscanthus

APPENDIX II 3 - Effect of potassium sulphate application on the alkali metal content of
Misacanthus leave

Sampling	Treatment	Avg. K content [ppm]	Avg. Na content [ppm]	Avg. Ca content [ppm]	Avg. Mg content [ppm]	Total alkali metal content [ppm]
1-Nov 05	N:50, KS:50	7141	71	6059	2886	16159
1-Nov 05	N:50, KS:100	6242	132	6211	2273	14859
1-Nov 05	N:150, KS:100	7626	77	6850	3085	17639
1-Nov 05	N:150, KS:50	8220	63	6890	2935	18110
2-Dec 05	N:50, KS:50	2419	139	5743	2394	10696
2-Dec 05	N:50, KS:100	2334	200	5855	1952	10341
2-Dec 05	N:150, KS:100	3080	137	6132	2323	11674
2-Dec 05	N:150, KS:50	3432	143	5927	2495	11998
3-Feb 06	N:50, KS:50	1210	127	6496	2340	10175
3-Feb 06	N:50, KS:100	1443	180	6198	1788	9610
3-Feb 06	N:150, KS:100	1291	111	6228	2248	9880
3-Feb 06	N:150, KS:50	2349	108	6993	2613	12065

12.2.4 Nitrogen fertiliser treatments on the stem content of Miscanthus

**APPENDIX II 4 - Effect of Nitrogen application on the alkali metal content of
Miscanthus stem**

Sampling	Treatment	Avg. K content [ppm]	Avg. Na content [ppm]	Avg. Ca content [ppm]	Avg. Mg content [ppm]	Total alkali metal content [ppm]
1-Nov 05	N:50	4227	41	615	691	5576
1-Nov 05	N:100, KCL:50	6379	37	487	652	7557
1-Nov 05	N:100	8092	40	667	1068	9869
1-Nov 05	N:200, KCL:50	6162	60	949	1080	8253
1-Nov 05	N:250, KCL:50	6290	46	907	1162	8406
2-Dec 05	N:50	3379	63	722	639	4804
2-Dec 05	N:100, KCL:50	5921	49	698	731	7400
2-Dec 05	N:100	6219	55	804	895	7974
2-Dec 05	N:200, KCL:50	4742	57	912	1024	6737
2-Dec 05	N:250, KCL:50	6440	42	641	965	8089
3-Feb 06	N:50	4082	69	716	677	5546
3-Feb 06	N:100, KCL:50	6316	55	606	739	7718
3-Feb 06	N:100	5185	50	644	810	6691
3-Feb 06	N:200, KCL:50	6130	57	665	932	7785
3-Feb 06	N:250, KCL:50	6517	44	761	1007	8331

12.2.5 Potassium chloride fertiliser treatments on the stem content of Miscanthus

**APPENDIX II 5 - Effect of potassium chloride application on the alkali metal content of
Miscanthus stem**

Sampling	Treatment	Avg. K content [ppm]	Avg. Na content [ppm]	Avg. Ca content [ppm]	Avg. Mg content [ppm]	Total alkali metal content [ppm]
1-Nov 05	KCL:50	4867	53	803	678	6402
1-Nov 05	N:50, KCL:100	7118	42	688	783	8633
1-Nov 05	N:50, KCL:50	5896	54	872	989	7813
1-Nov 05	N:150, KCL:100	8284	33	726	1123	10168
1-Nov 05	N:150, KCL:50	7341	49	744	950	9086
2-Dec 05	KCL:50	3212	58	764	535	4570
2-Dec 05	N:50, KCL:100	4995	49	727	675	6447
2-Dec 05	N:50, KCL:50	4567	53	742	817	6180
2-Dec 05	N:150, KCL:100	6873	48	675	929	8526
2-Dec 05	N:150, KCL:50	5422	63	763	904	7153
3-Feb 06	KCL:50	2753	55	586	447	3843
3-Feb 06	N:50, KCL:100	6110	45	646	722	7525
3-Feb 06	N:50, KCL:50	4129	56	677	741	5605
3-Feb 06	N:150, KCL:100	6236	51	643	953	7884
3-Feb 06	N:150, KCL:50	6843	59	667	899	8469

12.2.6 Potassium sulphate treatment fertiliser treatments on the stem content of
Miscanthus

APPENDIX II 6 - Effect of potassium sulphate application on the alkali metal content of
Misacanthus stem

Sampling	Treatment	Avg. K content [ppm]	Avg. Na content [ppm]	Avg. Ca content [ppm]	Avg. Mg content [ppm]	Total alkali metal content [ppm]
1-Nov 05	N:50, KS:50	4227	41	615	691	5576
1-Nov 05	N:50, KS:100	5363	71	673	590	6698
1-Nov 05	N:150, KS:100	8539	37	612	939	10128
1-Nov 05	N:150, KS:50	6731	38	841	1003	8614
2-Dec 05	N:50, KS:50	4689	64	819	779	6353
2-Dec 05	N:50, KS:100	3728	94	934	631	5389
2-Dec 05	N:150, KS:100	6878	53	763	971	8667
2-Dec 05	N:150, KS:50	5469	37	601	745	6854
3-Feb 06	N:50, KS:50	3283	57	805	744	4892
3-Feb 06	N:50, KS:100	3414	78	747	520	4760
3-Feb 06	N:150, KS:100	5785	58	678	927	7450
3-Feb 06	N:150, KS:50	7129	44	672	889	8735

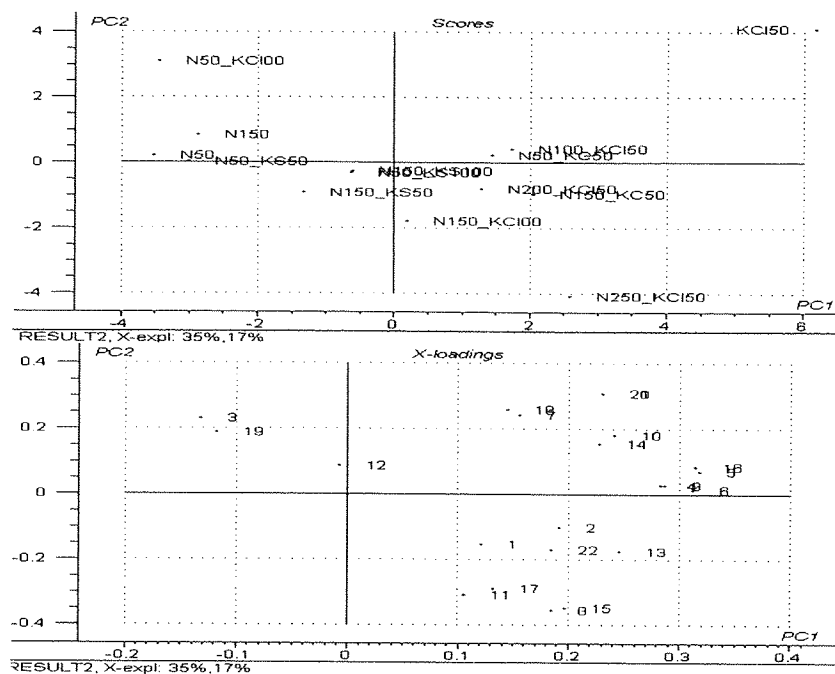
13 APPENDIX III

13.1 PCA Compounds analysis

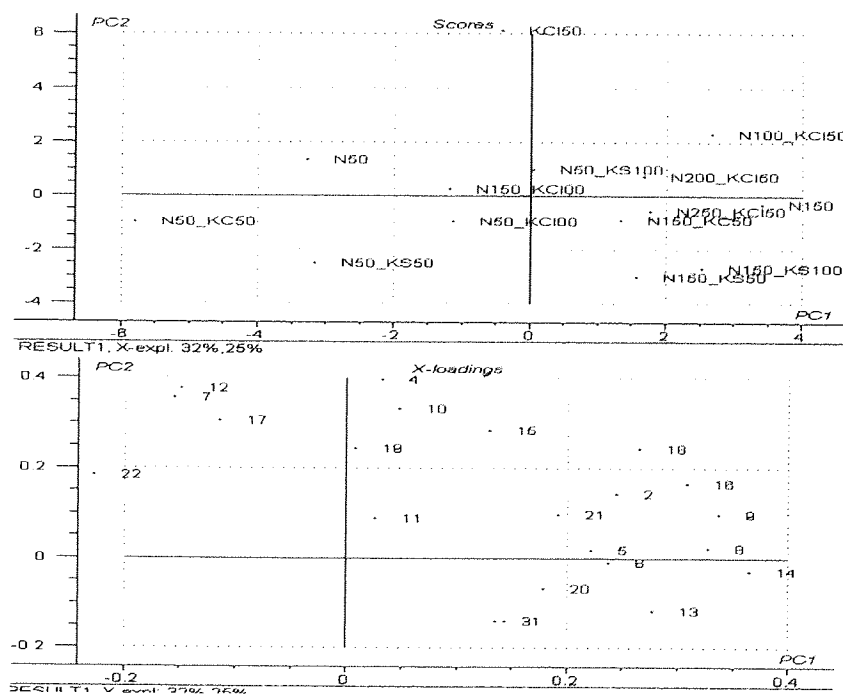
APPENDIX II 7 - PCA Compound number

Peak No.	Name of compound
1	2,3-Butandione
2	Hydroxyacetaldehyde
3	Hydroxypropanone
4	2-Furaldehyde
5	2 Furanmethanol
6	(5H)-Furan-2-one
7	4-Hydroxy-5,6-dihydro-(2H)-Pyran-2-one
8	Phenol
9	Guaiacol
10	4-Vinyl guaiacol
11	Eugenol
12	5-Hydroxymethyl-2-furaldehyde
13	Pyrocatechol
14	Syringol
15	Vanillin
16	4-Vinyl syringol
17	Levoglucosan
18	4-Propenyl syringol (trans)
19	Syringaldehyde
20	Acetosyringone
21	Coniferyl alcohol
22	Guaiacyl 4 ethyl

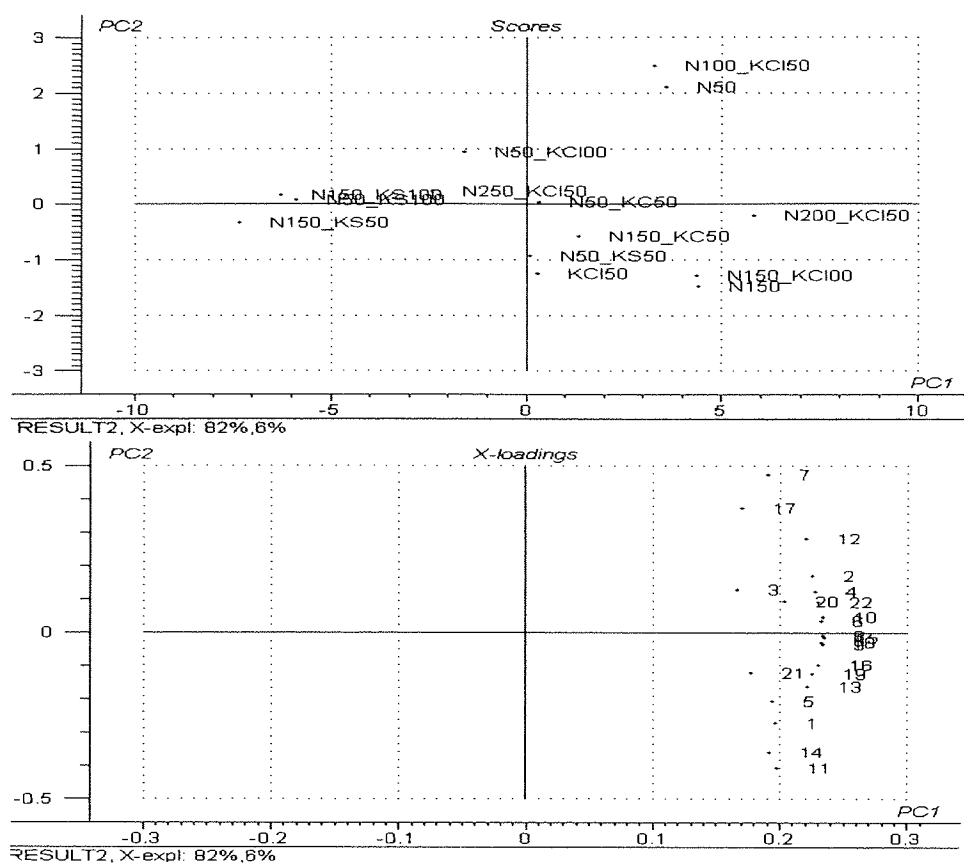
13.1.1 PCA results from pyroprobe-GC/MS for leaves



APPENDIX III, Figure 1 - 1st sampling leaves of fertiliser treatment on pyroprobe-GC/MS compounds

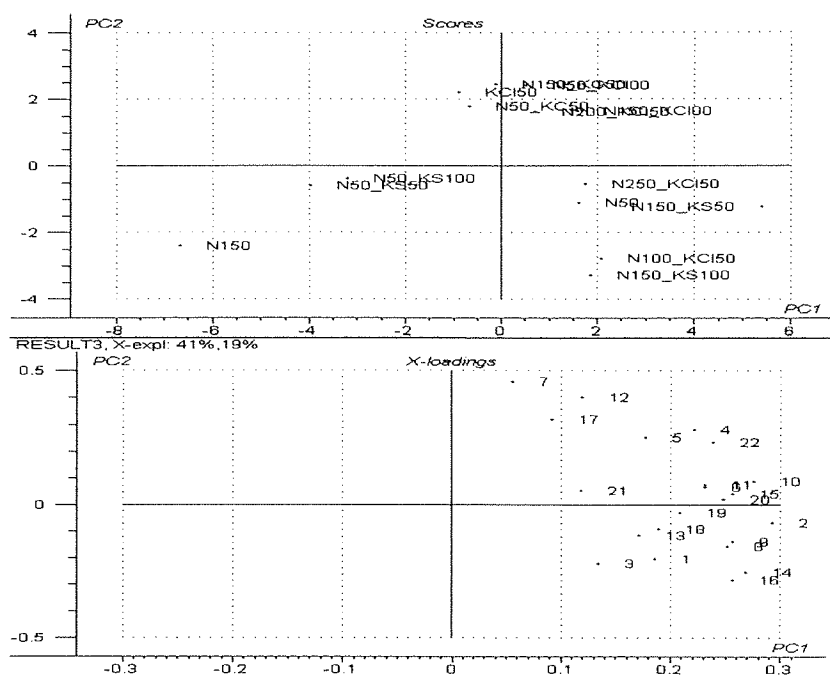


APPENDIX III, Figure 2 - 2nd sampling leaves of fertiliser treatment on pyroprobe-GC/MS compounds

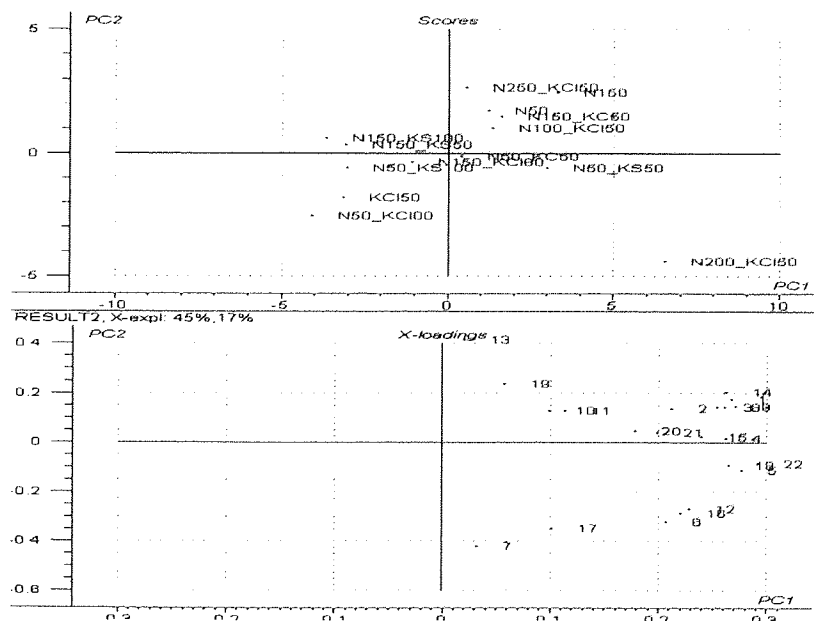


APPENDIX III, Figure 3 - 3rd sampling leaves of fertiliser treatment on pyroprobe-GC/MS compounds

13.1.2 PCA results from pyroprobe-GC/MS for stems



APPENDIX III, Figure 4- 1st sampling stems of fertiliser treatment on pyroprobe-GC/MS compounds



APPENDIX III, Figure 5 - 2nd sampling stems of fertiliser treatment on pyroprobe-GC/MS compounds

syringol respectively]. Treatment N:100_KCl:50 had a positive relationship with compounds 2, 16 and 18 [hydroxyacetaldehyde, 4-vinyl guaiacol and 4-propenyl syringol (trans) respectively], while treatment N:250_KCl:50 had a positive relationship with 5, 6 and 20 [2-furanmethanol, (5H)-furan-2-one and acetosyringone respectively] instead of compounds 1, 2 and 22 [2,3-butanedione, hydroxyacetaldehyde and 4-ethyl guaiacol respectively] from the first sampling. The third sampling for leaves showed that the majority of the treatments had no clear relationship with any of the compounds. However looking at the data for the third PCA analysis it can be deduced that treatments N:150, N:150_KCl:100 and N:200_KCl:50 had minor relationships with compounds 1, 5, 13, 19 and 21 [2,3 butanedione, 2 furanmethanol, pyrocatechol, syringaldehyde and coniferyl alcohol respectively] by showing a slight increase.

13.2.1.2 PCA analysis on nitrogen treatment on stems compounds:

The nitrogen treatments for the first sampling was scattered across the score plot with all the compounds clustering to the far right of the loading plot. Treatments N:150 had a negative relationship by showing a decrease for all the products evolved from the pyroprobe-GC/MS, while treatment N:100_KCl:150 had weak relationships with compound 3 [hydroxypropanone] by slightly increasing its yields. Treatments N:50 and N:250_KCl:50 possessed a weak positive effect on products 3, 13 and 18 [hydroxypropanone, pyrocatechol and 4-propenyl syringol (trans) respectively]. Treatment N:200_KCl:50 lied in a region in which no compounds were clustered. As the second sampling was analysed it was found that the majority of the treatments for nitrogen had a positive relationship by showing an increase on compounds 10, 11 and 19 [4-vinyl guaiacol, eugenol and syringaldehyde], while treatment N:200_KCl:50 effected the most on compounds 6, 12 and 16 [(5H)-furan-2-one, 5-hydroxymethyl-2-furaldehyde and 4-vinyl syringol] by an increase in yield. During the third sampling the majority of treatments had some level of a positive relationship with the majority of the compounds weak or strong, except for N:150_KCl:50 treatment. N:150 had an impact by slightly increasing compounds 9 and 16 [guaiacol and 4-vinyl syringol respectively], while N:250_KCl:50 had a relationship with 10 and 15 [4-vinyl guaiacol and Vanillin respectively] by showing an increase. However N:100_KCl:50 had major impacts on compounds 4, 5 and 18 [2-furaldehyde, 2 furan methanol and 4-propenyl syringol (trans) respectively] by increasing their yield.

13.2.2 Potassium chloride treatments

13.2.2.1 *PCA analysis on potassium chloride on leaf compounds:*

The first sampling data showed a cluster for all the treatments. Treatments N:150_KCl:100, N:150_KCl:50 had a positive result by increasing on compounds 1, 2, 13 and 22 [2,3 butanedione, hydroxyacetaldehyde, pyrocatechol and 4-ethyl guaiacol respectively], while treatments N:50_KCl:50, N:50_KCl:100 and KCl:50 lied in regions where no compounds were clustered and were close to the centre of the score plot. The second sampling treatments showed the product distribution became more spread with a reduction on compound relationships. The only treatment which had a positive increase was treatment N:150_KCl:50 on compound 20 [acetosyringone]. By the third sampling there was no relationship between any of the treatments with the compounds.

13.2.2.2 *PCA analysis on potassium chloride on stems compounds:*

All the treatments from the first sampling showed no clear relationship with any of the compounds, and this was demonstrated again in the second sampling, with the exception of treatment N:150_KCl:50 which had a positive increase relationship with compounds 10 and 11 and to a less extent compound 19 [4-vinyl guaiacol, eugenol and syringaldehyde respectively]. However by the third sampling it was found that all the potassium chloride treatments had a negative effect on the majority of the compounds.

13.2.3 Potassium sulphate treatments

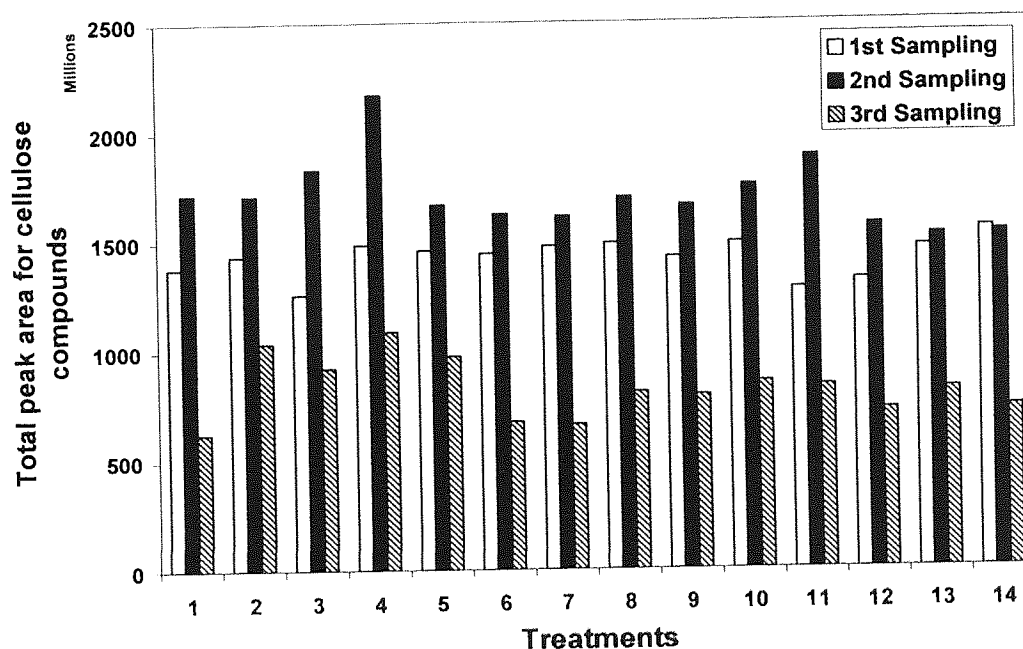
13.2.3.1 *PCA analysis on potassium sulphate on leaf compounds:*

From the first sampling of the sulphate fertiliser treatments it is noticeable that the majority of the treatments fell in the centre of the score plots, with the majority of the compound clustered on the far right of the load plot. Hence no relationship could be established from the first sampling. During the second sampling treatments N:50_KS:50, N:150_KS:50 and N:150_KS:100 remained to have no clear relationship with any of the products from pyroprobe-GC/MS. The only treatment which stood out in the second sampling was treatment with N:50_KS:100 which had positive effects on compound 11 [eugenol] by increasing its yield, and by the third sampling no relationship existed for any of the treatments.

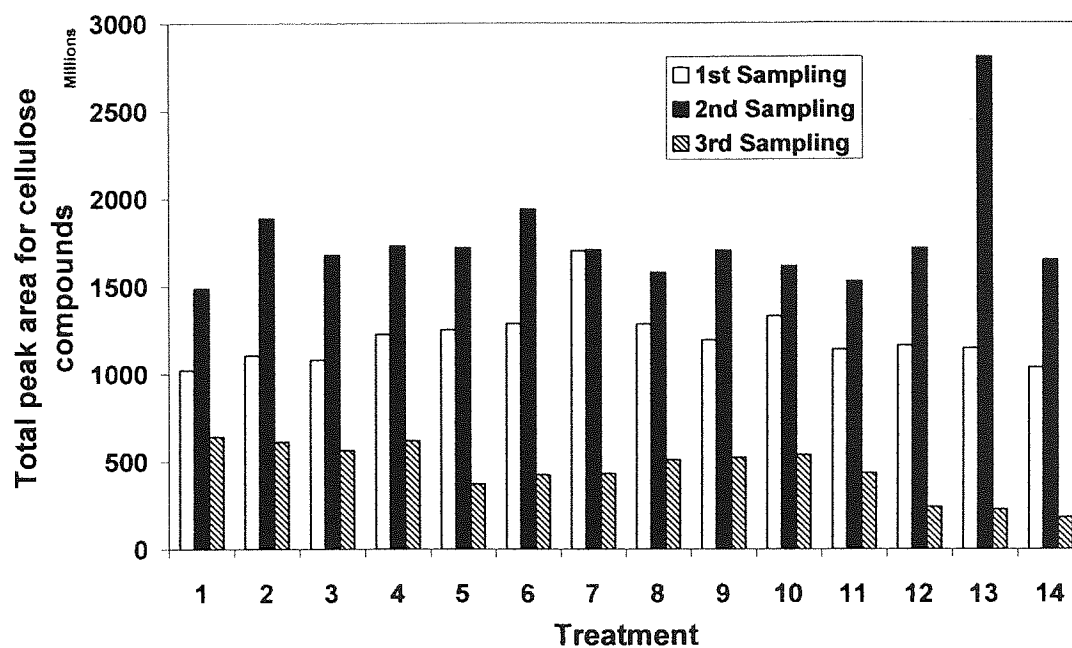
13.2.3.2 PCA analysis on potassium sulphate on stem compounds:

From all the sampling period results for the sulphur treatments, it was concluded that none of the treatments possessed any relationships with the compounds from pyroprobe-GC/MS.

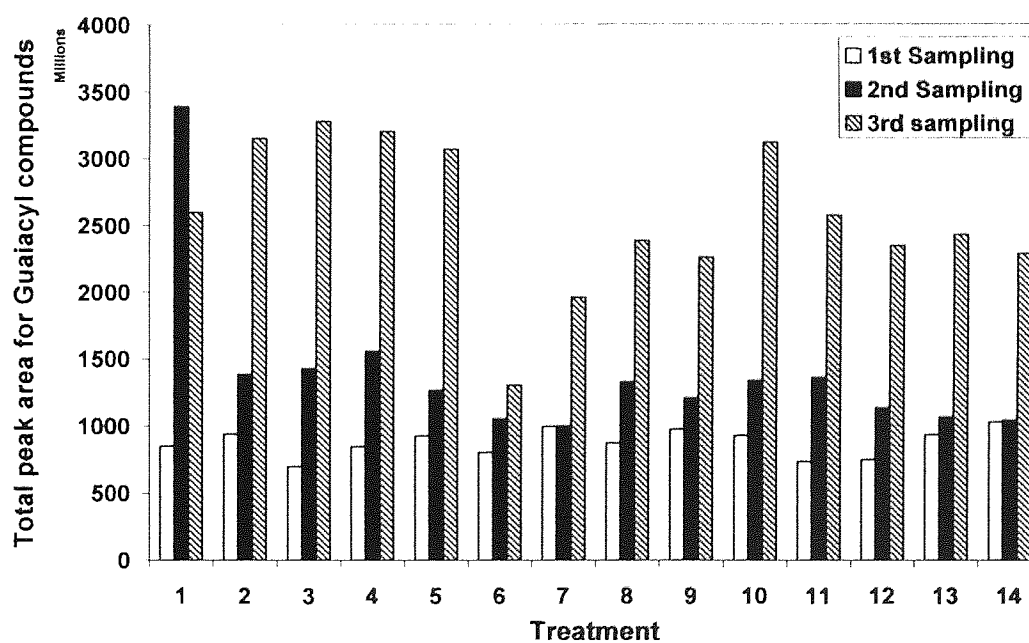
13.3 The effect of compound yields during sampling



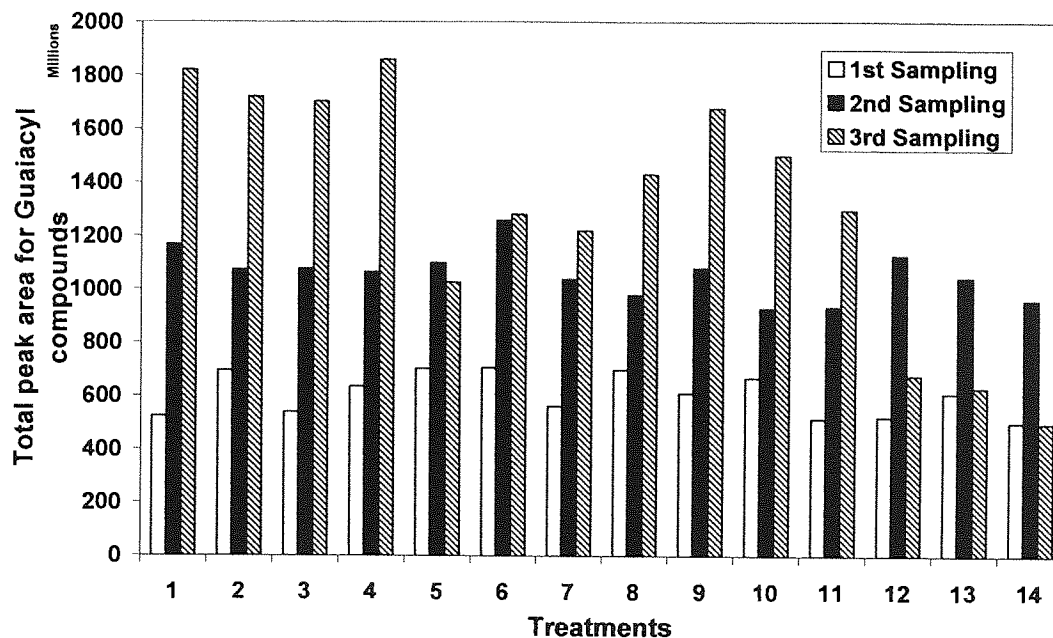
APPENDIX III, Figure 7 - Cellulose derived compounds from stems throughout sampling



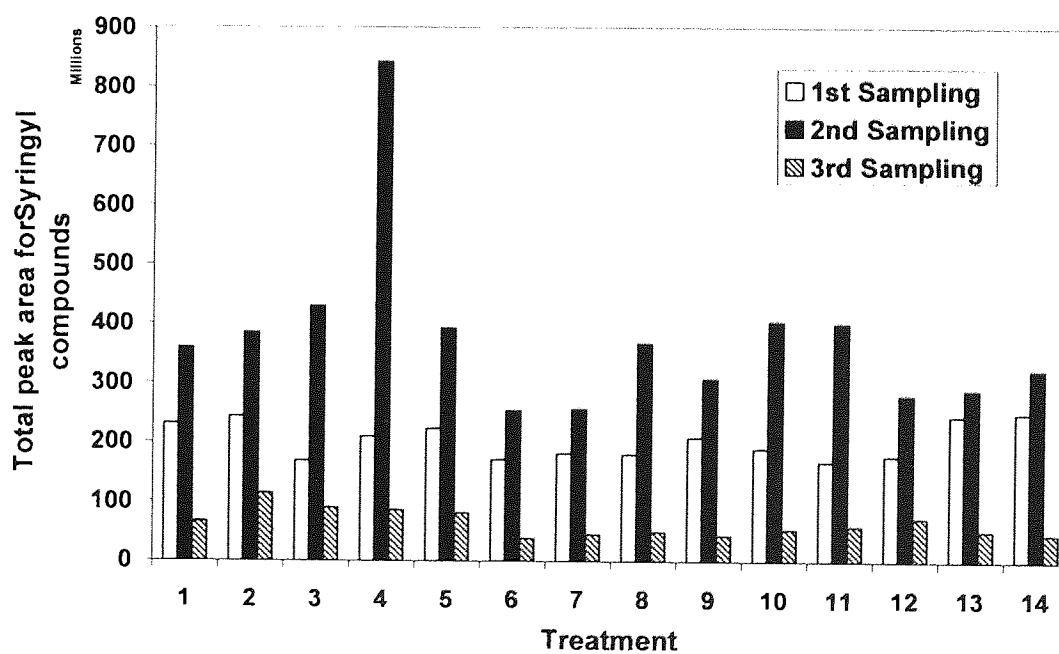
APPENDIX III, Figure 8 - Cellulose derived compounds from leaves throughout sampling



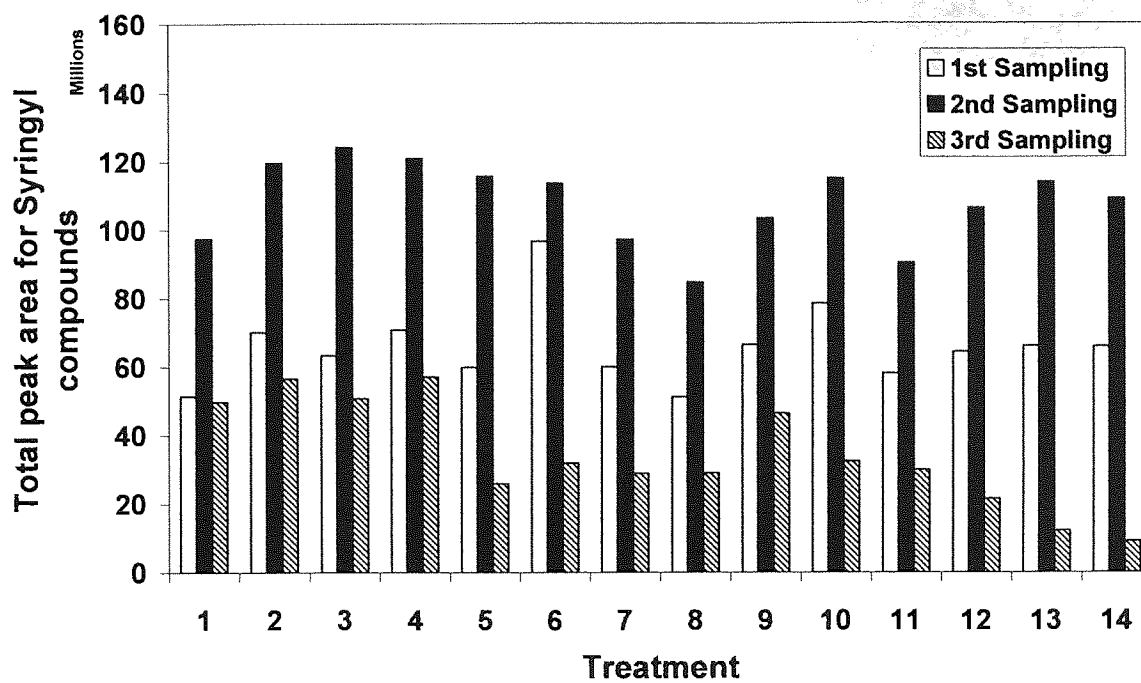
APPENDIX III, Figure 9 - Guaiacyl derived compounds from stems throughout sampling



APPENDIX III, Figure 10 - Guaiacyl derived compounds from leaves throughout sampling



APPENDIX III, Figure 11 - Syringyl derived compounds from stems throughout sampling



APPENDIX III, Figure 12 - Syringyl derived compounds from leaves throughout sampling